The diversity and drivers of bacterial assemblages in the euphotic zone from coastal seas to the open ocean.

Kimberley Elizabeth Bird

Doctor of Philosophy

University of East Anglia, UK

School of Environmental Sciences

September 2018

Abstract

Marine bacteria are ubiquitous in the world's oceans, contributing significantly to food webs and global biogeochemical cycles. Characterising the distribution and drivers of bacterial diversity is key to understanding their important roles in the marine ecosystem. This thesis characterised the diversity and drivers of bacterial communities in the euphotic zone from 1 mm to 250 m below the sea surface, covering a range of marine environments from the coastal and shelf seas to the open ocean, including biogeochemically important habitats such as the sea surface microlayer. Bacterioplankton communities vary seasonally and over local and global scales, in response to prevailing environmental characteristics. Using a multidisciplinary approach, interrogating 16S rRNA gene high-throughput sequence data with co-occurring physicochemical metadata has revealed that, in addition to the major overarching drivers of temperature and primary production, physical processes such as atmospheric deposition, mixing, and stratification can also influence the composition of bacterial communities and their vertical distribution in the water column. Enrichments of ecologically important bacteria such as *Alteromonas* sp. and *Trichodesmium* sp. in the sea surface microlayer have potential to influence the availability of resources arriving into the open ocean from the atmosphere. Using 16S rRNA transcripts to characterise active bacterioplankton communities has revealed that bacterioplankton activity is decoupled from abundance throughout the Atlantic Ocean, and may be influenced by the dominant primary producers. Furthermore, by combining culture-based techniques with functional amplicon sequencing, the physiological effects of CO-oxidation on the model bacterioplankton *R. pomeroyi* and a diversity of CO-oxidising bacterioplankton among the ecologically important Marine Roseobacter Clade in a temperate coastal environment have been identified. This thesis improves our understanding of bacterial ecology in the world's oceans, and demonstrates how holistic approaches to studying marine bacteria in the environment used in combination with molecular tools, can give a view of marine ecosystem function.

Contents

List of tables

Supplemental tables

List of figures

Chapter 1

Chapter 2

Chapter 3

Chapter 4

Chapter 5

Chapter 6

Chapter 7

Supplemental figures

List of equations

Dedication

To my parents,

Susan Lelliott and Peter Bird

Acknowledgements

Supervisory team

I would like to thank my primary supervisor Dr Michael Cunliffe at the Marine Biological Association of the UK (MBA) and my secondary supervisor Prof. Colin Murrell at the University of East Anglia (UEA) for their fantastic supervision and dedication; they have always had time for me and given the best advice. I could not have wished for a better supervisory team, they have made this an enjoyable and rewarding experience; I cannot thank them enough for helping me to full fill my potential. I would also like to thank the other members of Cunliffe Group and Murrell Group for their support it has been a pleasure working with them all. I acknowledge my funders the NERC EnvEast Doctoral Training Programme and the MBA for providing me with the opportunity to carry out this research and my institutes the UEA and the MBA.

Collaborators

This research has been supported by many people and this list by no means exhaustive, but I would like to mention and thank my collaborators: - Dr. Joe Taylor at the University of York (now at University of Salford) for teaching me bioinformatics and for carrying out the *coxL* sequencing for Chapter 4. Dr. Jon Todd, Simone Payne and the rest of the Todd lab at the UEA for providing the bacterial strains and primers used in Chapter 3, for their help and advice, and making me welcome in their lab. Dr Joseph Christie-Oleza at the University of Warwick for generously carrying out the proteomics for Chapter 3. Dr Oliver Wurl, Dr William Landing and Dr Chris Zappa and their teams for making their data available to me for use in Chapter 6.

Seagoing

I must also thank all who were involved in the seagoing part of this research, you made my time at sea an unforgettable experience, and many of you are now friends. I could not have collected the 100's of samples for this research without them. I would like to specifically mention: - The skipper, crew and seagoing team of the MBA's *R/V Sepia*. Especially Roger Pawley, Sean McTierney and Aisling Smith who supported the collection of samples at the Western Channel Observatory (WCO). I would also like to mention PML's *R/V Quest* and crew who also supported the WCO sampling effort, and Malin Tietjen for collecting my

samples when I was unable to do so. The captain, officers, crew and NERC technicians on board the *RSS James Clark Ross* during cruise JR15001 (AMT25) and participants: Arwen Bargery, Bita Sabbaghzadeh, Carolina Beltran, Bob Brewin, Cat Burd, Catherine Mitchell, Charlotte Smith, Giorgio Dall'Olmo, Glen Tarran, Pri Lange, Robyn Tuerena and Tim Smyth. I Thank the Scientific Committee on Oceanographic Research (SCOR) Working Group 141 Sea Surface Microlayer for the opportunity to take part in the AIR↓↑SEA study, and the Schmidt Ocean Institute for providing their research vessel *R/V Falkor* for the AIR↓↑SEA FK161010 cruise. I would also like to thank the captain and crew of the *R/V Falkor* and participants: Oliver Wurl, Christopher Zappa, William Landing, Mariana Ribas Ribas, Janina Rahlff, Rachel Shelley, Nur Ili Hamizah Mustaffa, Lea Oeljeschlaeger, Sophia Brumer, Scott Brown, Justin Armer, Scott Bowers, Joe McDaniel and Carson Witte, especially those who helped me glass plate sampling come rain, shine, waves and sea snakes.

Supporting metadata provision

I thank the NERC Earth Observation Data Acquisition and Analysis Service (NEODAAS), the British Oceanographic Data Centre, the Western Channel Observatory and Bearsbythesea for supplying supporting metadata used in this study.

Other important people

I would also like to extend thanks to the EnvEast team (David Craythorne, Alison henry and Bill Sturges), the rest of my friends and colleagues at the MBA and UEA especially those in the Murrell Lab, Cunliffe Lab, Cell and Molecular (especially Angela, Claire and Shea), the MBA PhD cohort and the EnvEast PhD cohort. Finally I thank my non-sciencey friends and family, especially my parents and Gavin for their love, support and gin when required!

Thank you

Kimberley Bird

Chapter 1

General Introduction

1.1 Marine bacteria

Bacteria are globally ubiquitous and estimated to have a total biomass of 70 Gt carbon (C), with pelagic marine bacteria (bacterioplankton) equating to 1.3 Gt C (Bar-On et al., 2018). Occupying the majority of the earth's surface, marine bacteria are billions per litre, having fundamental roles in global biogeochemical cycles, including driving transformations of organic and inorganic material (Azam et al., 1983, Falkowski et al., 1998, Azam and Malfatti, 2007).

Marine bacteria can broadly be divided into two main trophic categories based on their metabolism. Autotrophs are bacteria that gain energy from inorganic sources and can fix inorganic carbon. The majority of planktonic autotrophic marine bacteria are phototrophs and gain energy and carbon via photosynthesis (Partensky et al., 1999). Autotrophic marine bacteria contribute substantially to the marine carbon cycle (Hagström et al., 1988), with *Cyanobacteria* such as *Prochlorococcus* and *Synechococcus* responsible for 25 % of global net primary production (Flombaum et al., 2013). Heterotrophs are bacteria that gain both energy and carbon from organic substrates, and are estimated to consume a large proportion (10-50 %) of the total fixed carbon (secondary production) (Fuhrman and Azam, 1982). Bacterial secondary production contributes significantly to marine food webs and biogeochemical cycles (Azam et al., 1983, Ducklow, 2000, Azam and Malfatti, 2007).

Assigning trophic categories to marine bacteria is in reality more complex because in between full autotrophy and full heterotrophy are a range of bacteria that employ mixed strategies of energy and carbon acquisition (figure 1.1) (Eiler, 2006, Moran, 2015). Examples of strategies used by heterotrophs to obtain energy that deviate from full organoheterotrophy include photoheterotrophy, the acquisition of energy from light, and chemolithoheterotrophy, the acquisition of energy from inorganic substrates such as carbon monoxide (CO). Currently we know relatively little about the ecology of these alternative heterotrophic strategies in the marine environment but ‘resourceful’ heterotrophs such as the

carboxydovores (CO-oxidisers) are likely to change the way we view the marine carbon cycle (Moran and Miller, 2007).

Around 20% of coastal marine bacteria identified in the Global Ocean Survey metagenome data set are able to oxidise CO (Rusch et al., 2007), and the *coxL* Form I gene which encodes the large subunit of carbon monoxide dehydrogenase, is prevalent amongst ecologically relevant and ubiquitous bacteria such as the Marine Roseobacter Clade (MRC) (Tolli et al., 2006, Cunliffe, 2011). Bacterial CO-oxidation has potential to significantly contribute to the marine carbon cycle because CO produced by the photodegradation of dissolved organic matter is oxidised to carbon dioxide (CO_2) which equates to approximately 70 Tg of C per year (Zafiriou et al., 2003) that is available as CO_2 for primary production (figure 1.2).

Unlike carboxydotrophs that can grow autotrophically on CO, carboxydovores are chemolithoheterotrophs and cannot fix the resulting carbon, and must still acquire assimilatory carbon from organic substrates (King, 2003). However, trophic strategies, such as carboxydovory, come at a cost to marine bacteria (e.g. gene maintenance, protein synthesis), and therefore, must provide a benefit to the population in the long term (Eiler, 2006). It is hypothesised that CO is a supplementary energy source used by marine carboxydovores (King, 2003, Moran et al., 2004), presumably allowing for more efficient heterotrophic growth on the available organic substrates (Moran, 2015), however, this is yet to be shown empirically.

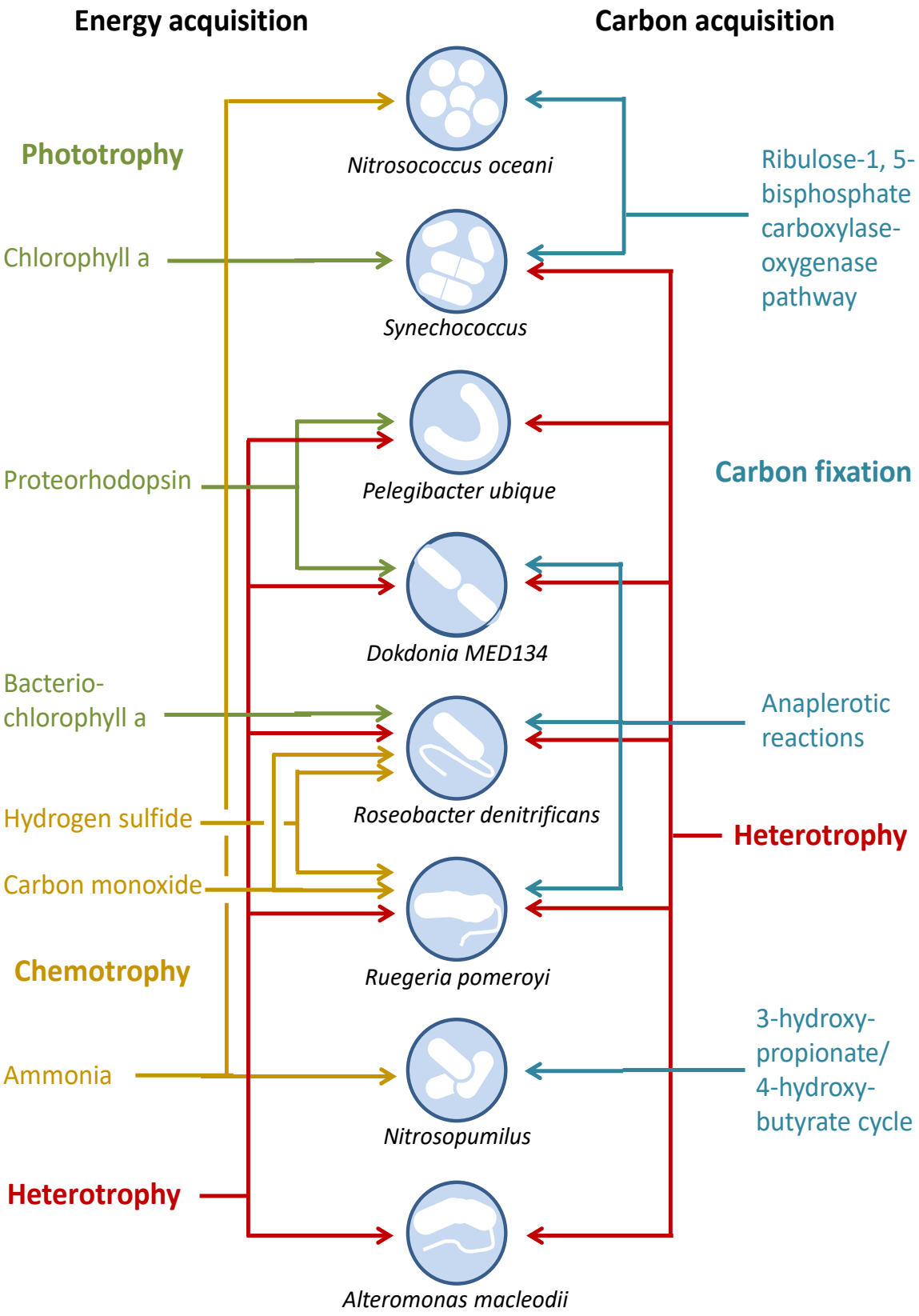

Figure 1.1. Categories of energy and carbon acquisition by bacteria in oxygenated seawater modified from Moran (2015).

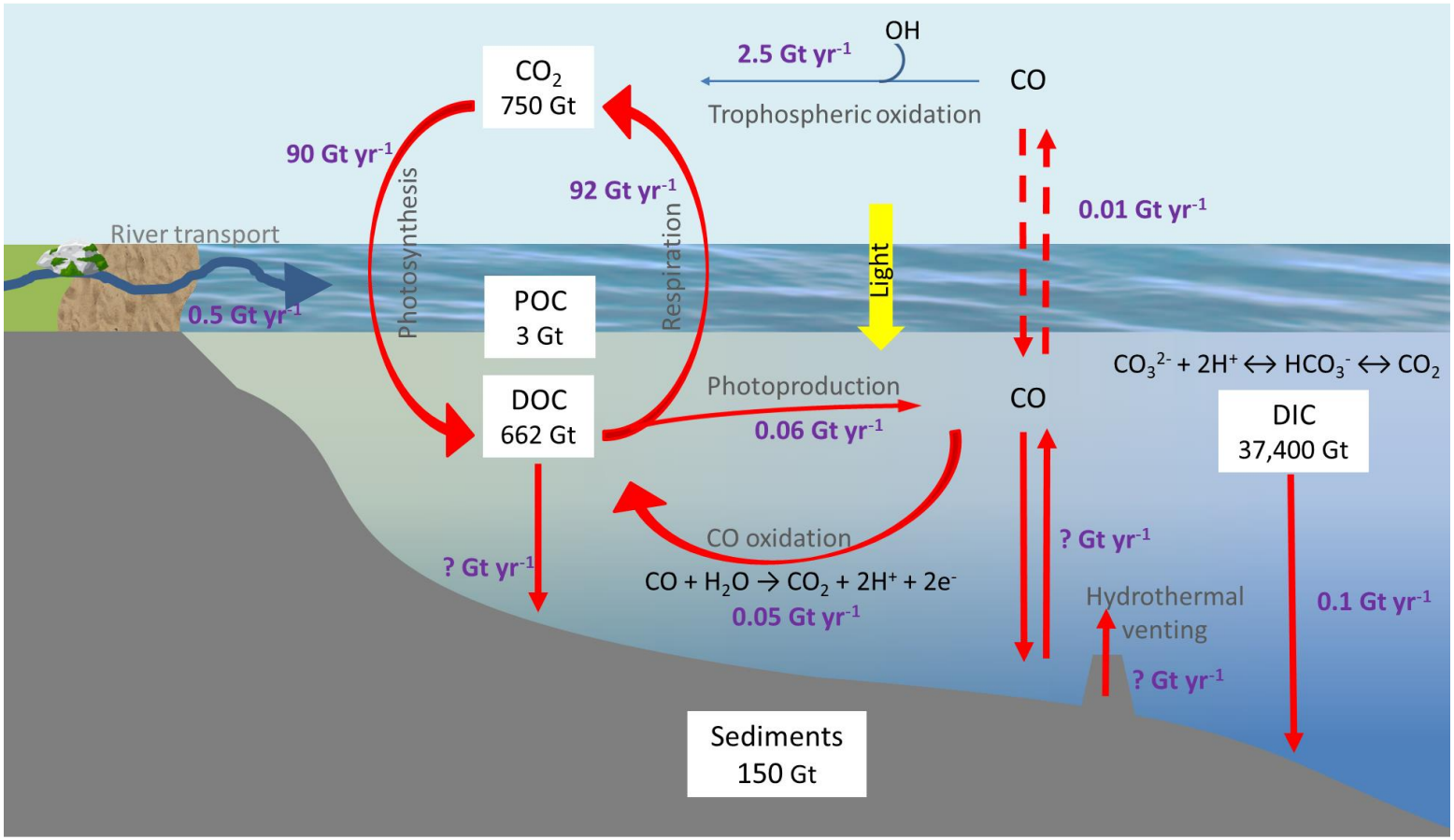

Figure 1.2. Illustration of the global marine carbon cycle including photochemically mediated carbon monoxide cycle. Carbon reservoirs are shown as rectangular blocks and sizes are in units of gigatons (Gt) of carbon. Flows between reservoirs are indicated by arrows and sizes are in units of gigatons (Gt) of carbon per year. Values are derived from Denman et al., (2007), King and Weber, (2007), Jiao et al., (2010) and Bianchi, (2011).

1.2 Geographical distribution and diversity of marine bacteria

Marine bacterial communities generally consist of a few dominant and many rarer taxa (Rappe et al., 2000, Zinger et al., 2011, Pedros-Alio, 2012, Sunagawa et al., 2015). It was previously hypothesised that the majority of marine bacteria should be universally distributed throughout the global ocean with little variation in community composition due to the lack of geographical barriers and large potential for dispersal (Hagström et al., 2000, Fenchel and Finlay, 2004). Since the development of culture independent methods, a large diversity of marine bacteria have been identified (DeLong and Pace, 2001, Doney et al., 2004, Karl, 2007) and contrary to this theory, the composition of bacterial communities has been shown to vary geographically (Pommier et al., 2007, Fuhrman et al., 2008, Zinger et al., 2011, Sunagawa et al., 2015).

Similarity between distant bacterial communities often occurs between similar ecosystem types, suggesting that prevailing environmental factors impact bacterial communities and therefore influence the geographical distribution of marine bacteria (Zinger et al., 2011, Sunagawa et al., 2015). The global seed bank theory suggests that the observed changes in community composition for a given ecosystem are driven by changes in the relative abundance (i.e. the number of reads as a percentage relative to the total number of reads) of each taxon according to ecological niches rather than their presence or absence in the community (Caporaso et al., 2012). Several studies have shown that bacterial communities are predictable by the characteristics of the environment they inhabit, with temperature thought to be the dominant driver of variation in bacterial communities on a global scale (Pommier et al., 2007, Fuhrman et al., 2008, Sunagawa et al., 2015). Other physicochemical characteristics such as nutrients, organic matter, light, chlorophyll, physical processes and biological factors such as predation and microbial interactions have also been shown to influence bacterial community composition (Long and Azam, 2001,

Fuhrman et al., 2006, Zinger et al., 2011, Gilbert et al., 2012, Buchan et al., 2014, Sarmento et al., 2016, Teeling et al., 2016, Bunse and Pinhassi, 2017).

As proposed by Baas-Becking (1934), it is clear that *"the environment selects"*, but whether it is from a global pool or local pool of bacteria, i.e. *"is everything really everywhere"*, remains to be determined (Green and Bohannan, 2006, Martiny et al., 2006, Pommier et al., 2007). Some studies suggest that few operational taxonomic units (OTUs) are actually cosmopolitan (Pommier et al., 2007, Sunagawa et al., 2015). Conversely, Gibbons et al. (2013) tested the global seed bank hypothesis and found that 32 – 66 % of the OTUs identified by Caporaso et al. (2012) could be found in a given biome and suggested with deep enough sequencing the phylogenetic diversity of all marine bacteria could be captured. Temporal studies show bacterial communities are seasonally reoccurring and high-resolution sampling efforts have revealed that bacterial communities undergo short-term, large peaks in single populations (Gilbert et al., 2012, Martin-Platero et al., 2018) supporting the notion that many bacteria are latently present. Testing this hypothesis will require the development of molecular techniques to better characterise the rare biosphere and the mechanisms that allow the existence of many taxa at low abundance (Pedros-Alio, 2006, Pedros-Alio, 2012).

Several studies have shown that the distribution of closely related phylotypes are determined by environmental factors (Schafer et al., 2002, Johnson et al., 2006, Six et al., 2007, Ivars-Martinez et al., 2008, Brown et al., 2012, Pittera et al., 2014, Bryson et al., 2017), and geographically distinct ecotypes are even present among the abundant and widespread bacteria such as the SAR11 clade (Field et al., 1997, Brown et al., 2012, Salter et al., 2014), *Prochlorococcus* (West and Scanlan, 1999, Bouman et al., 2006, Johnson et al., 2006) and the MRC (Selje et al., 2004). These findings suggest cosmopolitan bacteria may become endemic through environmental selection and genetic divergence, and also raises questions

as to whether current phylogenetic classification is suitable to accurately characterise microbial diversity (Callahan et al., 2017, Parks et al., 2018).

1.3 Temporal distribution of marine bacteria

Insights into the dynamics of microbial communities have been significantly advanced by time-series studies (Fuhrman et al., 2015, Bunse and Pinhassi, 2017). Bacterial communities vary temporally and exhibit seasonal-scale patterns in community composition in relation to changes in environmental properties. Seasonal patterns are observed in all regions, from the poles to the tropics, and in both coastal and open ocean environments, with the magnitude of change increasing with latitude (Fuhrman et al., 2015, Bunse and Pinhassi, 2017). Long term monitoring of bacterial communities and physicochemical characteristics have shown seasonal bacterial succession to be annually recurring with the greatest dissimilarity seen between opposing months (Gilbert et al., 2012, Fuhrman et al., 2015, Teeling et al., 2016, Bunse and Pinhassi, 2017). Seasonal patterns are comparable across geographical locations and over time (Fuhrman et al., 2015, Bunse and Pinhassi, 2017). Therefore a spring community is more likely to have greater similarities with a spring community from another location and or year than to an autumn community at the same location in the same year.

Temperate regions are strongly influenced by temperature, primary production and nutrient availability (Pinhassi and Hagström, 2000, Gilbert et al., 2012, Teeling et al., 2016). Sub-tropical and tropical regions are also influenced by temperature and nutrients, but also show greater influence of light (Giovannoni and Vergin, 2012, Karl and Church, 2014). Polar regions experience large and prolonged changes in response to extremes of light and temperature (Alonso-Saez et al., 2008, Ghiglione and Murray, 2012). Mixing and stratification processes also show seasonal variation and influence community composition. In the open ocean, seasonal variation is stronger in the upper mixed waters than deeper in

the water column, and in coastal regions strong water column mixing brings valuable nutrients to the surface (Cram et al., 2014, Bunse and Pinhassi, 2017). In oligotrophic environments where nutrients are low, seasonal changes in atmospheric deposition are also suggested to be important in structuring bacterial community composition (Boyd and Ellwood, 2010, Hill et al., 2010, Westrich et al., 2016). The dominant prevailing primary producer also strongly influences the bacterial community. In polar and temperate regions eukaryotic primary producers dominate, and phytoplankton blooms are often associated with higher abundances of copiotrophic bacteria such as the MRC, *Gammaproteobacteria* and *Bacteroidetes*. In sub-tropical and tropical regions *Cyanobacteria* dominate and are associated with a higher abundance of oligotrophs such as SAR11 and SAR86 (Bunse and Pinhassi, 2017).

1.4 Vertical distribution and diversity of marine bacteria

The global ocean is not just vast in terms of surface area, it also extends to the seafloor that is on average 3600 m deep, and is stratified into discrete layers over which temperature, light and nutrients are the main drivers of vertical variability in community composition (Giovannoni and Stingl, 2005, Behrenfeld et al., 2006, DeLong et al., 2006) as well as physical mixing processes (Zinger et al., 2011). Bacterial diversity generally declines with depth (Sunagawa et al., 2015, Walsh et al., 2016) and community composition varies less in deep water masses that undergo little biogeochemical variation in comparison to the surface ocean, which is more environmentally variable (Behrenfeld et al., 2006, Walsh et al., 2016).

The pelagic marine environment is dominated by *Cyanobacteria*, *Bacteroidetes* (mainly *Flavobacteriales*), *Alphaproteobacteria* (mainly SAR11), *Gammaproteobacteria*, *Deltaproteobacteria*, *Actinobacteria* and *Deferribacteres* (Zinger et al., 2011, Walsh et al., 2016). *Cyanobacteria* decrease in abundance with decreasing light levels (Zinger et al.,

2011) but still appear in the abundant fraction (~1 % of relative abundance) of the mesopelagic zone (Sunagawa et al., 2015), most likely being associated with sinking particles (Lochte and Turley, 1988). *Gammaproteobacteria*, *Deltaproteobacteria*, *Actinobacteria* and *Deferribacteres* increase with depth and dominate below the photic zone (Zinger et al., 2011, Walsh et al., 2016). *Alphaproteobacteria* are dominant throughout the water column and exhibit little variation with depth at the level of phyla (Zinger et al., 2011). Variation in the vertical distribution of marine bacteria is also seen within closely related taxa, for example distinct depth related ecotypes have been recorded for abundant taxa such as the SAR11 clade (Field et al., 1997) and *Prochlorococcus* (Johnson et al., 2006, Zinser et al., 2007).

Vertical differences in community composition also occur across very small scales; the upper 1 mm of the surface of the ocean known as the sea surface microlayer (SML) has physicochemical properties that are distinct from the surface water below (Zhang et al., 2003). This unique micro-habitat selects for the enrichment of bacteria from the water column below (Agogue et al., 2005a, Stolle et al., 2011), which leads to the formation of distinct SML bacterial communities (Franklin et al., 2005, Joux et al., 2006, Cunliffe et al., 2009) often dominated by *Gammaproteobacteria* (Agogue et al., 2005a, Franklin et al., 2005).

1.5 Functional diversity and activity of marine bacteria

The diversity and distribution of marine bacteria is fundamentally important to understanding ecosystem function (Azam and Malfatti, 2007, Fuhrman, 2009). However, we still know little about how bacterial communities function in the marine environment (Moran, 2015). Measuring function in the marine environment is difficult as the specific mechanisms by which communities mediate the transformations of organic carbon are

largely unknown. It is estimated only 1 % of the physiological and biochemical diversity of bacteria has been characterised (Rusch et al., 2007), since the vast majority of marine bacteria have not been isolated in culture, and cannot be kept in laboratory enrichments (DeLong and Pace, 2001, Rusch et al., 2007, Joint et al., 2010).

Genetic studies can provide information about the functional potential of bacterial communities but cannot demonstrate definitive function (Fuhrman, 2009, Krause et al., 2014). Most phylogenetic studies rely on the highly conserved 16S rRNA gene to identify bacteria in an evolutionary context, but 16S rRNA gene diversity does not represent well functional diversity, and the metabolic functions of bacteria can vary considerably within taxonomic lineages, such as the MRC (Moran et al., 2007, Christie-Oleza et al., 2012). In addition, functional diversity has been shown to exhibit different biogeographical patterns to phylogenetic diversity. Haggerty and Dinsdale (2017) found that functional diversity was most strongly influenced by latitude and showed little variation in response to environmental characteristics.

Complicating matters further, not all bacteria in the community are metabolically active (del Giorgio and Scarborough, 1995). Ratios between 16S rRNA transcripts and 16S rRNA genes suggest bacterial abundance in the community is not always indicative of bacterial activity in the community (Alonso-Saez et al., 2006, Alonso-Sáez et al., 2007, Alonso-Saez et al., 2008, Lami et al., 2009, Campbell et al., 2011, Hunt et al., 2013). Metagenomic and transcriptomics also show that functional genes can have far higher expression levels than their abundance suggests (Frias-Lopez et al., 2008).

Other approaches to defining ecological function in the environment, for example characterising individual components such as substrate composition (Arnosti et al., 2011) or extracellular enzymes (Arnosti and Steen, 2013), give an idea of the functions occurring in an ecosystem but do not identify the taxa responsible. Meta-omic studies allow the phylogenetic and functional diversity of whole and active communities and individual

ribotypes to be characterised (Rusch et al., 2007, Frias-Lopez et al., 2008). However, there are often a large number of unidentified genes due to a lack of representative reference genes in the genomic databases (Rusch et al., 2007, Gilbert et al., 2010a). Consequentially, there is still a need for *in vitro* trait-based studies to support the characterisation of functional genes from the environment (Krause et al., 2014).

1.7 Overarching thesis aims

The broad aim of this thesis was to improve our understanding of how marine bacterial communities are influenced by different environmental drivers (figure 1.3). I set out to characterise the biogeographical distribution of marine bacteria and investigate how bacterial communities respond to changes in their physiochemical environment. I specifically wanted to advance current knowledge by focusing on specific environments that are currently underrepresented in literature and to expand upon traditional DNA-based phylogenetic methods by investigating functional and active bacteria in the marine environment.

1.8 Specific thesis objectives

Chapter 3. Carboxydovory in the ecologically-relevant model marine bacterioplankton Ruegeria pomeroyi DSS-3

A major hurdle in environmental microbiology is assigning ecological functions to gene presence. In this chapter, I set out to confirm the function of the *coxL* gene in marine carboxydovores and to identify phenotypic responses to CO-oxidation in the ecologically relevant and important model marine bacterium *Ruegeria pomeroyi* DSS-3. Linking a functional gene to a confirmed metabolic function will enable more confident identification

of marine carboxydovores in the environment by *coxL*-based techniques and provide new insight into CO-based chemolithoheterotrophy.

Chapter 4. Seasonal diversity of bacterioplankton coxL genes: a time series study at the coastal Station L4 and open shelf Station E1 in the Western English Channel

In this chapter, I analyse weekly-scale dynamics of two temperate coastal bacterioplankton communities over a spring phytoplankton bloom transition, in relation to prevailing physicochemical drivers. Building on from Chapter 3, I have developed functional gene probes to investigate the diversity and distribution of marine carboxydovores, delivering an improved understanding of the ecology of carboxydovoric bacterioplankton in coastal waters.

Chapter 5. Diversity and distribution of total and active bacterioplankton communities in relation to light along a transect of the Atlantic Ocean

In this chapter, I investigated the bacterioplankton communities in the euphotic zone of the Atlantic Ocean, to gain a better understanding of their biogeographical distribution. I also investigated the activity of the bacterioplankton in these communities to gain insight into the relative contributions these taxa make to bacterial productivity. In addition, I investigated whether light affected the composition and distribution of bacterioplankton communities vertically through the water column.

Chapter 6. A multidisciplinary approach to studying the sea surface microlayer reveals the complexity of physicochemical influences on bacterioneuston diversity

In this chapter, I investigated bacterial diversity at the air-sea interface using a collaborative multidisciplinary approach in order to better understand the interactive effects of the physicochemical characteristics of the sea surface microlayer on the bacterioneuston. This provides new insight into the complexity of environmental influences on the bacterioneuston communities.

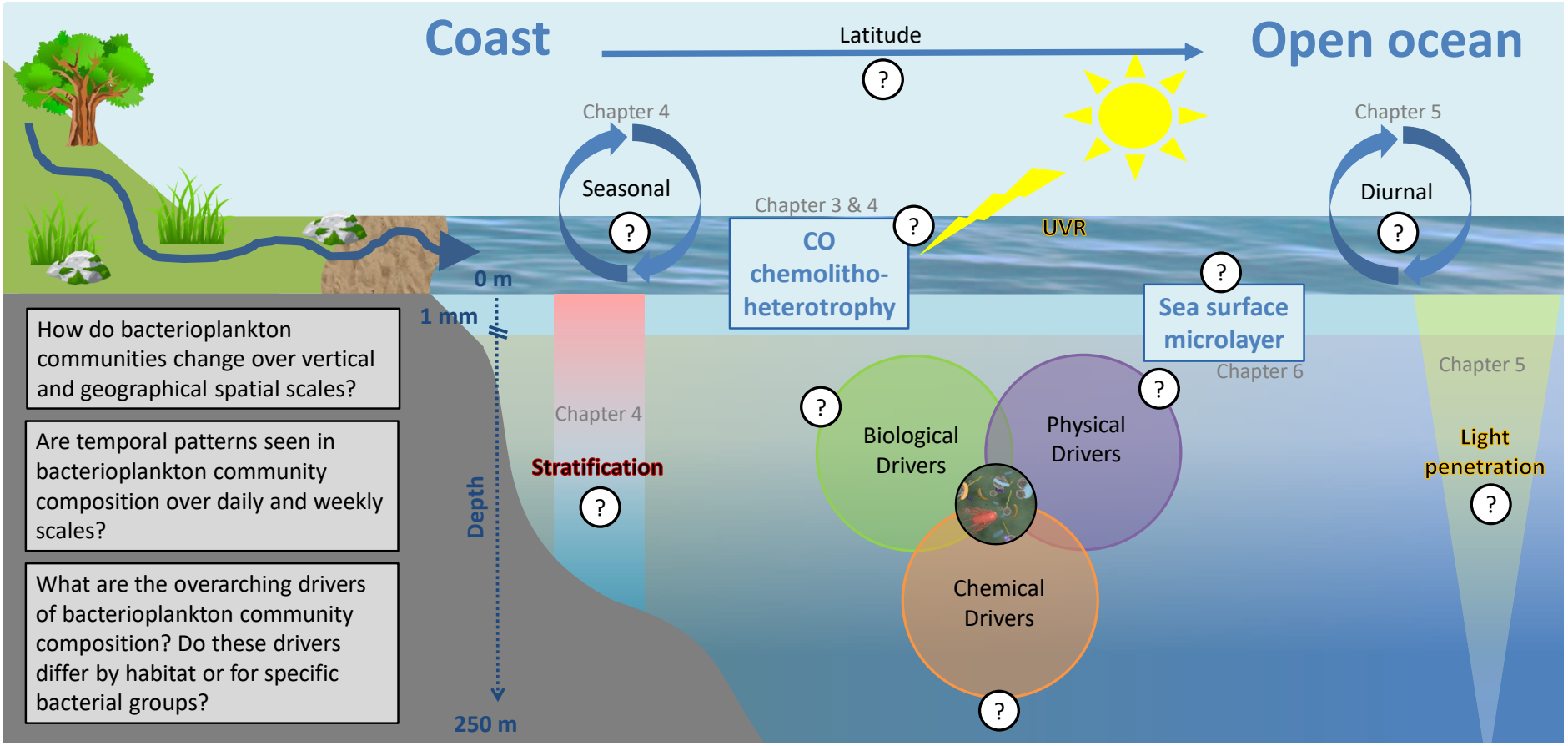

Figure 1.3. Conceptual diagram illustrating the knowledge gaps to be addressed in this thesis and how the different chapters sit together to collectively address the overarching aim to better understand how marine bacterial communities are influenced by different environmental drivers over spatial and temporal scales.

Chapter 2

Materials and Methods

2.1 Chemicals and reagents

Unless stated otherwise, all chemicals and reagents used for this research were obtained from Sigma Aldrich and Thermo Fisher Scientific.

2.2 Sterile working

Unless stated otherwise, all procedures were carried out wearing nitrile gloves on clean surfaces using sterile consumables and equipment. Clean surfaces refers to laboratory surfaces thoroughly cleaned using a chlorine disinfectant solution at 1000 ppm and/or Industrial Methylated Spirits (IMS) 70 % (v/v). Sterile refers to single use equipment certified as sterile by the manufacturer, equipment sterilised by autoclaving for 15 min at 121 °C and or by ultraviolet (UV) sterilisation for 30 min. All re-usable glass and plastic ware was washed as follows; 24 hr soak in 1000 ppm chlorine disinfectant solution, Decon®90 2 % (v/v) and hydrochloric acid solution 1 % (v/v) consecutively before being thoroughly rinsed with distilled water and dried in a drying cabinet. Equipment was scrubbed and rinsed with fresh tap water between each step.

2.2.1 Sterile working at sea

Routine cleaning was carried out between samples using IMS 70 % (v/v) for bench surfaces and pure molecular grade ethanol 99 % for filtration equipment. In addition, all surfaces and equipment were thoroughly cleaned with chlorine disinfectant solution 1000 ppm between each station. Filtration equipment was also rinsed with distilled water and covered when not in use. All work was carried out wearing nitrile gloves that were changed regularly. RNAlater® was divided into 50 mL aliquots to avoid repeated opening and potential contamination of the stock solution. Centrifuge tubes were pre-autoclaved and UV sterilised as required on board. Forceps were sterilised between each sample with pure molecular grade ethanol 99 % and flaming.

2.3 Media and solutions

All media were prepared using Milli-Q® water in sterile glassware and autoclaved for 15 min at 121 °C. Phosphate and vitamin stock solutions that could not be autoclaved were filter sterilised through a 0.2 µm sterile single use syringe filters and added to the autoclaved medium under laminar flow.

2.3.1 Half yeast, tryptone, sea salts (½ YTSS) medium

Dissolved into 1 L of water and autoclaved, final pH 7.0

- Yeast extract 2 g
- Tryptone 1.25 g
- Sea salts 20 g

2.3.2 Modified marine ammonium mineral salts (MAMS) medium

Added to 1 L of water (final volume) and autoclaved, phosphate and vitamin solutions were filter sterilised and added to cooled media after autoclaving.

- Sodium chloride (NaCl) 20 g
- Ammonium sulphate solution 10 mL
- Calcium chloride solution 10 mL
- Solution MS 10 mL
- Trace elements solution 1 mL
- Phosphate solution 10 mL
- Vitamins solution 5 mL

2.3.2.1 Trace elements solution

Dissolved into 1 L of water and autoclaved.

- Iron (II) chloride tetrahydrate ($FeCl_2$ - $4H_2O$) in 10 mL 25 % HCl 1.5 g
- Zinc chloride ($ZnCl_2$) 0.07 g
- Manganese (II) chloride tetrahydrate ($MnCl_2$- $4H_2O$) 0.1 g
- Boric acid (H_3BO_3) 0.006 g
- Cobalt (II) chloride ($CoCl_2$- $6H_2O$) 0.190 g
- Copper chloride dihydrate ($CuCl_2$- $2H_2O$) 0.002 g
- Nickel (II) chloride ($NiCl_2$- $6H_2O$) 0.024 g
- Sodium molybdate dihydrate (Na_2MoO_4 - $2H_2O$) 0.036 g

2.3.2.2 Vitamin solution

Dissolved into 1 L of water, filter sterilised and stored in the dark at 4 °C.

- Thiamine hydrochloride B1 0.010 g
- Nicotinic acid B3 0.020 g
- Pyridoxine hydrochloride B6 0.020 g
- Para-aminobenzoic acid 0.010 g
- Riboflavin B2 0.020 g
- Biotin 0.001 g
- Cyanocobalamin B12 0.001 g

2.3.2.3 Ammonium sulphate solution

Dissolved into 100 mL of water and autoclaved.

- Ammonium sulphate $(NH_4)_2SO_4$ 10 g

2.3.2.4 2 Calcium chloride solution

Dissolved into 100 mL of water and autoclaved.

- Calcium chloride ($CaCl_2$) 2 g

2.3.2.5 Solution MS

Dissolved into 100 mL of water and autoclaved.

- Magnesium sulphate heptahydrate ($MgSO_4$ - $7H_2O$) 10 g
- Iron (II) sulphate heptahydrate ($FeSO_4$ - $7H_2O$) 0.02 g
- Sodium molybdate dihydrate (Na_2MoO_4 - $2H_2O$) 0.20 g

2.3.2.6 Phosphate solution

Dissolved into 100 mL of water and autoclaved.

- Potassium di-hydrogen phosphate (KH_2PO_4) 3.6 g
- di-Potassium hydrogen phosphate (K_2HPO_4) 23.4 g

2.3.3 Phosphate buffered saline (PBS) 1 x

Dissolved into 1 L of water, pH adjusted to 7.4 with hydrochloric acid (HCl), and autoclaved.

- Sodium chloride (NaCl) 8 g
- Potassium chloride (KCl) 0.20 g
- Disodium phosphate (Na_2HPO_4) 1.44 g
- Potassium dihydrogen phosphate (KH_2PO_4) 0.24 g

2.3.4 Tris base acetic acid-EDTA (TAE) buffer 1x

50x TAE buffer concentrate (2 M Tris-Acetate, 100 mM Na-EDTA) mixed at a ratio of 1:49 with distilled water.

2.4 Bacterial strains

Table 2.1. List of bacterial strains used in this thesis.

Species	Type Strain	Genome	Source
Ruegeria pomeroyi (basonym *Silicibacter pomeroyi)*	DSS-3 DSM15171 ATCC700808	Chromosome RefSeq:NC_003911.12 INSDC:CP000031.2 Megaplasmid RefSeq:NC_006569.1 INSDC:CP000032.1	Dr Jonathan Todd, University of East Anglia, UK
Sagittula stellata	E37 DSM11524 ATCC700073	Whole Genome Shotgun RefSeq:NZ_AAYA00000000.1 INSDC:AAYA00000000.1	Leibniz Institute DSMZ-German Collection of Microorganisms and Cell Cultures, Germany

2.4.1 Routine maintenance of bacterial strains

All media and cultures were handled under a laminar flow or on occasion under flame. Roseobacter strains were routinely maintained on ½ YTSS agar and stored short term at 4 °C. For long term storage at -80 °C, glycerol stocks were prepared at a 1:1 ratio of exponential cells in ½ YTSS and 100 % glycerol (autoclaved). Flasks and plates were inoculated using sterile single use inoculation loops and incubated at 30 °C and 150 rpm in a Stuart shaking incubator (Cole-Parmer).

2.4.2 Bacterial strain purity checks

Strain purity was assessed regularly by examination at 1000x magnification using a Nikon TMS inverted phase contrast microscope (Nikon). In addition, occasional strain purity checks were performed using polymerase chain reaction (PCR) amplification and Sanger sequencing of the 16S rRNA gene (as described in section 2.15.1).

2.5 Physiological experimentation (Chapter 3)

A starting culture was prepared by inoculating 50 mL of modified MAMS supplemented with 10 mM glucose from a fresh (~3 day old) ½ YTSS plate and grown until mid-exponential phase (OD_{600} 0.5-0.8). Experimental replicates were then inoculated with 2 mL of starting culture. All experimental cultures were grown in sterile 250 mL jointed Erlenmeyer flasks containing 50 mL of the modified MAMS medium and stoppered with an air tight rubber turn-over closure stopper (Suba-Seal®). All experimental cultures were handled and incubated as described for the routine maintenance of cultures.

2.5.1 Producing carbon-starved cells

For carbon starvation experiments, the starting culture was washed twice by centrifuging for 10 min at 4000 G and 4 °C. The cell pellet was re-suspended in modified MAMS with glucose-free MAMS prior to inoculating the experimental replicates.

2.5.2 Harvesting of cells for nucleic acid and protein extraction

1 mL of culture was collected into a 1.5 mL centrifuge tube and centrifuged at 16,060 G for 20 min and the supernatant carefully removed before cell pellets were snap-frozen on liquid nitrogen and stored at -80 °C.

2.6 Addition of carbon monoxide to the culture flask headspace

Carbon monoxide (CO) was added to the flask headspace using a sterile single use syringe and needle fitted with gas tight valve. The headspace pressure was equalised by removing an equivalent volume of ambient air before adding the desired volume of 99 % pure CO (CK gases LTD). The syringe was pumped 5 times on taking up and on delivering the CO to ensure transfer of an exact volume of gas. Flasks already containing CO i.e. between

sampling time points, were allowed to vent under laminar flow for 30 min after experimental sampling before being re-stoppered and CO added to avoid an accumulation effect and to ensure a consistent starting headspace CO concentration.

2.6.1 Calculation of headspace volume

The headspace volume (290 mL) was calculated by subtracting the volume of culture (50 mL) from the total volume of the flask (less the stopper, 340 mL); the amount of CO to be added was then calculated as a percentage of the headspace volume (figure 2.1a).

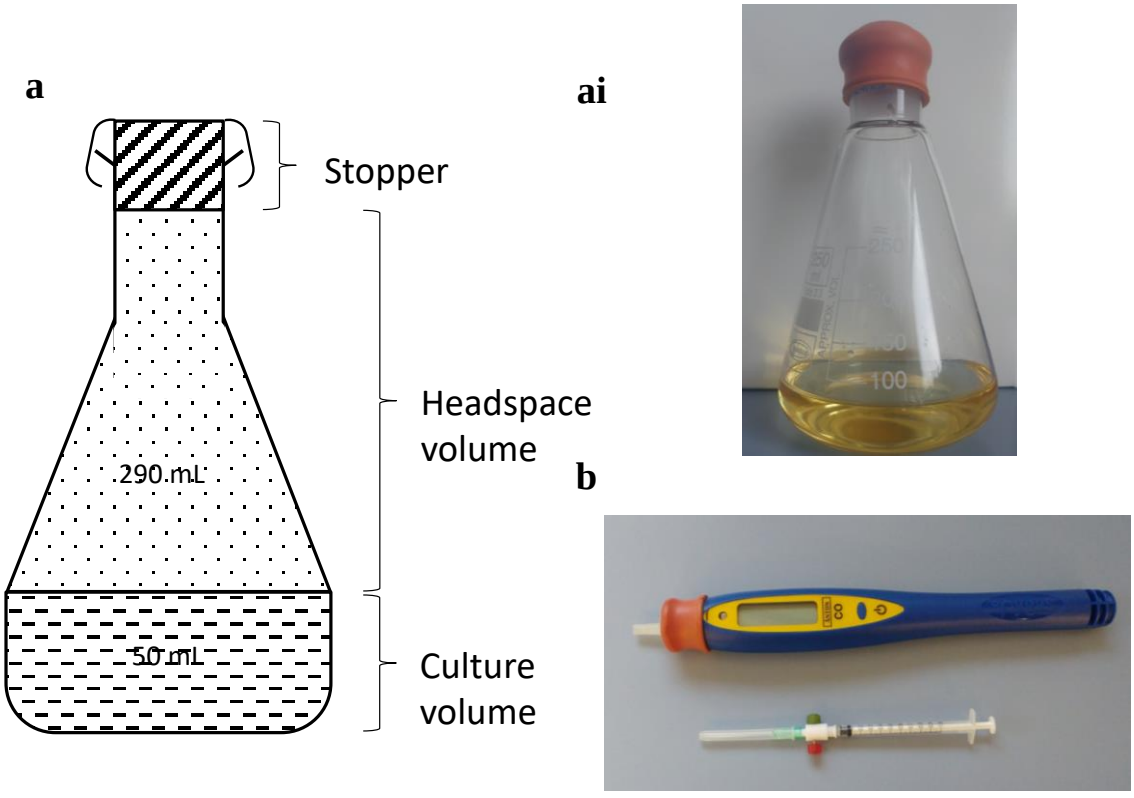

Figure 2.1. a) Diagram of experimental flask b) experimental flask and c) Carbon monoxide meter.

2.6.2 Quantification of headspace carbon monoxide concentration

Headspace CO concentration was quantified using a handheld CO meter (Anton). 0.5 mL of gas was collected from the headspace in the same manner as described previously and delivered into a rubber chamber fitted around the sensor of the meter (figure 2.1b). The sensor was vented and allowed to return to 0 between measurements.

2.7 Quantification of bacterial growth

Change in biomass (growth) was measured by optical density at 600 nm (OD_{600}). 1 mL of culture was added to a 1.5 mL BRAND® semi-micro cuvette and OD_{600} measured on an Eppendorf BioPhotometer® (Eppendorf). To keep values within a linear range, samples with OD_{600} greater than 0.6 were diluted with filter sterile PBS, the measured OD_{600} was multiplied by the dilution factor to determine the undiluted density.

2.7.1 Growth calculations

Growth rate (μ) was calculated from change in OD_{600} during the exponential growth phase (equation 1) (Widdel, 2007). Total growth (G) was calculated from the starting and the highest measured OD_{600} (equation 2) (Monod, 1978). For starvation experiments, loss of biomass was calculated using an adaption of equation 2 substituting $Biomass_{max}$ for biomass at a selected time point ($Biomass_{tx}$). Bacterial growth measurements for each treatment were averaged across biological replicates (n 4). Means of each treatment were compared using Welch's t-test performed in R version 3.2.2 (R-Core-Team, 2015).

Equation 1. Growth rate.

$$\mu = \frac{2.303(\log OD_{t2} - \log OD_{t1})}{(t_2 - t_1)}$$

Equation 2. Total growth.

$$G = Biomass_{max} - Biomass_{t0}$$

Where μ = growth rate, 2.303 = conversion to the decadic logarithm, OD_n = the OD_{600} at a given time point, t_n = time, G = total growth.

2.8 Proteomics

1 mL cell pellets were harvested for proteome analysis in parallel with the samples for DNA/RNA extraction and sent to collaborator Dr Joseph Christie-Oleza at the University of Warwick, UK, for proteome analysis. Pellets were re-suspended in 300 µl NuPAGE LDS sample buffer (Invitrogen), vortexed and incubated for 5 min at 95 °C three times. 30 µl of the sample was run on a 10 % Tris-Bis NuPAGE pre-cast gel (Invitrogen) using 3-(N-morpholino) propanesulfonic acid (MOPS) running buffer (Invitrogen). Sodium dodecyl sulphate polyacrylamide gel electrophoresis (SDS-PAGE) was performed for a short gel migration (1 cm). Polyacrylamide gel bands containing the whole cellular proteome were excised, and standard in-gel reduction with dithiothreitol, and alkylation with iodoacetamide were performed prior to trypsin (Roche) proteolysis. The resulting tryptic peptide mixture was extracted using 5 % formic acid in 25 % acetonitrile and concentrated at 40 °C in a speed-vac.

For mass spectrometry, the samples were re-suspended in 2.5 % acetonitrile containing 0.05 % trifluoroacetic acid and filtered using a 0.22 µm cellulose acetate spin column 16,000 g for 5 min in order to eliminate undissolved aggregates (Christie-Oleza et al., 2012). Samples were analysed using a nanoLC-ESI-MS/MS with an Ultimate 3000 LC

system (Dionex-LC Packings) coupled to an Orbitrap Fusion mass spectrometer (Thermo Scientific), using a 180 min LC separation on a 25 cm column and settings as previously described (Christie-Oleza et al., 2015).

Raw files were processed using the software package for shotgun proteomics MaxQuant version 1.5.5.1 (Cox and Mann, 2008) to identify and quantify proteins using the UniProt database of *R. pomeroyi* DSS-3. Samples were matched between runs. Other parameters were set by default. The list of detected peptides and polypeptides is provided in appendix 2. The bioinformatic analysis pipeline was completed using the software Perseus version 1.6.0.7 with settings as previously described (Christie-Oleza et al., 2012).

2.9 Seawater sampling

2.9.1 Sampling at the Western Channel Observatory (Chapter 4)

Seawater samples were collected during routine sampling at the Western Channel Observatory (WCO), using a 10 L Niskin bottle deployed from the stern of the vessel (figure 2.2b), with sample depth determined from meter markers along the length of the rope. 1 L samples were taken via a silicone tube into 1 L Nalgene collection bottles that were rinsed with sample water three times before sample collection. Samples were filtered immediately after collection, on occasion when the sea state was too rough, samples were stored in the dark in a cooler (4 °C) and transported back to the laboratory for processing within 4 hours of collection.

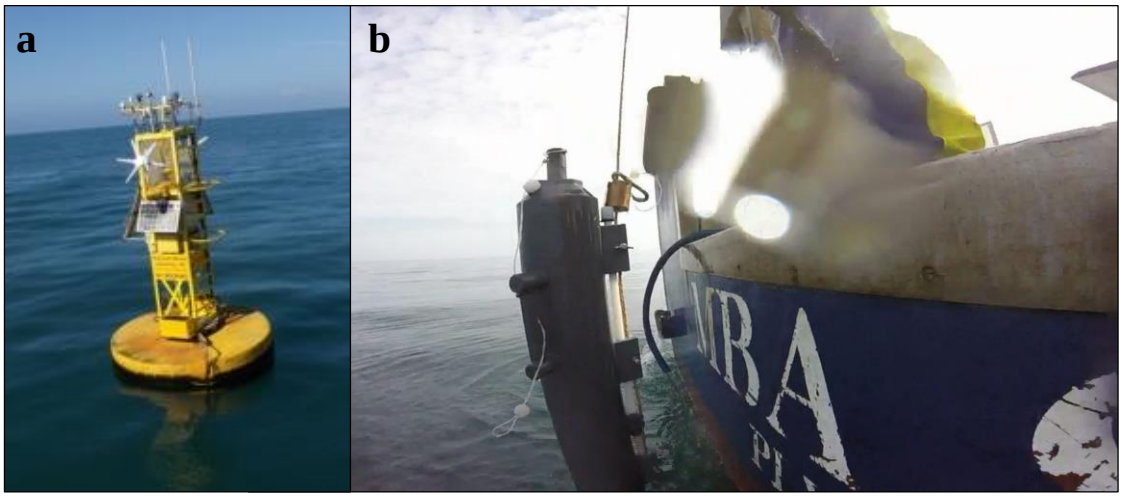

Figure 2.2. a) Station L4 buoy, b) deployment of the Niskin bottle from *R/V Sepia*.

2.9.2 Sampling during the Atlantic Meridional Transect 25 cruise (Chapter 5)

Seawater samples were collected from different light depths during routine water sampling from the *RRS James Clark Ross* during the JR15001 AMT 25 cruise (figure 2.3a). Seawater was collected into 20 L blacked-out carboys via a blacked-out silicone tubes from 20 L Niskin bottles fitted to a water sampling 24 bottle Seabird CTD (conductivity, temperature, depth) rosette system (figure 2.3b). Carboys were rinsed at least once (up to 3 times if water availability allowed) before filling. Samples were filtered immediately after collection.

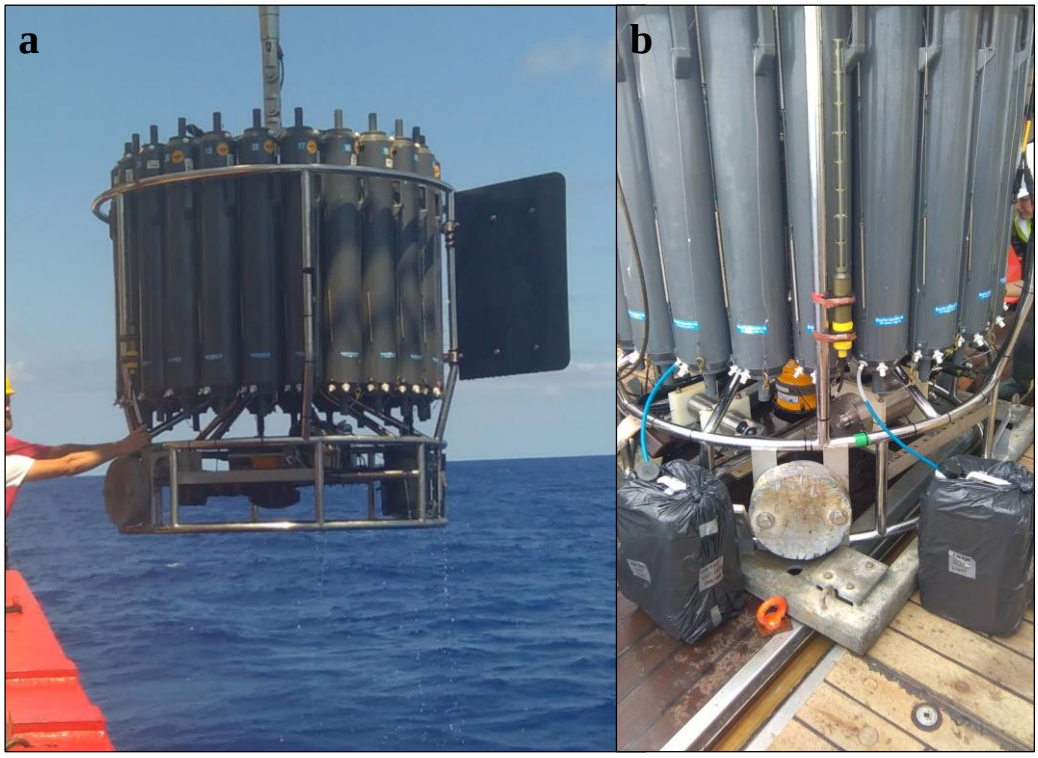

Figure 2.3. a) Water sampling carousel being recovered, b) water sampling carousel and carboys.

2.9.2.1 Calculation of light-dependent sampling depths

Light depths were calculated using the vertical diffuse attenuation coefficient (K_d) using equation 3a (see below). During noon casts, photosynthetically available radiation (PAR)

readings were taken from 5 depths spread throughout the water column and plotted as depth vs the negative natural log of PAR (figure 2.4). K_d is equal to the slope of the regression line (calculated using the least squares method) through the known data points (equation 3bi). For pre-dawn casts, light depths were calculated based on daily NEODAAS satellite images of calculated euphotic depth (Z_e) (the depth at which PAR is 1 % of the surface value) (Morel and Berthon, 1989), and K_d calculated using equation 3bii.

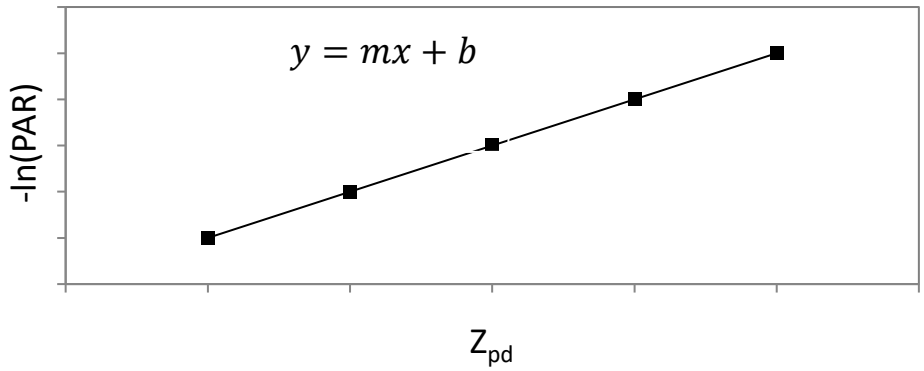

Figure 2.4. Example of known values plot (depth vs the negative natural log of PAR) with regression line and equation.

Equation 3. a) Calculation of penetration depth (Z_{pd}), b) Calculation of vertical diffuse attenuation coefficient (Kd), bi) noon CTD casts, bii) pre-dawn CTD casts.

a

$$Z_{pd} = \ln(PAR_{\%}) \times (\frac{1}{-Kd})$$

b

bi

$$Kd = \ m = \frac{y}{x + b} = \frac{-\ln(PAR)}{Z_{pd} + b}$$

bii

$$Kd = (\frac{-\ln(0.01)}{Z_e})$$

Where Z_{pd} is the penetration depth in m, $PAR_{\%}$ is the decimal percent of light at Z_{pd}, Kd is the vertical diffuse attenuation coefficient, m is the slope of the regression line, y is the -ln(PAR) y value, x is the Z_{pd} x value, b is the y-intercept and Z_e is the calculated euphotic depth.

2.9.4 Sampling during the Air to Sea cruise (Chapter 6)

All samples were collected from a workboat (6.3 m length) (figure 2.5c) that was deployed in the morning and afternoon to collect samples while drifting windward of the ship to avoid contamination or disturbance of the ocean surface by ship or other operations. All samples were collected into blacked-out polycarbonate Nalgene® bottles and stored on ice. Samples were returned to the ship within an hour of collection and filtered immediately. All sampling equipment was cleaned with 99 % pure molecular grade ethanol and rinsed 3 times with sample water prior to the collection of the actual sample. The sea surface microlayer was sampled using the glass plate method (Harvey, 1966, Cunliffe and Wurl, 2014) (figure 2.5a). A glass plate was dipped into the sea and withdrawn slowly perpendicular to the water surface (~5 cm s^{-1}). The collected microlayer was then transferred from the glass plate into the collection bottle via a funnel using a scraper. Underlying water from 1 m depth was collected using a 100 mL syringe attached to Ø12 mm silicone tube that was weighted to keep it vertical in the water column (figure 2.5b). The collected water was transferred directly to the collection bottle from the syringe.

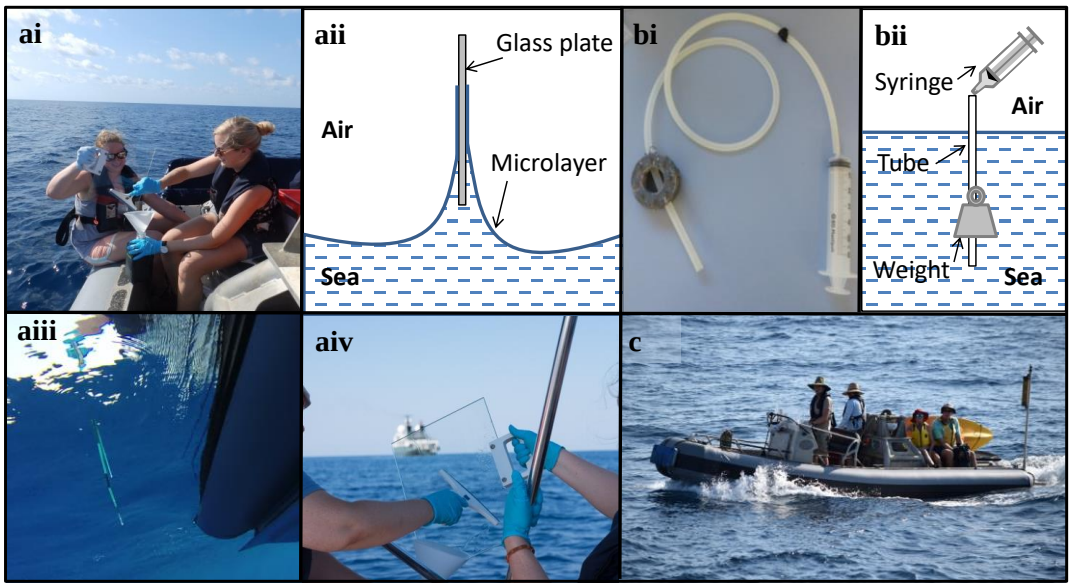

Figure 2.5. Sampling on the Air to Sea cruise. a) sea surface microlayer sample collection, ai) glass plate sampling aii) diagram of glass plate method aiii) glass plate viewed underwater aiv) sampling equipment. b) underlying water sample collection, bi) sampling equipment, bii) diagram of sampling method. c) workboat.

2.10 Seawater filtration

Seawater samples were filtered through sterile 0.2 µm cellulose nitrate membrane filters (Whatman) using a 6 funnel filter manifold and vacuum pump (figure 2.6). Using sterile forceps, membranes were carefully rolled and transferred to a sterile 2 mL centrifuge tube containing 1 mL of RNAlater® (Sigma) and immediately stored at -80 °C. For samples taken at the WCO (Chapter 4), no preservative was added. Samples were kept on dry ice and stored at -80 °C on return to the laboratory (within 4 hours of collection).

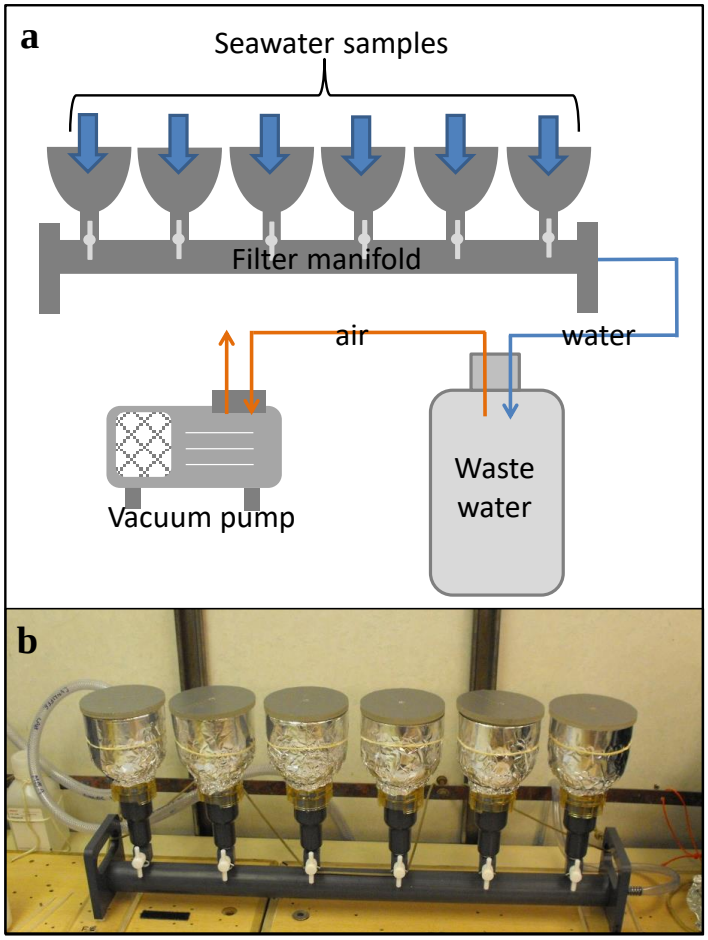

Figure 2.6. Filtration of environmental samples, a) diagram of filtration system, b) filter manifold.

2.11 Environmental metadata

Environmental metadata were available from collaborators and/or open access sources. The sources and details of these data are fully disclosed (appendix 3).

2.11.1 Metadata used in Chapter 4

Quality controlled physicochemical and biological metadata used in Chapter 4 were collected during routine sampling at Station L4 and Station E1 by the *R/V Plymouth Quest* and accessed via the WCO data repository (www.westernchannelobservatory.org.uk, 2011).

Meteorological metadata were recorded by a local weather station in Plymouth and accessed from (www.bearsbythesea.co.uk, 2018). For statistical analyses, only the metadata that corresponded to bacterial diversity water sampling dates (table 2.2) were used. Phytoplankton and microzooplankton counts at 10 m were assumed for all bacterial diversity sample depths.

Table 2.2. Water and metadata sampling dates for Chapter 4. ✓ denotes data collected concurrently with water samples, not available (NA) denotes missing data and dates indicate alternative sampling date.

Station	Water Sample	CTD data	Phytoplankton & microzooplankton	Meteorological	Nutrients
L4	10/03/2015	✓	✓	✓	✓
L4	23/03/2015	✓	✓	✓	✓
L4	07/04/2015	✓	✓	✓	✓
L4	20/04/2015	✓	✓	✓	✓
L4	07/05/2015	✓	✓	NA	✓
L4	20/05/2015	✓	✓	✓	✓
L4	03/06/2015	✓	✓	✓	✓
L4	15/06/2015	✓	✓	✓	✓
L4	29/06/2015	✓	✓	✓	30/06/2015
L4	30/07/2015	28/07/2015	28/07/2015	✓	28/07/2015
E1	10/03/2015	✓	✓	✓	✓
E1	25/03/2015	✓	✓	✓	✓
E1	09/04/2015	✓	✓	✓	NA
E1	24/04/2015	✓	30/04/2015	✓	30/04/2015
E1	08/05/2015	NA	NA	NA	NA
E1	21/05/2015	NA	✓	✓	✓
E1	05/06/2015	04/06/2015	04/06/2015	✓	04/06/2015
E1	16/06/2015	✓	✓	✓	✓
E1	29/06/2015	01/07/2015	01/07/2015	✓	01/07/2015
E1	30/07/2015	✓	✓	✓	✓

2.11.1.1 Metadata provided by the Western Channel Observatory

Depth resolved physicochemical data were collected using sensors attached to a sampling rosette. Seawater temperature and salinity were measured using a SeaBird SBE 19+. Fluorescence was measured using a Chelsea Technologies MINITracker and oxygen

measured using a SeaBird 43 Dissolved Oxygen sensor. Samples for phytoplankton and microzooplankton enumeration were collected from 10 m depth using a 10 L Niskin bottle and analysed as described in (Widdicombe et al., 2010). Samples for depth resolved nutrient quantification were also collected using a 10 L Niskin bottle and analysed according to the standard WCO protocol (appendix 4).

2.11.1.2 Metadata provided by the Plymouth weather station Bearsbythesea

Local weather data were collected using a Davis Vantage Pro2+ weather station and processed using Weather Display Software. Data were accessed via (www.bearsbythesea.co.uk, 2018).

2.11.2 Metadata used in Chapter 5

All metadata used in Chapter 5 are available through the Natural Environment Research Council (NERC) British Oceanographic Data Centre (BODC). Metadata were collected routinely during the AMT25 and processed at BODC (see BODC (2015) cruise JR15001 (AMT, JR864). The data presented in Chapter 5 includes all data from the upper 250 m over the entire transect (physicochemical = 1455 data points from 74 casts, nutrient = 888 data points from 70 casts). For statistical analysis, only data from the corresponding bottle (physicochemical) or equivalent depth (nutrients) to the nucleic acid samples were used.

2.11.2.1 Physicochemical metadata collected during the Atlantic Meridional Transect

The physicochemical data provided were taken from sensor readings at the depth from which the water sample was taken, where there were multiple sensors for a variable an average reading was taken. Temperature and salinity were measured using a Sea-Bird SBE 911plus CTD, dissolved oxygen was measured using a Sea-Bird SBE 43 dissolved oxygen sensor, fluorescence was measured using a Chelsea Technologies Group Aquatracka III fluorometer and PAR was measured using a Biospherical QCD-905L underwater PAR sensor. CTD casts were recorded using the Sea-Bird data collection software Seasave-Win32. The software

outputs were then processed following the BODC recommended guidelines using SBE Data Processing-Win32 v7.23.2. Additional water samples were collected from each cast to measure salinity (bench salinometer), chlorophyll-a (filtration, acetone extraction and fluorometer measurement) and oxygen (Winkler titration) in order to calibrate the respective sensor values. The method used for calibration was to generate an offset between the discrete water sample measurement and the nominal value from the sensor. The offsets were then plotted against the discrete sample values and a linear regression applied. Where the regression was significant the calibration equation was derived, where the regression was not significant the mean value of the offset was applied.

2.11.2.2 Nutrient metadata collected during the Atlantic Meridional Transect

Seawater samples for micro-molar nutrient measurements were taken from CTD bottle samples at every depth from each CTD cast. Samples were collected into acid-cleaned 60 ml high-density polyethylene (Nalgene) sample bottles and analysed on a 4-channel Bran and Luebbe AAIII segmented flow autoanalyser. The analytical chemical methodologies used were according to Brewer and Riley (1965) for nitrate, Riley (1977) for nitrite and Kirkwood (1989) for phosphate and silicate.

2.11.2.2 Microbial phytoplankton abundance metadata collected during the Atlantic Meridional Transect

Seawater samples from 200 m to the surface were collected in clean 250 mL polycarbonate bottles from each CTD cast. Samples were stored in a refrigerator and analysed within 3 hours of collection. Fresh samples were measured using a Becton Dickinson FACSort flow cytometer which characterised and enumerated *Prochlorococcus* sp. and *Synechococcus* sp. (Cyanobacteria) and eukaryotic phytoplankton, based on their light scattering and autofluorescence properties. The flow rate of the flow cytometer is calibrated by analysing

samples of Ø3.6 µm fluorescent microspheres (Beckman Coulter Flowset fluorescent microspheres) at a known concentration for a set length of time.

2.11.3 Metadata used in Chapter 6

2.11.3.1 Metadata provided by the Sea Surfaces Group at the Institute for Chemistry and Biology of the Marine Environment (ICBM), Carl von Ossietzky University of Oldenburg

The Sea Surface Scanner (SSS) is a remote controlled automated rotating glass disc sampler fitted with a suite of *in situ* sensors for measuring biogeochemical parameters (figure 2.7). pH, seawater temperature, chromophoric dissolved organic matter (FDOM) and salinity were measured in the sea surface microlayer (SML) and underlying water (ULW) (1 m) by on board sensors and calibrated as described in Ribas-Ribas et al., (2017). Chlorophyll derived from fluorescence was measured in the ULW by on board sensors and calibrated against discrete chlorophyll measurements. Air temperature, relative humidity, wind speed, UV and solar radiation were measured in the atmosphere by sensors at a height of 3 m fitted to the SSS mast (Ribas-Ribas et al., 2017). Details of the on-board sensors including manufacturers and specifications can be found in appendix 1, for further detail see Ribas-Ribas et al., (2017). Discrete SML and ULW samples were also taken for surface active substances (SAS), (a substance that lowers the surface tension of the liquid in which it is dissolved, also known as surfactants), and chlorophyll from the SSS bottle samples. SAS were measured using phase-sensitive alternating voltammetry (Model VA 747, Metrohm) with a hanging mercury drop electrode according to Ćosović and Vojvodić (1998). Unfiltered samples (10 mL) were measured three to four times using a standard addition technique, where the non-ionic surfactant Triton X-100 was used as a standard. Concentration of SAS was expressed as the equivalent concentration of Triton X-100 (Teq) (Wurl et al., 2009). Chlorophyll-a was measured using the method described by Arar and Collins (1997). The partial pressure of carbon dioxide (pCO_2) was measured using an

infrared gas analyser (IRGA) (SubCtech OceanPackTM, LI-COR LI-840x) fitted to an autonomous, drifting buoy with a floating chamber (Ribas-Ribas et al., 2018). The IRGA was calibrated using 5 CO_2 gas standards before and after sampling (accuracy better than 1.5%) (Ribas-Ribas et al., 2018). *p*CO2 flux was calculated based on the positivity or negativity of the slope ($dpCO_2/dt$) according to the equations as described in Ribas-Ribas et al., (2018), only flux values with an r^2 value greater than 0.95 were included in the dataset. The SSS and autonomous drifting buoy were usually deployed between 23:00 and 06:00 UTC. For statistical analysis with bacterial diversity data, the mean at each sampling station was determined for AM and PM sampling efforts and was defined as all data recorded before (AM) or after (PM) 12 noon (02:30 UTC at coastal stations and 02:00 UTC at oceanic stations).

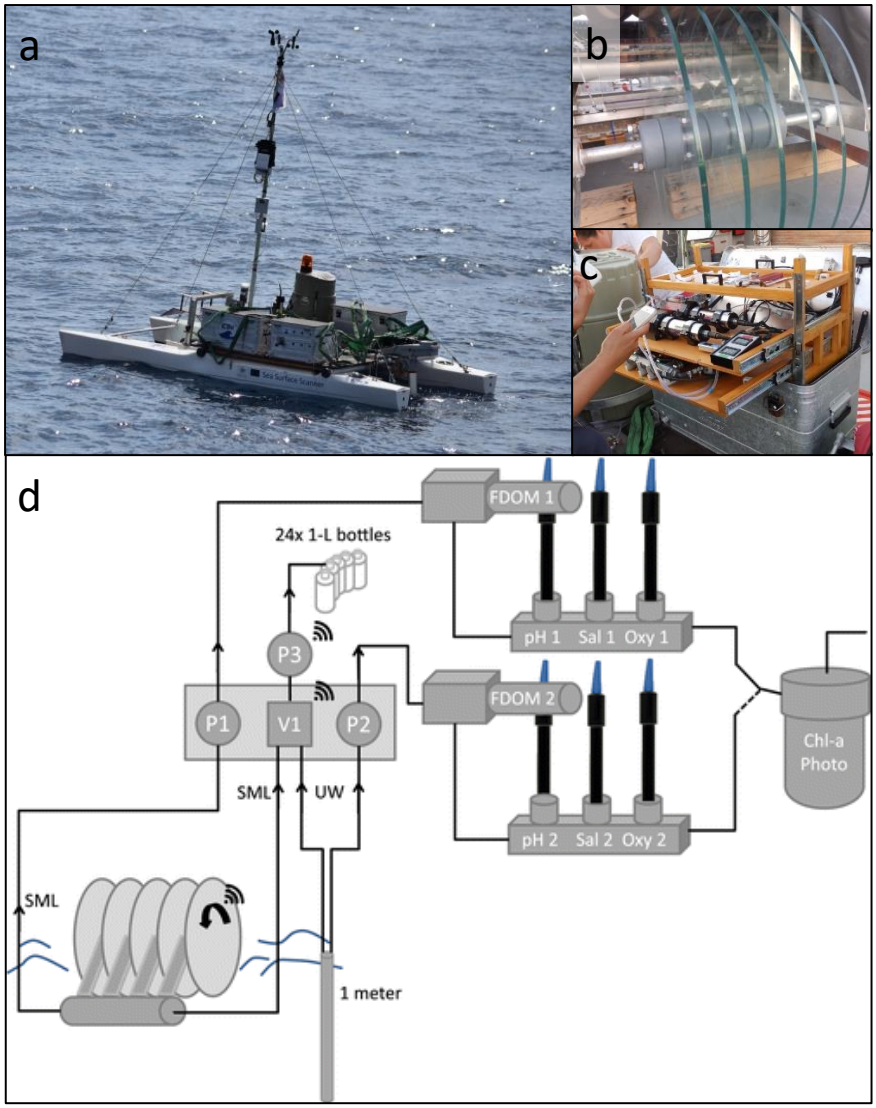

Figure 2.7. a) Sea surface scanner (SSS), (b) rotating glass discs onto which the sea surface microlayer (SML) is collected, c) on-board flow-through system, d) schematic view of the flow-through system with pumps (P1–P3), valves (V1), and sensor technology to measure salinity (Sal), pH, oxygen (Oxy), FDOM, Chl-a, and photosynthetic parameters (Photo) from Ribas-Ribas et al., (2017).

2.11.3.2 Data provided by the Zappa Group at the Lamont-Doherty Earth Observatory, Columbia University

Underway meteorological, navigational and physical measurements were recorded by the *R/V Falkor* on-board scientific computer system. Wind stress measurements were estimated from underway data using the algorithms defined in (Edson et al., 2013). For statistical analysis with bacterial diversity data, the mean was calculated for all data recorded 1 hour prior to, and during the collection of water samples for bacterial diversity.

2.11.3.3 Data provided by the Landing Group at the Department of Earth, Ocean and Atmospheric Science, Florida State University

Seawater samples were collected for the determination of particulate and dissolved trace metals from the SML (~50 µm thickness) and ULW (~30 cm depth) using a cylinder of pure quartz deployed from a plastic kayak (Ebling and Landing, 2015). 1 L of each sample was collected and immediately filtered onto 0.2 µm polycarbonate membranes on return to the ship's lab. The filters were frozen at -20 °C, and the filtrate acidified with 0.024 M HCl, for storage. On return to the home laboratory, the particulate material on the filter was digested using a strong acid digestion (Morton et al., 2013). Dissolved trace metals were extracted from the seawater matrix and pre-concentrated on to a Toyopearl AF-Chelate-650M chelating resin, (Tosoh Bioscience) (Milne et al., 2010). Particulate and dissolved trace metals were determined by high resolution magnetic sector field Element 2™ ICP-MS (Thermo-Fisher) at the National High Magnetic Field Laboratory at Florida State University.

2.12 DNA extraction using the DNeasy Blood and Tissue kit

DNA was extracted using the DNeasy Blood and Tissue Kit (Qiagen) following the manufacturer's protocol. A lysis mix containing 600 µL lysis buffer (DNeasy) and 10 µL of proteinase K (DNeasy) was added to the samples. The samples were prepared according to the sample type; for bacterial cells see (2.12.1) for seawater see (2.12.2). DNA was eluted for 5 min at room temperature in 100 µL of elution buffer (DNeasy) pre-heated at 40 °C.

2.12.1 Preparation of harvested bacterial cells for DNA extraction with the DNeasy Blood and Tissue kit (general use)

Frozen harvested cell pellets were thawed on ice and homogenised in the DNeasy lysis mix by vortexing before being incubated at 56 °C for 10 min. All of the lysate was then transferred to the DNeasy extraction column.

2.12.2 Preparation of filter membranes (seawater samples) for DNA extraction with the DNeasy Blood and Tissue kit

For the transfer and dissection of membranes, forceps and scalpels were sterilised between each use with ethanol and by flame. Mechanical homogenisation with FastPrep® Lysing Matrix B (2 mL matrix tubes containing 0.1 mm silica spheres) (MP Biomedicals) was performed in a Mini-BeadBeater-8 (BioSpec) for 2 min on maximum speed.

2.12.2.1 Preparation of seawater samples collected at the Western Channel Observatory (Chapter 4)

Frozen membranes were transferred directly to a FastPrep® Lysing Matrix B tube with the DNeasy lysis mix and homogenised mechanically. Homogenised samples were incubated at 56 °C for 10 min before being centrifuged for 1 min at 16,060 G, the lysate was recovered and transferred to the DNeasy extraction column by pipette.

2.12.2.2 Preparation of surface microlayer and underlying seawater samples collected during the Air to Sea cruise (Chapter 6)

Frozen membranes were thawed on ice and transferred ensuring minimal carryover of RNAlater® to sterile petri dishes. To maximise the lysis of the small amount of material collected, membranes were un-rolled and cut using a sterile scalpel into ~12 pieces. The dissected membranes were then transferred to sterile FastPrep® Lysing Matrix B tubes with the DNeasy lysis mix and homogenised mechanically. Homogenised samples were incubated at 56 °C for 10 min before being centrifuged for 1 min at 16,060 G the lysate was recovered and transferred to the DNeasy extraction column by pipette.

2.13 Simultaneous extraction of DNA and RNA using the E.Z.N.A. DNA/RNA isolation kit

RNA and DNA were extracted simultaneously from the lysate (prepared according to the sample type), using the E.Z.N.A. DNA/RNA isolation kit (VWR) following the manufacturers protocol. An on column DNase digestion step using the RNase-Free DNase set (VWR) was also performed according to the manufacturer's protocol. RNA and DNA were eluted for 5 min at room temperature in 40 µL of DEPC treated water (EZNA) pre-heated to 70 °C and 40 µL of elution buffer (EZNA) pre-heated to 40 °C respectively.

2.13.1 Lysis of harvested Ruegeria pomeroyi DSS-3 cells for use with the E.Z.N.A. DNA/RNA isolation kit (Chapter 3)

Frozen harvested cell pellets were thawed on ice and with 350 µL GTC lysis buffer (EZNA) containing 20 µL mL^{-1} of 2-mercaptoethanol added. Cell pellets were homogenised in the lysis buffer by vortexing. All of the lysate was then transferred to the DNeasy extraction column.

2.13.2 Lysis of seawater samples for use with the E.Z.N.A. DNA/RNA isolation kit (Chapter 5)

Membranes were thawed on ice and transferred ensuring minimal carryover of RNAlater® to sterile 2 mL FastPrep® Lysing Matrix B tubes. Membranes were snap frozen with liquid nitrogen and broken up using a sterile pellet pestle (Sigma). 700 µL of GTC lysis buffer (EZNA) containing 20 µL mL^{-1} of 2-mercaptoethanol was added and the membranes homogenised mechanically using a Mini-BeadBeater-8 (BioSpec, US) for 3 min at maximum speed. Matrix tubes were then centrifuged for 1 min at 16,060 G, the lysate was recovered and transferred to the EZNA DNA extraction column by pipette.

2.14 PCR primers

2.14.1 qPCR primer design

Functional gene qPCR primers specific to *R. pomeroyi* DSS-3 were designed from the DSS-3 genome (table 2.3) (Moran et al., 2004). Primers coxL-2F and coxL-2R were selected by hand using the genome viewing software Artemis (Wellcome Sanger Institute) and were donated to me by Simone Payne, from the University of East Anglia, UK. Primer sets pyrGPOMF and pyrGPOMR, and rpoBPOMF and rpoBPOMR were selected using Primer-BLAST (Ye et al., 2012). Primers were verified by PCR with *R. pomeroyi* DSS-3 genomic DNA and Sanger sequencing.

2.14.2 coxL Form I primer design for high-throughput sequencing

The amplicon length (1200 bp) of the combined OMPF and OBR primer set was not suitable for high-throughput sequencing on an Illumina platform; therefore, a new reverse primer was designed. Based on the original King (2003) literature, known *coxL* Form I sequences representing a range of bacterial orders (*Rhodobacterales*, *Rhizobiales*, *Burkholderiales*, *Actinobacteria* and *Bacillales*) were selected from GenBank (figure 2.8b). An alignment

(figure 2.8a) was made and the OMPF forward primer sequence was identified. Conserved regions ~400-600 bp from the forward primer were identified as potential new reverse primers. A 100 % conserved region was not found, however relatively conserved regions were identified (~60 %). These regions were scanned for homologous and heterologous bases; degenerate bases were called if more than two bases at that position were heterologous. Only degenerate bases representing two bases were allowed, for heterologous positions containing more than two different bases, a base was called according to the most abundant two bases. Potential new reverse primers were paired with OMPF and verified by PCR with a range of bacterial genomic DNA samples and Sanger sequencing. After verification the new reverse primer NGSR was selected (figure 2.8a).

The length of the amplicon (~650 bp, which increased to ~800 bp with the addition of adapter sequences) would not be suitable for paired end sequence analysis. A phylogenetic tree was constructed from the alignment to confirm if the forward reads (~250 bp) alone would be able to resolve taxonomy to a suitable level (appendix 5). Comparison of the tree with the original alignment (1200 bp) (figure 2.8) suggested some taxonomic resolution would be achievable using unpaired reads.

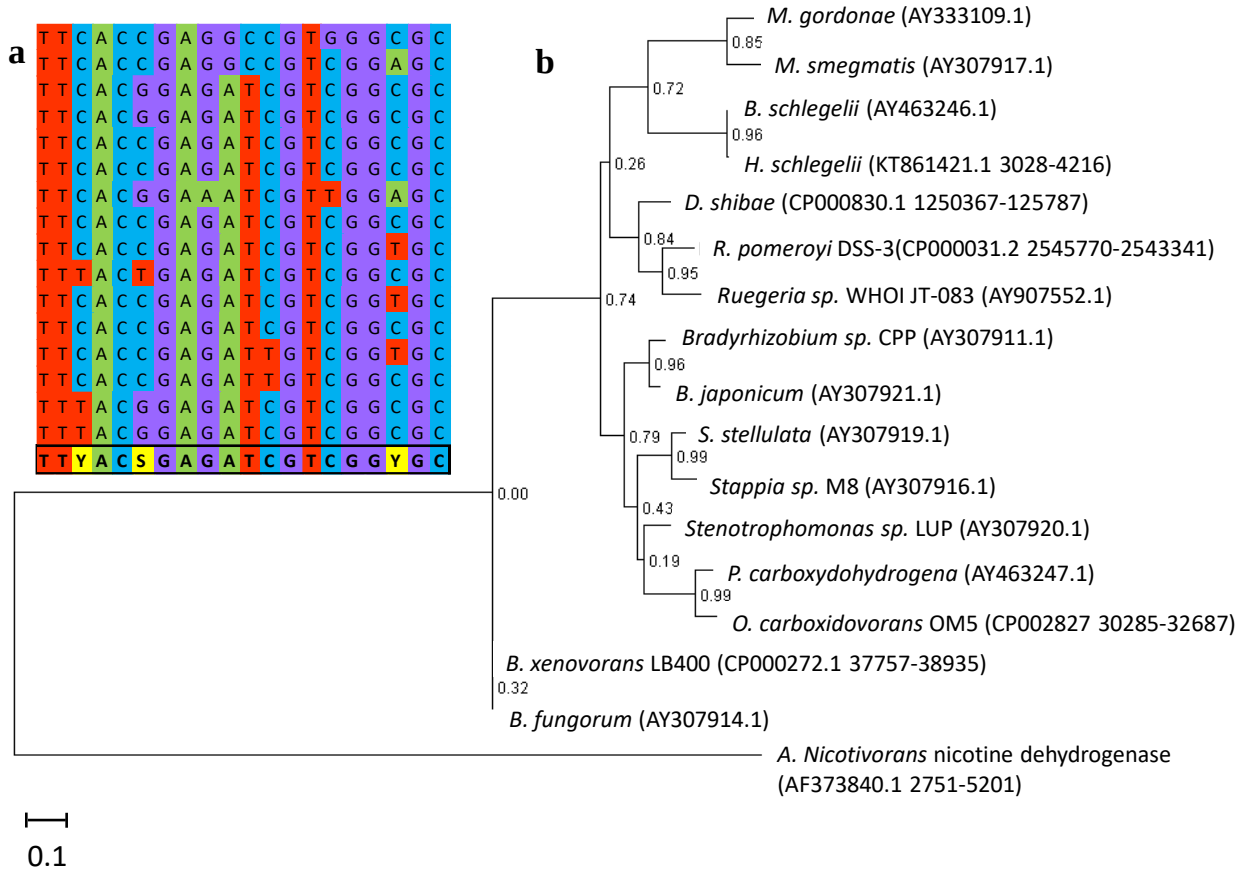

Figure 2.8. a) Region of the aligned *coxL* Form I sequences corresponding to the new primer NGSR. b) Maximum Likelihood analysis (1000 bootstrap replications) of aligned *coxL* Form I sequences (1200 bp) used for the design of primer NGSR.

Table 2.3. Sequences of the primer pairs used in this study.

Name (direction)	Use (size)	Target gene	Target gene product	Sequence	Reference	Anne-aling temp.
OMPF (forward)	PCR (1200 bp)	*coxL* Form I	carbon monoxide dehydrogenase (CODH)	GGCGGCTTYGGSAASAAGGT	(King, 2003)	58 – 62 °C
BMSF (forward)		*coxL* Form II		GGCGGCTTYGGSTCSAAGAT		
OBR (reverse)		*coxL* Form I & II		YTCGAYGATCATCGGRTTGA		
coxL-2F (forward)	qPCR (120 bp)	DSS-3 *coxL* Form I		CTGACGGCCAAGGATCTG	Simone Payne (UEA)	59 °C
coxL-2R (reverse)				GCCACACAAAGGCTACTTC		
OMPF/SEQ (forward)	HTS (650 bp)	*coxL* Form I		TCGTCGGCAGCGTCAGATGTGTATAAGAGACAG-A-NNNHNN NW NNNH-GGCGGCTTYGGSAASAAGGT	Adapted from (King, 2003)	56 °C
NGSR/SEQ (reverse)				GTCTCGTGGGCTCGGAGATGTGTATAAGAGACAG-T-GCRCCGACGATCTCSGTRAA	This study, Chapter 4	
27F (forward)	PCR (1465 bp)	16S rRNA	16S ribosomal RNA	AGAGTTTGATCMTGGCTCAG	(Lane, 1991)	55 °C
PROK 1492R (reverse)				GGWTACCTTGTTACGACTT	(Suzuki et al., 2000)	
pyrGPOMF (forward)	qPCR (120 bp)	DSS-3 *pyrG*	CTP synthase (NH_3, glutamine)	CCTCGGCGATCGACTTGTAG	This study, Chapter 3	59 °C
pyrGPOMR (reverse)				CGGACCTGACCAAATGGGAG		
rpoBPOMF (forward)		DSS-3 *rpoB*	β subunit of bacterial RNA polymerase	ATAGATGTCCATGAGCGCGG		
rpoBPOMR (reverse)				AACGGCGTCACCAATATCCC		

2.15 Quantification of nucleic acids and manipulation techniques

Routine nucleic acid quantification was carried out spectrophotometrically using a NanoDrop® ND-1000 (Thermo Scientific). Nucleic acids that were to be used for downstream analysis such as reverse transcription, sequencing and qPCR were also quantified fluorescently using the QuantiFluor® dsDNA System or QuantiFluor® RNA System (Promega) for DNA and RNA respectively.

2.15.1 Polymerase chain reaction (PCR)

Routine PCR was performed in 25 or 50 µL volumes in a Mastercycler™ Nexus Gradient (Eppendorf) or a Gradient Palm-Cycler™ CG1-96 (Corbett Life Science Pty. Ltd., AU) thermo cycler using GoTaq® Flexi DNA Polymerase (Promega). A typical reaction would contain a final concentration of 0.2 µM of each forward and reverse primer, 2 mM of MgCl, 1.25 u GoTaq®, x1 GoTaq® Flexi Buffer and 0.2 mM of each dNTP and up to 0.5 µg DNA. For *coxL* amplification using OMPF/BMSF and OBR or OMPF/SEQ, and NGSR/SEQ, bovine albumen serum (BSA) was added at a final concentration of 0.1 µg μL^{-1}.

2.15.2 DNA purification

PCR products were purified and cleaned using the GenElute™ PCR Clean-Up Kit (Sigma) according to the manufacturer's protocol.

2.15.3 Agarose gel electrophoresis

Typically, 5 µL of PCR product (plus an equal volume of loading dye such as Orange G if required) was loaded onto a 1.5 % (w/v) agarose gel containing ethidium bromide (0.4 µg mL^{-1}) in 1 x TAE buffer. HyperLadder™ 50 bp DNA ladder (Bioline) was used to estimate DNA fragment size. Gels were run for 40 min at 110 v and imaged on a G:Box image analyser (Syngene).

2.15.4 Reverse transcription (RT)

RNA was reverse transcribed using the Omniscript RT Kit (Qiagen) according to the manufacturer's protocol. Final reaction volumes were 15 µL for *Ruegeria pomeroyi* RNA (Chapter 3) or 10 µL for seawater RNA (Chapter 5) see table 2.4 for reaction mixes. Primers pyrGPOMR, rpoBPOMR or coxL-2R were used for the reverse transcription of RNA from *Ruegeria pomeroyi* and primer PROK1492R was used for the reverse transcription of RNA from seawater (table 2.3). RNA was thawed on ice and denatured in RNase-free water for 5 min at 60 °C prior to the addition of the reaction master mix. Reactions were then incubated at 37 °C for 60 min (seawater RNA) or 90 min (cell pellet RNA).

Table 2.4. Reverse transcription reaction mixes.

Component	Final concentration per reaction	
	RNA from cell pellets (Chapter 3)	RNA from seawater (Chapter 5)
Buffer RT (10 x)	1 x	1 x
dNTPs (5 mM each)	0.5 mM each	0.5 mM each
Gene specific reverse primer (10 µM)	1 µM	1 µM
Omniscript reverse transcriptase (4 units per µL)	0.2 units per µL	0.2 units per µL
Target RNA	50 ng (total)	200 ng (total)
RNase free water	Up to 15 µL	Up to 10 µL

2.16 Quantitative PCR (qPCR)

qPCR amplifications were performed with three technical replicates using SensiFAST™ SYBR® No-ROX Kit (Bioline). Reactions contained a final concentration of 1 x SensiFAST SYBR® No-ROX Mix, 0.3 µM of both the forward and reverse primers, 4 µL of cDNA as template and made up to a final volume of 10 µL using molecular grade water. 3 step cycling

was performed with a Rotor-Gene Q3000 (Qiagen) cycling conditions were; 95 °C for 30 s, 40 cycles of denaturation 95 °C for 10 s, annealing 59 °C for 15 s and extension 72 °C for 20 s followed by melt curve analysis from 72 °C to 95 °C.

2.16.1 Reference genes

To validate the effect of the CO treatment (Chapter 3) on the transcription of the target gene *coxL*, reference 'housekeeping' genes *rpoB* (β subunit of bacterial RNA polymerase) and *pyrG* (cytidine triphosphate (CTP) synthase) were chosen (Rocha et al., 2015). The reference genes act as an internal control to determine a normal expression level for each sample irrespective of the treatment.

2.16.2 qPCR standards

Non-degenerate gene specific primers were used to target the *Ruegeria pomeroyi* DSS-3 *coxL* Form I, *rpoB* and *pyrG* genes (table 2.3). qPCR standards were created from a dilution series of purified amplicon DNA. PCR was performed in duplicate with 20 ng of *R.pomeroyi* DSS-3 genomic DNA as a template and amplification confirmed by electrophoresis. PCR products were then pooled, purified and quantified fluorescently. Gene copy number was determined using equation 4.

.

Equation 4. Equation to calculate gene copy number.

$$number\ of\ copies = \frac{ng\ \times (6.022 \times 10^{23})}{molecular\ mass\ \times (1 \times 10^{9})}$$

Where ng = ng of DNA, 6.022×10^{23} = Avogadro's number, molecular mass = molecular mass of the DNA and 1×10^{9} = conversion to ng.

2.16.3 Relative quantification of qPCR data

Threshold (C_t) values and gene transcript copy numbers were determined from the standard curve of the qPCR standard dilution series using the Rotor-Gene Q Series Software version 2.3.1 (Qiagen). The ratio of *coxL* gene transcription in the treatment vs the control was calculated using the $\Delta\Delta C_t$ method (Livak and Schmittgen, 2001) and normalised to the reference genes *pyrG* and *rpoB* (equation 5). Pair-wise fixed reallocation randomisation tests (n 2000) were performed using REST 2009 software version 2.0.13 (Pfaffl et al., 2002). Calculated *coxL* copy number for each sample was normalised to the reference genes by dividing by a normalisation factor. The normalisation factor for each sample was calculated by dividing the geometric mean of the reference gene copy numbers by their grand geometric mean for each experimental time point (table 2.5).

Equation 5. Calculation of transcription fold change using the ΔΔCT method.

$$\Delta Ct_{exp} = (Ct_{GOI} - Ct_{REF})$$

$$\Delta Ct_{con} = (Ct_{GOI} - Ct_{REF})$$

$$\Delta\Delta Ct = \left(\Delta Ct_{exp} - \Delta Ct_{con}\right)$$

$$Fold\ change = 2^{-(\Delta\Delta Ct)}$$

Where Ct = threshold values, exp = form experimental treatment, con = from control treatment, GOI = gene of interest and REF = reference gene (or the mean of reference genes if multiple).

Table 2.5. Calculation of normalisation factors for calculated gene copy number.

Sample	Ref gene 1 (Xa)	Ref gene 2 (Xb)	Geo mean (GM)	Normalisation factor (NF)
Sample 1	Xa^1	Xb^1	GM^1	$NF^1 = GM^1 / GGM$
Sample 2	Xa^2	Xb^2	GM^2	$NF^2 = GM^2 / GGM$
Sample 3	Xa^3	Xb^3	GM^3	$NF^3 = GM^3 / GGM$
	Grand geomean (GGM)		GGM	

Sample	Gene of interest copy No. (N)	Normalised copy no.
Sample 1	N^1	N^1 / NF^1
Sample 2	N^2	N^2 / NF^2
Sample 3	N^3	N^3 / NF^3

2.17 Sequencing

For general purposes such as strain and primer target verification, purified amplicons were Sanger sequenced by Source BioScience in Rochdale, UK, following their standard protocol. Samples are prepared using the Applied Biosystems™ Big Dye® Terminator kit, v3.1 (Thermo fisher), purified using a magnetic bead clean-up process and sequenced on an Applied Biosystems™ 3730xl DNA Analyser (Thermo fisher). DNA sequences were examined in Chromas (Technelysium Pty LTD) and verified using the National Center for Biotechnology Information (NCBI) basic local alignment search tool (BLAST) (Altschul et al., 1990).

2.17.1 High-throughput sequencing: bacteria 16S rRNA encoding genes

Bacterial 16S rRNA gene library preparation and sequencing were performed at the Integrated Microbiome Resource (IMR) at the Centre for Comparative Genomics and Evolutionary Bioinformatics (CGEB) (Dalhousie University, CA) as described by (Comeau

et al., 2017). DNA samples were PCR amplified and barcoded using gene specific fusion primers, the V4-V5 region of the bacterial 16S rRNA gene was targeted using primer set 515F and 926R (Walters et al., 2016) with the addition of an Illumina Nextera adapter and indices. Amplicons were then verified, cleaned and normalised before being pooled to produce the sample library which was sequenced using the Illumina MiSeq platform.

2.17.2 High-throughput sequencing: bacterial coxL Form I (coxL-2) genes

DNA samples were PCR amplified targeting the *coxL* Form I gene with primer pair OMPF/SEQ and NGSR/SEQ. Both primers included the addition of a NextEra Illumina kit adapter sequence and a single base spacer to the 5', in addition 12 random bases were added to the forward primer only (table 2.3). *coxL* amplicons were purified and sent to collaborator Dr Joe Taylor at the University of York, UK, for library preparation and sequencing. Purified amplicons were cleaned and size selected using Agencourt® AMPure® XP magnetic bead kit (Beckman Coulter). Amplicons were then barcoded, libraries prepared using the NextEra XT library prep kit (New England Biolabs) and sequenced on an Illumina MiSeq using the Illumina MiSeq v3 reagent kit.

2.18 High-throughput sequence processing

All sequences were processed using the Quantitative Insights Into Microbial Ecology (QIIME) software version 1.9.1 (Caporaso et al., 2010) workspace run on VirtualBox (Oracle).

2.18.1 16S rRNA gene high throughput sequence processing

Raw paired reads were first merged using the programme VSEARCH version 2.4.3 (Rognes et al., 2016). Using the programme USEARCH version 9 (Edgar, 2010), primers were trimmed from the reads (left 19 and right 20 bp) and quality filtering performed to discard reads less than 250 bp or with an expected error rate of > 5 %. The quality filtered reads

were truncated to 250 bp, de-replicated, singletons removed and sorted by size annotation before operational taxonomic units (OTUs) were clustered at 97 % similarity and chimeras removed. OTUs were mapped to the original merged reads and an OTU table created. Taxonomy was assigned to the OTUs from the SILVA database release 128 (Quast et al., 2013) using the RDP Classifier 2.2 (Wang et al., 2007) and added to the OTU table using BIOM 2.1.6 (McDonald et al., 2012). Using QIIME, the OTU table was filtered to remove any OTUs assigned as eukaryote, archaea or organelles (e.g. chloroplasts) and normalised by rarefaction to allow comparison between samples. A phylogenetic tree was created from the OTU sequences using USEARCH. The tree and OTU table (filtered and rarefied) was then used with QIIME to make a weighted distance matrix using UniFrac metrics (Lozupone and Knight, 2005).

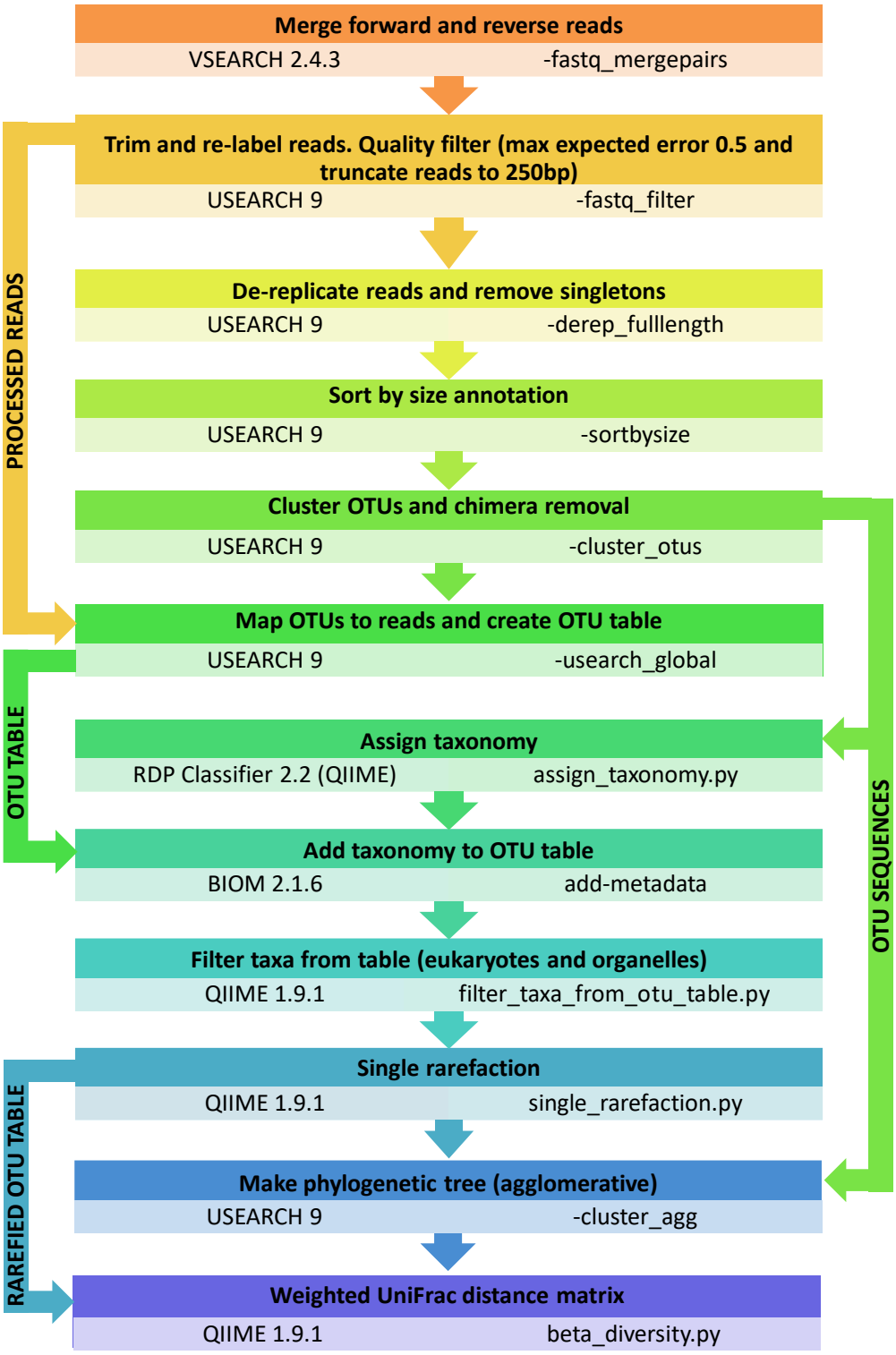

Figure 2.9. Flow chart showing bacterial 16S rRNA gene sequence processing pipeline detailing the programme and script used to carry out each step starting from raw reads (top) through to an OTU table and distance matrix (bottom) that are used for further analysis.

2.18.2 coxL Form I (coxL-2) high-throughput sequence processing

For *coxL* Form I (*coxL-2*) gene sequences only the forward reads were used because the amplicon was too long for paired end analysis and the reverse reads were of poorer quality. Using the programme USEARCH version 9 (Edgar, 2010), random bases (left 13 bp) were trimmed from the forward reads and quality filtering performed, discarding any reads less than 175 bp or with an expected error rate of > 5 %. The quality filtered reads were truncated to 175 bp, de-replicated, singletons removed and sorted by size annotation before operational taxonomic units (OTUs) were clustered at 97 % similarity and chimeras removed. OTUs were mapped to the original merged reads and an OTU table created. To assign taxonomy, the OTU sequences were searched against the NCBI non-redundant protein database using BLASTx. The OTU table was filtered to include only sequences with a hit to *bona fide* carbon monoxide dehydrogenase and normalised by rarefaction to allow comparison between samples. A phylogenetic tree was created from the CODH OTU sequences using USEARCH. The tree and OTU table (filtered and rarefied) was then used with QIIME to make a weighted distance matrix using UniFrac metrics (Lozupone and Knight, 2005).

2.19 Limitations of high throughput sequencing

Established genomic methods have been used in this thesis, however, there are always methodological limitations to consider. 16S rRNA gene approaches are the standard in bacterial identification but bias can be introduced during processing steps. DNA extraction can select easier to lyse cells like gram negative over gram positive bacteria. Bias can also be introduced during PCR amplification and by primer specificity due to the strength of binding at the annealing site and or downstream secondary structures during extension (Gohl et al., 2016, Comeau et al., 2017). Consequently all primer sets will under or over represent certain groups once OTU clustering has been performed. In these studies a mechanical and

chemical lysis step was employed to minimise any extraction bias. Amplicons were PCR-amplified in duplicate using separate template dilutions and using high fidelity polymerase by the sequencing centre to produce the highest quality starting material for high through put sequencing. The V4-V5 region primers chosen for these studies were selected as the best choice based on the taxa that were expected e.g. the alternative V6-V8 region primers are known to over represent proteobacteria which feature abundantly in the data set (Comeau et al., 2017). Amplicons were sequenced using Illumina MiSeq technology which produces reads of a high quality. Using a paired end approach, strict quality filtering and normalisation of sequencing depth provides further confidence in the data produced.

It must also be acknowledged that no process controls were used in these studies but should be considered in future studies where possible. Running replicate samples can help better identify what is a rare sequences from sequence errors. The inclusion of process blanks and kitome samples allows methodological contaminants to be identified and removed (Salter et al., 2014), and the inclusion of mock community samples will help to identify any sequencing bias (Yeh et al., 2018). Although independent process controls were not carried out here, the sequencing centre used to generate the data for this thesis has conducted testing of the of library preparation and sequencing protocol used, details can be found in Comeau et al., (2017).

2.20 Statistics, data analysis and graphical representation

Unless otherwise stated, all data were entered and edited in Microsoft Excel 2010. Data frames were stored as .xlsx, .csv or .tsv. Graphical representations of data were generated using Microsoft Excel or using R version 3.2.2. Data-Interpolating Variational Analysis (DIVA) gridded section plots and station maps (Chapters 4 and 6) were created using Ocean

Data View version 4 (Schlitzer, 2015). The station map for Chapter 5 was created in ArcGIS version 10.3 using longhurst_v4_2010 shape file.

2.20.1 Sequence analysis

For the analysis of small groups of sequences (e.g. Sanger results and BLAST hits etc.), alignments were made using Multiple sequence comparison by log-expectation (MUSCLE) (Edgar, 2004) in Molecular evolutionary genetics analysis (MEGA) version 6 (Tamura et al., 2013). Phylogenetic analysis was also carried out in MEGA6 and edited in Dendroscope version 3.5.9 (Huson and Scornavacca, 2012).

2.20.2 High throughput sequence data analysis

Processed sequences from high-throughput sequence runs were analysed in R version 3.2.2 (R-Core-Team, 2015) for packages and programmes used see table 2.6a and QIIME version 1.1.9 (Caporaso et al., 2010) for commands used see table 2.6b.

Table 2.6. Details of statistical analyses carried out in a) R and b) QIIME.

a.

Software	Package	Function	Reference
R version 3.2.2	vegan	anova.cca spantree dbrda	(Oksanen et al., 2013)
	stats	cmdscale t.test	(R-Core-Team, 2015)
	Hmisc	rcorr	(Harrell Jr, 2016)

b

Software	Test	command	Reference
QIIME version 1.1.9	PERMANOVA	compare_categories.py	(Caporaso et al., 2010)
	G-TEST	group_signifcance.py	

Chapter 3

Carboxydovory in the ecologically-relevant model marine bacterioplankton *Ruegeria pomeroyi* DSS-3

3.1 Introduction

Aerobic bacterial carbon monoxide (CO) utilisation has been studied for several decades and has focused principally on carboxydotrophy in the model bacteria *Oligotropha carboxidovorans* and *Pseudomonas carboxydohydrogena*, which utilise CO as a source of assimilatory carbon and energy (Meyer and Schlegel, 1983, King and Weber, 2007). Carbon monoxide dehydrogenase (CODH) is the key enzyme in the utilisation of CO by carboxydotrophic bacteria and is encoded by the genes *coxS, M* and *L* (Meyer et al., 1993). CODH is a molybdenum-containing oxidoreductase that is associated with the inner aspect of the cytoplasmic membrane and respiratory chain in *O. carboxidovorans*, reacting CO with H_2O to produce CO_2 and conserved reducing power (Meyer et al., 1993). Carboxydotrophs subsequently assimilate the CO-derived CO_2 through the Calvin Benson Bassham Cycle via ribulose-1,5-bisphosphate carboxylase/oxygenase (RuBisCO) and use the electrons through the electron transfer chain to reduce a dioxygen terminal acceptor and produce ATP (Meyer, 1989).

Principally through genome sequence analysis and molecular ecology studies, a second functional group of aerobic CO-utilising bacteria has been more recently identified that are termed carboxydovores (King, 2003, King and Weber, 2007). Even though carboxydovores can readily oxidise CO, they are unable to assimilate the resulting CO_2 because they lack RuBisCO and/or the higher CO concentrations that are typically used to grow carboxydotrophs are inhibitory (King, 2003, King and Weber, 2007).

Carboxydovory appears to be particularly prevalent in some heterotrophic marine bacterioplankton groups, including the abundant and ecologically important Marine Roseobacter Clade (MRC), with CO proposed to be utilised chemolithoheterotrophically as a supplementary energy source (Newton et al., 2010). Marine bacterioplankton carboxydovory is biogeochemically important because microbial oxidation is the dominant

CO sink in seawater, accounting for up to 86 % of the CO produced by photolysis of organic matter and subsequently diminishing the potential impact of marine-derived CO on atmospheric processes (Zafiriou et al., 2003).

Ruegeria pomeroyi DSS-3 (basonym *Silicibacter pomeroyi*) is a member of the MRC and one of the first groups of carboxydovores identified (Moran et al., 2004, King, 2003). *R. pomeroyi* DSS-3 has become a well-established model bacterioplankton and has been used to help elucidate the biological mechanisms that underpin a range of marine biogeochemical and ecological processes, including elemental cycling e.g. (Cunliffe, 2016, Todd et al., 2011) and microbe-microbe interaction e.g. (Christie-Oleza et al., 2017).

The *R. pomeroyi* DSS-3 genome contains two different *cox* gene operons (Form 1 and Form 2) and lacks RuBisCO (Moran et al., 2004). The *R. pomeroyi* DSS-3 Form 1 *cox* genes are homologous to the verified CODH-encoding *cox* genes in the well characterised carboxydotrophs *O. carboxidovorans* and *P. carboxydohydrogena*. The Form 2 is a putative CODH, with function inferred from sequence similarity with the Form I *coxL* gene encoding the large catalytic subunit of CODH (King, 2003, King and Weber, 2007). From a study of nine MRC strains (including *R. pomeroyi* DSS-3) with genomes that contain either both forms or only the Form 2, only strains that had both the Form 1 and the Form 2 *cox* operons could oxidise CO. MRC strains with only the putative Form 2 CODH encoding genes could not oxidise CO under the conditions tested (Cunliffe, 2011).

Even though *R. pomeroyi* DSS-3 has been shown to readily oxidise CO (King, 2003, Moran et al., 2004, Cunliffe, 2013), the physiological effects of CO oxidation on *R. pomeroyi* or any other marine bacterioplankton remain poorly understood. Given that marine bacterioplankton CO oxidation appears widespread based on genome/metagenome (Moran et al., 2007, Newton et al., 2010) and biogeochemical evidence (Zafiriou et al., 2003), there are still substantial gaps in our understanding of the principal underpinning biological mechanisms controlling potential CO-supported chemolithoheterotrophy. The aims of this

study were to address these knowledge gaps by focusing on the following specific research questions; is there a physiologically beneficial response (i.e. chemolithoheterotrophy) to CO oxidation in *R. pomeroyi*, and what is the supporting molecular machinery (i.e. mRNA and proteins/enzymes) involved in sustaining *R. pomeroyi* CO-oxidation and potential CO-supported chemolithoheterotrophy.

3.2 Results

3.2.1 Impacts of CO on growth and organic carbon starvation response

The effect of CO on the growth of *R. pomeroyi* DSS-3 was examined in marine ammonium minimal salts (MAMS) medium with 10 mM glucose. CO was added at 10 % of the headspace volume and compared to the ambient air only control. Growth was measured via optical density (OD_{600}) and showed that there was no significant difference in growth rate (μ) between the CO-exposed cultures (μ 0.11 ± 0.001) and the control cultures (μ 0.10 ± 0.007) (Welch's t-test p =0.33) during the exponential phase. The CO-exposed cultures, however, achieved greater final biomass in the stationary phase when glucose became depleted compared to the control cultures (Welch's t-test p =0.03) (figure 3.1a).

To further determine the impact of CO oxidation on organic carbon starved *R. pomeroyi* DSS-3, cultures were grown in MAMS medium with 10 mM glucose to mid-exponential phase (OD_{600} 0.5-0.8), washed and re-suspended in glucose-free MAMS medium. The addition of CO (10 % headspace volume) caused *R. pomeroyi* DSS-3 to maintain significantly greater biomass (Welch's t-test p =0.02) compared to the control cultures exposed to ambient after 42 hours for up to 97 hours (figure 3.1b).

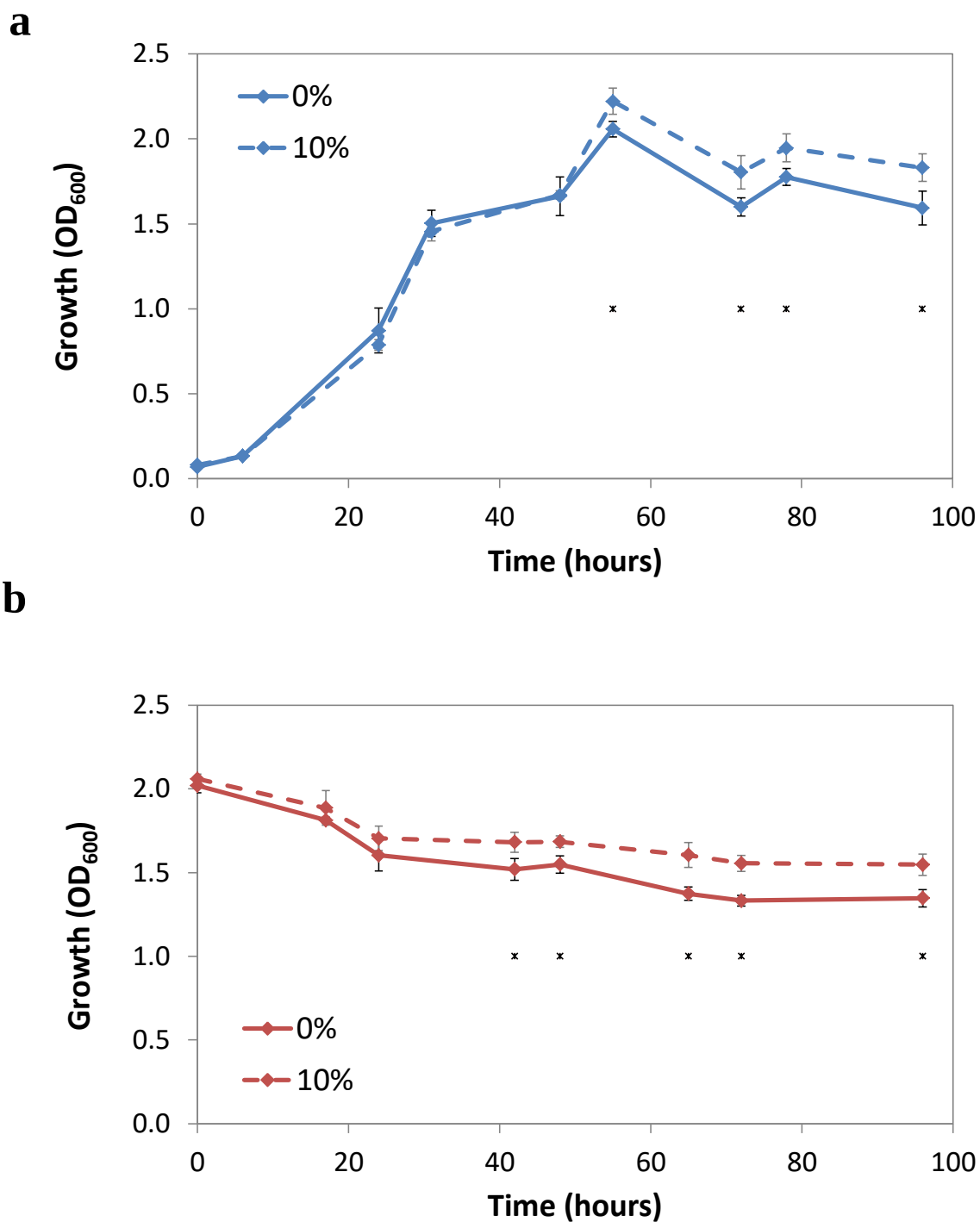

Figure 3.1. Growth of *R. pomeroyi* DSS-3 on MAMS with a) 10 mM glucose and b) no additional carbon source, over time in hours. 0 % control contains ambient air, 10 % treatment contains 10,000 ppm CO addition to the flask headspace. Values represent means (n 4), error bars represent standard deviation. Symbol * shows significant p <0.05 time points calculated by Welch's t-test.

To confirm that 10% CO does not also have a positive effect on a MRC bacterium without the Form 1 *cox* genes (i.e. Form 2 only), growth was also assessed in *Sagitulla stellata* E37 and showed no evidence of CO oxidation or change in growth parameters (figure 3.2).

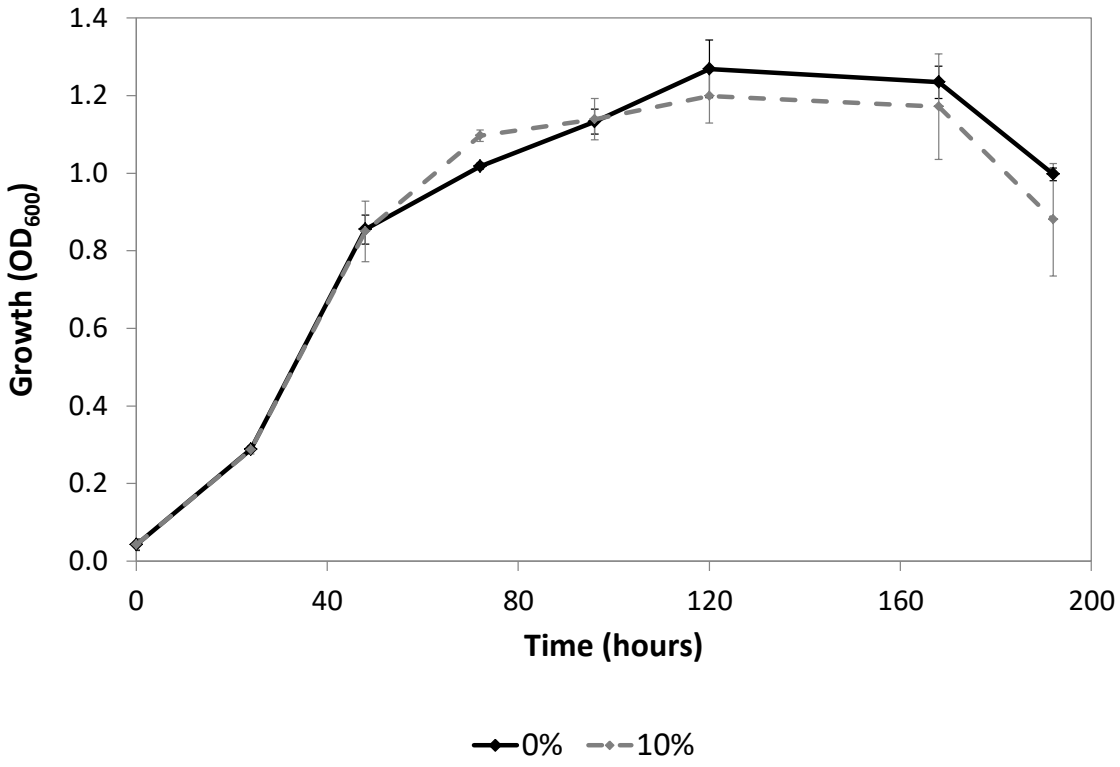

Figure 3.2. Growth of *S. stellata* E37 with MAMS with 10 mM glucose over time (in hours). 0 % control contains ambient air, 10 % treatment contains 10,000 ppm CO addition to the flask headspace. Values represent means (n 3), error bars represent standard deviation.

3.2.2 Impact of CO on Form 1 coxL transcription

To determine the impact of CO on *coxL* transcription, RNA was extracted from cell pellets harvested from 24, 48 and 72 hours during the growth experiment (figure 3.1a) and at 0 and

96 hours during the organic carbon starvation experiment (figure 3.1b). RT-qPCR analysis of *coxL* mRNA transcripts normalised against mRNA transcripts of the 'housekeeping' genes *pyrG* and *rpoB*, showed that *coxL* transcription was significantly increased in the presence of CO after 72 hours (figure 3.3a) coinciding with the significantly increased biomass (figure 3.1a). The same RT-qPCR analysis performed on the RNA extracted from the organic carbon starvation experiment, showed that after 96 hours *coxL* transcription was significantly increased in the presence of CO compared to the control (i.e. ambient air) (figure 3.3b).

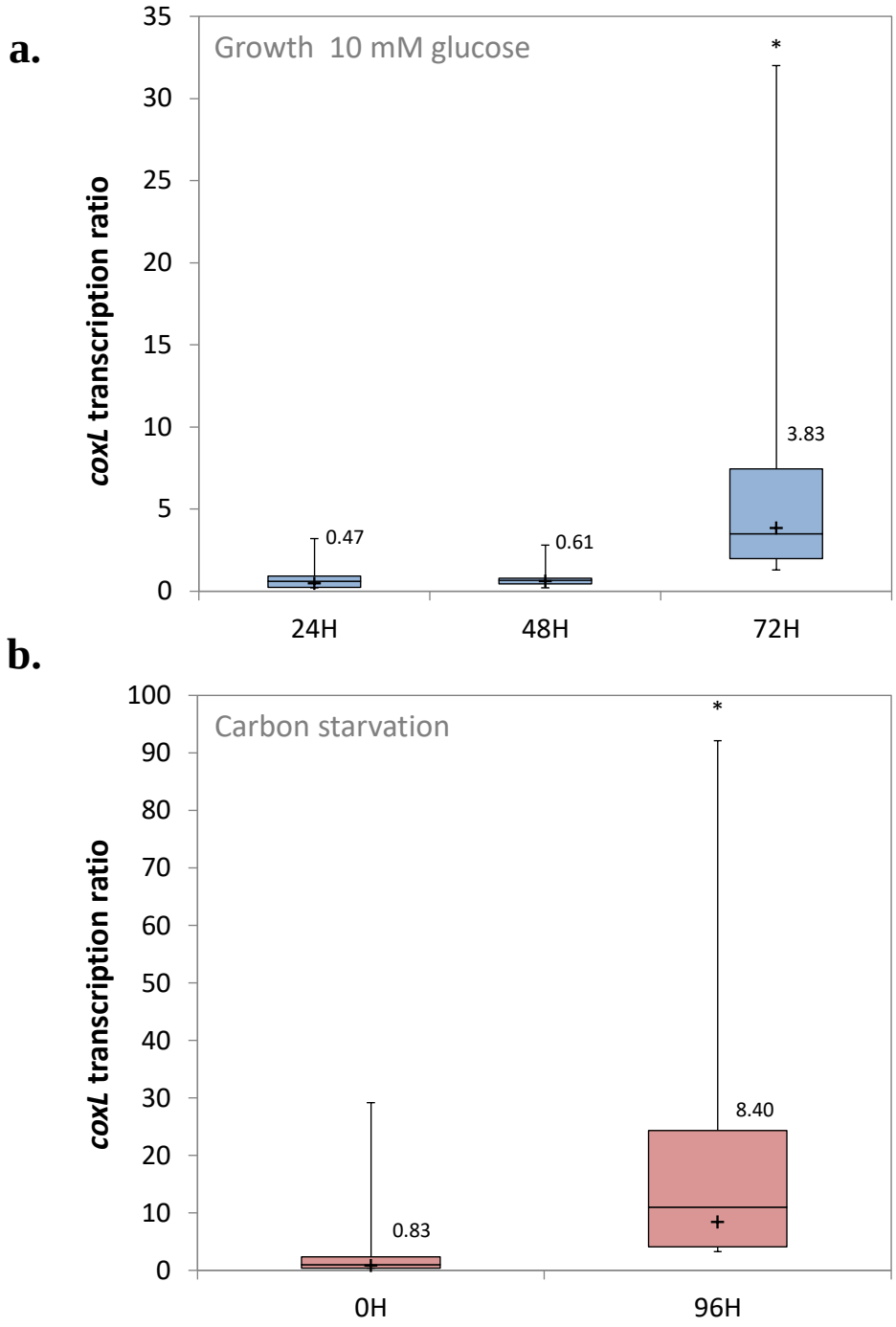

Figure 3.3. Normalised relative gene transcription of the *coxL* Form I gene from *R.pomeroyi* during a) growth on 10 mM glucose and b) during carbon starvation. *p* values (* = $p < .001$) are derived by pair-wise fixed reallocation randomisation test (n 2000). Error bars represent 95 % confidence interval and crosses and numbers show mean transcription ratio in the plus CO treatment compared to the no CO control.

3.2.3 Impact of CO on the R. pomeroyi DSS-3 proteome

The proteins SPO2397, SPO2398 and SPO2399 (carbon monoxide dehydrogenase, CODH) that are encoded by the Form 1 genes *coxL*, *coxS* and *coxM* respectively, significantly increased in the presence of CO at 10 % of the headspace volume compared to the ambient air only control (student t-test $p < 0.05$) (figure 3.4a and figure 3.5a). The other associated proteins encoded through the CODH operon (operon 1606), namely SPO2393 (*coxG*), SPO2394 (*coxF*), SPO2395 (*coxE*) and SPO2396 (*coxD*) were also significantly increased in abundance in the presence of 10 % CO compared to the control (student t-test $p < 0.05$) (figure 3.4a and figure 3.5a).

In the glucose-starved samples, the *R. pomeroyi* proteomes from the cells exposed to 10 % CO showed reduced expression of the CODH operon proteins (figure 3.5a) compared to the proteomes from the exponential phase grown cells (figure 3.5a). However, when compared to the control glucose-starved cells (i.e. ambient air), the CODH proteins SPO2397 (*coxL*), SPO2398 (*coxS*) and SPO2399 (*coxM*) were still significantly higher (student t-test $p < 0.05$) in the presence of 10% CO. as were, SPO2393 (*coxG*) and SPO2394 (*coxF*) (figure 3.4b and figure 3.5a).

The control 'housekeeping' proteins SPO1312 (CTP synthase) and SPO3508 (DNA-directed RNA polymerase beta subunit), which are encoded by the genes *pyrG* and *rpoB* respectively, showed no difference in expression between treatments (figure 3.5b), matching the associated mRNA abundances (figure 3.6).

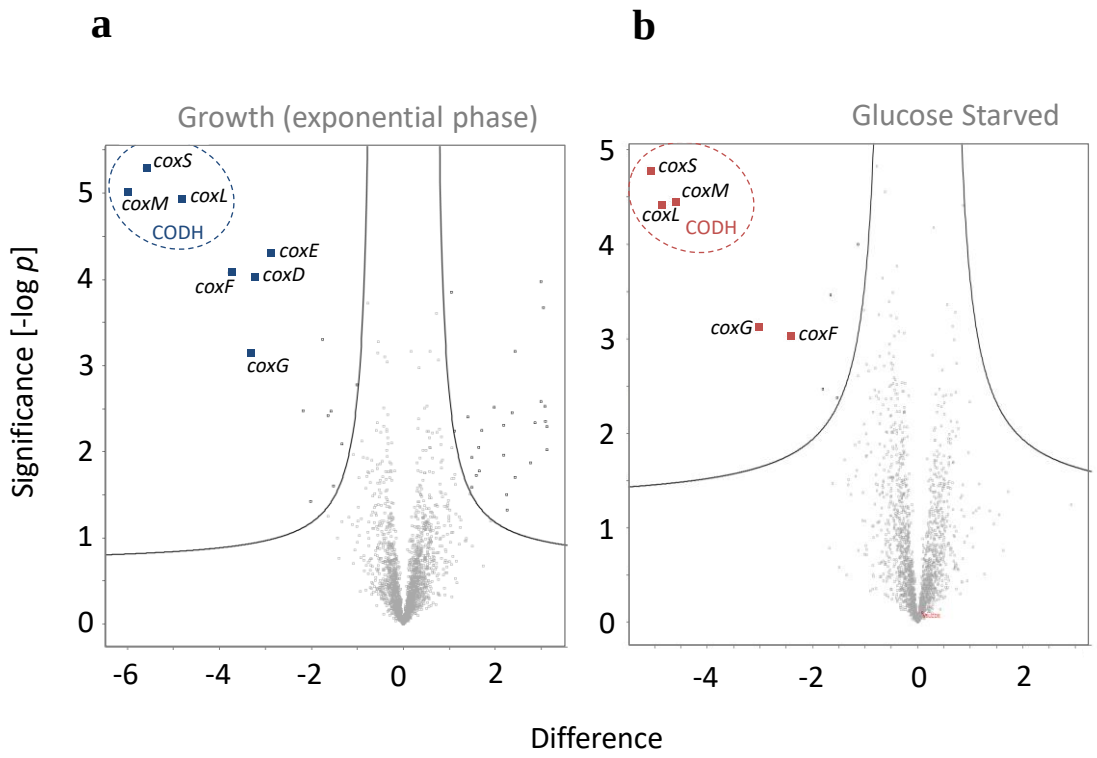

Figure 3.4. Volcano plot of statistical significance against fold change between the 10 % CO treatment and no CO control. Differentially expressed genes, *coxS* (SPO2398), c*oxM* (SPO2399), *coxL* (SPO2397) of CODH are highlighted along with other CODH operon genes *coxG* (SPO2393), *coxF* (SPO2394), *coxE* (SPO2395) and *coxD* (SPO2396).

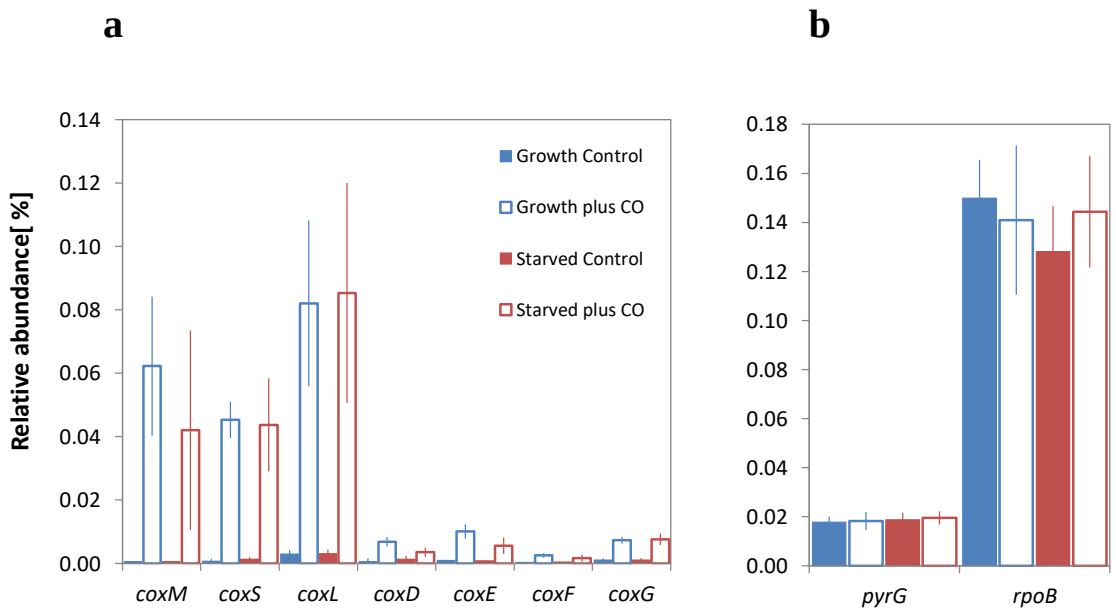

Figure 3.5. a) Relative abundance of carbon monoxide dehydrogenase (CODH) proteins SPO2398 (*coxS*), SPO2399 (*coxM*), SPO2397 (*coxL*), and other CODH operon proteins SPO2393 (*coxG*), SPO2394 (*coxF*), SPO2395 (*coxE*) and SPO2396 (*coxD*). b) Relative abundance of housekeeping proteins SPO1312 (*pyrG*) and SPO3508 (*rpoB*).

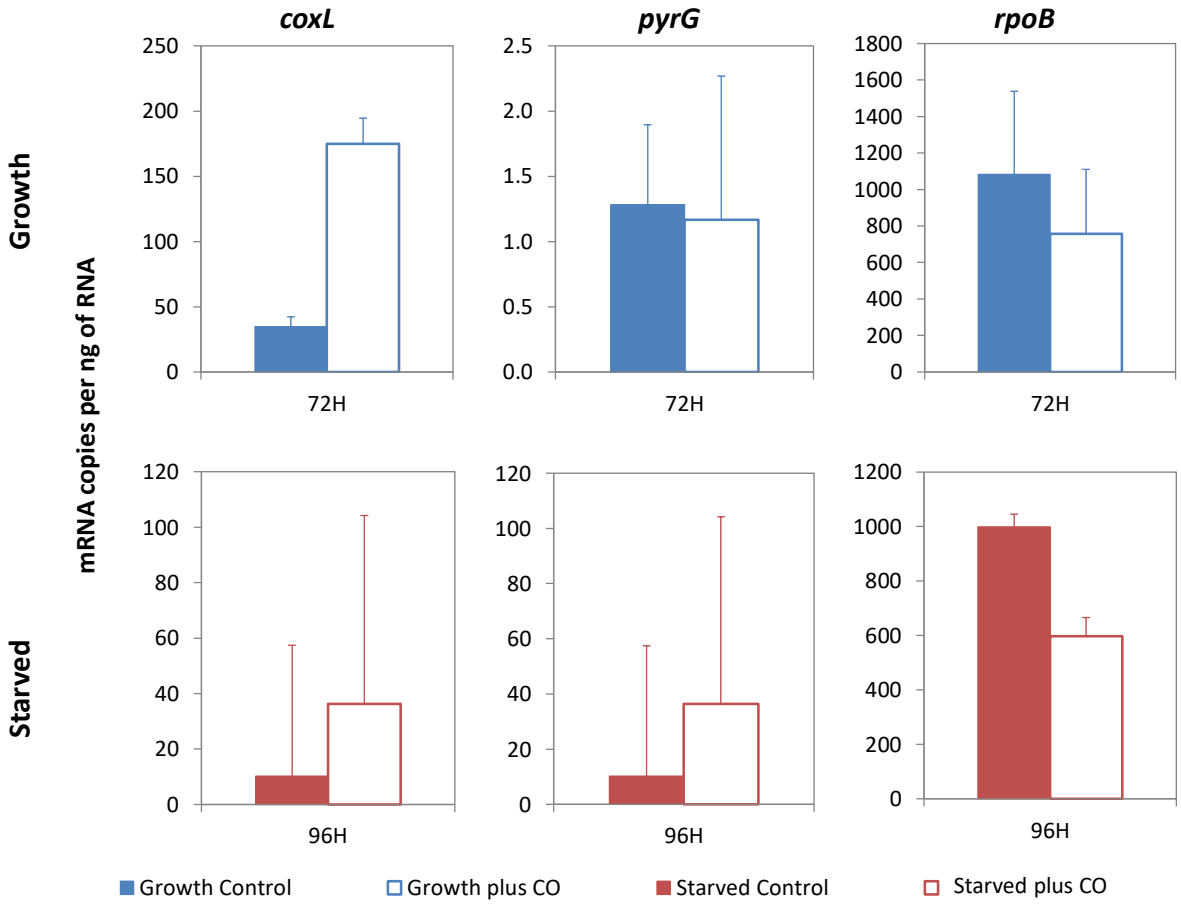

Figure 3.6. Mean (n 4) mRNA copies per ng of RNA for target gene *coxL* and housekeeping genes *pyrG* and *rpoB* in the 10 % CO treatment and no CO control for growth (10 mM glucose) and carbon starvation experiments.

3.2 Discussion

The results presented here have demonstrated a sustained increase in *R.pomeroyi* DSS-3 biomass through CO oxidation during stationary growth phase (i.e. when organic carbon was depleted), and greater maintained biomass of carbon starved cells also through CO oxidation. Both responses to CO show empirically that *R.pomeroyi* DSS-3 is able to utilise CO chemolithoheterotrophically. mRNA RT-qPCR and proteome analysis show that the Form 1 CODH is active at both the transcript and protein level during CO chemolithoheterotrophy.

Previous studies have demonstrated similar effects of CO on the growth of carboxydotrophs, which unlike carboxydovores have the ability to grow autotrophically, assimilating CO_2 from CO-oxidation (Meyer and Schlegel, 1978, Krüger and Meyer, 1984). When grown on organic substrates in addition to CO, carboxydotrophs (e.g. *Acinetobacter*) can grow mixotrophically assimilating organic and CO-derived carbon simultaneously (Kim and Kim, 1989). Some bacteria (e.g. *Pseudomonas carboxydoflava*) can grow chemolithoheterotrophically, using CO-oxidation only as an additional energy source and allowing more efficient use of organic substrates (Kiessling and Meyer, 1982). Even in the most efficient CO autotrophs, almost all CO is converted to CO_2 as an energy source and only 4-16% is further assimilated into cell carbon (Zavarzin and Nozhevnikova, 1977, Meyer and Schlegel, 1978). The observation that autotrophic growth on CO is slower than mixotrophic or chemolithoheterotrophically growth with CO (Meyer and Schlegel, 1978, Kiessling and Meyer, 1982) coupled with the small amount of cell biomass derived from CO-oxidation implies that the primary role of CO-oxidation in CO-oxidising bacteria is as an energy source.

In this study, the effect of CO on *R.pomeroyi* DSS-3 biomass was only detectable at relatively high CO concentrations and evident only during stationary growth phase once the organic carbon source (i.e. glucose) had been depleted, or during deliberate carbon starvation. This suggests the effect of CO on bacterial growth in carboxydovores is far

subtler than in carboxydotrophs, and supports the hypotheses suggesting that CO-oxidation in carboxydovores is used as complementary fitness strategy. This may also explain why previous studies did not detect any significant effects of CO on carboxydovore growth, including *R.pomeroyi* DSS-3, which used lower CO headspace concentrations (King, 2003, Cunliffe, 2013).

The 10% headspace volume CO concentration used in this study has limited environmental relevance because naturally occurring equivalent CO concentrations are only found in a few niche environments such as hydrothermal vents (Lilley et al., 1982). However, this concentration was used because this was the only condition in which CO-dependent chemolithoheterotrophically growth was detectable. High biomass was also needed for mRNA RT-qPCR and proteome analysis. The highest concentrations recorded in the marine environment exist in productive coastal surface waters (~15 nM) and are lower for the open ocean (~2 nM) (Tolli and Taylor, 2005). We were unable to detect the effects of CO at lower, more environmentally relevant concentrations ≤ 1% (results not shown).

CODH is conserved throughout the otherwise taxonomically and phenotypically diverse CO-oxidiser group, including autotrophic, mixotrophic and chemolithoheterotrophic utilisers (Kang and Kim, 1999). However, based on the response to CO in *R.pomeroyi* DSS-3 and the low concentration of CO in seawater, CO-dependent chemolithoheterotrophy is more likely a mechanism that allows a population to be sustained rather than one to proliferate in the marine environment. Recent studies have hypothesised that core members of marine bacterial communities are persistent throughout time and vary not by presence or absence but by abundance in response to environmental factors (Caporaso et al., 2012, Gibbons et al., 2013). The ability to oxidise CO may be an ecological trait that allows specific bacterial populations to exist in low numbers in the 'microbial seed bank' during less favourable conditions. This strategy would be advantageous in temperate coastal and shelf seas, which are well known for seasonal cycles in productivity and associated changes

in bacterial community structure (Chapter 4). These ecosystems also have the highest reported CO-production and oxidation rates (Jones, 1991, Jones and Amador, 1993).

In recent years, genomic studies have revealed a diversity of *coxL* genotypes within marine bacterioplankton (Tolli et al., 2006, Weber and King, 2007, Cunliffe et al., 2008). Of particular magnitude is the prevalence of *coxL* genes in the MRC (Cunliffe, 2011, Tolli et al., 2006), a metabolically diverse and ubiquitous group of marine bacteria (Buchan et al., 2005). As such, the MRC are likely involved in the significant marine CO sink (Cunliffe, 2011), and potentially represent an underestimated component of the marine photochemically mediated carbon cycle.

In conclusion, I have linked CO-oxidation specifically with *coxL* Form I gene function and shown chemolithoheterotrophy in the model MRC CO-oxidiser *R. pomeroyi* DSS-3. These findings can be used to infer function from the presence of *coxL* Form I genes (Chapter 4) in natural bacterioplankton communities, allowing for a better understanding of the distribution and diversity of CO-oxidisers in the marine environment.

Chapter 4

Seasonal diversity of bacterioplankton and *coxL* genes: a time series study at the coastal Station L4 and open shelf Station E1 in the Western English Channel

4.1 Introduction

4.1.1 Seasonal diversity of bacterioplankton communities in temperate coastal seas

Heterotrophic bacterioplankton have major roles in nutrient and elemental fluxes, re-mineralising up to 50% of phytoplankton derived organic matter (DOM) via the microbial loop (Azam, 1998, Ducklow, 2000). One of the major hurdles in modelling global fluxes is the ability to upscale local observations to predict broad scale processes due to high spatial and temporal variation in microbial assemblages (Azam and Malfatti, 2007). Shifts in bacterioplankton community composition in response to changes in environmental conditions occur throughout the marine environment over multiple timescales and have been recently reviewed (Fuhrman et al., 2015, Bunse and Pinhassi, 2017). Some of the greatest variation in bacterioplankton diversity occurs in coastal ecosystems, which in contrast to the open ocean, are highly dynamic (Longhurst et al., 1995). Coastal seas represent only a small fraction of the total global ocean (~7 % by surface area) (Frankignoulle and Borges, 2001), but are highly productive accounting for ~19 % of net primary production (Field et al., 1998). Consequently, the processes that are occurring in coastal ecosystems are important in understanding global-scale biogeochemical cycles.

The majority of seasonal-scale bacterioplankton succession studies have been conducted in northern hemisphere temperate regions (Bunse and Pinhassi, 2017). By far the most comprehensive of these studies have been carried out at time series stations in the North Sea (Teeling et al., 2016) and the Western English Channel (Gilbert et al., 2012), which have shown seasonal patterns in bacterioplankton succession to be annually recurrent (Gilbert et al., 2012, Teeling et al., 2016). Generally, coastal bacterioplankton communities are dominated by Alphaproteobacteria, *Bacteroidetes* and *Gammaproteobacteria* taxa (Zinger et al., 2011). These core dominant phyla exhibit seasonal changes in their abundance at both low and high taxonomic resolution (Schauer et al., 2003, Mary et al., 2006a) according to

ecological niche optima (Caporaso et al., 2012, Gibbons et al., 2013), with changes driven by complex interactions of abiotic and biotic variables such as temperature, light, inorganic nutrients, organic substrates, phytoplankton and other biological interactions that control mortality (Rodríguez et al., 2000, Gilbert et al., 2012). The extents to which these drivers directly influence the succession of specific bacterioplankton populations still remain poorly resolved (Bunse and Pinhassi, 2017).

Typically, winter is characterised by water column mixing, high nutrients, low temperatures, low light and low primary productivity. Bacterioplankton are lower in abundance and dominated by oligotrophs such as *Pelagibacterales* (SAR11) and *Prochlorococcus*. Spring is characterised by high inorganic nutrient levels following winter mixing and coastal input (e.g. estuarine), increasing temperature and increasing light, which increases phytoplankton primary productivity. Subsequently bacterioplankton abundance increases in response to the organic substrates made available from the spring phytoplankton bloom. Spring bacterioplankton communities are typically dominated by copiotrophs, such as *Flavobacteriales* and *Rhodobacterales*. During summer, high temperatures can lead to water column thermal stratification, and inorganic nutrients are depleted by the spring phytoplankton bloom resulting in lower primary productivity. Summer bacterioplankton communities are characterised by increasing abundances of *Rhodobacterales*, *Gammaproteobacteria* and SAR11. During autumn, temperature begins to decrease and thermal stratification breaks down releasing nutrients that have regenerated over summer in underlying water triggering a secondary phytoplankton bloom. In the bacterioplankton community, SAR11 abundance continues to increase, while *Rhodobacterales* abundance decreases and a second peak in *Flavobacteriales* abundance appears in response to the increase in primary productivity (Rodríguez et al., 2000, Alonso-Sáez et al., 2007, Caporaso et al., 2012, Gilbert et al., 2012).

Seasonal bacterioplankton succession in temperate coastal environments has almost exclusively been studied in surface waters (table 4.1), with relatively little known about community dynamics vertically throughout the water column. The stratification of microbial populations has been shown in oceanic environments (Giovannoni et al., 1996, Field et al., 1997, DeLong et al., 2006, Treusch et al., 2009), and is thought to be related to eukaryotic phytoplankton distribution (Treusch et al., 2009) and local hydrological influences such as fronts, mixing and thermal stratification processes (Casotti et al., 2000, Treusch et al., 2009). Although coastal shelf seas are shallow in comparison to the open ocean, processes such as vertical mixing and stratification are present and likely to influence the vertical structure of bacterioplankton communities (Salter et al., 2014, Lindh et al., 2015).

Bacterioplankton are also known to vary along productivity gradients (Horner-Devine et al., 2003, Traving et al., 2017). Given the diversity and dynamic nature of coastal environments (Longhurst et al., 1995), and their proximity to terrestrial and anthropogenic influences, the physicochemical drivers of bacterioplankton community structure are likely to vary over a conserved spatial area. Very few studies have compared seasonal bacterioplankton succession at more than one study site at the same time (table 4.1). Those that have suggest that temporal variation is stronger than spatial variation, but either lack high temporal resolution (Feng et al., 2009) or pre-date contemporary high-throughput sequencing (HTS) technologies (Rooney-Varga et al., 2005). Caporaso et al., (2012) and Gilbert et al., (2012) suggested that riverine and other hydrological influences are not significant in determining seasonal succession. Conversely, a study by Taylor et al. (2014) at the same location showed the similarity between nearby estuarine and coastal sites varied over a spring bloom. In addition, Alonso-Sáez et al. (2007) concluded that the high abundance of SAR11 in the Mediterranean compared to other coastal sites could be due to oceanic influence.

Table 4.1. Literature investigating bacterioplankton dynamics in northern hemisphere temperate coastal seas.

Reference	Location	Province	Spatial resolution		Temporal resolution		Method
			Sampling Site	Depth	Frequency	Duration	
(Wright and Coffin, 1983)	N Massachusetts	NWCS	Essex, Ipswich and parker estuaries	1 m	Monthly (every 45 min High - Low Tide), seasonally	1 year	Enumeration, activity
(Campbell et al., 2009)	Delaware		Delaware Bay	Surface	Monthly	2 years	DGGE, sequencing
(Rooney-Varga et al., 2005)	SW Bay of Fundy		6 Stations	Surface	Bimonthly	Feb-Sep 00	DGGE, sequencing
(Feng et al., 2009)	East China Sea	CHIN	9 Stations (2 sites estuary & coastal)	Surface, sediment	Seasonally	May & Oct 07	Sequencing
(Schauer et al., 2003)	NW Mediterranean	MEDI	Blanes Bay	Surface	Monthly (Weekly Feb-Mar)	Dec 97 - Dec 98	DGGE, sequencing
(Alonso-Sáez et al., 2007)			Blanes Bay	Surface	Monthly	Mar 03 - Mar 04	DGGE, CARD-FISH, RFLP
(Sapp et al., 2006)	North Sea	NECS	Helgoland Roads	1 m	Fortnightly	Feb-May 2004	DGGE, sequencing
(Alderkamp et al., 2006)			Royal Netherlands Institute for Sea Research (NIOZ)	Surface	Monthly	Mar-Aug 04	CARD-FISH, microautoradiography
(Teeling et al., 2012)			Helgoland Roads Kabeltonne	Surface	Twice weekly	Jan 09-Jan 10	CARD-FISH, HTS (16S rRNA, metagenome, metaproteome)
(Klindworth et al., 2014)				Surface	Weekly	Feb-Sep 09	HTS (16S rRNA)
(Teeling et al., 2016)				Surface	Biweekly, Bimonthly	Jan 09-Jan 10, Jan 10 - Dec 12	CARD-FISH, HTS (16S rRNA, metagenome)
(Alonso-Saez et al., 2015)	Bay of Biscay		Station E2	Surface	Monthly	Jul 09-Dec 12	HTS (16S rRNA)
(Pinhassi and Hagström, 2000)	Baltic Sea		Station NB1	4 m	Twice monthly, monthly	Mar-Nov 95	Enumeration, activity
(Andersson et al., 2010)			Landsort Deep station	3 m	Every 1-3 weeks	May 03 - May 04	HTS (16S rRNA)
(Lindh et al., 2015)			Linnaeus Microbial Observatory (LMO)	2 m	Twice weekly	2011	HTS (16S rRNA)
(Rodríguez et al., 2000)	Western English Channel		Western Channel Observatory (WCO) Station L4	10 m	Weekly	Oct 92- Jan 94	Enumeration
(Mary et al., 2006a)				2 m	Weekly	Aug 03 – Aug 04	Enumeration, FISH
(Gilbert et al., 2009)				Surface	Monthly	Feb – Dec 07	HTS (16S rRNA)
(Gilbert et al., 2010b)				Surface	Monthly	Jan 03-Dec 08	HTS (Metagenome, metatranscriptome)
(Gilbert et al., 2010a)				0-2 m	Monthly	Jan 03-Dec 08	HTS (16S rRNA, metagenome, metatranscriptome)
(Caporaso et al., 2012)				Surface	Monthly	Jan 03-Dec 08	HTS (16S rRNA)
(Gilbert et al., 2012)				Surface	Monthly	Jan 03-Dec 08	HTS (16S rRNA)
(Taylor et al., 2014)			WCO Station L4, Plym and Tamar estuaries	Microlayer, 2 m	Twice weekly	Feb-Jul 2012	HTS (16S rRNA)

4.1.1 Functional diversity of bacterioplankton communities in temperate coastal seas

Copiotrophs such as *Rhodobacterales*, *Flavobacteriales* and members of the *Gammaproteobacteria* are abundant in coastal bacterioplankton communities especially in spring when primary productivity is high (Gilbert et al., 2012, Teeling et al., 2012, Teeling et al., 2016,). Although often referred to as generalists (Mou et al., 2008, Newton et al., 2010), these phylogenetic groups preferentially degrade different organic substrates (Sarmento and Gasol, 2012) and are metabolically diverse. Consequently, they play an important role in re-mineralising the large flux of organic matter following phytoplankton blooms (Buchan et al., 2014). The metabolic traits of individual taxa are hypothesised to play a role in the structuring of bacterioplankton communities (Bryson et al., 2017, Bunse and Pinhassi, 2017), however, currently little is known about the functional diversity or the specific mechanisms of carbon and energy acquisition utilised by many of these taxa (Buchan et al., 2014). Only a handful of coastal succession studies have characterised the functional diversity of the community (Gilbert et al., 2010a, Gilbert et al., 2010b, Teeling et al., 2012, Klindworth et al., 2014).

The Marine Roseobacter Clade (MRC), dominant members of the *Rhodobacterales* (Pujalte et al., 2014), possess multiple mechanisms of carbon and energy acquisition (Buchan et al., 2005, Moran et al., 2007). Due to their cultivability, many of these mechanisms have been characterised in model organisms (Buchan et al., 2005, Moran et al., 2007, Newton et al., 2010), however, assigning ecological function to *in situ* phylogenetic diversity data remains difficult as often the presence of functional genes vary between MRC genomes (Newton et al., 2010). The specific example used in this study is carboxydovory, the oxidation of carbon monoxide (CO) as a supplementary energy source (see Chapter 3). Existing surveys of the *coxL* gene functional marker for CO-oxidation have identified a high abundance of potential CO-oxidisers among the MRC (Cunliffe, 2011, Tolli et al., 2006) and suggest the ability is unevenly distributed among the clade (Cunliffe, 2011).

CO in seawater is produced by the photodegradation of DOM, with up to 86% (equivalent to ~70Tg of carbon per year globally) of the CO produced oxidised by bacterioplankton to CO_2 (Zafiriou et al., 2003, Stubbins et al., 2006) and, with the production and consumption of seawater CO greatest in productive waters such as coastal seas (Conrad and Seiler, 1980, Jones, 1991, Jones and Amador, 1993). CO-oxidation by carboxydovores is a form of chemolithoheterotrophy and provides an energetic advantage facilitating more efficient exploitation of organic substrates (King, 2003, Moran et al., 2004). This trait may influence bacterioplankton community structure by facilitating higher biomass production during bloom conditions or by prolonging survival during suboptimal conditions (Chapter 3).

In the current study, bacterioplankton diversity was characterised over a spring phytoplankton bloom from three different depths at the coastal Station L4 and, for the first time, at open-shelf Station E1 in the Western English Channel. The study aim was to provide insight into depth resolved community dynamics as well as making a comparison between the bacterioplankton communities present at the two stations, testing the hypothesis that bacterioplankton communities differ vertically as well as temporally in response to seasonal stratification and mixing processes at the WCO (Southward et al., 2005, Smyth et al., 2010). And in addition, investigating whether the pattern of bacterioplankton seasonal succession differed between Station L4, which receives greater influence from the local river system, and Station E1, which receives greater influence from Atlantic water masses (Southward et al., 2005, Smyth et al., 2010).

Furthermore, this study also attempts novel high-throughput functional gene sequencing, investigating a subset of samples for potential CO-oxidising bacterioplankton using a trait based approach to characterise the diversity of carboxydovores over a spring-summer seasonal transition. Testing the hypotheses that CO-oxidising genes will be present

at the WCO and that the MRC's will contribute heavily to the CO-oxidising community following the spring phytoplankton bloom.

4.2 Methodology in brief (full materials and methods in Chapter 2)

4.2.1 Sampling sites

Station L4 and Station E1 are principle fixed sampling locations in the Western English Channel (figure 4.1) forming part of the Western Channel Observatory (WCO) time series programme, which has been recording the physical, chemical and biological characteristics of the Western English Channel since 1888 (Southward et al., 2005). Station L4 (Lat 50.25, Lon -4.22) is located 14 km south from Plymouth (UK) and Station E1 (Lat 50.03, Lon -4.36) is located 40 km south from Plymouth (UK). Both stations are influenced by tidal processes (Pingree, 1980) and are generally seasonally stratified from April through to September (Smyth et al., 2010). The biological characteristics at L4 and E1 display seasonal patterns which are strongly influenced by local meteorological and hydrographic conditions (Eloire et al., 2010, Widdicombe et al., 2010, Highfield et al., 2010, Gilbert et al., 2012). Station L4 is coastal (depth 50 m) and is strongly influenced by periodic riverine inputs from the Tamar estuary (Rees et al., 2009, Smyth et al., 2010), whereas Station E1 is an open shelf station (depth 75 m) that is less influenced by land-sea exchanges and, based on salinity measurements, thought to be influenced more by the North Atlantic Ocean (Laane et al., 1996, van Leussen et al., 1996).

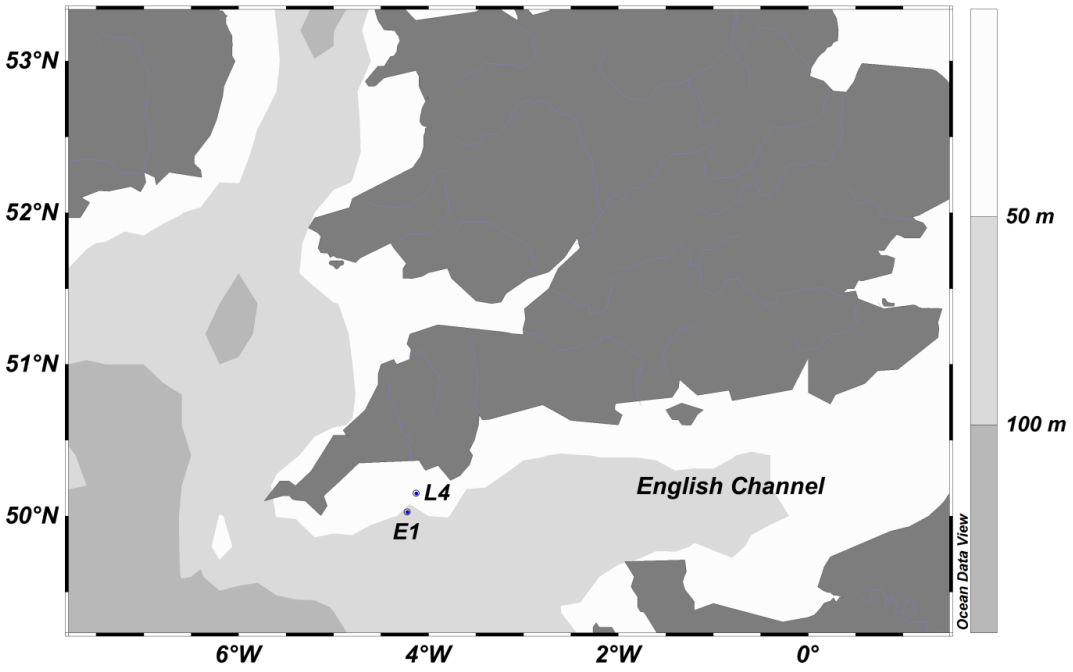

Figure 4.1. Location of Western Channel Observatory time series stations L4 and E1.

4.2.2 Sampling strategy.

1 L of seawater was collected from 1 m, 25 m (L4)/30 m (E1) and 50 m (L4)/60 m (E1) between 09:00 and 11:00 am GMT using a 10 L Niskin bottle. Samples were collected into 1 L aged sterile plastic bottles that were rinsed with sample water x3 prior to filling. Seawater samples were immediately filtered onto sterile 0.2 µm cellulose nitrate membranes. Each depth was filtered simultaneously in replicates of four using a 6 funnel filter manifold and vacuum pump. Membranes were transferred using sterile forceps into 1.5 mL autoclaved centrifuge tubes and frozen on dry ice before being stored at -80 °C on return to the laboratory.

4.3 Results

4.3.1 Physicochemical and general plankton characteristics at the Western Channel Observatory

Environmental metadata was obtained from the Western Channel Observatory, the majority of which was concurrent with water sampling for the bacterial analysis with the exception of a few data points that were collected a day or two before or after seawater sampling (table 2.2). During the 2015 spring-summer study period, seawater temperature at both stations increased steadily from 9 °C in March to 16 °C in July, with thermal stratification appearing in late April at Station L4 (surface-bottom ≥0.5 °C) and by early June (surface-bottom ≥1 °C) at Station E1 (figure 4.2a). Salinity at Station L4 was variable, but overall increased from March to July and ranged from 35.09–35.35 PSU. In contrast, salinity at Station E1 was more uniform and ranged from 35.25–35.43 PSU, decreasing slightly from March to July. The upper 20 m became fresher than the underlying water column from late April at Station L4 and late May at Station E1 (figure 4.2b). Seawater oxygen ranged from 231.9–296.2 µM at Station L4 with peaks in March and April, and from 236.6–290.7 µM at Station E1 with a peak in April. Oxygen was also higher in the upper 20 m than the underlying water column from June onwards at both stations (figure 4.2c). Two main fluorescent peaks were observed at Station L4, the first appeared throughout the water column in early April and a second more intense peak was seen between 25 and 50 m from late April to early May. The fluorescent signal remained at approximately 1 FSU throughout May and was very low throughout June with a surface peak seen in July. A peak in fluorescence was present throughout April at Station E1, but was otherwise low, except for two small intense peaks seen in the mid water column mid-June and Late July (figure 4.2d).

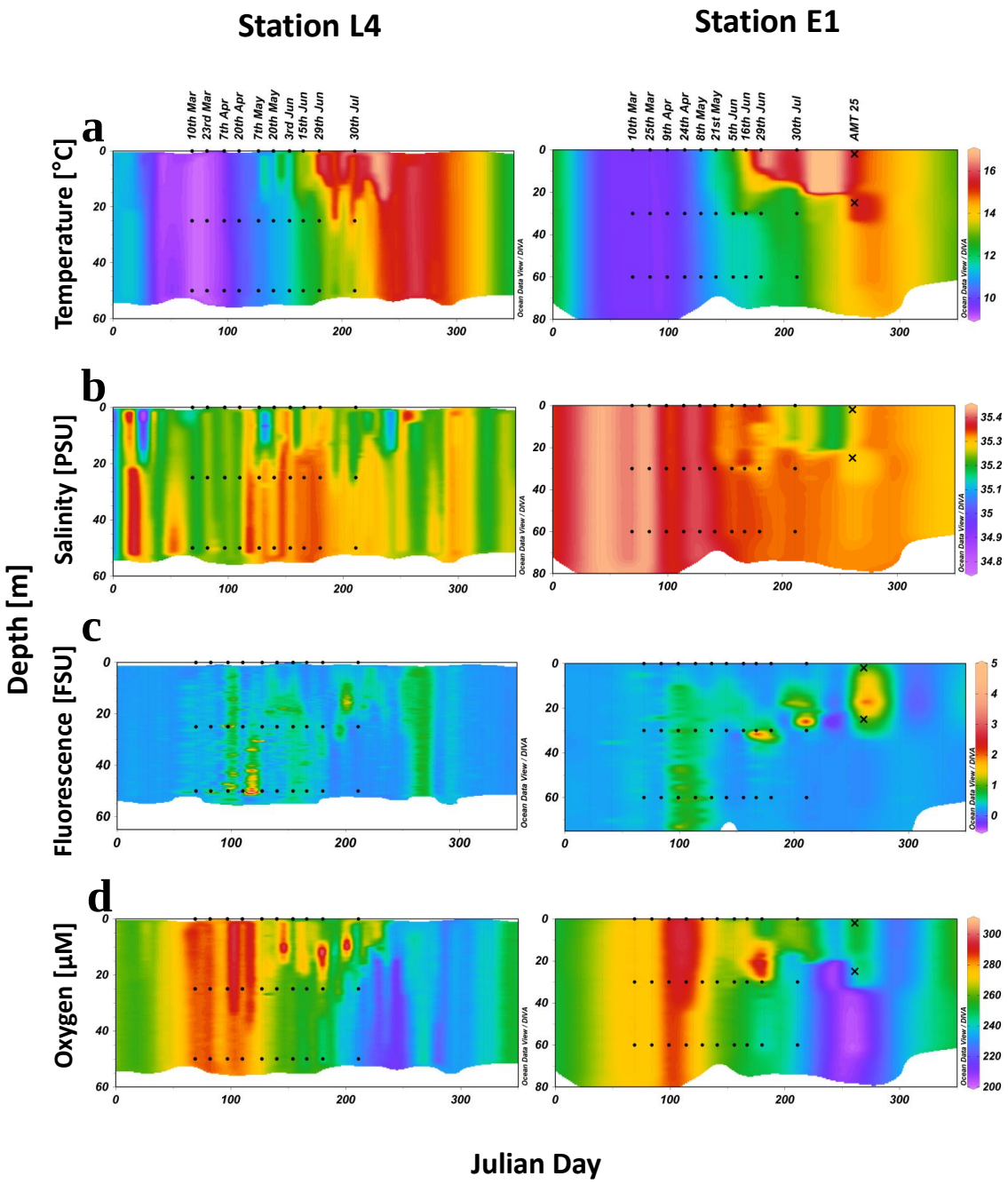

Figure 4.2. Data-Interpolating Variational Analysis (DIVA) gridded section plots showing physicochemical data for stations L4 and E1 measured weekly (L4) and fortnightly (E1) during 2015. a) temperature [°C], b) salinity [PSU], c) photosynthetically available radiation (PAR) [µE m^{-2} S^{-1}] and d) oxygen [µM]. Depth [m] on the Y axis vs. Julian day on the X axis. Black symbols (•) represent the day and vertical position of water samples analysed in this study.

Key nutrients nitrite, nitrate and phosphate all decreased from March to July, with nitrite and nitrate becoming depleted from late April at Station L4 and from early April at Station E1. Phosphate was not depleted until late June at Station L4 and early June at Station E1. All three nutrients were completely depleted below the detection limit in the upper water column from late May at Station L4 and early May at Station E1 (figure 4.3).

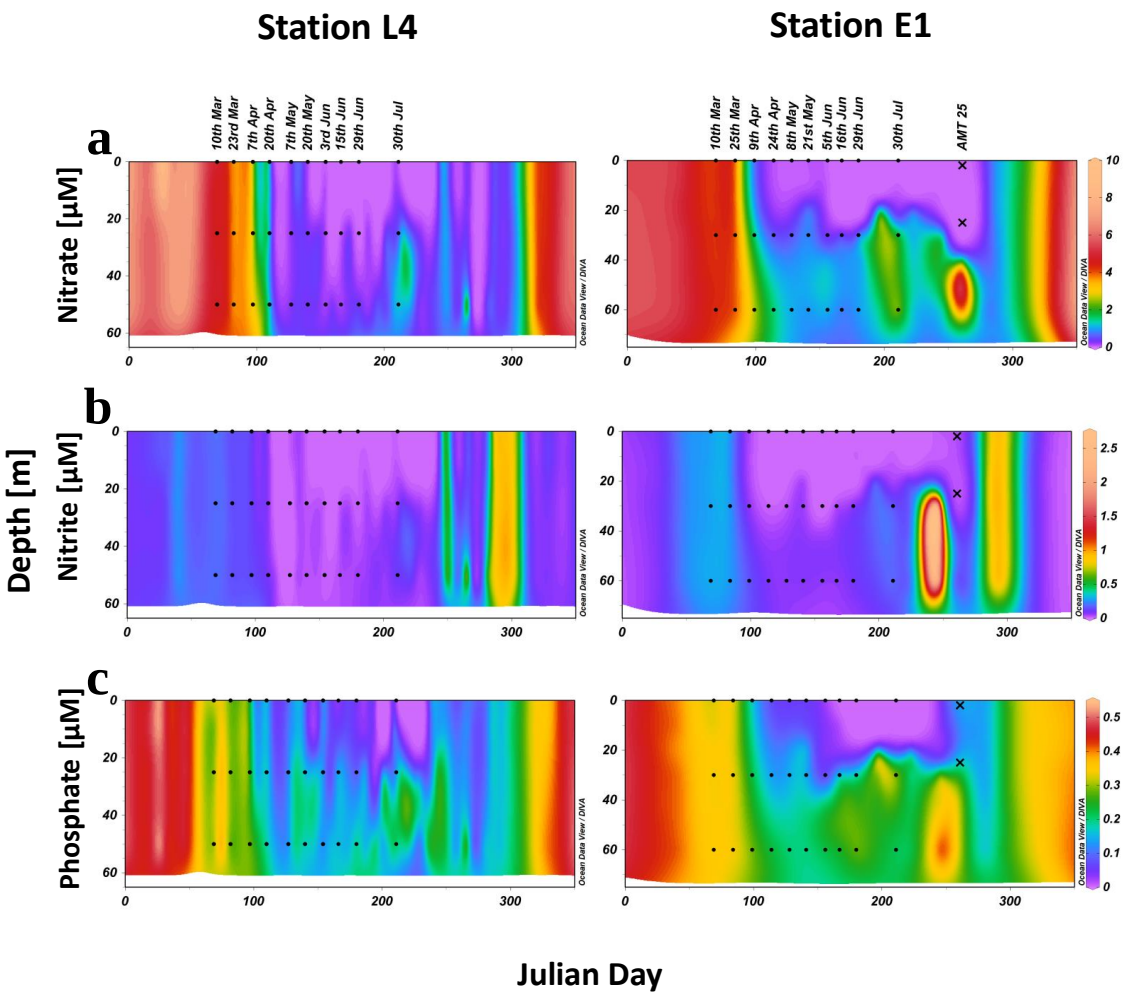

Figure 4.3. Data-Interpolating Variational Analysis (DIVA) gridded section plots showing nutrients data [µM] for stations L4 and E1 measured weekly (L4) and fortnightly (E1) during 2015. a) nitrate, b), nitrite, c) ammonia and d) phosphate. Depth [m] on the Y axis vs. Julian day on the X axis. Black symbols (•) represent the day and vertical position of water samples analysed in this study.

Phytoplankton and zooplankton counts were only available from a 10 m depth. Phytoplankton abundance at both stations peaked in April and July with a smaller peak also observed in May. Phytoplankton abundance was dominated by phytoflagellates, which accounted for >70% relative abundance (RA) of the community in any one month at both stations (figure 4.4a). However, the distribution of phytoplankton groups was more informative when quantified by biomass. At Station L4, diatoms dominated in March (71 % RA) and peaked again in May (40 % RA). Phytoflagellates were most abundant in April (59 % RA) and autotrophic dinoflagellates were most abundant in July (91 % RA) (figure 4.4bi). At Station E1, phytoflagellates dominated in March (60% RA) and April (55 % RA), diatoms were also most abundant in March (35% RA) and April (31 % RA), and dinoflagellates dominated May to July (mean 66% RA) (figure 4.4bii). Coccolithophorids reached a maximum biomass of 5 % and 2 % RA in April at Station L4 and E1 respectively.

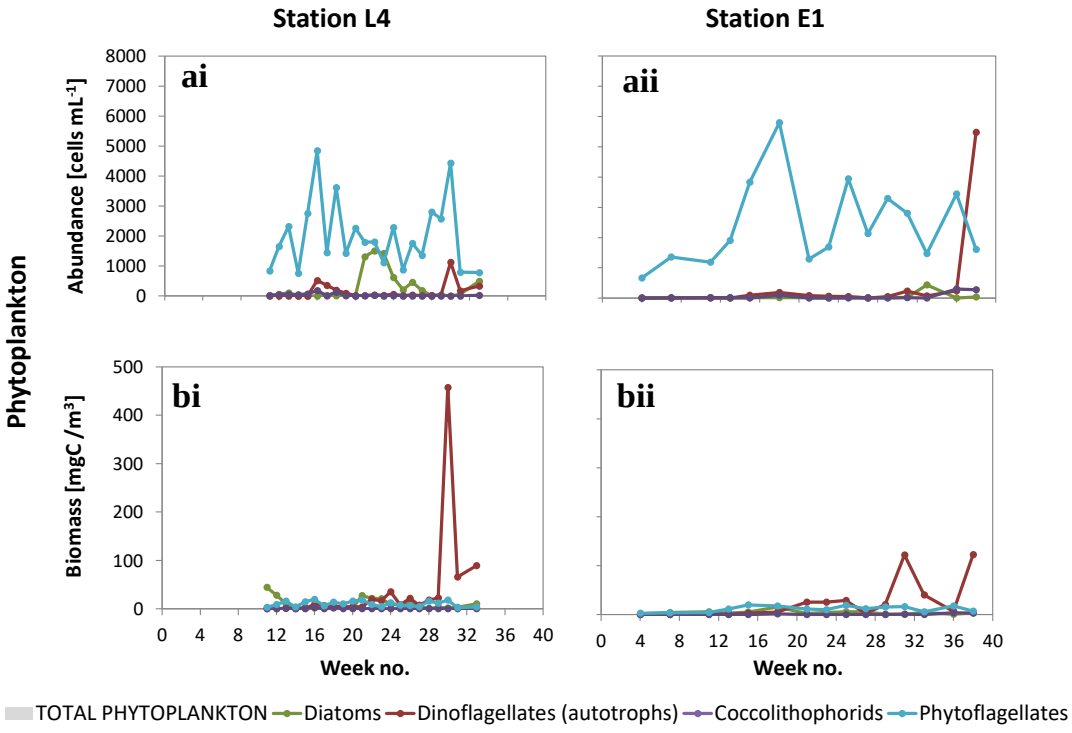

Figure 4.4. Phytoplankton a) abundance [cells mL^{-1}] and b) biomass [mgC/ m^3] at i) Station L4 and ii) Station E1.

Microzooplankton abundance at Station L4 was dominated by zooflagellates >70 % RA in all months except June when ciliates (50 % RA) and colourless dinoflagellates (34 % RA) dominated (figure 4.5ai). In contrast, zooflagellates made up relatively little of the zooplankton population by biomass (mean 6 % RA). Colourless dinoflagellates dominated (mean 54% RA) and were most abundant in June (69 % RA) and July (78 % RA), followed by ciliates (mean 40 % RA) which peaked in April (63 % RA) (figure 4.5bi). At station E1, zooflagellates also dominated zooplankton abundance (mean 47 % RA) but were most abundant during March and April (mean 82%). Colourless dinoflagellates (mean 34 % RA) were most abundant during May (65 % RA) and July (52% RA), and ciliates (mean 20 % RA) were most abundant in June (50 % RA) (figure 4.5aii). However, at E1 zooflagellates only accounted for ~1 % RA of zooplankton biomass, whereas the biomass of heterotrophic dinoflagellates (mean 50% RA) and ciliates (48 % RA) were abundant across all months (figure 4.5bii).

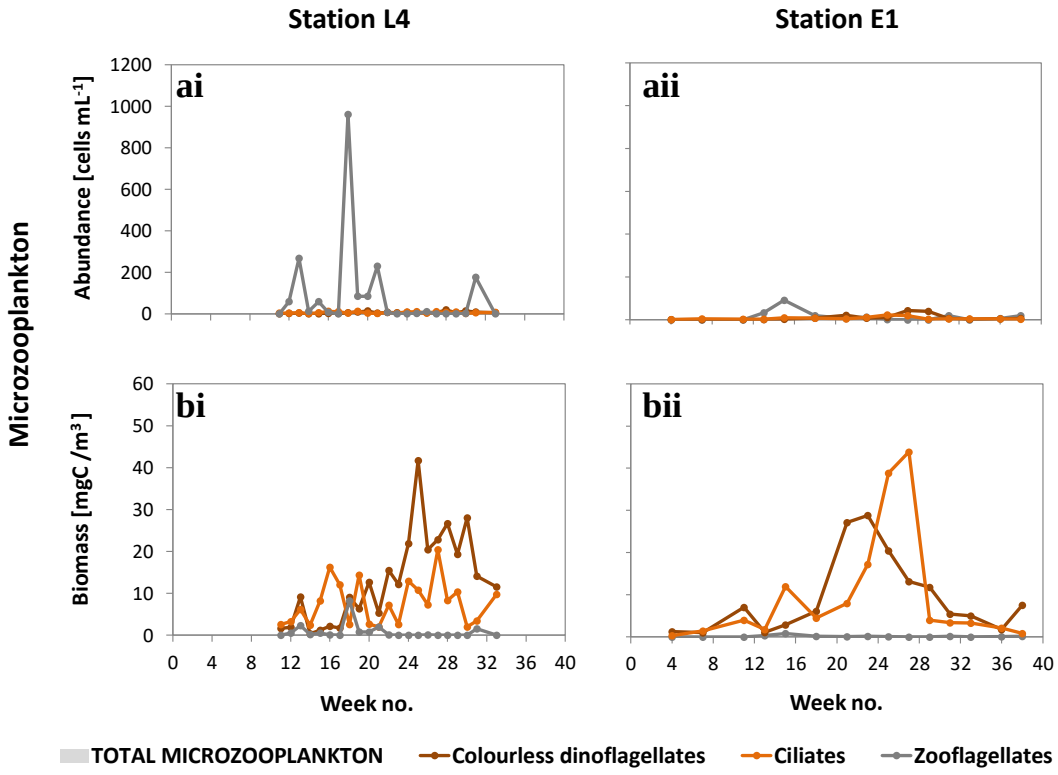

Figure 4.5. Zooplankton a) abundance [cell mL^{-1}] and b) biomass [mgC/ m^3] at i) Station L4 and ii) Station E1.

4.3.2 General bacterioplankton diversity

The bacterioplankton communities at stations L4 and E1 were assessed by 16S rRNA gene amplicon high-throughput sequencing (HTS). Reads were filtered to exclude singletons, eukaryotic, archaeal and organelle sequences and rarefied to a depth of 5266 reads per sample resulting in a total of 310,694 high quality reads that represented 878 operational taxonomic units (OTUs) based on 97% similarity. 26 abundant (>0.1 % RA) orders at Station L4 and 32 abundant (> 0.1 % RA) orders at Station E1 were identified. The bacterioplankton communities at both stations were dominated by 3 major bacterial orders, which accounted for 78 % of the total normalised abundance across all samples; the *Rhodobacterales* were most abundant (33 %), followed by the SAR11 clade (24%) and the *Flavobacteriales* (20%) (figure 4.6a and b).

Log-likelihood ratio tests showed that the orders *Rhodobacterales* (statistic =73, Bonferroni p <0.000), Caulobacterales (statistic =15, Bonferroni p =0.009) and *Flavobacteriales* (statistic =14, Bonferroni p =0.019) were significantly more abundant at Station L4, whereas the SAR11 clade (statistic =78, Bonferroni p <0.000) and the orders *Alteromonadales* (statistic =68, Bonferroni p <0.000) were significantly more abundant at Station E1. Log-likelihood ratio tests also showed that 2 orders were significantly different by depth; *Alteromonadales* (statistic =72, Bonferroni p <0.000) was more abundant in deep samples and *Flavobacteriales* (statistic =26, Bonferroni p <0.000) was more abundant in mid water column and surface samples at both station L4 and E1.

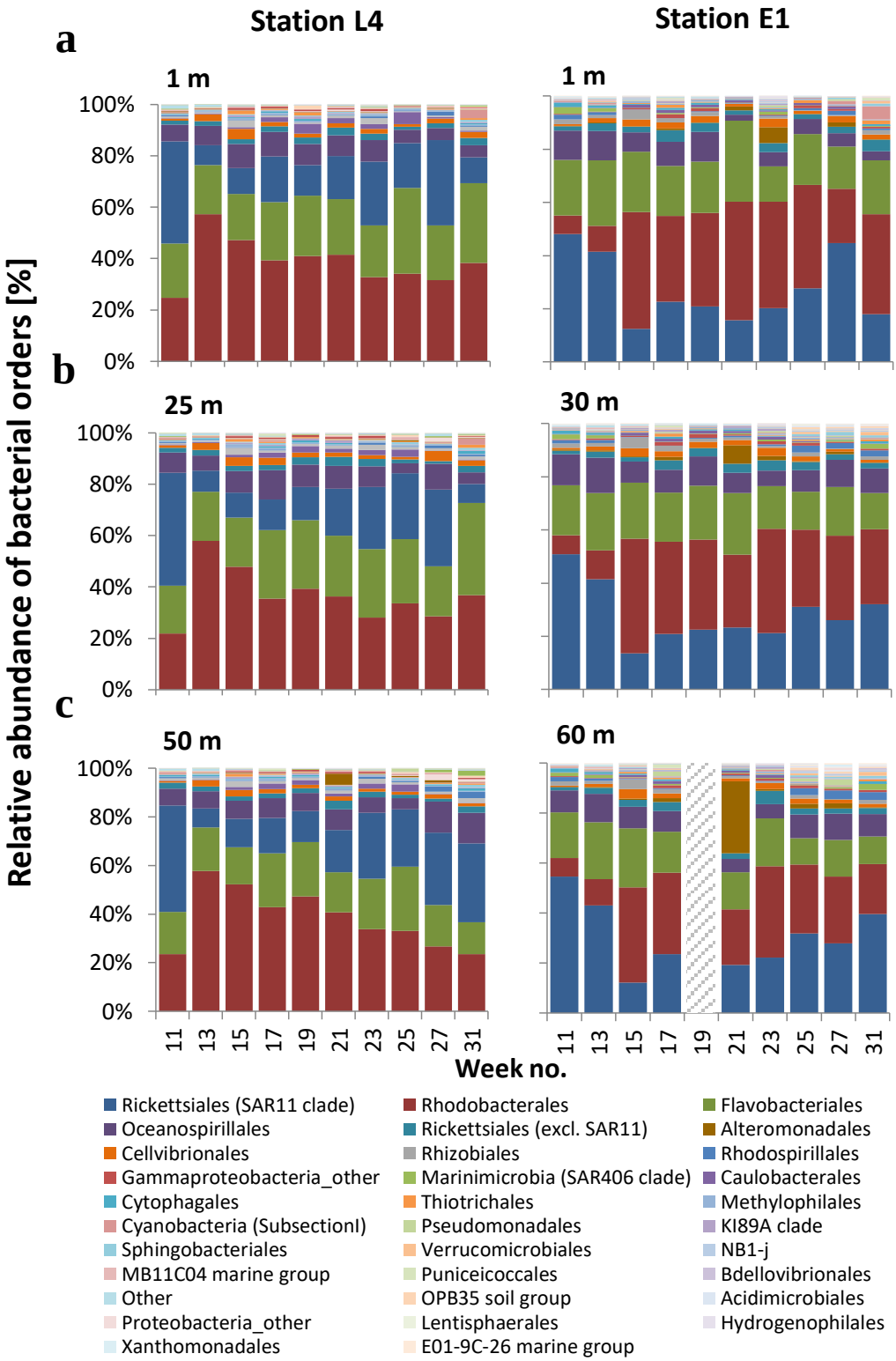

Figure 4.6. Variation of bacterial orders (>0.1% relative abundance) by week at the time series stations L4 and E1 for each sampling depth; a) surface (1 m) b) Mid-water column (L4 25 m / E1 30 m) and c) deep (L4 50 m / E1 60 m) shaded bars indicate missing data.

4.3.3 Temporal and spatial variance in community structure by beta diversity analyses

Weighted UniFrac distance matrices were used to compare the diversity between samples. L4 and E1 samples were on average 25 % (SD 12 %) dissimilar to each other, with the greatest dissimilarity (58 %) seen during week 13 (6^{th}-12^{th} April). Overall, there was little dissimilarity (generally <10 %) between sample depths, however greater dissimilarity (mean 21 %, SD 10) was seen between depths from weeks 25-31 at Station L4 and from weeks 21-31 at Station E1 (Supplemental figure 4.1).

Principle coordinates analysis (PCoA) (figure 4.7a) showed that samples clustered into 3 main groups; group 1 = March samples excluding L4 week 13, group 2 = L4 week 13, all April samples and May week 19, and group 3 = May samples excluding week 19, all June and July samples. A minimum spanning tree (MST) model (figure 4.7b) was also used to connect samples by their minimum distance (i.e. to the most closely related sample). The MST confirms the grouping observed in the PCoA and reveals more details of the relationships between samples within the suggested groupings. Group 1 was most similar to the July deep (L4 50 m, E1 30 and 60 m) samples. Stations L4 and E1 in Group 2 were distinct from each other except during week 15, stations L4 and E1 remained distinct from each other throughout May. Samples in group 1 and 2 varied little by depth whereas samples in group 3 showed more variation by depth, especially during weeks 21 and 25-31 at Station E1 and during weeks 25-31 at Station L4. Permutational multivariate analysis of variance (PERMANOVA) showed that stations L4 and E1 were significantly different to each other (*pseudo-F* 6.7, p = 0.001) and that samples were significantly different to each other when grouped by month (*pseudo-F* 8.2, p = 0.001). No significant difference was seen between samples grouped by depth.

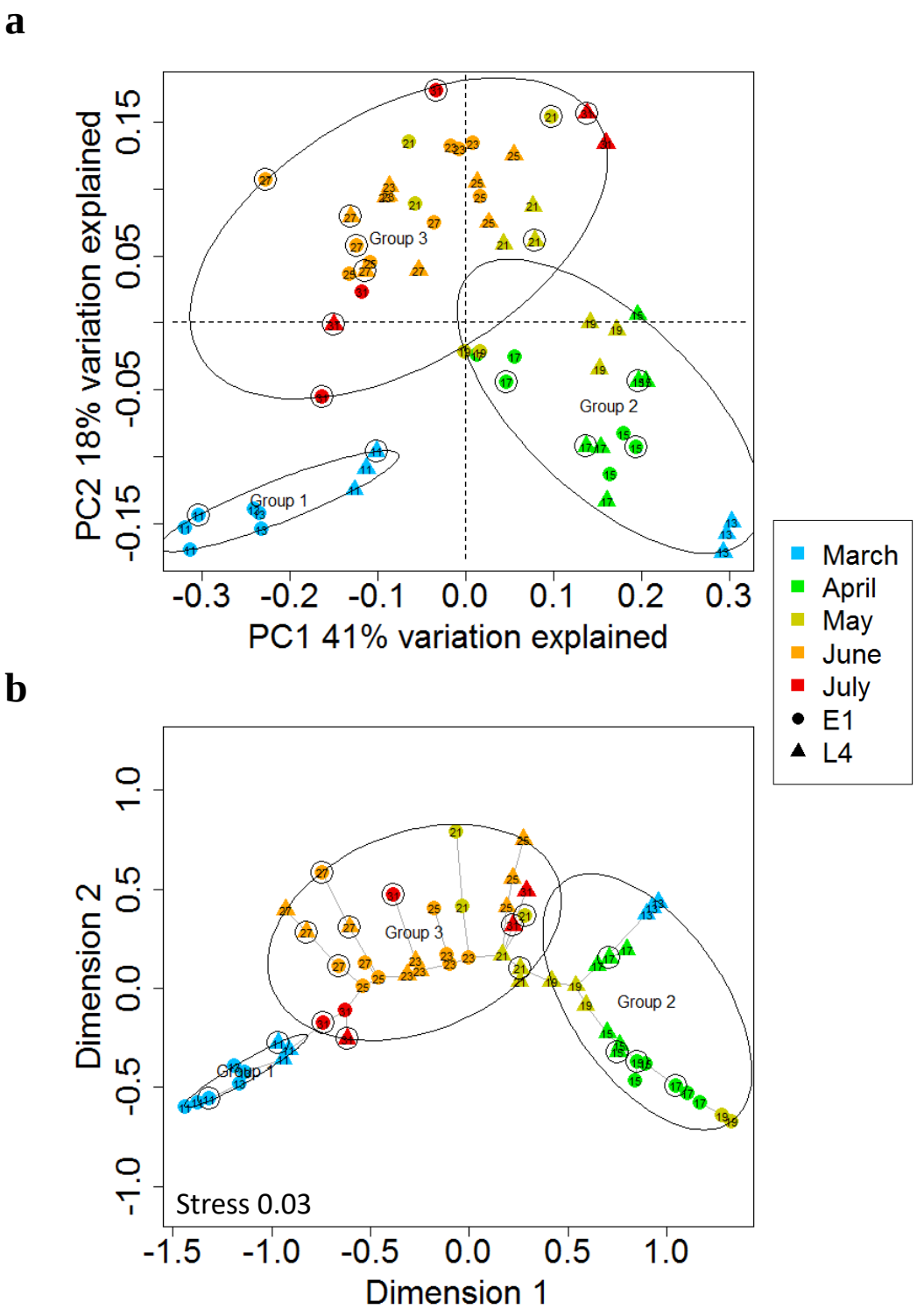

Figure 4.7. a. Principle coordinates analysis (PCoA) and b. minimum spanning tree (MST) using weighted UniFrac distance metrics of all 16S rRNA gene samples. Points represent an individual sample and are coloured by month, symbols represent the sampling station (circles = E1, triangles = L4). Circled points identify *coxL-2* sequenced samples and numbers indicate sample week.

4.3.4 CO-oxidising bacterioplankton diversity

The CO-oxidising bacterioplankton communities at stations L4 and E1 were assessed by *coxL* Form I gene amplicon high-throughput sequencing. Reads were filtered to exclude singletons and clustered into OTUs based on 97 % similarity. DNA sequences were translated to amino acid sequence and bacterial *coxL* identified from the NCBI RefSeq non-redundant protein record, resulting in 241 bona fide *coxL* OTUs that were then rarefied to a depth of 1185 reads per sample. 53 abundant (> 0.1 % RA) OTUs at Station L4 and 48 abundant (> 0.1 % RA) OTUs at Station E1 were identified. The CO-oxidising bacterioplankton community at both stations was dominated by 6 OTUs that accounted for 74 % of the total normalised abundance across all samples (OTU_2 = 25 %, OTU_3 = 16 %, OTU_5 = 11 %, OTU_4 = 7%, OTU_7 = 8% and OTU_11 = 6%) (figure 4.8).

Log-likelihood ratio tests showed only 2 OTUs were significantly different between stations L4 and E1; OTU_5 was 1.6 times higher at Station L4 (statistic =15, Bonferroni p <0.000) and OTU_3 was 1.5 times higher at Station E1 (statistic =15, Bonferroni p <0.000). Log-likelihood ratio tests also showed 16 OTUs were significantly different by month (Bonferroni $p < 0.05$) (supplemental table 4.1).

Focusing on the 6 most abundant OTUs from both stations, OTU_2 abundance steadily decreased from March to July, whereas OTU_3 and OTU_4 increased in abundance, with the greatest increase seen between May and July. OTU_5, OTU_7 and OTU_11 were more uniformly distributed between months. OTU_5 peaked in May, where as OTU_7 and OTU_11 showed small peaks in April and June.

Log-likelihood ratio tests also showed the 6 most dominant OTUs were significantly different by depth; OTU_11 (statistic =66, Bonferroni p <0.000), OTU_2 (statistic =45, Bonferroni p <0.000) and OTU_7 (statistic =44, Bonferroni p <0.000) were respectively 27.2, 3.8 and 4.0 times higher in the deep samples compared to the surface samples. OTU_3 (statistic 21, Bonferroni p <0.000), OTU_5 (statistic =19, Bonferroni p <0.000) and OTU_4

(statistic =19, Bonferroni p <0.000) were 6.2, 1.5 and 1.4 times higher in the surface samples compared to the deep samples.

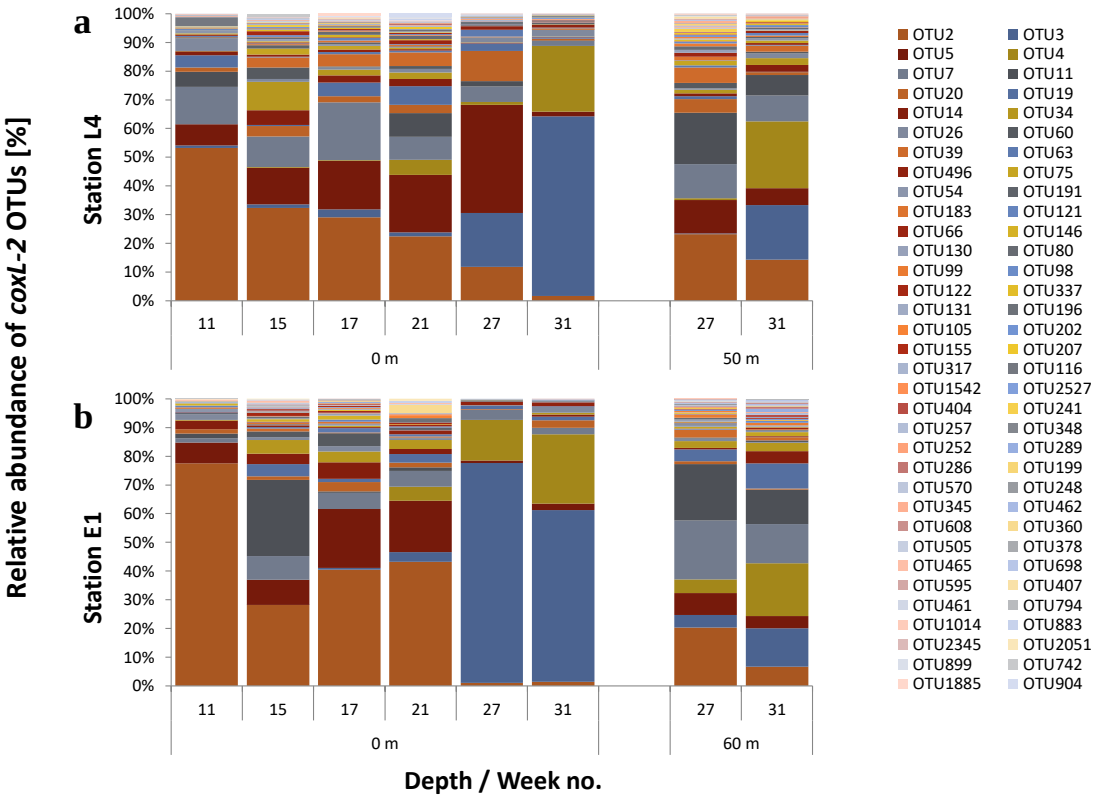

Figure 4.8. Relative abundance showing the variation of bacterial *coxL* OTUs (>0.1% relative abundance) by week at the time series stations a) L4 and b) E1.

4.3.5 Variance in bacterial CO-oxidising communities by beta diversity analyses

Weighted UniFrac distance metrics were used to compare *coxL* diversity between samples. The dissimilarity between the surface samples at stations L4 and E1 increased steadily from 12 % in week 11 to 53 % in week 27, then declined rapidly to 7 % by week 31. In addition to the surface samples, deep samples were included for weeks 27 and 31. Dissimilarities between Station L4 and E1 deep samples were 35 %. The dissimilarity between surface and deep samples was greater at E1 (mean 61 %, SD12) than at L4 (mean 42 %, SD6), with the greatest difference between depths at both stations seen during week 27 (supplemental figure 4.1b).

PCoA (figure 4.9a) showed that April, May and June (excl. June E1 surface) formed a cluster and together with March samples, were distinct from the July samples (including June E1 surface) that were separated along axis PC1. The July surface (including June E1 surface) and deep samples were also distinct from each other and separated along axis PC1 and PC2. MST confirms the grouping of samples seen in the PCoA and shows more intra-variability by May and June samples than by March and April samples (figure 4.9b). PERMANOVA showed that samples were significantly different to each other when grouped by month (*pseudo-F* =3.7, *p* =0.029), but no significant difference was seen between samples grouped by depth or by station.

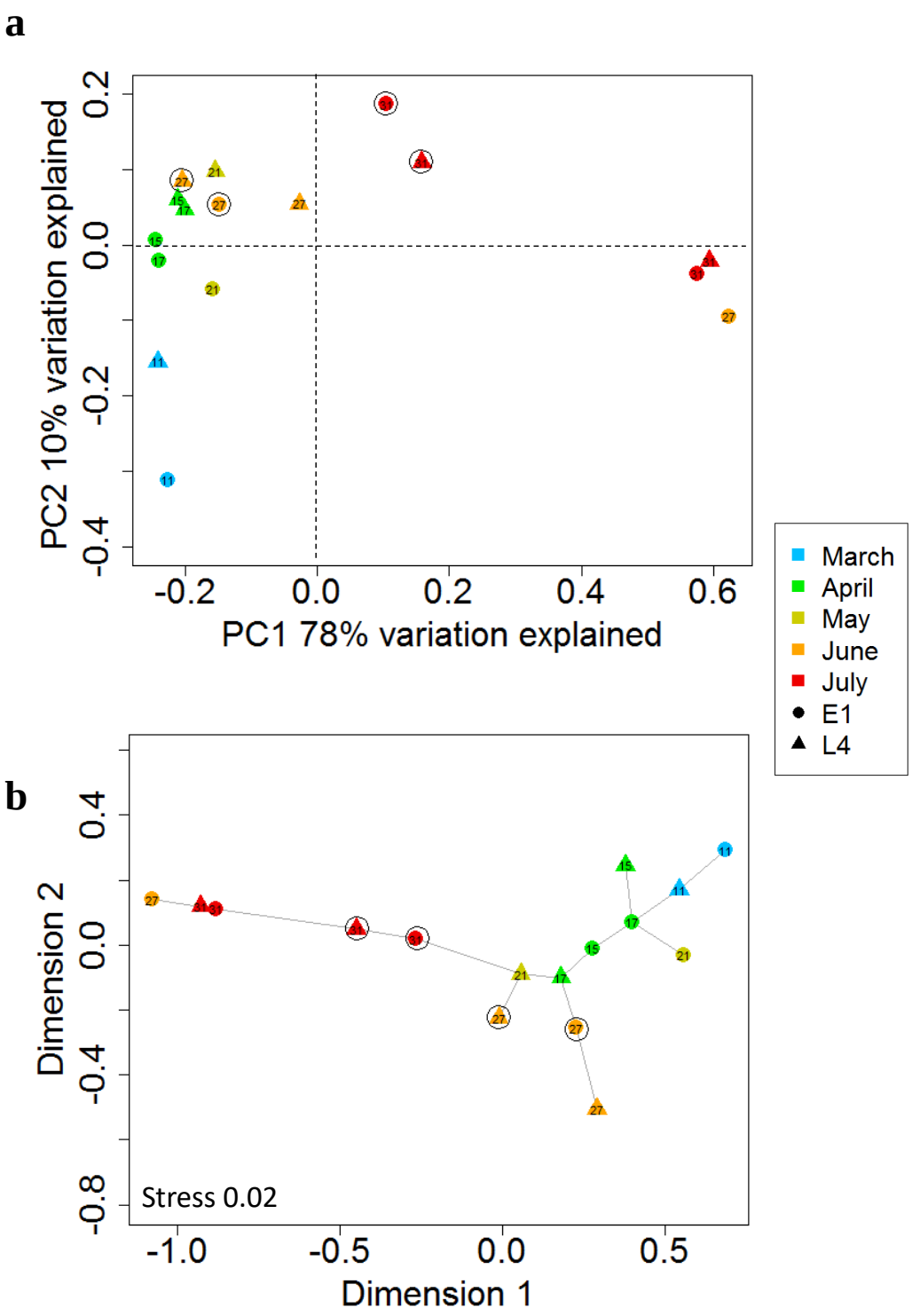

Figure 4.9. a. Principle coordinates analysis (PCoA) and b. minimum spanning tree (MST) using weighted UniFrac distance metrics of all *coxL* sequenced samples. Points represent an individual sample and are coloured by month. Symbols represent the sampling station (circles = E1, triangles = L4), numbers indicate sample week and circles identify deep samples.

4.3.6 Relationship between total bacterial and CO-oxidising bacterial communities with physicochemical and biological metadata

Spearman's rho correlations were performed with the microbial sequence data and cognate physicochemical metadata. For the 16S rRNA samples, PC1 correlated positively with fluorescence (R = 0.37, p =0.004) and oxygen (R =0.36, *p* =0.005), and negatively with salinity (R =-0.45, *p* <0.000), nitrite (R =-0.33, *p* =0.015) and wind speed (R =-0.39, *p* =0.004). PC2 correlated positively with seawater temperature (R =0.78, *p* <0.000), UV (R =0.75, *p* <0.000) and solar energy (R = 0.68, *p* <0.000), and negatively with oxygen (R =-0.61, *p* <0.000), nitrite (R =-0.69, <0.000), nitrate (R =-0.77, *p* <0.000) and phosphate(R =-0.74, *p* <0.000). PC1 and PC2 also correlated positively with several phytoplankton and microzooplankton groups (supplemental table 4.2).

For the *coxL* samples, PC1 correlated positively with seawater temperature (R =0.89, *p* <0.000), solar energy (R =0.66, *p* =0.005) and UV (R =0.65, *p* =0.007), and negatively with oxygen (R =-0.79, *p* <0.000), nitrate (R =-0.52, *p* =0.048), phosphate (R =-0.59, *p* =0.026 and precipitation (R =0.51, *p* =0.044). PC2 correlated positively with depth [m] (R =0.61, *p* =0.62) and negatively with PAR (R =-0.51, *p* =0.045).

Redundancy analysis (RDA) was performed on the 16S rRNA gene samples, constraining the ordination by significantly correlated physicochemical variables to see how these characteristics influence the ordination of samples. Variables with >2 missing data points were excluded, and where associated variables co-correlated (e.g. seawater temperature and solar energy), only one representative was used in the analysis. The RDA model using significantly correlated physicochemical metadata (figure 4.10) significantly explained the variation in the samples and showed a similar ordination of samples to the original PCoA. The RDA model using significantly correlated biological metadata distorted the ordination but maintained the same core grouping of samples seen in the original PCoA. Permutation tests on the RDA models revealed that the physicochemical RDA model was

stronger (*pseudo-F* =6.82, *p* =0.001) than the biological RDA model (*pseudo-F* =4.7, *p* =0.001) at explaining the variation between samples. The combined RDA model (*pseudo-F* =5.39, *p* =0.001) showed that salinity (*pseudo-F* =13.54, *p* =0.001), seawater temperature (*pseudo-F* =12.36, *p* =0.001) and phytoflagellate biomass (*pseudo-F* =5.14, *p* =0.002) were the strongest metadata variables that explained variation between samples.

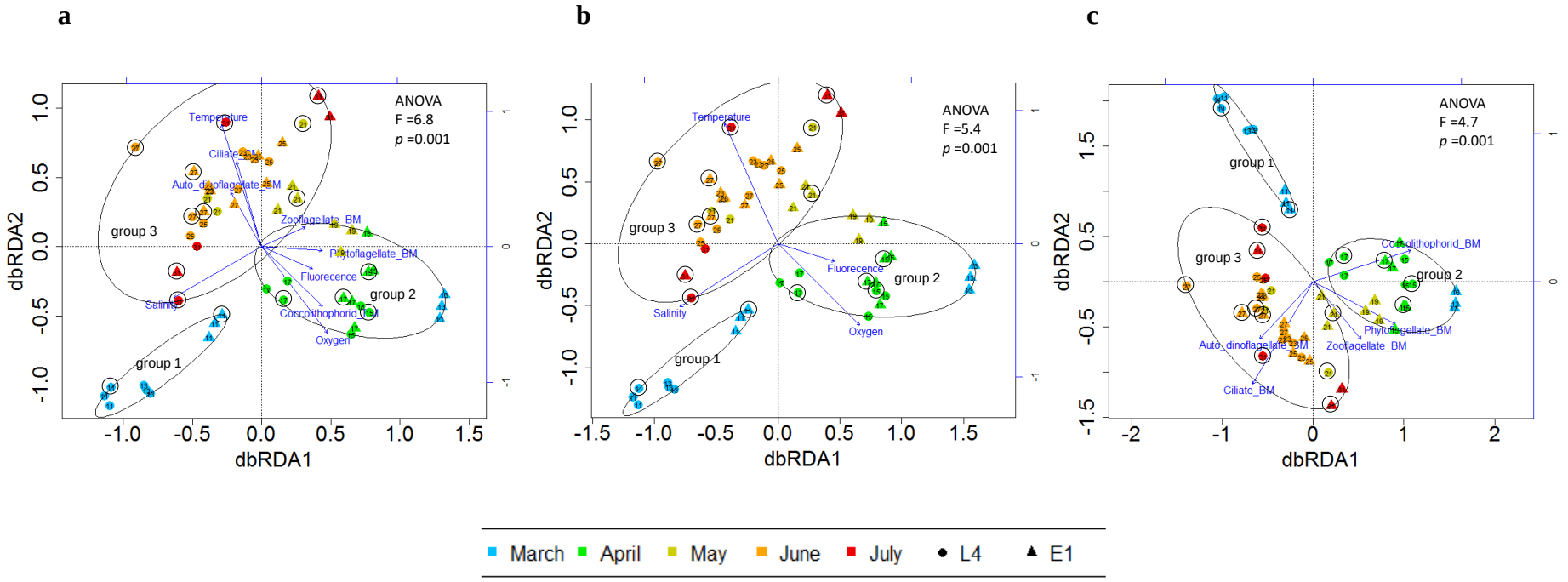

Figure 4.10. Redundancy analysis of weighted UniFrac distance metrics on all 16S rRNA gene sequenced samples. Ordination is constrained by selected significantly correlated metadata variables a) combined physicochemical and biological metadata, b) physicochemical metadata and c) biological metadata. Blue arrows represent continuous explanatory variables fitted to the ordination; direction indicates the maximum change whereas the length indicates the magnitude of change for a variable. Points represent an individual sample and are coloured by month, symbols represent the sampling station (circles = E1, triangles = L4) and numbers indicate sample week and circled points identify *coxL* sequenced samples.

4.4 Discussion

4.4.1 General environmental characteristics at Station L4 and E1.

Temperature and salinity at Station L4 and E1 in 2015 were typical for the Western Channel Observatory (WCO) and followed previously described patterns (Smyth et al., 2010). The main phytoplankton blooms at Station L4 typically occur as a spring diatom-dominated bloom in April which occurs in response to high nutrients, increasing temperatures and light levels, and a secondary summer diatom and flagellate bloom in subsurface waters as a result of nutrient regeneration below the thermocline (Southward et al., 2005, Widdicombe et al., 2010). During this study, the patterns observed in the fluorescence corresponded well with peaks in phytoplankton and oxygen that described a typical phytoplankton abundance cycle at Station L4. With the exception of diatoms, which were in an unusually low abundance during April and gave way to a phytoflagellate dominated spring bloom, the patterns in phytoplankton abundance and biomass were also typical for this study area (Widdicombe et al., 2010). The anomaly seen in diatom abundance at Station L4 in 2015 is not characteristic of a typical year, however inter-annual variation in phytoplankton at Station L4 has been reported previously (Widdicombe et al., 2010). This atypical spring bloom may be caused by change in climatological, hydrological or grazing processes (Southward et al., 2005, Irigoien et al., 2000, Irigoien et al., 2005, Widdicombe et al., 2010). The abundance of diatoms has been shown to correlate with the winter North Atlantic Oscillation (NAO) index which is characterised by increased mixing processes (Irigoien et al., 2000). April 2015 had below average rain fall of 10 mm compared to an 8 year mean of 46 mm for April (supplemental figure 4.2a), which may have favoured a phytoflagellate bloom due to increased light (reduced cloud cover) and stability (reduced mixing) (Irigoien et al., 2000).

4.4.2 Depth resolved bacterioplankton diversity and community succession at the Western Channel Observatory

Previous studies that have characterised bacterioplankton abundance and diversity at the WCO have focused primarily on the surface waters (<10 m) at Station L4. Bacterioplankton abundance and biomass at Station L4 typically increase from March to July (Rodríguez et al., 2000, Mary et al., 2006a). The Station L4 bacterioplankton community is dominated by the *Alphaproteobacteria*, the bulk of which are within the SAR11 clade, and the *Rhodobacterales* which are dominated by the MRC. *Bacteroidetes* (mainly *Flavobacteria*) and members of the *Gammaproteobacteria* are also found in abundance at Station L4. In addition to the dominant community, sporadic blooms of rare taxa have also been recorded at Station L4 (Gilbert et al., 2012). In this study, Station L4 and Station E1 were sampled weekly at three depths spanning the entire water column. The bacterioplankton community composition at Station L4 and Station E1 throughout the water column was very similar to existing studies describing Station L4 surface waters (Mary et al., 2006a, Gilbert et al., 2009, Gilbert et al., 2012), and was dominated by SAR11, *Rhodobacterales* and *Flavobacteriales*.

The seasonal succession of bacterioplankton has also been well characterised in the surface waters of Station L4 and is typified by a SAR11 dominated community in the winter, transitioning to a *Rhodobacterales* (*Rhodobacteraceae*) dominated community in the spring and summer (Mary et al., 2006a, Gilbert et al., 2012). This pattern of succession is characteristic of other temperate coastal and shelf seas (Alonso-Sáez et al., 2007, Teeling et al., 2016). Owing to the long time-series at the WCO, we know this annual cycle of succession in community composition is robust and predictable (Gilbert et al., 2012). During this study, we also observed significant seasonal variation in the bacterioplankton community, at both station L4 and E1 that was comparable to previous studies at Station L4. 24 of the 26 orders at Station L4 and 28 of the 32 orders at E1 were significantly different in abundance by month. Beta diversity analyses showed that generally the community

exhibited succession by consecutive month and three main groups were identified 1) a pre-bloom community, 2) a spring bloom community and 3) a summer community.

At both Station L4 and E1, pre-bloom and spring bloom communities were uniform throughout the water column, whereas summer communities became distinct above and below the thermocline. Deep summer communities below the thermocline were more similar to pre-bloom communities than their corresponding surface community. The between depth dissimilarity increased 3 fold during summer at both stations and coincided with the formation of thermal stratification evidenced by a 1 °C change in temperature between the surface and bottom of the water column. Thermal stratification at Station L4 has previously been described by a more conservative cut-off (Δ0.5 °C between 0 and 30 m) than Station E1 (Δ1 °C between 0 and ~75 m) (Smyth et al., 2010). Our result suggests that the bacterioplankton community is only affected by thermal stratification processes when the temperature difference is ≥ 1° C between the surface and bottom of the water column, which in this study occurred later at Station L4 than at Station E1. Summer bacterioplankton communities play an important role in the regeneration of nutrients, which fuel the late summer phytoplankton bloom on the breakdown of stratification (Rodríguez et al., 2000). The presence of distinct communities within the water column during summer suggests this process is more complex than previously thought. Further work is required to determine the individual contribution that these communities to nutrient regeneration.

4.3.3 Environmental drivers of bacterioplankton seasonal succession at the Western Channel Observatory

Rodríguez et al. (2000) showed that bacterial abundance was determined by seawater temperature driven growth rates versus countering bacterivorous grazing rates, and that bacterial biomass was influenced by seawater temperature during autumn and winter and by biological interactions during spring and summer. Gilbert et al. (2009) found that seawater

temperature and nutrients (e.g. phosphate and silicate) influenced the bacterioplankton community, and in a later study Gilbert et al. (2012) went on to describe complex physicochemical and biological interactions at Station L4. This study also found significant correlations with physicochemical and biological parameters. To identify which of these parameters were most important in the seasonal structuring of the microbial community, redundancy analysis was performed to test the response of the bacterioplankton community to different explanatory variables. The results showed that physicochemical variables explained the variation more strongly than biological variables, and that salinity closely followed by seawater temperature were the most influential drivers of community structure.

Salinity showed contrasting trends between the stations over the study period, and consequently it is difficult to infer the ecological significance of this variable in determining bacterioplankton succession. Salinity at Station E1 showed a slightly decreasing trend over the study period and was generally higher than at Station L4, which showed an overall increasing trend over the study period and was much more variable due to influences from the river Tamar (Rees et al., 2009, Smyth et al., 2010). The RDA analysis reflected the trend in salinity seen at E1 suggesting salinity is a more influential variable at Station E1 than at Station L4. Given the similarity in the overall pattern of succession between the two stations, salinity may describe between station variability better than between month variability. The spring bloom community was associated with lower seawater temperature and increased primary production, whereas summer communities showed the opposite trend. Pre-bloom communities were associated with both lower seawater temperatures and lower primary productivity. This suggests that bacterioplankton are primarily responding to changing temperature until a threshold of primary productivity is reached after which phytoplankton also influence the community composition as has previously been suggested (Rodríguez et al., 2000).

Of the phytoplankton, phytoflagellate biomass was the strongest significant influencing biological variable and was more strongly associated with the spring bloom community, whereas the summer community was more strongly associated with dinoflagellate biomass. These associations fit with the patterns seen in the phytoplankton abundance data, however, as surface measurements were assumed for the entire water column, it is difficult to make complete conclusions about influence of phytoplankton on the bacterioplankton community from this dataset.

This study focused on a few key variables and cannot account for trophic interactions or mortality, the complexities of which have been discussed previously (Rodríguez et al., 2000, Gilbert et al., 2012). The comparable bacterioplankton community succession seen in 2015 (this study) with previous studies (Gilbert et al., 2009, Gilbert et al., 2012), coupled with the non-typical spring bloom, supports the earlier result that physicochemical factors are stronger than biological factors in determining bacterioplankton community structure.

Phytoplankton communities at the WCO also show a strong seasonal scale pattern of community succession (Widdicombe et al., 2010), which has been linked to climate and hydrological processes (Southward et al., 2005), and the dominant spring bloom forming species varying considerably inter-annually (Widdicombe et al., 2010). These data suggest that although specific microbe-microbe interactions are potentially important in structuring the bacterioplankton community (Gilbert et al., 2012), ultimately the seasonal bacterioplankton community structure at the WCO is directly and indirectly influenced by climatological and hydrological process altering the physical, chemical and biological components of the environment.

A fundamentally important consequence of these overarching physicochemical drivers is the coupling of bacterioplankton and phytoplankton community succession. The switch from the metabolically streamlined, oligotrophic, free-living strategy of the SAR11 (Giovannoni et al., 2005) to the phytoplankton-associated, copiotrophic, metabolically

diverse strategy of the *Rhodobacteraceae* (Pujalte et al., 2014) following the spring phytoplankton bloom has been reported in coastal and shelf sea ecosystems globally (Bunse and Pinhassi, 2017). This switch is driven by an increase in phytoplankton-derived organic matter that alters the trophic regime favouring generalist bacterioplankton (Buchan et al., 2014) such as the *Rhodobacterales* and *Flavobacteriales*. The resulting bacterioplankton bloom regenerates nutrients that in turn fuel the subsequent summer phytoplankton blooms (Rodríguez et al., 2000, Bunse and Pinhassi, 2017). The importance of these bacterial groups in secondary production has been reviewed previously by Buchan et al. (2014), who concluded that the ability of bacterioplankton like the *Rhodobacterales* and *Flavobacteriales* to respond to phytoplankton derived substrate is likely due to their metabolic diversity. Recent studies at the WCO have linked changes in the bacterioplankton communities, including the *Rhodobacterales*, to specific phytoplankton derived materials such as microgel particles (Taylor et al., 2014, Taylor and Cunliffe, 2017) and nucleic acids (Taylor et al., 2018).

4.3.4 A comparison of total bacterioplankton communities at Station L4 and E1

Despite the apparent similarity in the taxa present at order and OTU level, Station L4 and E1 bacterioplankton communities were found to be significantly different to each other. In total, Station E1 was slightly more diverse with 730 OTUs in comparison to L4 with 708 OTUs. Station E1 also had a higher number of abundant (>0.1 % relative abundance) orders than Station L4, however these 6 orders 'unique' to Station E1 were present at a low relative abundance (0.11-0.17 %) and were also recorded in the rare fraction (<0.1 % relative abundance) at Station L4.

There were two main drivers of dissimilarity between Station L4 and E1 identified. Firstly, there were significant differences in the abundance of the dominant taxa. The *Rhodobacterales*, *Flavobacteriales* and *Caulobacterales* were found to be significantly

higher at Station L4, whereas SAR11 and were significantly higher at E1. The bacterioplankton community at both stations were characteristic of productive coastal shelf seas (Rappe et al., 2000, Zinger et al., 2011), however, the higher abundance of the metabolically diverse and often phytoplankton-associated taxa at Station L4 points toward a more productive ecosystem than the relatively more oligotroph dominated Station E1. The significant abundance of *Alteromonadales* at E1 was due to an acute peak in May, and is most likely a 'sporadic bloom' in response to increased substrate availability which is typical of these taxa (López-Pérez and Rodriguez-Valera, 2014). Secondly, there are different phenological changes in bacterioplankton communities. The succession from pre-bloom to post-bloom communities occurred earlier (week 11-13) at Station L4 than at Station E1 (week 13-15), and the stratification of bacterioplankton communities was evident earlier at Station E1 (week 21) than at Station L4 (week 25). Station E1 is further offshore than Station L4 and it is likely that the two stations receive different levels of influence from the land and other water bodies, which drives the subtle differences between the stations. Smyth et al. (2010) concluded than coastal Station L4 was influenced more strongly by land-sea exchanges that open-shelf Station E1. Conversely Station E1 is more strongly influenced by larger scale climatic and hydrological influences from the North Atlantic (Laane et al., 1996, Smyth et al., 2010).

4.4.5 CO-oxidising bacterioplankton at the Western Channel Observatory

Not all phytoplankton derived organic matter is directly assimilated by bacterioplankton. A significant fraction of DOM is photo-oxidised to a range of compounds including carbon monoxide (CO) (Conrad and Seiler, 1980, Miller and Zepp, 1995, Moran and Zepp, 1997). The distribution of CO in the marine environment is therefore closely linked to productivity (Jones and Amador, 1993, Jones, 1991, Conrad and Seiler, 1980, Tolli and Taylor, 2005), and the major sink for CO in the seawater is bacterioplankton oxidation (Zafiriou et al., 2003, Xie et al., 2005). Representative subsets of the samples used in the 16S rRNA gene analysis

were assessed for the presence of the carbon monoxide dehydrogenase (CODH) encoding gene *coxL* (King, 2003). A total of 241 bona fide *coxL* OTUs were identified, with the majority of abundance attributed to 6 OTUs.

Most of the *coxL* OTUs were identified as *Rhodobacterales* (family *Rhodobacteraceae*), with OTUs representing *Actinobacteria*, *Rhizobiales* and *Burkholderiales* also identified (supplemental figure 4.3). Short read lengths and possible bias towards MRC's in the NCBI database due to a lack of reference sequences meant taxonomy could not confidently be assigned at a higher resolution, and other bacterial groups may be under represented as only OTUs with high similarity to confirmed CODH were included. The prevalence of *Rhodobacteraceae coxL* sequences was not however surprising given the prevalence of the *Rhodobacteraceae* in the total bacterioplankton community in this study and the high abundance of *coxL* genes previously reported amongst the MRC (Tolli et al., 2006, Cunliffe, 2011), a major group within *Rhodobacteraceae* (Pujalte et al., 2014). The abundance of CO-oxidisers in the dominant *Rhodobacteraceae* suggests CO-oxidation may play an important role in bacterioplankton secondary production at the WCO.

The CO-oxidising bacterioplankton community was significantly different by month, with the greatest dissimilarity seen between spring (March, April and May) and summer (June and July) communities. The abundance of dominant OTUs showed a seasonal switch from OTU_2 which declined steadily over the study period, to OTU_3 which peaked more acutely in June and July. Two deep samples from June and July were also assessed for *coxL* gene presence; deep CO-oxidising communities more closely resembled the spring community than the summer community suggesting that stratification significantly affects the composition of the CO-oxidising community.

CO-oxidation is used as a supplementary energy source in carboxydovores such as the MRC and may provide an advantage by increasing heterotrophic efficiency when

substrate turnover or competition for substrate is high (Chapter 3). Caporaso et al. (2012) and Gibbons et al. (2013) have suggested that the existence of a microbial seed bank at the WCO, where variation in community composition is determined by the relative abundance of taxa selected for by the environment from a reservoir of persistent taxa. CO-oxidation alone is unlikely a dominant driver of community succession, but given the diversity of metabolic strategies utilised by members of the *Rhodobacteraceae* (Buchan et al., 2005, Moran et al., 2007), CO-oxidation potentially contributes to the success of this group at the WCO and in other coastal and shelf sea ecosystems.

4.4.6 Conclusions

In conclusion, this study made the first characterisation of bacterioplankton community dynamics at both Station L4 and E1, and throughout the entire water column. We found that the bacterioplankton present are typical of previous studies at Station L4 and exhibit strong seasonal patterns in response to physicochemical and biological influences (figure 4.11).

Using a depth resolved approach, this study has identified vertical changes in the bacterioplankton community composition in relation to thermal stratification. A 1°C difference between the surface and bottom of the water column in summer coincides with the formation of distinct surface and deep bacterioplankton communities. Our findings show that significant patterns in bacterioplankton community dynamics are missed by only sampling the surface of the water column in stratified coastal systems. This may have implications for our understanding of nutrient regeneration processes in coastal systems.

We also show that differences in the meteorological and hydrographic conditions at the coastal Station L4 and open-shelf Station E1 influence the bacterioplankton community. The dominance of SAR11 suggests a more open ocean regime at Station E1, and is supporting evidence that the meteorological and hydrographic influence from the North Atlantic reaches Station E1. Future studies should consider a larger transect encompassing

the entrance of the English Channel into the Atlantic Ocean. Despite the importance of long-term data sets, fewer recent studies are conducted at multiple WCO Stations. Future plans for the WCO should consider including these historic stations to better represent the Western English Channel, especially when monitoring the area for impacts of climate change.

Biodiversity alone is insufficient to understand ecosystem functioning especially within natural microbial assemblages. Here, by identifying the *coxL* gene which has been conclusively linked to CO oxidation (see Chapter 3) in the environment, we have successfully demonstrated the use of a trait-based approach to characterise potential CO-oxidising bacterioplankton. We found a prevalence of the functional *coxL* gene amongst the *Rhodobacteraceae* and identified seasonal changes in the community in relation to the spring phytoplankton bloom. CO-oxidation is not only an important sink of CO in coastal environments but also potentially important in bacterioplankton secondary production and may contribute to bacterial succession. Although progress has been made, we can only speculate at the potential of the CO-oxidising community identified. More evidence is required to fully understand the ecological role of CO-oxidation in the marine ecosystem. We suggest future studies of this kind should focus on transcripts to confirm activity of these genes in the environment.

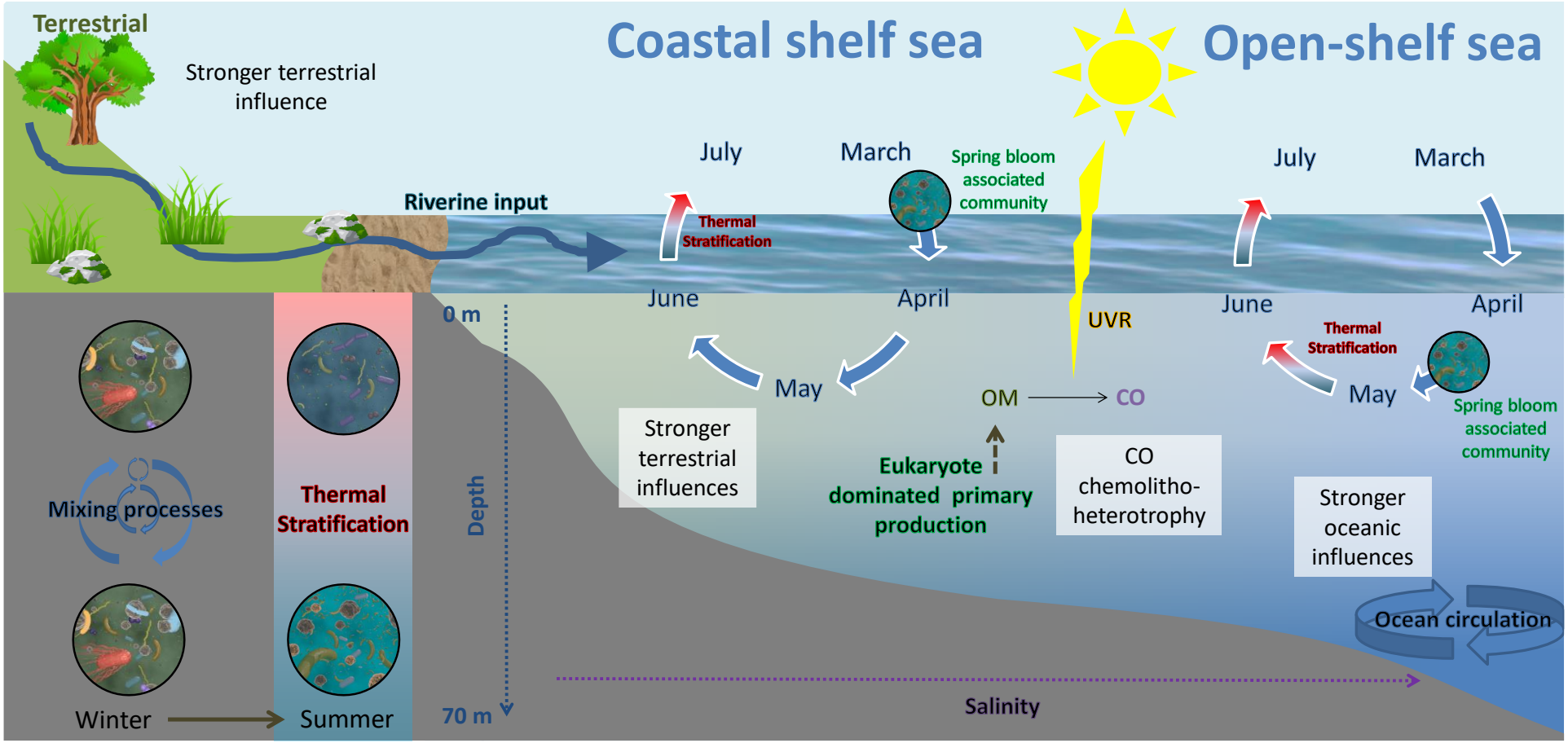

Figure 4.11. Conceptual diagram of the coastal environment illustrating the seasonal changes in bacterioplankton community composition over a spring bloom cycle at a coastal shelf sea and open shelf sea site.

4.5 Supplementary material

Supplemental table 4.1. *coxL-2* OTUs showing significantly different (Bonferroni corrected *p* value <0.05 from Log-likelihood ratio tests) abundance when grouped by month.

OTU	Test-Statistic	Bonferroni *p* value	March mean	April mean	May mean	June mean	July mean
OTU2	836.75	0.000	761.00	370.00	374.00	156.00	68.75
OTU3	1112.49	0.000	5.00	13.50	27.00	292.75	451.75
OTU5	167.80	0.000	84.50	167.50	215.50	165.25	40.25
OTU7	22.82	0.031	84.50	127.25	76.00	114.50	76.25
OTU4	559.37	0.000	0.00	1.25	58.00	59.50	255.75
OTU11	40.65	0.000	40.00	79.00	55.00	108.00	54.25
OTU20	24.42	0.015	18.00	28.50	25.50	47.00	13.00
OTU14	42.54	0.000	25.00	48.75	24.00	4.75	21.50
OTU34	78.68	0.000	2.50	57.50	31.00	10.25	17.00
OTU39	41.27	0.000	1.00	26.00	29.50	22.00	10.75
OTU26	24.92	0.012	37.00	12.75	10.50	9.75	17.75
OTU60	40.29	0.000	4.00	31.25	7.00	6.25	3.75
OTU196	21.94	0.047	0.50	3.00	13.00	3.00	0.50
OTU116	56.50	0.000	18.50	0.00	0.00	0.00	0.00
OTU360	48.43	0.000	0.00	0.00	16.50	0.25	0.00
OTU122	26.44	0.006	0.00	10.50	5.50	0.50	0.00

Supplemental table 4.2. Significant (in bold) Spearman's correlations between principle components axes (16S rRNA PCoA) and, phytoplankton and microzooplankton (Ab = abundance, BM = biomass at 10 m).

Variable	**PC1**		**PC2**	
	R value	***p* value**	**R value**	***p* value**
Diatom (Ab)	-0.10	0.46	**0.33**	**0.01**
Autotrophic dinoflagellate (Ab)	**0.29**	**0.03**	**0.32**	**0.02**
Coccolithophorid (Ab)	0.25	0.06	**-0.72**	**0.00**
Total Phytoplankton (BM)	0.02	0.88	**0.48**	**0.00**
Autotrophic dinoflagellate (BM)	-0.08	0.57	**0.70**	**0.00**
Coccolithophorid (BM)	**0.26**	**0.05**	**-0.69**	**0.00**
Phytoflagellate (BM)	**0.33**	**0.01**	-0.02	0.86
Total Microzooplankton (Ab)	**0.55**	**0.00**	0.00	0.99
Ciliate (Ab)	-0.04	0.78	**0.53**	**0.00**
Heterotrophic dinoflagellate (Ab	**0.46**	**0.00**	0.18	0.18
Total Microzooplankton (BM)	0.07	0.58	**0.51**	**0.00**
Ciliate (BM)	-0.06	0.66	**0.56**	**0.00**
Zooflagellate (BM)	**0.48**	**0.00**	-0.12	0.38

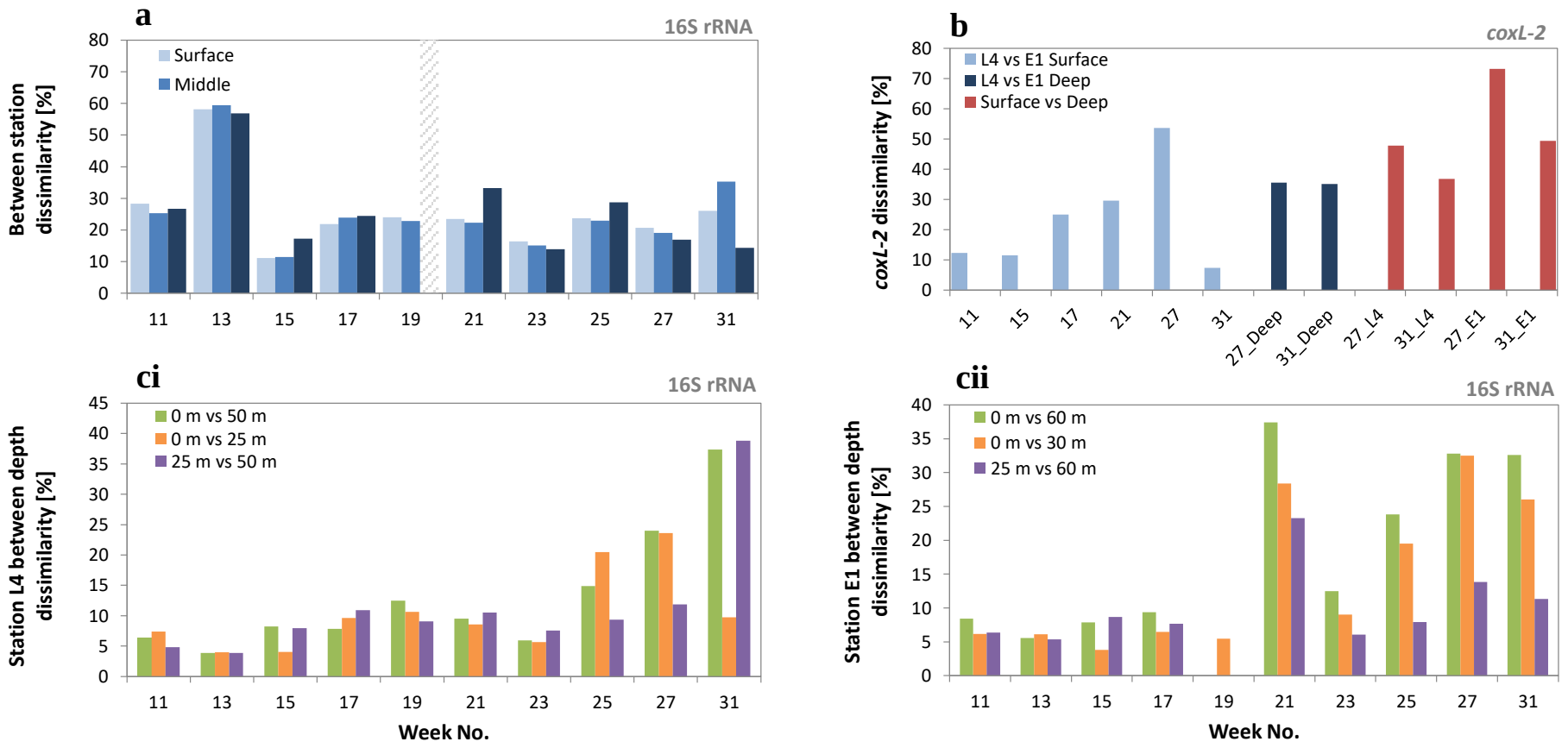

Supplemental figure 4.1. Weighted UniFrac dissimilarity scores a) 16S rRNA between station L4 and E1 by week, b) *coxL-2* between station and or depth by week, ci) 16S rRNA Station L4 between depth by week and cii) 16S rRNA Station E1 between depth by week.

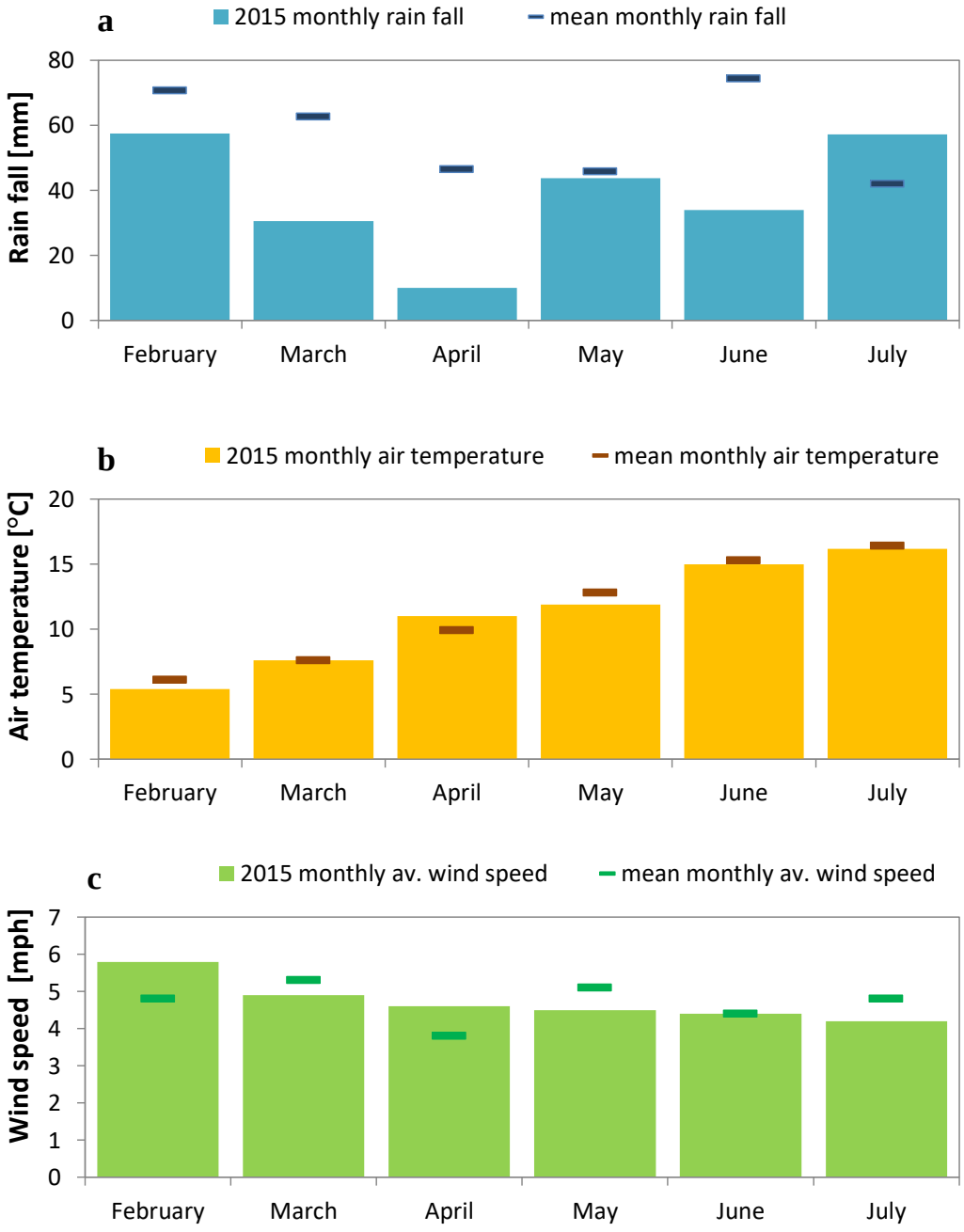

Supplemental figure 4.2. Meteorological metadata a) rainfall, b) air temperature and c) wind speed. Bars show the monthly mean for 2015 and points show the monthly mean taken over an 8 year period.

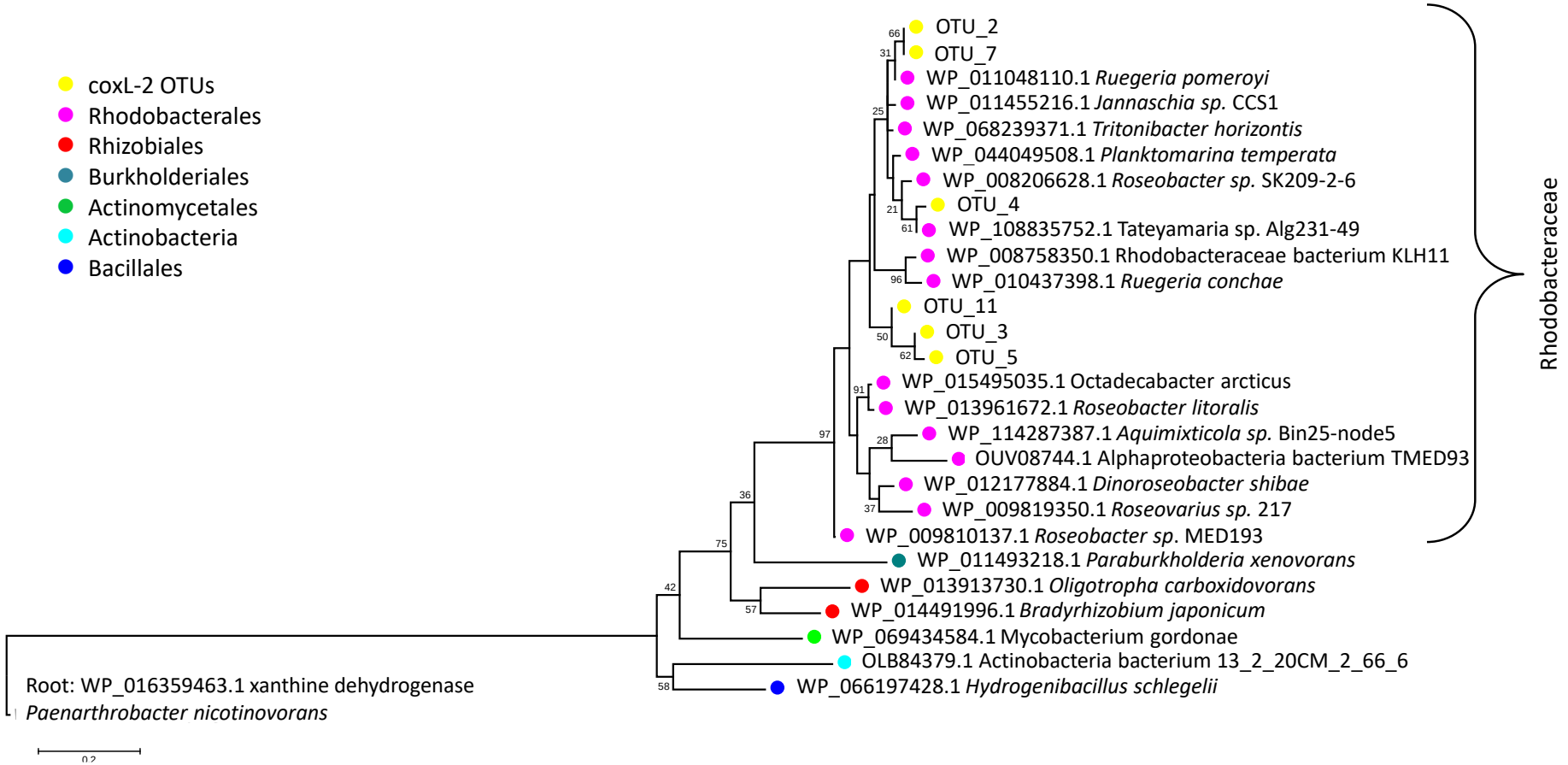

Supplemental figure 4.3. Molecular Phylogenetic analysis by Maximum Likelihood method showing an amino acid alignment of the 6 most abundant OTUs and other carbon monoxide dehydrogenase Form I sequences from the non-redundant protein sequence database. The percentage of trees in which the associated taxa clustered together is shown next to the branches.

Chapter 5

Diversity and distribution of total and active bacterioplankton communities in relation to light along a transect of the Atlantic Ocean

5.1 Introduction

Marine bacterioplankton sustain global-scale biogeochemical cycles and significantly contribute to primary (Richardson and Jackson, 2007) and secondary production (Ducklow, 2000). The total diversity of bacterioplankton (i.e. from DNA) has been characterised from a variety of different locations globally (Zinger et al., 2011, Sunagawa et al., 2015). However, not all bacteria in these communities are metabolically active at a given time (del Giorgio and Scarborough, 1995). Therefore, total bacterioplankton diversity can only provide information about the potential of bacterial communities in the environment.

Bacterial activity has been shown to vary both spatially and temporally (Alonso-Sáez and Gasol, 2007, Alonso-Saez et al., 2008, Lami et al., 2009, Campbell et al., 2011, Hunt et al., 2013) and in response to changes in environmental factors such as nutrient availability, organic substrates, temperature and light (Alonso-Saez et al., 2006, Alonso-Sáez and Gasol, 2007, Alonso-Saez et al., 2008, Lami et al., 2009, Hunt et al., 2013). These findings have implications for our current understanding of biogeochemical cycles. Bacterial production estimates used in global models are most likely inaccurate as these models generally assume bacterial production to be uniform across all taxa (Fasham et al., 1999). In addition bacterial abundance is de-coupled from bacterial activity (Alonso-Sáez and Gasol, 2007, Alonso-Saez et al., 2008, Lami et al., 2009, Campbell et al., 2011, Hunt et al., 2013,), suggesting that estimates of ecological function based on gene presence and abundance are also likely to be inaccurate (Krause et al., 2014, Rocca et al., 2015). In order to better understand the ecological function of bacterioplankton communities and how they interact with biogeochemical cycles, we must not only understand which taxa are present but also which taxa are active in a community.

Light has a critical effect on several marine biogeochemical cycles, providing energy directly and indirectly to bacterioplankton (Karl, 2002, Moran and Miller, 2007, Richardson

and Jackson, 2007). Ultraviolet radiation (UVR) from light also causes cellular damage, negatively affecting metabolic processes, bacterial abundance, substrate uptake and activity (Bailey et al., 1983, Herndl et al., 1993, Müller-Niklas et al., 1995, Sommaruga et al., 1997). Bacterioplankton are exposed to daily fluctuations in light levels and many taxa have developed resistance mechanisms to UVR (Arrieta et al., 2000, Agogue et al., 2005b). Sensitivity to light and the metabolic requirement for light has been shown to influence the vertical distribution of some Cyanobacteria (Six et al., 2007, Mella-Flores et al., 2012). Light could also be a determining factor of general community composition (Alonso-Saez et al., 2006), but so far, no significant effect of light has been shown (Winter et al., 2001, Schwalbach et al., 2005).

The Atlantic Meridional Transect (AMT) programme is a multi-disciplinary and collaborative time series that has been running since 1995 (Rees et al., 2015). Unlike most other time series, the AMT is not a fixed station but instead takes the form of an annual research cruise from the UK to the South Atlantic. Spanning multiple biogeochemical provinces from sub-polar and temperate coastal shelf seas to open ocean tropical gyres, the AMT provides an almost pole-to-pole oceanographic research platform. The aims of the AMT have developed and grown, but the primary aims remain largely unchanged: To record the biogeochemical properties of the Atlantic Ocean in order to validate and develop global ocean models, provide a long-term observatory for monitoring the effects of change on the ocean and to provide a platform for multidisciplinary research and training in 3 key areas. 1) The structure and function of planktonic ecosystems, 2) processes controlling the fate of organic matter and 3) atmosphere to ocean exchange processes.

Over 20 years, the physicochemical properties of the Atlantic have been well characterised (Aiken et al., 2000, Robinson et al., 2006). However, biological monitoring has largely relied on the measurement of photosynthetic pigments, bulk biomass and productivity estimates often relying on remote sensing methods. Although bacterioplankton

communities have been investigated, these studies have focused on specific functional groups such as methanol utilizers (Dixon et al., 2013) or have been based on flow cytometry analysis (Zubkov et al., 2000).

Geographical patterns of bacterial diversity are today relatively well characterised and have been greatly advanced by global data sets such as Tara Oceans (Sunagawa et al., 2015) and ICoMM (Pommier et al., 2007). However, a large proportion of the euphotic global ocean remains poorly characterised. For example, there is a lack of research in the southern hemisphere and few ocean time series none of which, to our knowledge, that are basin-wide. Currently, little is known about the latitudinal distribution of bacterioplankton communities in the Atlantic Ocean. There have been two genomic studies of bacterial diversity over a latitudinal transect of the Atlantic. Milici et al. (2016) characterised bacterioplankton diversity throughout the water column but did not report phylogenetic diversity, and Reintjes (2017), who characterised phylogenetic diversity of particle associated and free living bacterioplankton, did so only at 20 m below the surface. The AMT is a long-term observatory for monitoring the effects of change on the Atlantic Ocean but to date has largely overlooked bacterial communities. I used the AMT platform to record the microbial diversity of the Atlantic Ocean. Doing so on an annual basis could help improve our understanding of the effects of change on the oceans and help to develop global ocean models.

The primary aim of this study was to characterise the diversity and distribution of total and active bacterioplankton communities along AMT using high throughput sequencing techniques. We hypothesise the community will be dominated by a core set of taxa but the abundance and activity of these taxa will vary independently in response to differing environmental characteristics along the transect. This study also aimed to investigate the specific effect of light on the composition of bacterioplankton communities by comparing samples collected from three different depths ranging 97 to 1 %

photosynthetically available radiation (PAR). We hypothesise there will be variation in the community in response to light, and that taxa will be partitioned into different light niches based on their resistance/tolerance to light stress and metabolic requirement for light, which in turn, will lead to diurnal differences in the community composition.

5.2 Method summary

5.2.1 Seawater sampling

Seawater samples were collected during the AMT 25 cruise on board the *RSS James Clark* Ross, which sailed from Immingham, UK to Stanley, Falkland Islands (18^{th} Sep to 4^{th} Nov 2015). The cruise track crossed nine biogeochemical provinces (Longhurst et al., 1995) in the North and South Atlantic Ocean (figure 5.1), which represented a range of marine ecosystems from temperate coastal seas to tropical ocean gyres (table 5.1).

Seawater samples were taken from three different light depths (97 %, 55 % and 1 % PAR) during 16 casts at eight stations that consisted of paired pre-dawn (~04:30 local time = 04:00 – 07:00 UTC) and solar noon (~13:30 local time =13:00 – 16:00 UTC) casts, which were approximately 150 km apart. Two additional samples were also collected from 4 m and 27 m (08:00 UTC) at the Western Channel Observatory Station E1 (Chapter 4). Seawater samples were immediately filtered onto a 0.2 µm filter membrane and stored in a nucleic acid preservative at -80 ^{0}C. On return to the laboratory, DNA and RNA were co-extracted from the membranes using commercially available DNA/RNA isolation kit (E.Z.N.A). DNA and cDNA, synthesised from the RNA by reverse transcription were sent for 16S rRNA gene amplicon sequencing (see Chapter 2 for further details).

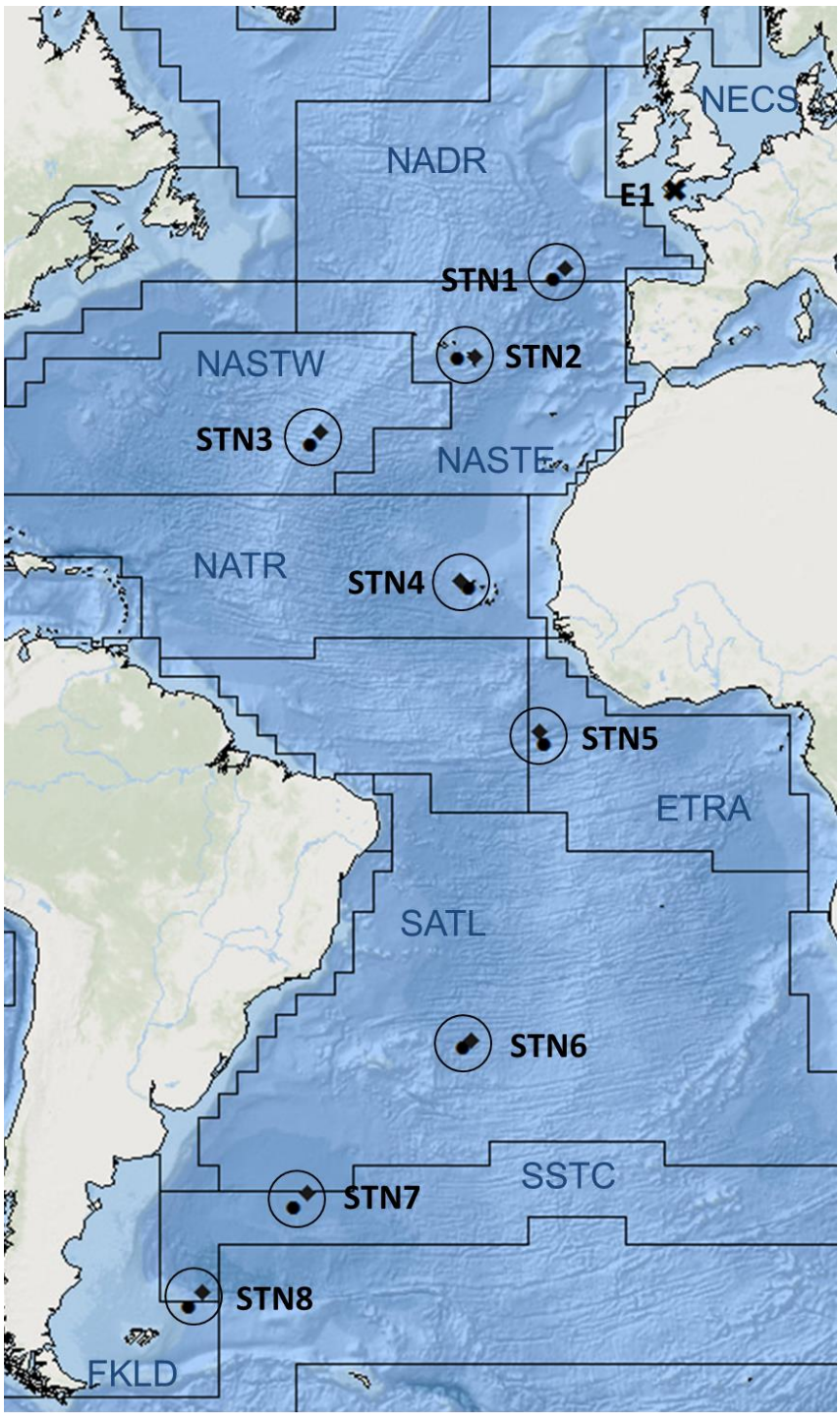

Figure 5.1. Map showing location of samples taken during the Atlantic Meridional Transect (AMT) 25 that were analysed in this study. Symbols represent the geographical position of casts (● noon, ◆ pre-dawn and ✕ Western Channel Observatory Station E1), open circles indicate paired casts and represent a station. Lines show borders of biogeochemical provinces annotated by their abbreviation (table 5.1).

Table 5.1. Atlantic Meridional Transect 25 sampling stations, including details of Longhurst provinces and climatic regions.

Station	Cast ID	Longhurst Province		Domain	Region
E1	CTD001	NECS	North East Atlantic Continental Shelf	Coastal	Temperate (Boreal Autumn)
STN1	CTD006	NADR	North Atlantic Drift	Westerlies	
	CTD007				
STN2	CTD012	NASTE	North Atlantic Tropical Gyral East		
	CTD013				
STN3	CTD021	NASTW	North Atlantic Tropical Gyral West		Sub-Tropical (North)
	CTD022				
STN4	CTD033	NATR	North Atlantic Tropical Gyral	Trades	Tropical
	CTD034				
STN5	CTD042	ETRA	Eastern Tropical Atlantic		
	CTD043				
STN6	CTD066	SATL	South Atlantic Gyral		Sub-Tropical (South)
	CTD067				
STN7	CTD076	SSTC	South Subtropical Convergence	Westerlies	Temperate (Austral Spring)
	CTD077				
STN8	CTD080				
	CTD081	FKLD	South West Atlantic Continental Shelf	Coastal	

5.3 Results

5.3.1 Physicochemical characteristics of the Atlantic Meridional Transect

Seawater temperature ranged from 4.4 °C in the southern temperate regions to 29.6 °C in the surface waters of the tropical regions (figure 5.2a). Salinity ranged from 34.1 to 37.6 PSU and was highest in the gyral regions and lowest in the southern temperate regions (figure 5.2b). Generally, seawater temperature and salinity decreased with depth, and stratification was evident from 50°N to 30°S, after which the water column became mixed. Fluorescence was highest (2.6 RFU) at Station E1 in the Western English Channel and lowest in the northern and southern gyres. A deep chlorophyll maximum (DCM) was present throughout the transect, and was deepest (100-150 m) in the gyral regions (figure 5.2c). Oxygen ranged from 57.1 to 305.2 µM L^{-1} and was lowest between 20°N and 20°S below 50-75 m and highest in the southern temperate regions (figure 5.2d).

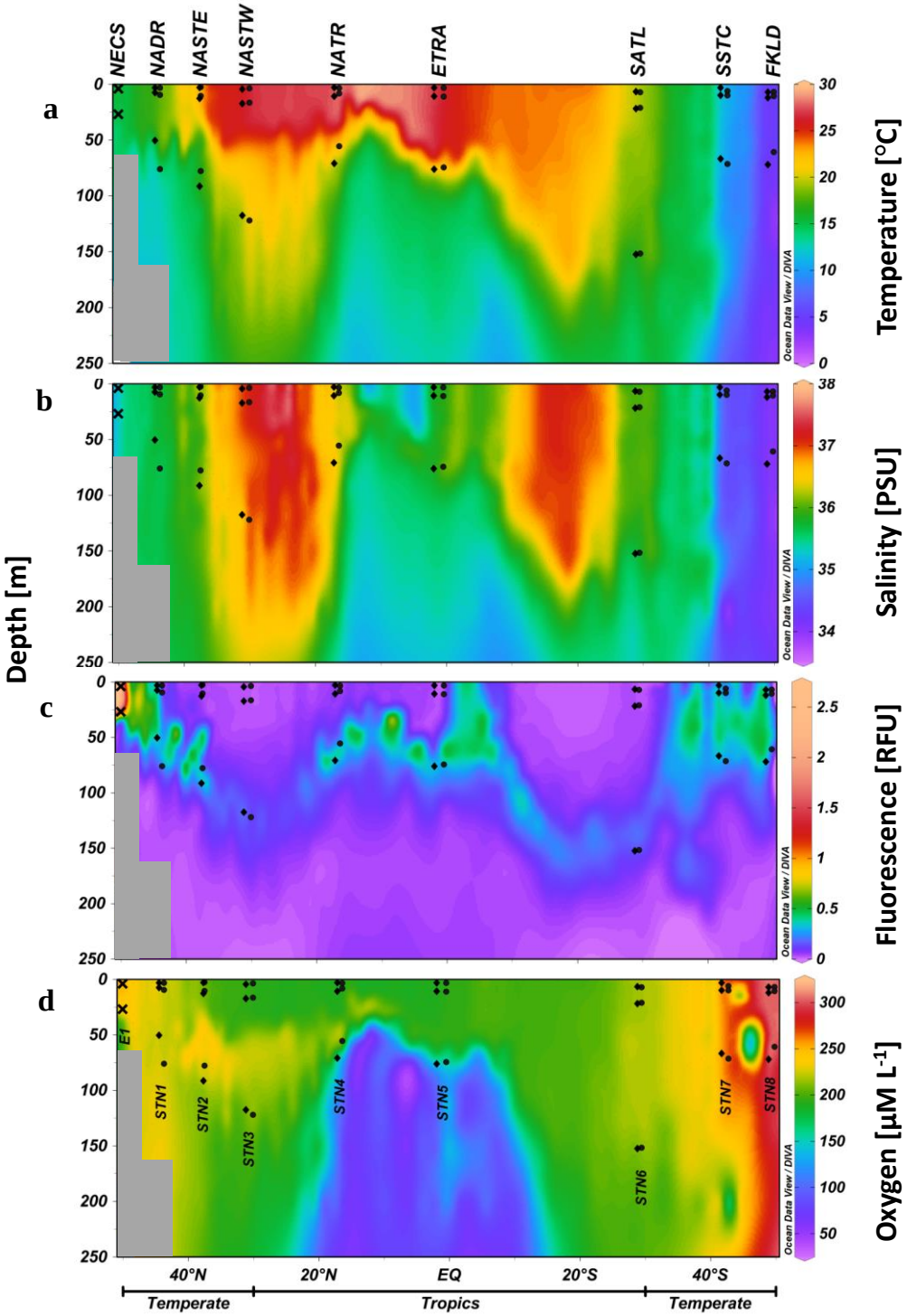

Figure 5.2. Data-Interpolating Variational Analysis (DIVA) gridded section plots showing physicochemical data from 73 CTD casts totalling 912 data points along the AMT25. a) temperature [°C], b) salinity [PSU], c) fluorescence [RFU] and d) oxygen [µM L^{-1}]. Depth [m] on the Y axis vs. latitude on the X axis. Symbols represent the position of water samples analysed in this study (● noon, ◆ pre-dawn and ✕ Western Channel Observatory Station E1).

Photosynthetically available radiation (PAR) ranged from 3 to 1,340 W m^{-2} during noon sampling and was highest at the surface declining with depth (figure 5.2a). PAR was much lower during pre-dawn sampling and was consistently <1.5 W m^{-2} (figure 5.2b). PAR at 97 % (mean 4.3 m), 55 % (mean 12.5 m) and 1 % (mean 86.7 m) light depths were on average 745.1, 371.6 and 8.7 W m^{-2} respectively. The two additional samples collected from 4 m and 27 m at the Western Channel Observatory Station E1 were equivalent to 55 % and 1 % light depths based on the *in situ* PAR measurements.

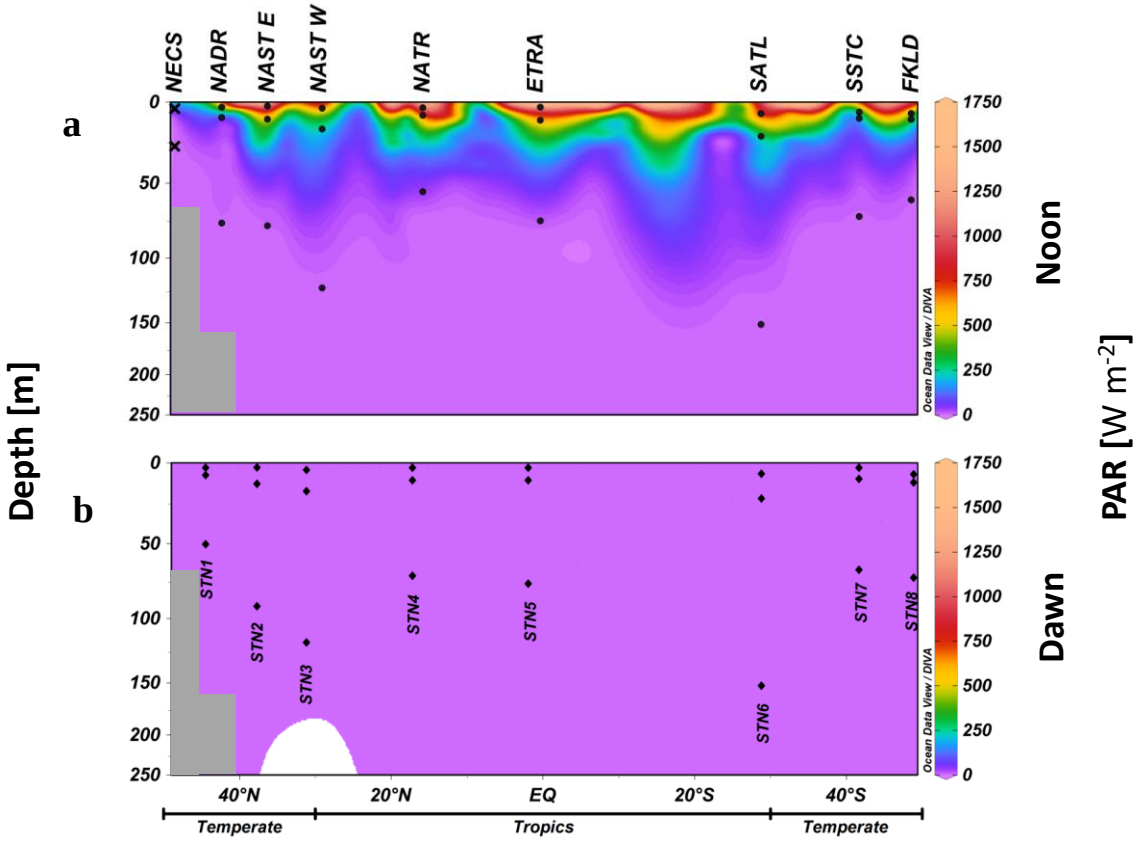

Figure 5.2. Data-Interpolating Variational Analysis (DIVA) gridded section plots showing photosynthetically available radiation (PAR) data [W m^{-2}] along the AMT25 during 2016. a) noon and b) pre-dawn. Depth [m] on the Y axis vs. latitude on the X axis. Symbols represent position of water samples analysed in this study (● noon, ◆ pre-dawn and ✕ Western Channel Observatory Station E1).

The seawater nutrients nitrate and nitrite combined, phosphate and silicate were low < 1 µM L^{-1} and often below the limits of detection for phosphate (< 0.02 µM L^{-1}), nitrate + nitrite (< 0.02 µM L^{-1}) and nitrite (< 0.01 µM L^{-1}) throughout the upper 50 m of the water column and down to ~150 m in the gyral regions (figure 5.4). Maximum values up to 34.5 µM L^{-1} nitrate and nitrite (figure 5.4a), 2.3 µM L^{-1} phosphate (figure 5.4b) and 11.4 µM L^{-1} silicate (figure 5.4c) were recorded in the southern temperate regions throughout the water column and between 20°N and 20°S below a depth of 50 m. Due to the high number of missing data points, nitrate and nitrite could not be separated, although mean nitrite when recorded was ~0.03 µM L^{-1} suggesting nitrate and nitrite values are composed mostly of nitrate.

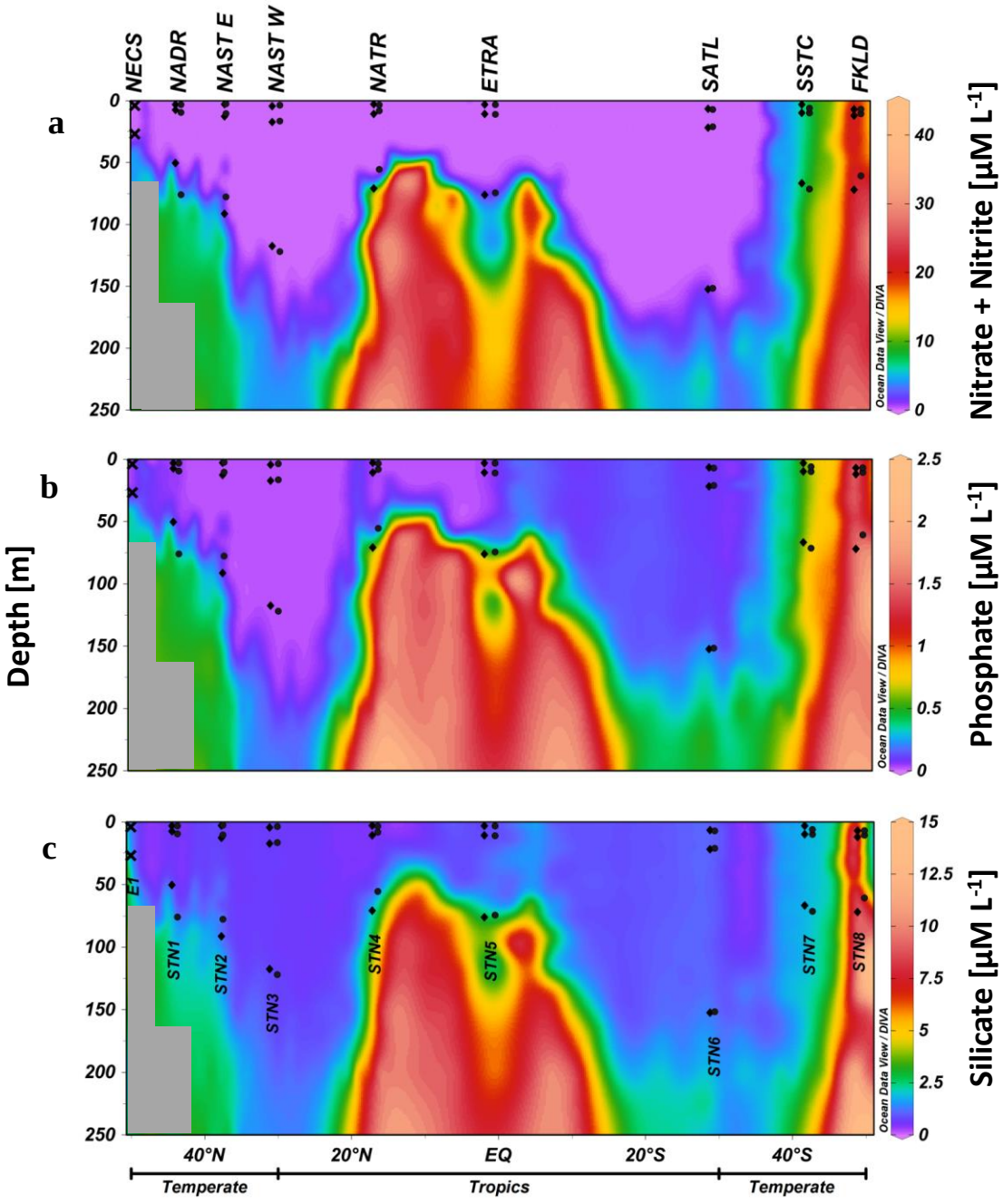

Figure 5.4. Data-Interpolating Variational Analysis (DIVA) gridded section plots showing nutrient data [µM L^{-1}] along the AMT25 during 2016. a) nitrate and nitrite, b) phosphate and c) silicate. Depth [m] on the Y axis vs. latitude on the X axis. Symbols represent position of water samples analysed in this study (● noon, ◆ pre-dawn and ✕ Western Channel Observatory Station E1).

5.3.2 Total (DNA) and active (RNA) bacterioplankton diversity along the Atlantic Meridional Transect

Bacterioplankton diversity was assessed by bacterial 16S rRNA gene and 16S rRNA high-throughput sequencing. Reads were filtered to exclude singletons, non-bacterial and organelle sequences, then rarefied to a depth of 8,391 reads per sample resulting in a total of 83,910 high quality reads (250 bp) that represented 2,366 operational taxonomic units (OTUs) based on 97 % similarity. 134 taxonomic groups identified to order level were detected, 38 were considered abundant (>0.1 % relative abundance) in DNA samples and 29 were considered abundant (>0.1 % relative abundance) in RNA samples, resulting in 40 abundant taxa at order level (figure 5.5).

The majority (~80 %) of the relative abundant (RA) taxa was contributed by just seven taxa mostly at order level. However, the relative contribution of these taxa varied significantly between DNA and RNA samples (table 5.2). Total bacterioplankton communities assessed by 16S rRNA gene abundance (DNA) were dominated by *Prochlorococcus*, followed by *Flavobacteriales*, SAR11 clade, *Oceanospirillales*, *Rhodobacterales* and *Synechococcus* (figure 5.5a). Active bacterioplankton communities assessed by 16S rRNA (RNA) were dominated by *Prochlorococcus* followed by *Flavobacteriales*, *Synechococcus*, Oceanospirillales, unidentified *Cyanobacteria* (Subsection I Other) and *Rhodobacterales*. The *Cyanobacteria Prochlorococcus*, *Synechococcus* and Subsection I Other were almost twice more abundant in RNA samples than DNA samples. In contrast, the SAR11 clade was 30 times less abundant in RNA samples compared to DNA samples. *Flavobacteriales*, *Oceanospirillales* and *Rhodobacterales* were also less abundant in RNA samples than DNA samples but to a lesser degree (1.2 – 1.8 times lower).

Table 5.2. Contribution to bacterioplankton community of the seven overall most abundant taxa by number of normalised reads and relative abundance.

Taxa	All samples		DNA samples		RNA samples	
	reads	RA %	reads	RA %	reads	RA%
Prochlorococcus	380678	45.4	141091	33.1	239587	58.0
Flavobacteriales	106275	12.7	65141	15.5	41134	9.8
SAR11 clade	51226	6.1	49476	11.8	1750	0.4
Oceanospirillales	43851	5.2	23737	5.7	20114	4.8
Rhodobacterales	41098	4.9	26389	6.3	14709	3.5
Synechococcus	33456	4.0	11675	2.7	21781	5.3
Subsection I Other	22850	2.7	7862	1.8	14988	3.6

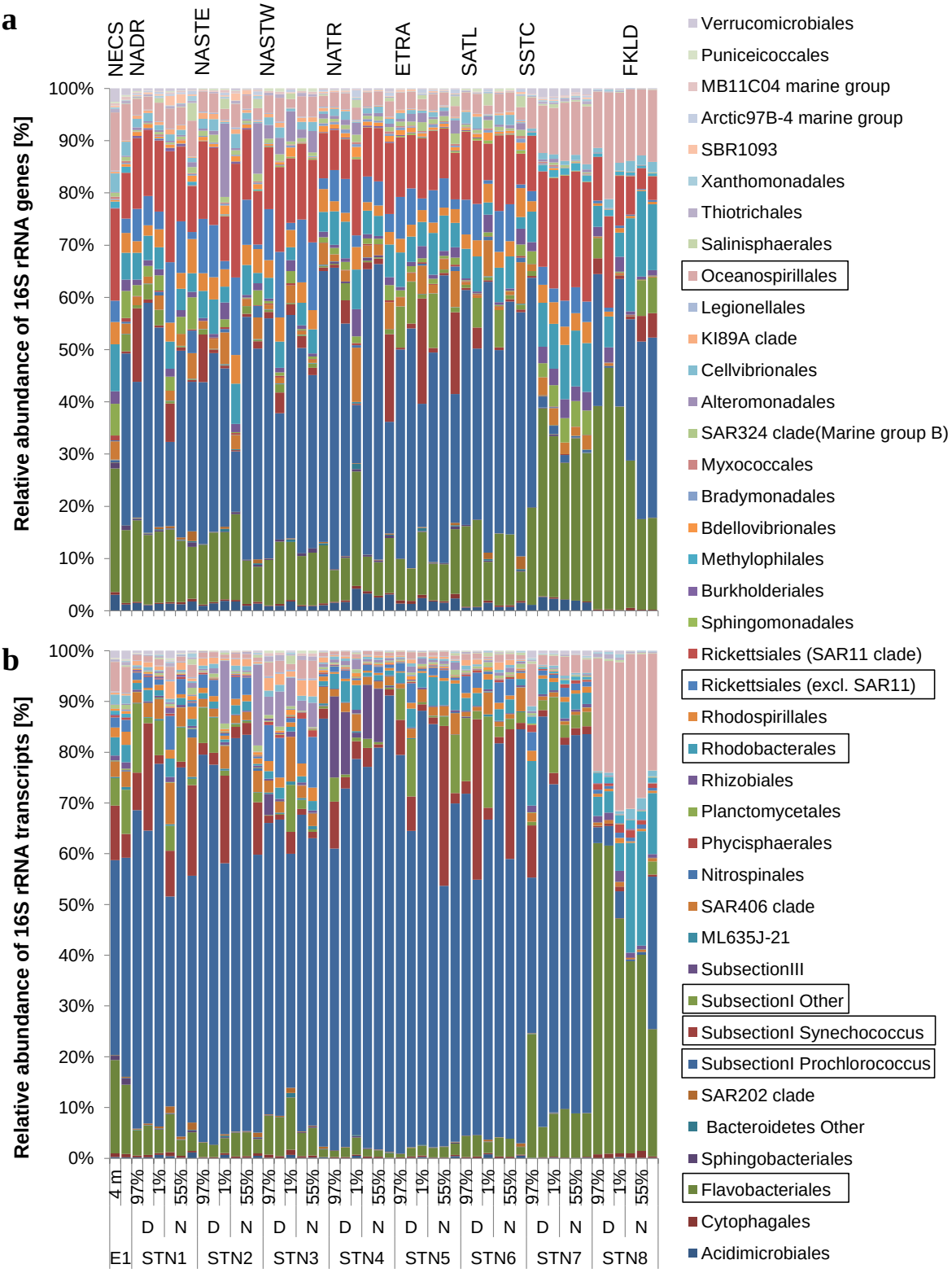

Figure 5.5. Relative abundance of bacterioplankton taxa along the AMT25 of a. DNA samples (16S rRNA gene abundance) and b. RNA samples (16S rRNA transcript abundance). Outlines highlight the seven overall most abundant taxa.

5.3.3 Bacterioplankton community structure along the Atlantic Meridional Transect

Permutational multivariate analysis of variance (PERMANOVA) on weighted UniFrac metrics showed that DNA and RNA samples were significantly different to each other (p <0.05), as were samples grouped by province and by light depth (table 5.3). Overall there was no significant difference between noon and pre-dawn samples (table 5.3), although Log-likelihood ratio tests on abundant orders (RA >0.1%) of combined DNA and RNA samples showed that *Prochlorococcus* (statistic =49.34, p <0.000), *Rhodobacterales* (statistic =48.58, p <0.000) and *Oceanospirillales* (statistic =10.72, p <0.042) were significantly higher in noon samples. Whereas *Flavobacteriales* (statistic =27.52, p <0.000) and Subsection I Other (statistic =15.15, p <0.004) were significantly higher in pre-dawn samples.

PERMANOVA on DNA and RNA samples separately showed that DNA samples were significantly different when grouped by province and light depth, whereas RNA samples were only significantly different when grouped by province (table 5.3). PERMANOVA on all DNA samples by paired light depths showed the bacterioplankton community at 97 % and 55 % light depths were not significantly different to each other but were both significantly different (p <0.05) to the community at the 1 % light depth (table 5.3). Log-likelihood ratio tests on DNA samples showed 21 taxa were significantly different (Bonferroni p <0.05) when grouped by light depth, of these taxa Subsection I Other, *Cellvibrionales*, *Puniceicoccales* and *Rhodobacterales* were higher in abundance in surface samples (97 % and 55 % light depths) than the 1% light samples. 14 taxa from RNA samples were also significantly different (Bonferroni p <0.05) when grouped by light depth. Cyanobacteria Subsection III (identified as *Trichodesmium spp.*), *Rickettsiale*s (excl. SAR11 clade) and KI89A clade were more abundant in surface samples compared to 1 % light samples except *Synechococcus* which was most abundant in 55 % light samples. Log-

likelihood ratio tests on both DNA and RNA samples showed nearly all taxa were significantly different when grouped by province (Bonferroni p <0.05).

Table 5.3. Permutational multivariate analysis of variance (PERMANOVA) of categorical variables, bold text highlight significant differences.

Category	ALL samples		DNA samples		RNA samples	
	pseudo-F	*p*-value	*pseudo-F*	*p*-value	*pseudo-F*	*p*-value
Pre-dawn vs Noon	1.02	0.359	0.63	0.623	0.55	0.712
DNA vs RNA	**10.17**	**0.001**	NA	NA	NA	NA
Province	**16.53**	**0.001**	**11.17**	**0.001**	**13.93**	**0.001**
Light Depth (97, 55 & 1 %)	**2.24**	**0.025**	**2.13**	**0.033**	0.91	0.511
97 % vs 55 %	0.17	0.975	0.09	0.995	0.12	0.987
1 % vs 97 %	**3.27**	**0.017**	**3.24**	**0.015**	1.35	0.261
55 % vs 97 %	**3.45**	**0.009**	**3.28**	**0.019**	1.36	0.256

To further investigate the bacterioplankton communities by biogeochemical province, Principal Coordinates Analysis (PCoA) were conducted on DNA samples and RNA samples separately using weighted UniFrac metrics. DNA and RNA PCoA plots showed similar patterns of sample orientation (figure 5.6). Samples from the same province clustered well with the exception of samples from SSTC. Provinces FKLD, SSTC and NECS were distinct from the other provinces along axis PC1 and were grouped tightly by cast along axis PC2. Other provinces were more closely clustered, forming two groups along axis PC2. Group 1 was composed mostly of samples from 97 % and 55 % light depths of provinces NADR, NASTE and SATL. Group 2 was composed of provinces NATR, ETRA and the 1 % light depths of the 1st group. The only province to show a difference in sample grouping between DNA and RNA PCoAs was NASTW, which was clustered with group 1 in the DNA PCoA (figure 5.6a) and with group 2 in the RNA PCoA (figure 5.6b).

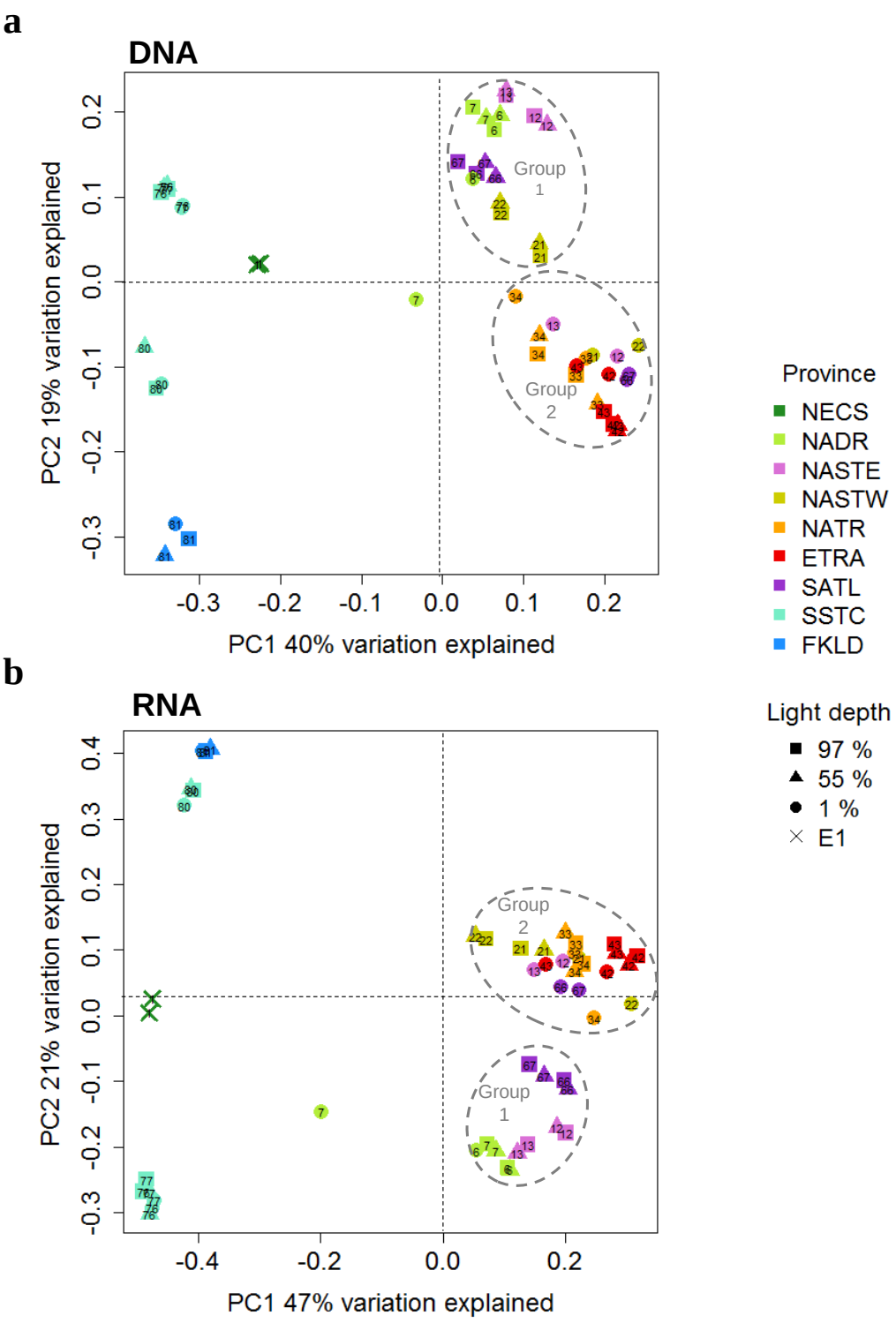

Figure 5.6. Principal Coordinates Analysis (PCoA) using weighted UniFrac distance metrics of a. DNA samples and b. RNA samples. Symbols represent light depth (● 1 %, ▲ 55 %, ■ 97 % and ✕ Western Channel Observatory Station E1) colours represent biogeographical province and numbers indicate cast number.

Minimum spanning trees (MST) were also constructed from the weighted UniFrac metrics for DNA and RNA samples (figure 5.7). Corresponding samples from different light depths were closely related to each other in provinces FKLD, SSTC and NECS. Whereas, in all other provinces, samples from 97 % and 55 % light depths were more closely related to each other than the corresponding samples from the same station from 1 % light depth. This pattern was strongest in the DNA MST (figure 5.7a), where samples from 1 % light depth of different provinces with the exception of NADR were clustered together and more related to each other than corresponding surface (97 % and 55 %) samples. The RNA MST (figure 5.7b) was generally linear, with minimal branching. SSTC and FKLD samples were linked by NECS to NADR, NASTE, SATL, NASTW, ETRA and NATR in succession. In contrast the DNA MST was more heavily branched. SSTC and FKLD samples were linked by NECS to NASTW and the other provinces that were branched forming 2 groups as per the PCoA plot, with Group 2 being further branched into surface and 1 % light depth samples.

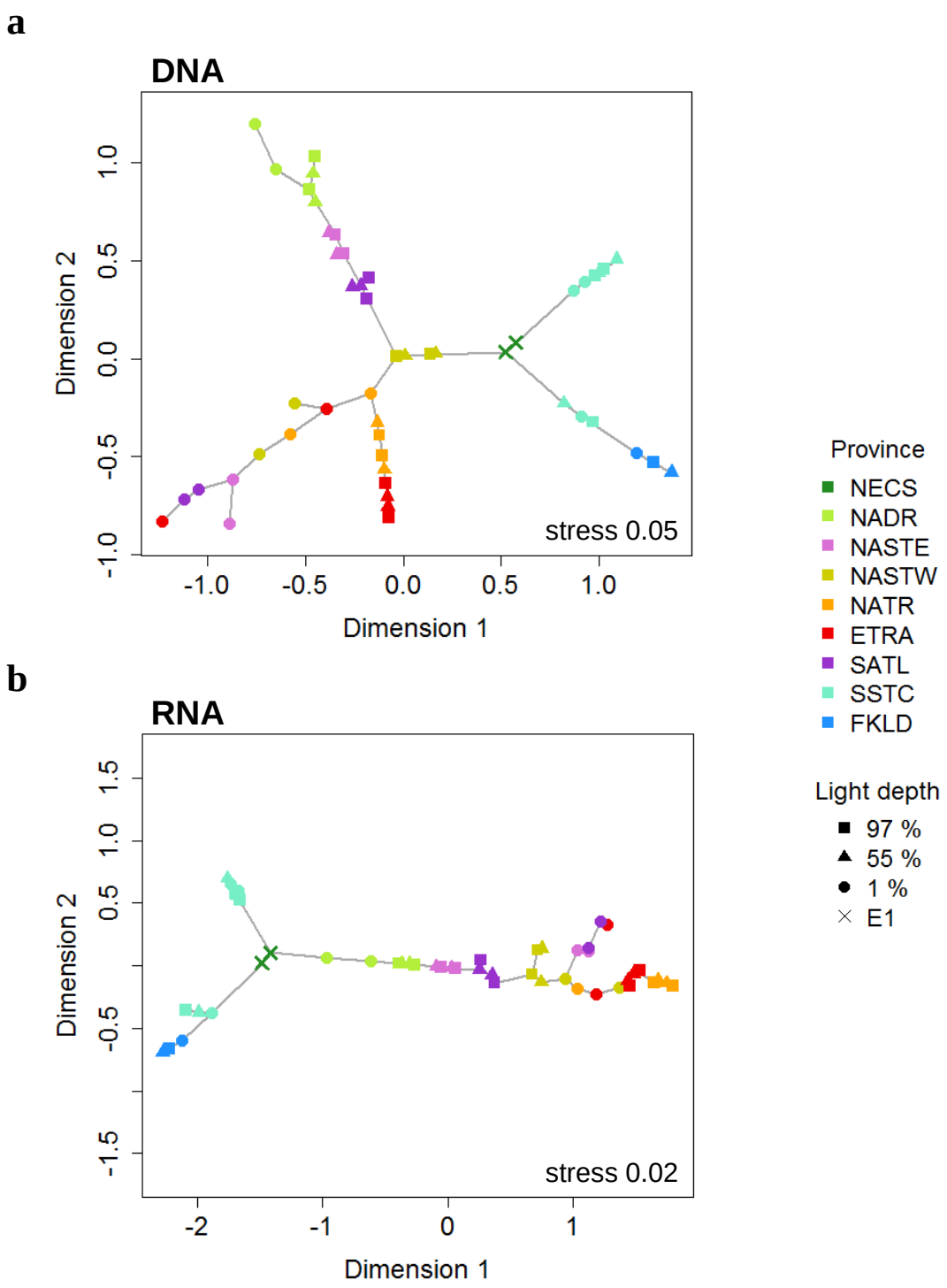

Figure 5.7. Minimum spanning tree (MST) using weighted UniFrac distance metrics of a. DNA samples and b. RNA samples. Symbols represent light depth (● 1 %, ▲ 55 %, ■ 97 % and ✕ Western Channel Observatory Station E1) colours represent biogeographical province.

5.3.4 Linking bacterioplankton community structure with physiochemical parameters along the Atlantic Meridional Transect

Spearman's rho correlations were conducted on the principle component axes PC1 and PC2. PC1 from both DNA and RNA PCoAs correlated positively with seawater temperature and salinity, and negatively with oxygen, fluorescence and all nutrients (nitrate/nitrite, phosphate and silicate). Axis PC2 (RNA) correlated positively with nitrate/nitrite and axis PC2 (DNA) correlated negatively with all nutrients.

Redundancy analysis (RDA) was also performed on weighted UniFrac metrics of RNA and DNA samples. Analysis of variance on RDA models showed that overall, the physicochemical data explained the ordination of the samples (figure 5.8) and temperature, salinity and oxygen were significant explanatory variables in the DNA RDA and temperature, salinity, oxygen and fluorescence were significant explanatory variables in the RNA RDA (table 5.4).

Table 5.4. Analysis of variance (ANOVA) of Redundancy analysis (RDA) models, bold text indicates significant values.

Variable	DNA		RNA	
	F value	*p* value	F value	*p* value
Temperature	**28.2**	**0.001**	**27.9**	**0.001**
Salinity	**9.3**	**0.001**	**5.4**	**0.004**
Oxygen	**5.7**	**0.002**	**2.9**	**0.037**
Fluorescence	2.0	0.080	**3.5**	**0.019**
PAR	0.5	0.758	0.6	0.652

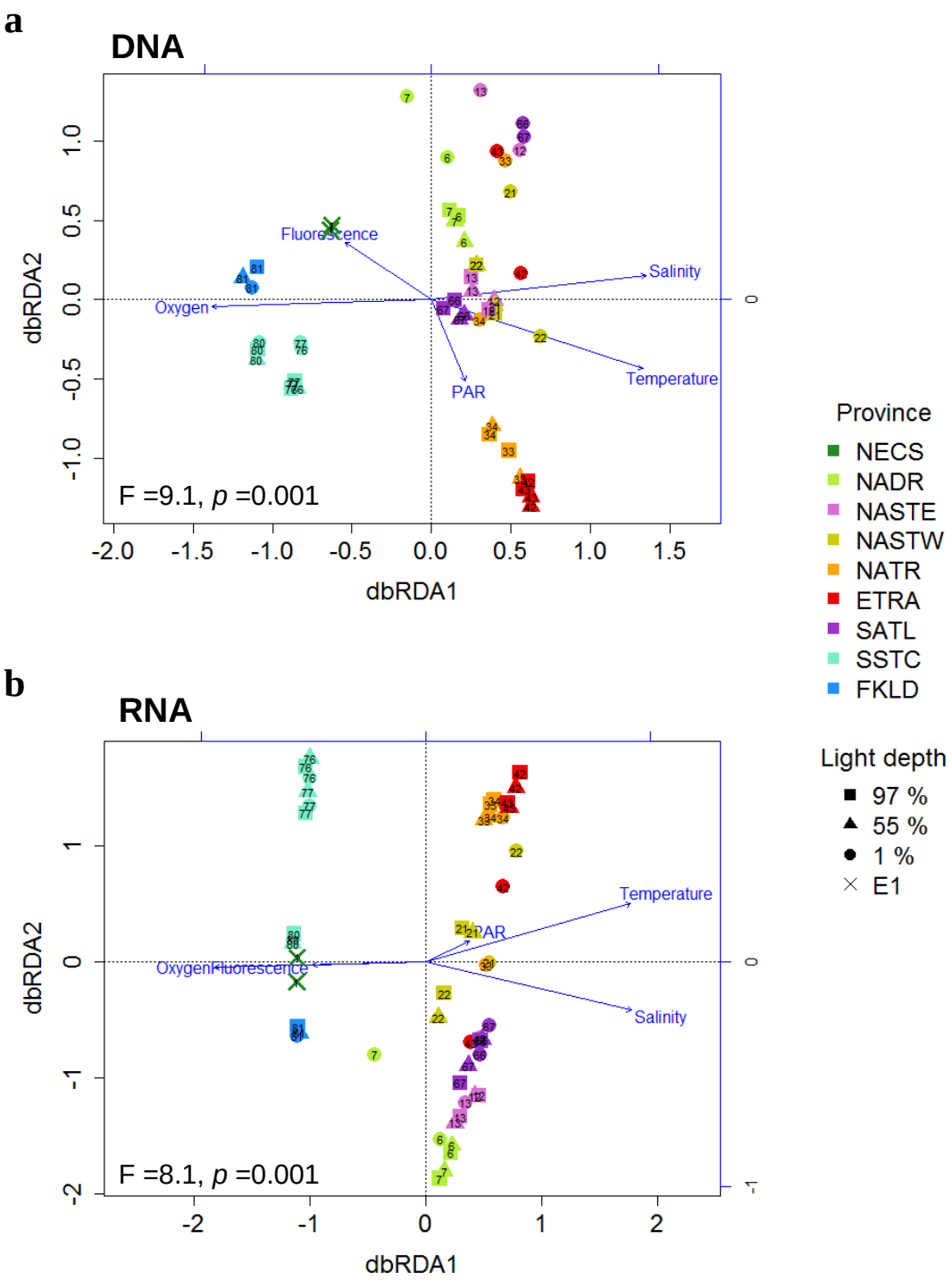

Figure 5.8. Redundancy analysis (RDA) using weighted UniFrac distance metrics of a. DNA samples and b. RNA samples. Symbols represent light depth (● 1 %, ▲ 55 %, ■ 97 % and ✕ Western Channel Observatory Station E1) colours represent biogeographical province and numbers indicate cast number.

5.3.5 Comparison between total (DNA) and active (RNA) diversity

Log likelihood-ratio tests were used to compare RNA abundance to DNA abundance for each abundant (>0.1 % RA) taxon. Over the whole transect, only 5 taxa, 4 of which belonged to the Cyanobacteria (*Prochlorococcus*, *Synechococcus*, Subsection I other and *Trichodesmium*) and the *Gammaproteobacteria* KI89A clade, had a significantly (Bonferroni p <0.05) higher abundance in RNA samples compared to DNA samples. 13 taxa had a significantly lower abundance in RNA samples compared to DNA samples and the remaining 22 taxa showed no significant difference between RNA and DNA abundance.

When grouped by province, 29 of the 38 taxa showed a significant difference between RNA and DNA abundance in at least one province. The ratio of RNA to DNA abundance was calculated for each taxon in each province. Across all provinces, 45 % of taxa (n 17) had a mean ratio of ~1:1, 39 % (n 15) had a mean ratio <1:1) and 16 % (n 6) had a mean ratio >1:1 (figure 5.9).

NECS	NADR	NASTE	NASTW	NATR	ETRA	SATL	SSTC	FKLD		
0.14	**0.31**	**0.17**	**0.11**	**0.04**	**0.08**	**0.21**	**0.10**	1.27	**Acidimicrobiales**	▼
2.20	1.19	1.20	1.58	0.76	0.40	0.99	3.00	**2.09**	**Cytophagales**	—
1.10	**0.32**	**0.33**	**0.46**	**0.19**	**0.20**	**0.25**	**0.87**	**1.10**	**Flavobacteriales**	—
1.37	**0.30**	0.67	**0.32**	0.40	0.30	0.24	0.67	0.17	**Sphingobacteriales**	▼
1.60	0.62	0.54	0.56	0.28	0.27	0.11	1.44	nd	**Bacteroidetes Other**	—
3.78	1.04	1.03	2.68	0.64	0.47	**0.27**	2.10	2.00	**SAR202 clade**	▲
2.48	**1.70**	**2.11**	**1.26**	**1.91**	**1.99**	**1.45**	**3.49**	**0.28**	**SubsectionI Prochlorococcus**	▲
34.15	**2.24**	**3.08**	0.70	0.95	1.14	**10.45**	**2.23**	**0.04**	**SubsectionI Synechococcus**	▲
4.47	**4.16**	**6.17**	**2.27**	**2.08**	1.10	**2.39**	**3.82**	**0.15**	**SubsectionI Other**	▲
nd	nd	2.00	**29.27**	**31.39**	5.00	nd	1.00	nd	**SubsectionIII**	▲
4.72	2.45	2.44	**4.00**	1.60	1.36	2.10	0.71	nd	**ML635J-21**	▲
1.41	**1.61**	0.89	**1.46**	**0.55**	**0.66**	**0.65**	0.72	**2.66**	**SAR406 clade**	—
0.56	**0.37**	**0.21**	nd	0.34	**0.17**	**0.14**	0.17	0.62	**Nitrospinales**	▼
0.06	**0.02**	**0.01**	**0.08**	**0.03**	**0.01**	**0.05**	0.17	0.07	**Phycisphaerales**	▼
0.05	**0.03**	**0.03**	**0.04**	**0.02**	**0.02**	**0.04**	**0.02**	0.08	**Planctomycetales**	▼
0.60	**0.33**	**0.22**	**0.42**	**0.18**	**0.19**	**0.17**	**0.39**	0.75	**Rhizobiales**	▼
0.65	**0.33**	**0.25**	**0.30**	**0.45**	**0.72**	**0.43**	**0.62**	**0.79**	**Rhodobacterales**	—
0.69	**0.30**	**0.28**	**0.43**	**0.25**	**0.23**	**0.28**	**0.49**	0.80	**Rhodospirillales**	▼
0.79	**0.31**	**0.36**	**0.65**	**0.24**	**0.29**	**0.47**	0.66	1.76	**Rickettsiales (excl. SAR11)**	—
0.04	**0.02**	**0.02**	**0.05**	**0.01**	**0.01**	**0.03**	**0.06**	**0.13**	**Rickettsiales (SAR11 clade)**	▼
0.00	0.55	0.50	0.54	0.51	0.51	0.34	0.94	0.55	**Sphingomonadales**	▼
1.06	0.97	0.79	1.53	0.75	1.02	0.91	2.11	1.73	**Burkholderiales**	—
0.79	0.32	0.19	nd	0.50	0.20	0.44	1.13	**2.10**	**Methylophilales**	—
1.15	**0.40**	**0.32**	**0.31**	**0.33**	**0.36**	**0.26**	0.72	0.83	**Bdellovibrionales**	—
0.97	0.52	0.33	**0.16**	**0.15**	**0.27**	0.29	0.72	0.00	**Bradymonadales**	▼
0.23	0.25	0.14	0.12	**0.04**	**0.07**	**0.07**	0.20	0.12	**Myxococcales**	▼
1.21	0.82	0.65	**0.44**	**0.43**	**0.39**	0.63	1.30	1.25	**SAR324 clade(Marine group B)**	—
1.31	0.80	1.18	1.01	0.97	0.61	0.68	0.93	1.09	**Alteromonadales**	—
0.70	**0.30**	**0.50**	**0.61**	**0.40**	0.48	**0.27**	**0.40**	**0.60**	**Cellvibrionales**	▼
2.20	1.62	1.70	**3.06**	1.66	1.56	**2.27**	3.60	3.33	**KI89A clade**	▲
1.73	1.56	0.62	1.49	0.54	0.77	0.54	2.42	nd	**Legionellales**	—
0.77	**0.34**	**0.31**	**0.66**	**0.27**	**0.32**	**0.32**	1.05	**1.38**	**Oceanospirillales**	—
4.00	**0.31**	**0.23**	0.75	**0.27**	**0.31**	**0.38**	1.49	2.33	**Salinisphaerales**	—
1.13	0.86	1.11	1.52	0.39	0.37	1.07	1.38	2.76	**Thiotrichales**	—
0.67	0.87	0.58	18.00	0.48	0.79	0.97	1.21	1.50	**Xanthomonadales**	▲
0.21	**0.06**	**0.10**	0.04	**0.08**	**0.08**	**0.01**	0.11	0.33	**SBR1093**	▼
0.14	**0.06**	**0.05**	**0.10**	**0.03**	**0.02**	**0.03**	0.10	0.00	**Arctic97B-4 marine group**	▼
0.17	**0.03**	**0.08**	1.12	0.02	0.00	0.08	0.08	nd	**MB11C04 marine group**	▼
0.94	0.98	0.51	0.81	0.31	0.20	0.44	1.00	nd	**Puniceicoccales**	—
1.05	1.32	0.53	1.08	0.29	0.76	0.64	1.00	0.80	**Verrucomicrobiales**	—

Figure 5.9. Heat map showing the ratio of RNA to DNA abundance for all abundant taxa (>0.1% RA). Symbols indicate mean RNA:DNA ratio for each taxa across the whole transect (▲ >1:1, ▼ <1:1 and — =1:1). Bold numbers indicate a significant difference (Bonferroni p <0.05) between RNA and DNA abundance by province. Underlined taxa indicate a significant difference (Bonferroni p <0.05) between RNA and DNA abundance over all samples.

5.4 Summary of the physicochemical characteristics along the Atlantic Meridional Transect

The Atlantic Ocean can be partitioned into domains and provinces that are based on physical oceanographic features and biological production estimates (Longhurst et al., 1995), the details of which have been reviewed for the AMT previously (Aiken et al., 2000). During AMT25, twice daily casts recorded core physicochemical data along the transect that crossed ten biogeochemical provinces (figure 5.1). The northern temperate region (66-33°N) was relatively well mixed and characterised by lower seawater temperatures (~15 °C) and salinity (~36 PSU). Nutrients were low (mean 2.2 µM L^{-1} nitrate+nitrite, 1.4 µM L^{-1} silicate and 0.2 phosphate µM L^{-1}) and oxygen high (mean 224 µM L^{-1}), fluorescence was very high in the upper 50 m especially in the coastal domain at Station E1 (maximum 2.6 RFU), suggesting the presence of a seasonal phytoplankton bloom typical of boreal autumn (Bunse and Pinhassi, 2017). This was further evidenced by a high abundance of mainly pico-eukaryote primary producers (supplemental Figure 5.1). Seawater temperature (15-27 °C) and salinity (36-37 PSU) increased moving southward into the sub-tropical (33-23°N) and tropical northern Atlantic (23°N-0°), which was characterised by high surface seawater temperatures (25-30 °C) and salinity (37-38 PSU). Fluorescence (<0.1RFU) and oxygen (57 µM L^{-1}) were low, increasing slightly around 100-150 m at the DCM to maximum of 0.5 RFU and 223 µM L^{-1} respectively. Temperatures remained high into the equatorial region but salinity decreased (35-36 PSU). Fluorescence increased slightly to 1 RFU around the equator as did the abundance of eukaryotic primary producers (supplemental Figure 5.1); the DCM was located at ~ 50 m close to a high nutrient/low oxygen zone that existed below the thermocline between 20°N and 20°S. The characteristics of southern tropical Atlantic (0°-23°S) were much the same as the north although temperatures were slightly lower (12-24 °C) and the DCM extended to ~200 m. Nutrient levels throughout the tropical Atlantic were close to or at detection limits, either side of the equator this nutrient deplete area extends from the

surface to around 200 m and describes the northern and southern oligotrophic gyres. Temperature and salinity decreased heading south into the southern sub-tropical (23-33°S) and temperate Atlantic (33-66°S). The southern temperate region was well mixed and characterised by lower temperatures (4-12°C) and salinity (33-35 PSU) especially below 40°S (<10 °C and <35 PSU). Nutrient levels (mean 17 µM L^{-1} nitrate+nitrite, 5 µM L^{-1} silicate and 1 µM L^{-1}phosphate) and oxygen (mean 280) were high, with the highest values recorded below 40°S. Fluorescence and the abundance of eukaryotic primary producers was also higher in the upper 50 m compared to the oligotrophic gyres, but lower than the northern temperate ocean suggesting the austral spring bloom was not yet established due to lower seawater temperatures.

5.5 Discussion

5.5.1 Diversity and distribution of total and active bacterioplankton along the Atlantic Meridional Transect

Each province has distinct physicochemical characteristics (Longhurst et al., 1995) that could influence the composition of the resident microbial community. A recent study by Milici et al. (2016) showed that bacterioplankton communities in the Atlantic exhibit strong biogeographical patterns in response to differing environmental drivers but did not report the composition of the communities. In this study, bacterioplankton communities were also found to vary significantly by province, and the physicochemical seawater properties temperature, salinity, oxygen and fluorescence significantly influenced provincial differences in agreement with Milici et al. (2016). The bacterioplankton present were generally uniform across all provinces, with communities dominated by members of the Cyanobacteria, *Alphaproteobacteria*, *Bacteroidetes* and *Gammaproteobacteria*. However, the relative contribution of individual taxa to the communities varied significantly, agreeing

with the suggestion that bacterioplankton community composition is determined by abundance rather than presence i.e. by changes in the abundance of the bacteria present in the community rather than by changes in the presence or absence of specific bacterial taxa (Caporaso et al., 2012, Gibbons et al., 2013).

Prochlorococcus dominated the communities in all provinces except those in the temperate coastal domains (NECS and FKLD), where the relative abundances of heterotrophic bacterioplankton such as *Flavobacteriales*, *Rhodobacterales*, the SAR11 clade and *Oceanospirillales* were higher. This pattern largely followed the distribution of eukaryotic primary producers, which are thought to out compete prokaryotic phytoplankton in productive regions (Zinger et al., 2011). The coupling between eukaryotic phytoplankton and heterotrophic bacterioplankton is well documented (Buchan et al., 2014) and has been discussed previously (Chapter 4). Province SSTC which is the convergence zone between the productive Southern Ocean and the more oligotrophic Southern Atlantic Ocean was also characterised by a higher abundance of these heterotrophs and the Cyanobacterium *Synechococcus* which is associated with more productive nutrient regimes (Flombaum et al., 2013, Pittera et al., 2014). Consequently, bacterioplankton communities in these three provinces were more similar to each other than with neighbouring sub-tropical/tropical provinces and considered to be mesotrophic. The remaining provinces which had a higher abundance of the oligotrophs *Prochlorococcus* and the SAR11 clade were closely grouped and considered to be oligotrophic.

The oligotrophic provinces could also be further divided into sub-tropical (NASTW and SATL) and tropical (NATR and ETRA) provinces. The provinces NADR and NASTE are geographically temperate (i.e. >33°N) but were more similar to the provinces in sub-tropical regions, and so were included in the sub-tropical grouping. Bacterioplankton communities from sub-tropical provinces were generally quite similar to the bacterioplankton communities from tropical provinces, but had a slightly higher relative

abundance of copiotrophic heterotrophs such as the *Flavobacteriales* and a slightly lower relative abundance of *Prochlorococcus*. This distribution of bacterioplankton coupled with physicochemical variables that are midway between the mesotrophic (NECS, SSTC and FKLD) and tropical oligotrophic provinces (NATR and ETRA) suggest that changes in the bacterioplankton community occur over a latitudinal gradient and/or with distance from the coast, presumably in response to changing environmental conditions. Therefore, sub-tropical provinces are transitional regions connecting temperate and tropical regions of the ocean.

Interestingly, NASTW was the only province to vary between total community and active community in the ordination analyses. This apparent switch in group is possibly due to an increase in the abundance of Rickettsiales (excluding the SAR11 clade) in the active community. The abundance of *Alteromonadales* also increased in both total and active communities of the NASTW province. *Alteromonadales* are typical r-strategists, blooming rapidly in response to increased available substrates (Vergin et al., 2013, López-Pérez and Rodriguez-Valera, 2014). In addition, the abundance of *Trichodesmium* sp., which are known to bloom in response to atmospheric iron deposition (Capone et al., 1997, Chen et al., 2011, Rubin et al., 2011), increased in neighbouring province NATR. These two provinces are within the influence of nutrient and trace metal inputs from Saharan dust (Baker et al., 2006), it is possible that these taxa were responding to atmospheric deposition of terrestrial nutrients.

Seasonal scale variations in bacterioplankton communities are greatest in temperate regions compared to sub-tropical and tropical regions (Bunse and Pinhassi, 2017). In this study, the mesotrophic provinces showed greater variability than oligotrophic provinces, most likely due to differences in nutrient status between the northern and southern hemisphere in opposing seasons. Northern province NECS (autumn) had low nutrient levels in common with oligotrophic provinces but high eukaryotic primary production in common with southern temperate provinces SSTC and FKLD (spring). *Prochlorococcus* were

dominant in province NECS, but less dominant in province SSTC and FKLD when *Flavobacteriales* became more dominant. These diversity patters agree with seasonal scale studies of temperate regions discussed in detail in Chapter 4, which show that oligotrophic bacterioplankton increase in abundance during summer and autumn seasons in contrast to spring when copiotrophs (e.g. *Rhodobacterales*) dominate (Bunse and Pinhassi, 2017).

It is also worth noting that in this study each province was represented by samples within a relatively localised area (~150 km), while this is representative when comparing the bacterioplankton community over the entire transect, it is possible that the community could vary within a province. STN8 was divided across the two adjacent provinces SSTC and FKLD, with the bacterioplankton communities from these samples more closely related by their spatial proximity than their province grouping. This may be due to seasonal variation in the geographical position of the classic Longhurst province boundary (Reygondeau et al., 2013) or may be evidence that transitional gradients exist over province boundaries.

5.5.2 Bacterioplankton presence vs. bacterioplankton activity

Using RNA:DNA ratios Hunt et al. (2013) showed that bacterial activity was decoupled from bacterial abundance in the Pacific (i.e. high abundance does not denote high activity). To investigate the active communities in this study, 16S rRNA gene transcripts were compared to 16S rRNA gene abundance. Although the overall diversity and distribution of the total and active communities were comparable, the relative abundance of individual taxa varied significantly between total and active communities leading to variations in the RNA:DNA ratios.

On the whole, marine bacterioplankton communities are considered active according to previous methods (Campbell et al., 2011, Hunt et al., 2013,), with a mean activity to abundance RNA:DNA ratio of 1.18. However, this activity level was not uniformly distributed across provinces or taxa. Overall, the activity of heterotrophs was low in contrast

to the autotrophic Cyanobacteria, which were highly active members of the community. The high activity of the Cyanobacteria is predictable given their significant role in photosynthetic primary production in the open ocean (Partensky et al., 1999, Richardson and Jackson, 2007, Uitz et al., 2010).

In this study, bacterioplankton communities were more active in the mesotrophic provinces compared to the communities in oligotrophic provinces. The increased activity in the northern and southern mesotrophic provinces was largely attributed to members of the *Bacteroidetes*, *Alphaproteobacteria* and *Gammaproteobacteria*. Cyanobacteria (excluding *Prochlorococcus* and *Trichodesmium*) also contributed to increased activity in the northern mesotrophic provinces. Bacterial (secondary) production shows a positive relationship with chlorophyll-a (a proxy for primary production) (del Giorgio and Scarborough, 1995, Ortega-Retuerta et al., 2008). Heterotrophic bacterioplankton (including members of the *Bacteroidetes*, *Alphaproteobacteria* and *Gammaproteobacteria*) have also been shown to be less active in the uptake of dissolved organic matter (DOC) derived from *Prochlorococcus* (the dominant primary producer in this study) than from other primary producers such as S*ynechococcus* and diatoms (Sarmento and Gasol, 2012). Therefore it is likely that the higher heterotrophic activity in coastal provinces was stimulated by substrates produced by eukaryotic phytoplankton, which had a higher abundance in the mesotrophic provinces in this study.

In agreement with other studies using RNA:DNA ratios (Lami et al., 2009, Hunt et al., 2013), the abundant SAR11 clade had low activity across all provinces, which is likely a reflection of their oligotrophic life strategy (Giovannoni, 2017). However, several studies that have investigated the assimilation of specific compounds such as leucine, glucose and other amino acids, suggest that the SAR11 clade are very active in the community (Malmstrom et al., 2004, Mary et al., 2006b, Laghdass et al., 2012). Considering the global abundance of the SAR11 clade, it is important to elucidate their contribution to

bacterioplankton secondary production. The discrepancies in reported SAR11 clade activity may be because of the different methodologies used (RNA:DNA ratios vs substrate uptake); seawater incubated with supplementary substrates stimulate SAR11 clade activity whereas *in situ* RNA:DNA ratios suggest SAR11 clade activity is low in the environment. These results taken together show the SAR11 clade has potential to be a highly active member of the community when conditions suit, (i.e. when concentrations of labile substrates such as amino acids are more abundant) but otherwise exhibit low activity. These results also suggest more environmentally relevant substrates such as organic matter (OM) derived from phytoplankton cultures should be used to determine heterotrophic productivity as suggested by Sarmento and Gasol (2012), who showed that the SAR11 clade have very low interaction strength with *Prochlorococcus* derived DOC but very high interaction strength with leucine.

In contrast to the SAR11 clade, the oligotrophic *Gammaproteobacteria* K189A clade had a higher than average activity in all provinces but was generally a rarer member of the community. The K189A clade is a member of the oligotrophic marine *Gammaproteobacteria* group (OMG) and has slow growth rates (Cho and Giovannoni, 2004). Therefore the high RNA:DNA ratio seen in the K189A clade is likely a result of increased metabolic activity rather than increased growth. These results suggest that abundant oligotrophs employ a different strategy to rare oligotrophs, with the SAR11 clade displaying a less active but abundant strategy versus K189A clade that displays a rare but active strategy.

5.5.3 The vertical distribution of total and active bacterioplankton in relation to light

Solar radiation impacts the activity of some bacteria and has been shown to alter bacterioplankton community composition (Alonso-Saez et al., 2006). The effect of light on the composition of the bacterioplankton community was examined by comparing samples taken at three different light depths; NECS was excluded from these analyses as the sampling

occurred at a different time of day from only two nominal depths. The overall active bacterioplankton community (i.e. RNA-derived) in this study did not differ significantly with light intensity, although several individual taxa did show some significant differences. Conversely, an overall significant difference in total bacterioplankton communities (i.e. DNA-derived) was seen between 'high' (97 % and 55 %) and 'low' (1 %) light depths.

Of the total and active bacterioplankton communities, the majority of taxa to show a significant difference by light depth were lower in abundance at high light depths than at low light depths (e.g. Rhizobiales, SAR406 clade, *Alteromonadales*, Acidimicrobiales). Taxa that showed a significant difference in both the active community and the total community showed the same relationship, suggesting that the RNA:DNA ratio i.e. activity level did not change in response to light but their abundance did. The *Gammaproteobacteria* K189A clade and the Cyanobacteria *Trichodesmium* sp. had a significantly higher abundance in the active community at depths where there was high light intensity with no difference seen in the abundance of the total community, suggesting that these taxa were more active at high light depths and have some form of UVR resistance or tolerance. *Trichodesmium* sp. are known to produce protective compounds such as mycosporine-like amino acids (Cai et al., 2017) enabling them to inhabit near surface waters (Capone et al., 1997). A high proportion of *Gammaproteobacteria* have also been shown to be resistant to UVR (Agogue et al., 2005b). UVR resistance in the K189A clade has not been determined, although other members of the OMG group are known to contain genes enabling mixotrophic growth using light (Spring et al., 2015).

Previous studies have shown that *Prochlorococcus* are more sensitive to UVR stress than *Synechococcus* (Llabrés and Agustí, 2006, Six et al., 2007, Zinser et al., 2007, Mella-Flores et al., 2012). However, the vertical distribution of Cyanobacteria in this study did not show any distinctive patterns that suggested light-dependant niche partitioning within this phylum. This is possibly because vertical partitioning according to high and low light is less

defined in *Synechococcus* which exhibits stronger latitudinal niche partitioning (Pittera et al., 2014, Zwirglmaier et al., 2007) and the OTU cut off of 97 % used in this study would not distinguish between light ecotypes of *Prochlorococcus* (Johnson et al., 2006, Zinser et al., 2007).

5.5.4 Diurnal patterns in the distribution of total and active bacterioplankton

Circadian rhythms are established in *Cyanobacteria* and some heterotrophic bacteria have also been shown to possess genes associated with 'time keeping' (Johnson et al., 2017). Whether bacteria contain true biological clocks or just diurnally regulated genes, they are exposed to variations in light and other physicochemical variables over a diurnal cycle potentially influencing bacterioplankton community structure. Diurnal effects of light on the bacterioplankton community were investigated by comparing samples taken during pre-dawn and solar noon casts. For these analyses, NECS was also excluded for the same reasons mentioned before. Although overall there was no significant difference between noon and pre-dawn bacterioplankton communities, some specific dominant taxa showed a significant difference in noon and pre-dawn abundance.

In both the total and active bacterioplankton communities *Rhodobacterales* were more abundant in noon samples and *Flavobacteriales* were more abundant in pre-dawn samples. Members of both *Bacteroidetes* and *Rhodobacterales* have also been shown to have rhythmical genes that are expressed with a periodicity of 24 h, such as circadian clock genes *kaiBC* and oscillator gene *prx* (Loza-Correa et al., 2010, Hörnlein et al., 2018). Building upon the substrate controlled succession/niche separation of heterotrophic bacterioplankton proposed by Teeling et al. (2012) and Buchan et al. (2014) the metabolic wave theory proposes diurnal variation in heterotrophic activity is also coupled to the production and availability of organic matter from primary producers (Gasol et al., 1998, Ottesen et al., 2014). Given these two taxa occupy co-occurring niches and are often

associated with phytoplankton, their contrast in total and active abundance may be a result of substrate specialisation. *Flavobacteriales* degrade high-molecular weight OM (e.g. phytoplankton-derived polysaccharides), and *Rhodobacterales* degrade associated low-molecular weight OM (e.g. monosaccharides) (Buchan et al., 2014).

Although OM concentration was not recorded in this study, a previous study by Obernosterer et al. (2001) found that DOC in the sub-tropical Atlantic to be higher in the morning (08:00) than at noon, similar patterns have also been observed for amino acids and particulate organic carbon (POC) in the Baltic sea (Mopper and Lindroth, 1982, Szymczycha et al., 2017). Assuming the same pattern is true for this study, the higher abundance seen in primary degraders (*Flavobacteriales*) at pre-dawn and higher abundance seen in the secondary degraders (*Rhodobacterales*) at noon would be explained by the metabolic wave hypothesis.

The abundance of some *Cyanobacteria* taxa also varied significantly between pre-dawn and noon sampling times, *Prochlorococcus* was more abundant at noon in the total and active community and Subsection I other which was most closely related to *Synechococcus* sp., was more abundant at dawn in the active community. However because these taxa also varied significantly by light depth, further comparison was made between pre-dawn and noon at each different light depth. In the total community (DNA-derived) *Prochlorococcus* and *Synechococcus* showed little variation in abundance between noon and pre-dawn, although their abundance increased with depth at noon and decreased with depth pre-dawn. In the active community (RNA-derived), *Prochlorococcus* and *Synechococcus* were both more abundant pre-dawn and decreased in abundance with depth at both noon and pre-dawn sampling times. The same relationship was also seen for the putative *Synechococcus* but was less pronounced.

The patterns seen in the total community suggest that trade-offs exist between photosynthesis and UVR stress; although the vertical distribution of *Cyanobacteria* appears

to be influenced diurnally by light, *Cyanobacteria* are overall more abundant during the day when PAR is higher. The higher abundance seen in the active community pre-dawn is more likely indicative of cell division rather than other metabolic processes such as photosynthesis. Zubkov et al. (2000) showed a higher proportion of *Prochlorococcus* in the Atlantic contained double the amount of DNA at night than during the day. A diurnal strategy of cell division at night and photosynthesis during the day may allow for more efficient use of light hours, and limit UVR damage which has been linked to cell activity (Alonso-Saez et al., 2006). Also growth at night may boost the population which probably becomes depleted throughout the day by UVR induced cell death (Llabrés and Agustí, 2006).

5.5.5 Conclusions

This study characterised the bacterioplankton communities from nine different biogeochemical provinces spanning the north and South Atlantic Ocean, showing that the bacterioplankton community composition was typical of the environments investigated (e.g. open ocean and coastal), and exhibited strong biogeographical variation in response to prevailing seawater characteristics (figure 5.10).

The data presented here suggest that the physicochemical properties that define provinces occur across gradients. While biogeochemical provinces are a useful tool to estimate environmental conditions the variation in physicochemical properties within a province can affect the bacterioplankton community. Therefore, the general characteristics of a province are not enough to accurately predict bacterioplankton community composition and activity without more specific physicochemical data, which may have implications for biogeochemical modelling.

A major aim of this study was to compare total and active bacterioplankton communities. We have shown that bacterioplankton activity is decoupled from abundance throughout the Atlantic, although the two community types show similar patterns in beta

diversity. *Cyanobacteria* were among the most active members of the community, compounding their important role in primary production in the open ocean. In contrast, the abundant SAR11 clade were one of the least active members of the community, raising uncertainty about their potential contribution to bacterial secondary production. Organic carbon source (i.e. the dominant primary producer) is potentially important in determining the activity of dominant heterotrophic bacterioplankton with the activity of copiotrophs most likely coupled with eukaryotic primary producers.

There are limitations in using RNA as a measure of activity; RNA concentration does not always correlate to growth rate and this relationship can differ between taxa. Without a better understanding of how RNA concentration relates to different metabolic activities it is not possible to determine if the activity measured in the environment relates to growth activities or non-growth activities (Blazewicz et al., 2013). However, there is still merit in using RNA as a measure of activity, here we have normalised RNA to DNA concentration and shown changes in activity for different taxa over a range of environments, in this context using RNA:DNA ratios as an estimate of bacterial activity could help improve our understanding of bacterioplankton production in the oceans, and if applied to functional gene transcription and abundance has potential to improve measures of ecosystem function by individual taxa or the community as a whole.

This study suggests that light contributes to the vertical distribution of bacterioplankton communities in the open ocean. Surprisingly, light did not significantly affect the overall structure of the active community. However, the activity of a few taxa such as the *Cyanobacteria* did vary according to light depth. Although not identified in this study, light niches are likely to exist but require a higher taxonomic resolution to resolve different ecotypes. Using a higher OTU cut off or amplicon sequence variants (ASVs) to identify variation in highly similar sequences could help to further resolve distribution patterns within closely related taxonomic lineages.

Whole bacterioplankton communities did not vary between noon and pre-dawn, but ecologically important members of the community did show distinct differences in activity. Our data provides supporting evidence that *Prochlorococcus* and other *Cyanobacteria* have higher growth rates during dark hours. We also show diurnal patterns in heterotrophic bacterioplankton and suggest that this is a result of the metabolic wave theory proposed previously (Ottesen et al., 2014).

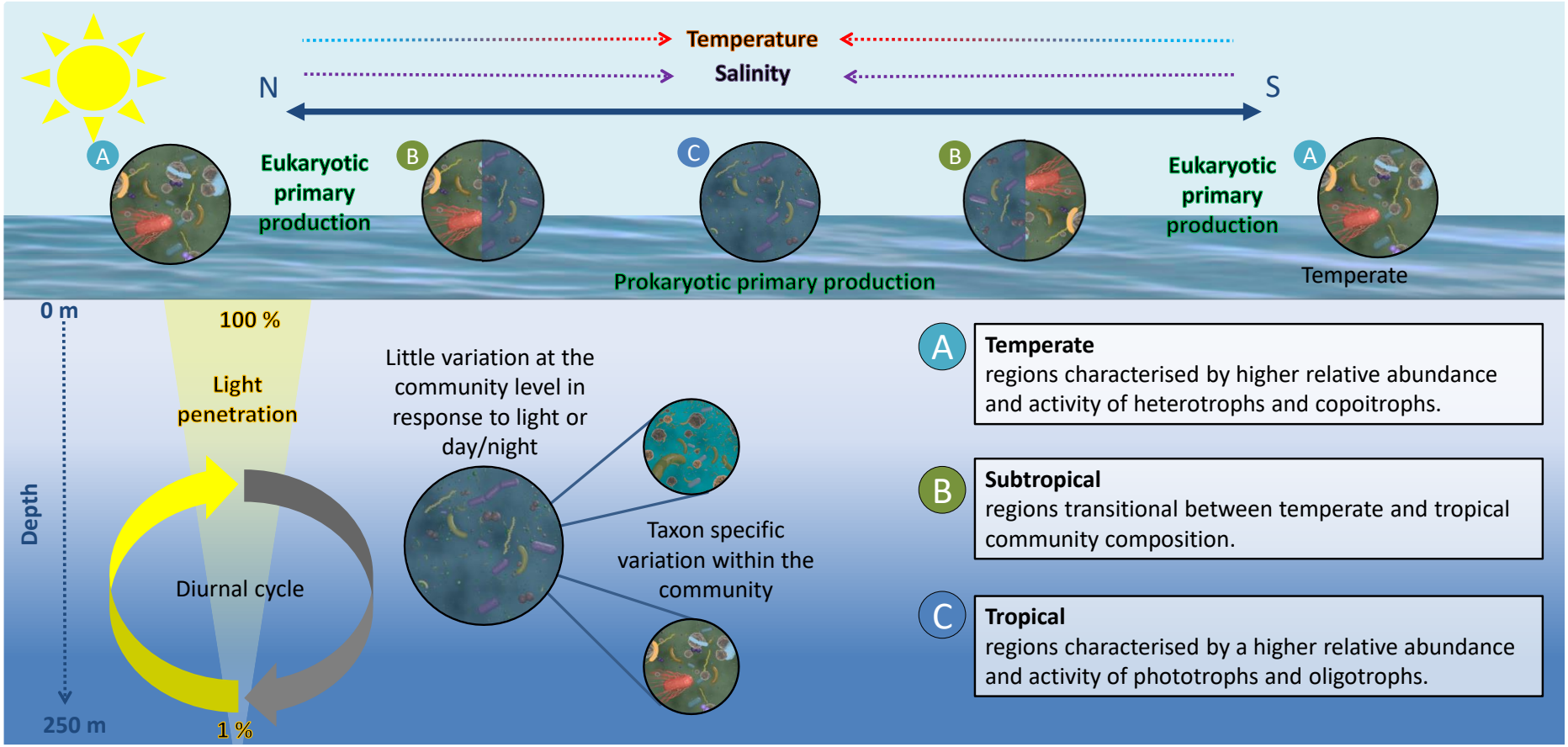

Figure 5.10. Conceptual diagram of the open ocean environment illustrating the typical bacterioplankton community composition in response to different biogeographical environments over a latitudinal transect of the Atlantic including a schematic of depth resolved variation in response to light.

5.6 Supplemental material

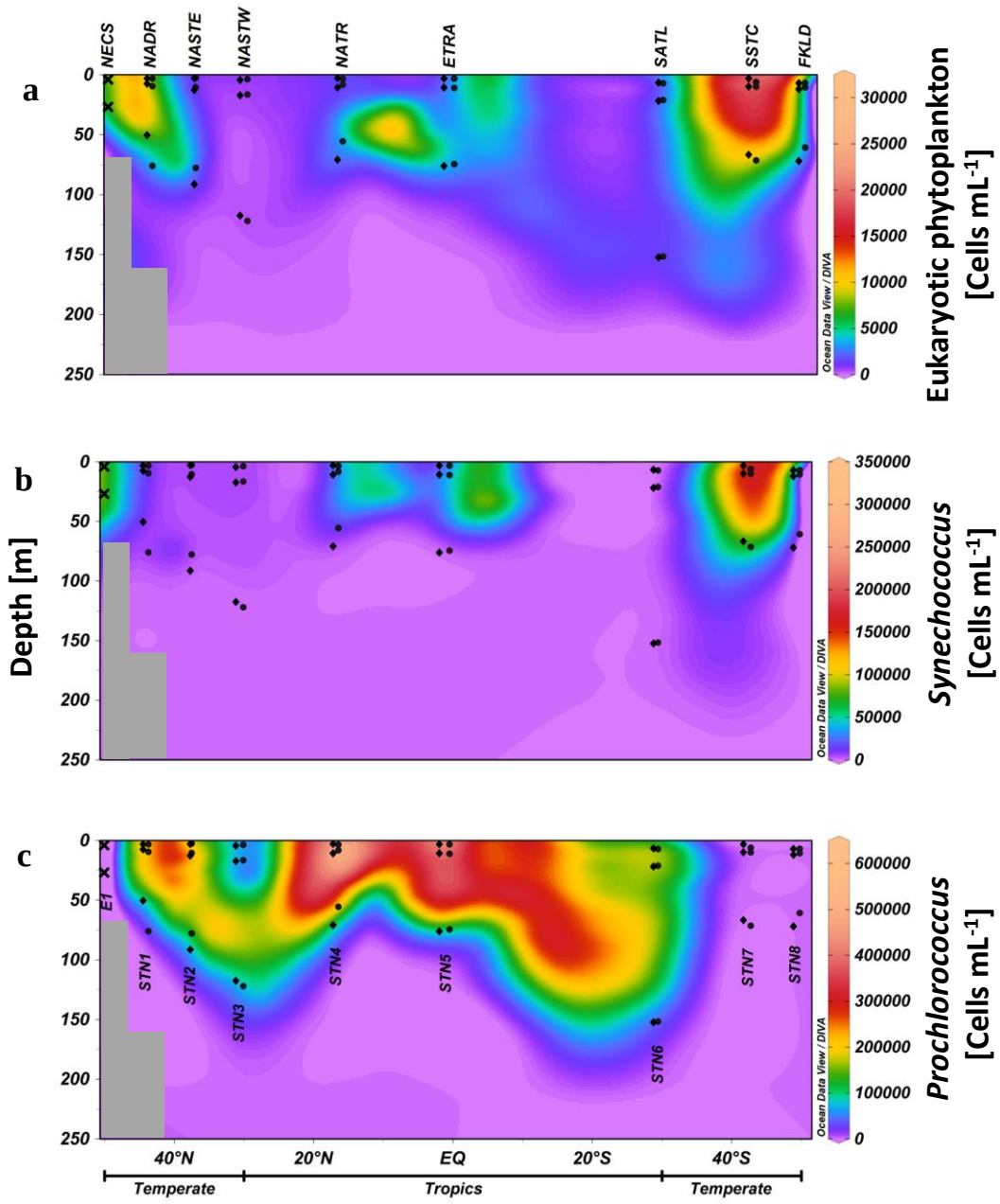

Supplemental figure 5.1. Data-Interpolating Variational Analysis (DIVA) gridded section plots showing flow cytometry data [Cells mL^{-1}] along the AMT25 during 2016. a) total eukaryotic phytoplankton, b) *Synechococcus* and c) *Prochlorococcus*. Depth [m] on the Y axis vs. latitude on the X axis. Symbols represent position of water samples analysed in this study (● noon, ◆ pre-dawn and ✕ Western Channel Observatory Station E1).

Chapter 6

A multidisciplinary approach to studying the sea surface microlayer reveals the complexity of physicochemical influences on bacterioneuston diversity

6.1 Introduction

The sea surface microlayer (SML) is the physical boundary between the atmosphere and the marine environment, generally defined as the upper most 1mm of the surface ocean (Hunter, 1980). The SML is a biogenic particle-enriched biofilm layer (Sieburth, 1983, Wurl and Holmes, 2008, Cunliffe and Murrell, 2009) that can exist as an invisible (to the eye) layer or visible layer that is often referred to as a 'slick' resulting from the increased supply of organic matter (OM) to the SML (Salter et al., 2011). The SML has physicochemical properties that differ significantly from the underlying water (ULW) (Zhang et al., 2003), forming a unique microhabitat and often creating distinct biological communities termed neuston (Naumann, 1917). Covering 70% of the Earth's surface, the SML influences everything that passes through the air-sea boundary and therefore has a major role in global biogeochemical and climate processes.

Bacterioneuston communities originate from the underlying bacterioplankton community (Agogue et al., 2005a, Joux et al., 2006, Stolle et al., 2011) but can have markedly different community structure (Franklin et al., 2005, Joux et al., 2006, Cunliffe et al., 2009). It is largely accepted that the differences between the bacterioneuston and bacterioplankton community structure are in response to SML-specific ecological drivers (Cunliffe et al., 2011). Previous studies have demonstrated changes in bacterioneuston community composition and distribution in response to different biological, chemical and physical characteristics of the SML, such as prevailing meteorological conditions (Stolle et al., 2010, Stolle et al., 2011, Rahlff et al., 2017) and organic matter (OM) composition (Obernosterer et al., 2005, Cunliffe et al., 2009, Zäncker et al., 2017). However, few studies have examined a large range of co-occurring physicochemical measurements simultaneously. The need for a wide-ranging holistic approach when studying the SML has been highlighted in review articles over the past decade (Cunliffe et al., 2011, Cunliffe et al., 2013, Engel et al., 2017, Wurl et al., 2017). Despite many conceptual models of the sea

surface microlayer being proposed (e.g. figure 6.1), no previous studies have investigated the hypothesised interactions of the major physical, chemical and biological components of the SML.

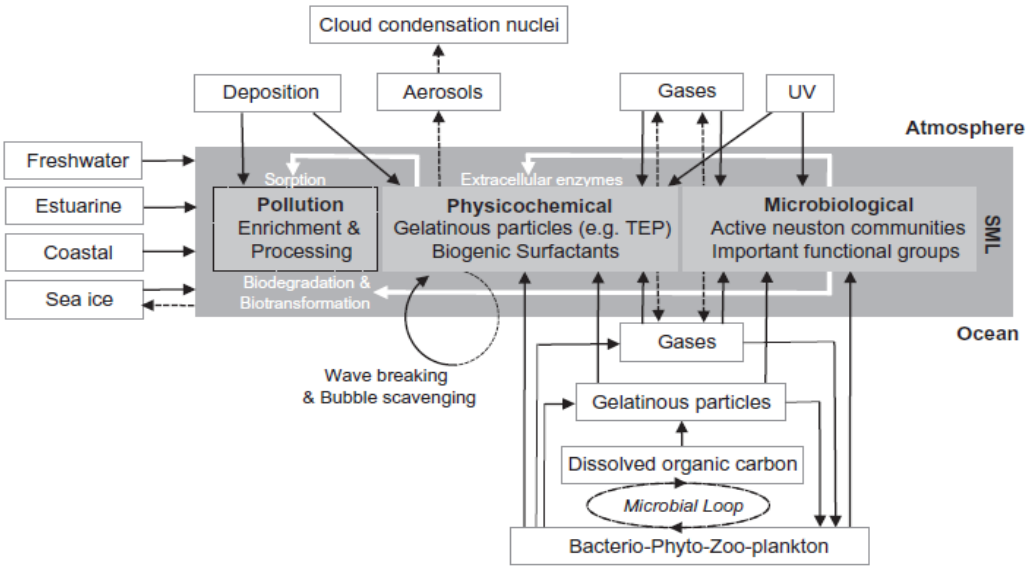

Figure 6.1. Conceptual model of the sea surface microlayer (Cunliffe et al., 2013).

OM is often enriched in the SML (Wurl et al., 2009, Kattner and Brockmann, 1978, Wurl et al., 2011a) and exists in a variety of forms such as soluble, colloidal and particulate material. Rich in nitrogen (N), phosphorous (P) and carbon (C), OM in the SML is a reservoir of valuable substrate for bacterial growth (Zäncker et al., 2017). The SML varies spatially and temporally in response to biological, chemical and physical influences (Wurl et al., 2011b), and recently OM in the SML has been shown to vary according to the prevailing nutrient regime (Zäncker et al., 2017). Yet very little is known about how bacterioneuston communities respond to differing geochemical regions.

In addition to OM, biologically important trace elements are also enriched in the SML (Hunter, 1980, Ebling and Landing, 2017). Trace elements enter the SML via atmospheric deposition and, based on estimates of residence time in the SML, could be altered by biological and chemical processes before passing to the ULW (Ebling and

Landing, 2017). Despite the importance of trace elements to microbial community composition and biogeochemical functioning in the ocean (Boyd et al., 2017), relatively little is known about the fate of trace elements in the SML and microbe-trace element interactions remain an underestimated but potentially important component of marine nutrient cycles (Wurl et al., 2017).

Bacterial production in the SML can be limited by physical stressors such as high levels of solar radiation and increased exposure to turbulent processes (Stolle et al., 2011, Santos et al., 2012). SML 'stability' is often defined by wind speed, with the SML reported as stable (i.e. distinct from the ULW) at wind speeds up to 5 m s^{-1} (Stolle et al., 2011, Wurl et al., 2011b, Rahlff et al., 2017). Wind speeds in excess of this threshold have been shown to inhibit the formation of distinct bacterioneuston communities under experimental mesocosm conditions, however, in the marine environment, OM enrichments have been shown to persist in the SML under wind speeds up to 10 m s^{-1} (Wurl and Holmes, 2008, Reinthaler et al., 2008, Wurl et al., 2011b). The OM composition of the SML can alter the effect of physical stress acting on the surface ocean, including by capillary wave-dampening (Salter et al., 2011) or increased viscoelastic properties allowing the SML to rapidly reform after disturbance (Wurl et al., 2011b). It has been proposed that OM, especially particulate OM, could aid the enrichment of bacterioneuston to persist at increased wind speeds (Stolle et al., 2011). However, we currently know little about how the interaction of physical, chemical and biological characteristics of the SML, influence the structure of bacterioneuston communities.

The aim of this study was to identify the potential links between the SML physicochemical environment and bacterioneuston diversity. The study focused on simultaneously examining the influences of physical stress, dust deposition, and meteorological processes on the chemical composition of the SML and bacterioneuston communities in two contrasting marine environments; the productive coastal Sunda-Arafura

shelf region off the north coast of Australia and the oligotrophic open ocean warm pool region in the West Pacific Ocean. The extensive collection of co-occurring physicochemical data during this study facilitated an unprecedented comprehensive analysis of the SML physiochemical environment. In this study, we address three novel questions: 1) Are bacterioneuston communities uniform across different broad-scale marine environments? 2) What bacterioneuston taxa are enriched in the SML, and what are the physicochemical drivers of their enrichment? 3) Do interactions of physical and chemical SML characteristics influence the bacterioneuston community composition?

6.2 Method summary

6.2.1 Seawater sampling

Sampling was carried out during the Schmidt Ocean Air to Sea cruise (FK161010) from Darwin, AU to Guam, US (October 11–November 10, 2016; *RV Falkor*). Samples were collected at nine coastal stations located in the Sunda-Arafura shelf region off the north coast of Australia (figure 6.2a and c) and at 7 oceanic stations in the warm pool region of the west Pacific (figure 6.2a and b). SML and ULW samples were collected during AM (~23:00 UTC) and PM (~04:00 UTC) workboat deployments. Samples were filtered onto 0.2 µm membrane filters and stored in a nucleic acid preservative at -80 ^{0}C. On return to the laboratory at the MBA, DNA was extracted from the membranes using a commercially available extraction Kit and sent for 16S rRNA gene sequencing.

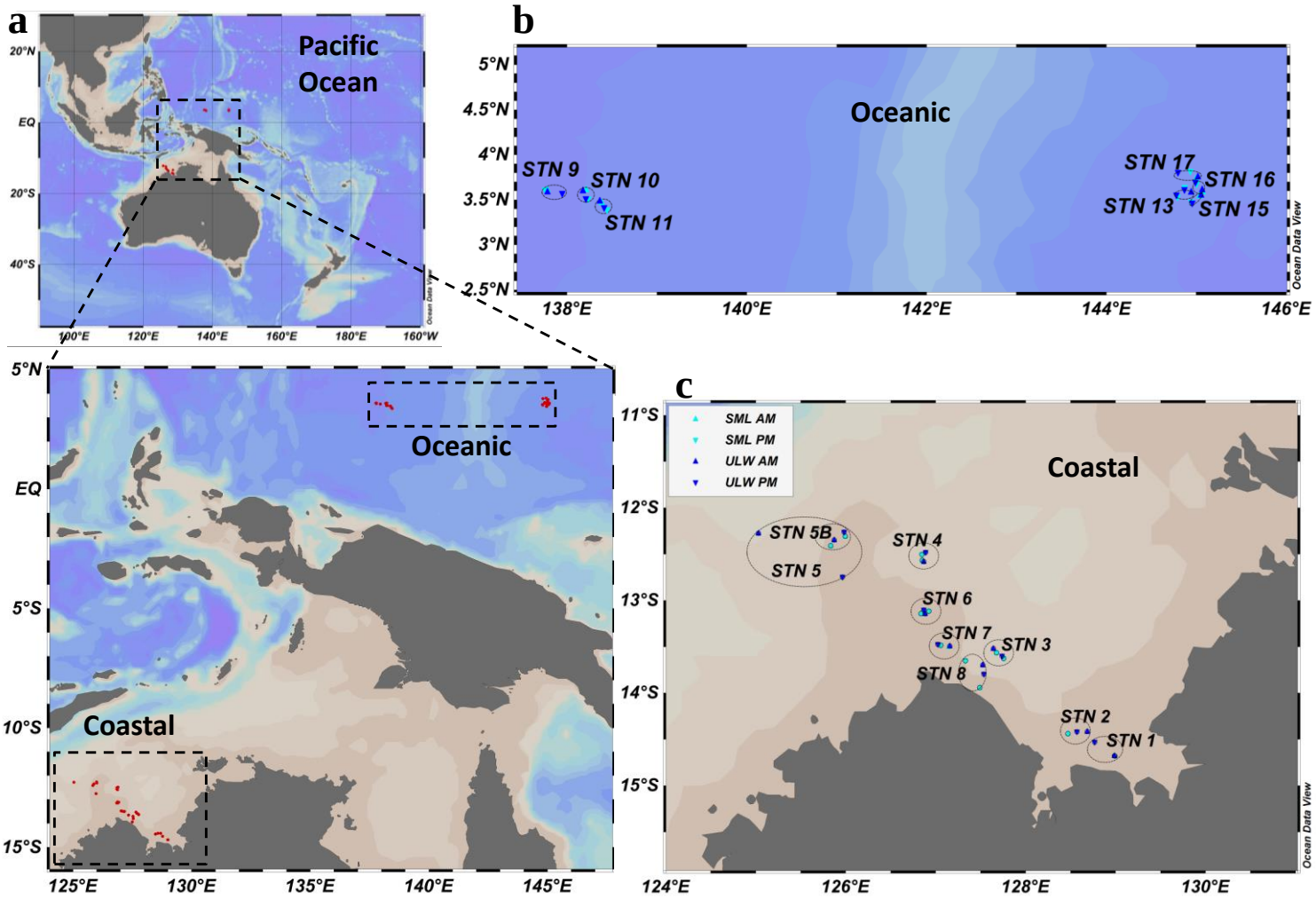

Figure 6.2. Map showing a location of study, ai coastal and oceanic sites, b oceanic sampling stations and c coastal sampling stations.

6.3 Results

6.3.1 Physicochemical and meteorological properties

Overall there was little difference in temperature between the SML and the ULW at both coastal and oceanic stations, although temperature showed that the SML was more often slightly cooler than the ULW. Seawater temperature ranged 28.0 - 33.6 °C (mean 30.9 °C) in the SML and 29.2 - 33.8 °C (mean 30.8 °C) in the ULW at coastal stations (figure 6.3a), and 29.0 - 33.6 °C (mean 30.5) in the SML and 29.1 - 32.9 (mean 30.6) in the ULW at oceanic stations (figure 6.3b). The SML was generally more saline than the ULW at both coastal and oceanic stations, although delta salinity was more varied at oceanic stations. Salinity ranged 31.6 - 37.0 PSU (mean 34.90 PSU) in the SML and 32.0 - 36.0 PSU (mean 34.7 PSU) in the ULW at coastal stations (figure 6.4a) and 31.6 – 35.8 PSU (mean 34.1 PSU) in the SML and 32.0 - 34.9 PSU (mean 33.88 PSU) in the ULW at oceanic stations (figure 6.4b). The pH at coastal stations (figure 6.5a) was generally higher in the SML, range 7.83 - 8.28 (mean 8.15) than the ULW, range 8.02 - 8.26 (mean 8.12). At stations 4 and 7, the pH showed sporadic large drops of ~ 0.15 units in the SML compared to the ULW. The difference in pH between SML and ULW was more variable at oceanic stations (figure 6.5b), but was generally lower in the SML, range 8.09 - 8.27 (mean 8.18) than the ULW, range 8.18 - 8.62 (mean 8.62), especially at stations 15 – 17, where the pH of the ULW increased by ~ 0.4 units above that of the SML.

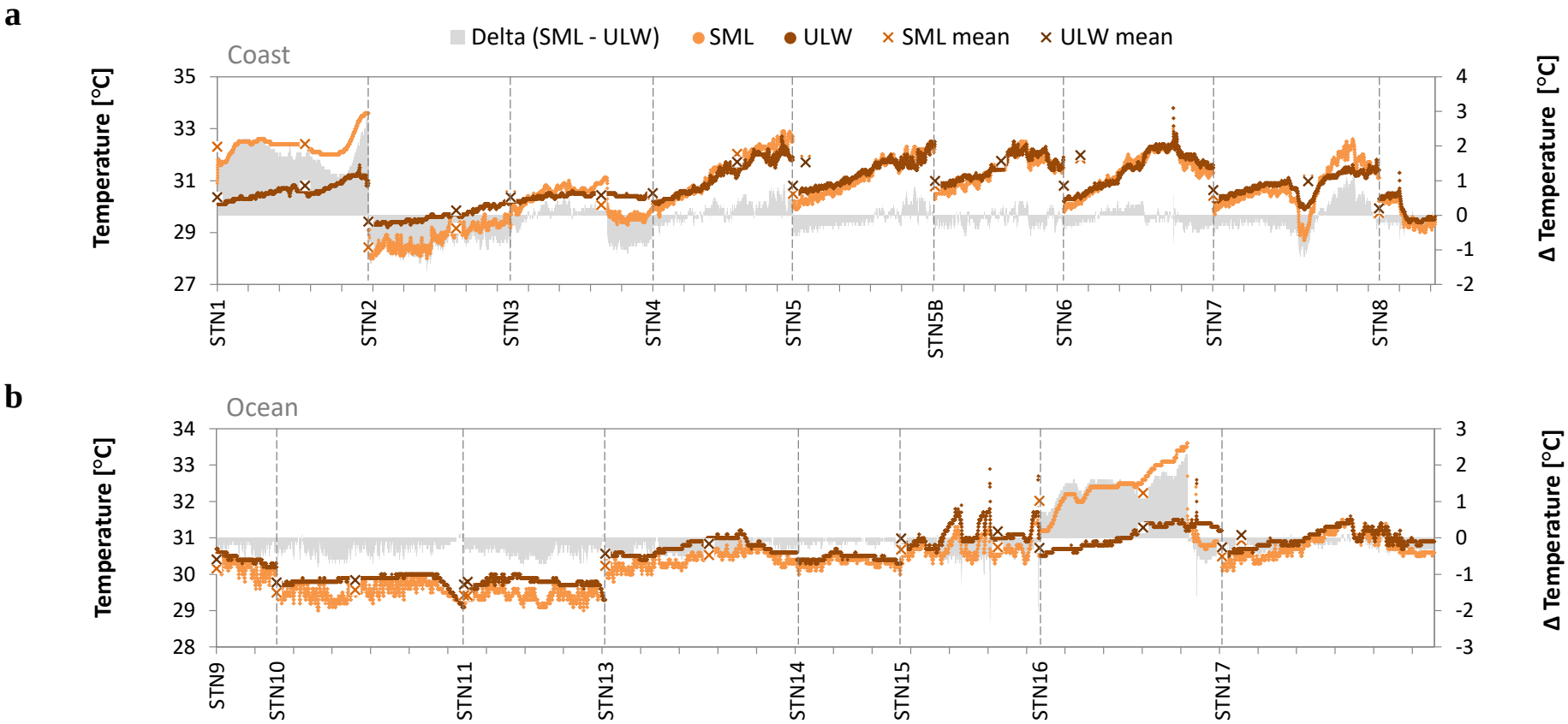

Figure 6.3. Temperature [°C] measured in the sea surface microlayer (SML) and underlying water (ULW) at a) coastal stations b) oceanic stations. Points represent an individual data point, bars represent the difference between the SML and the ULW, and crosses represent the mean for each station at AM and PM sampling times. Data is not continuous between stations, intervals between each station are indicated by dashed gridlines.

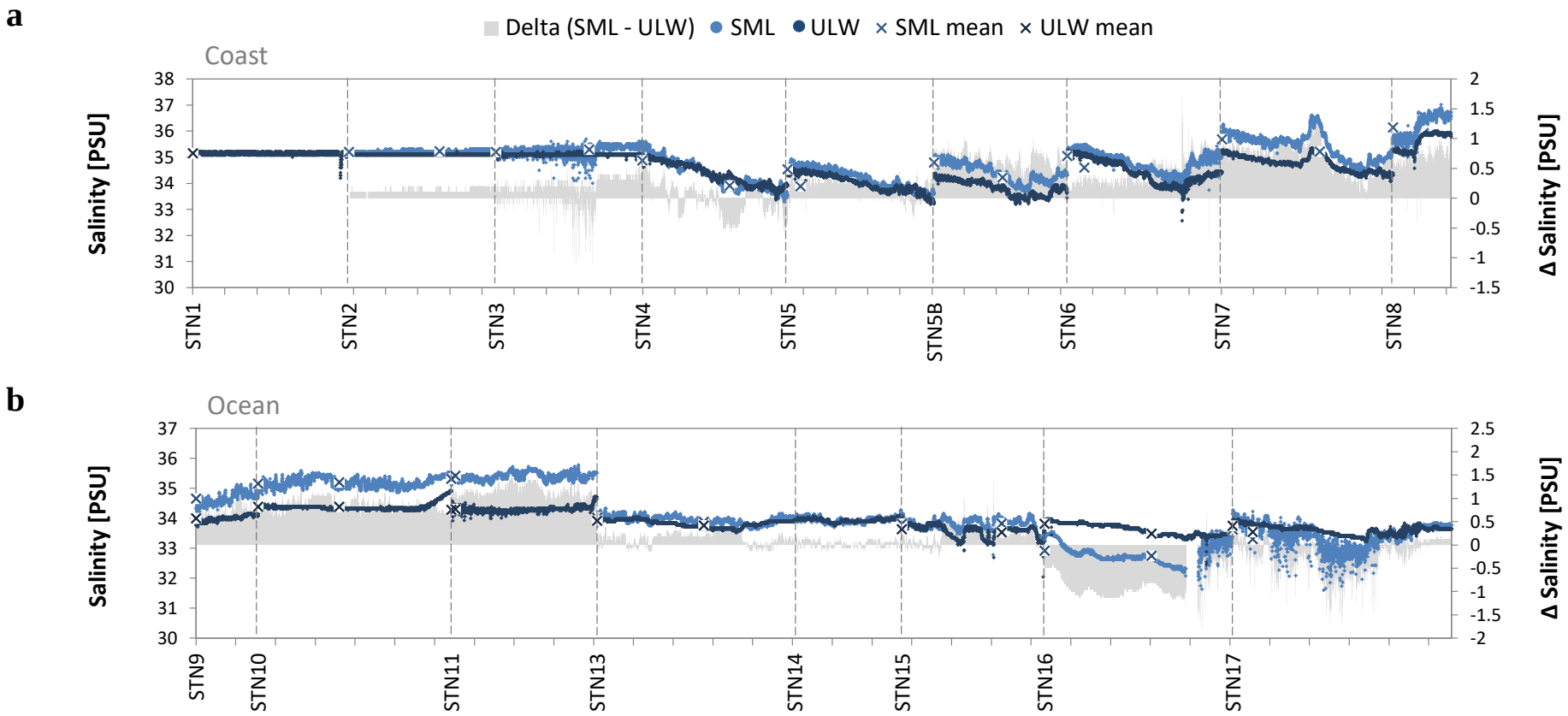

Figure 6.4. Salinity [PSU] measured in the sea surface microlayer (SML) and underlying water (ULW) at a) Coastal stations b) oceanic stations. Points represent an individual data point, bars represent the difference between the SML and the ULW, and crosses represent the mean for each station at AM and PM sampling times. Data is not continuous between stations, intervals between each station are indicated by dashed gridlines.

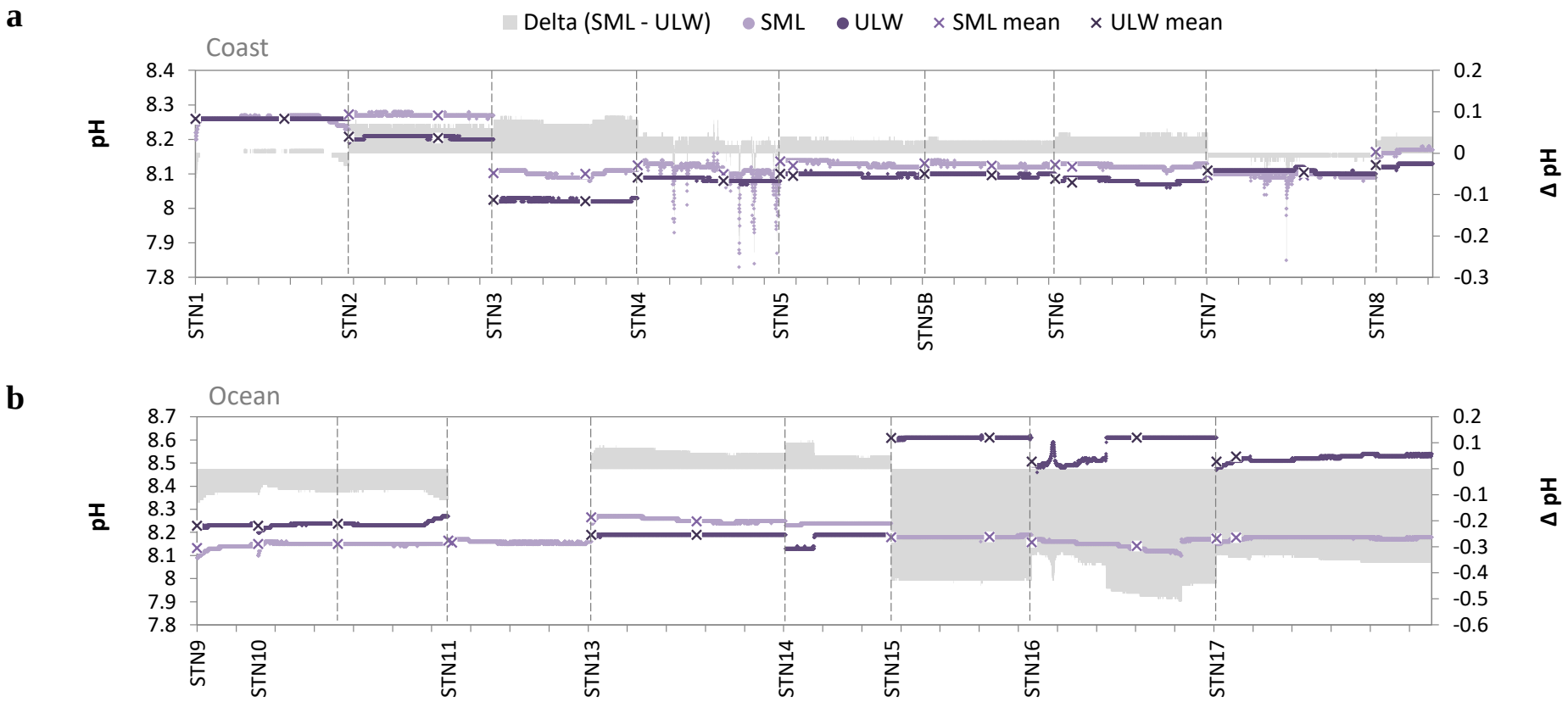

Figure 6.5. pH measured in the sea surface microlayer (SML) and underlying water (ULW) at a) coastal stations b) oceanic stations. Points represent an individual data point, bars represent the difference between the SML and the ULW, and crosses represent the mean for each station at AM and PM sampling times. Data is not continuous between stations, intervals between each station are indicated by dashed gridlines.

Fluorescent dissolved organic matter (fDOM) was only recorded for coastal stations (figure 6.6) and was generally higher in the SML (mean 2.79 µg L^{-1}; range 0.4 - 31.6 µg L^{-1}) than the ULW (mean 1.22 µg L^{-1}; range 0.4 - 6.8 µg L^{-1}), with large peaks above average in the SML at stations 5, 5B, 6 and 7 and an extreme peak reaching 31.6 µg L^{-1} at station 4.

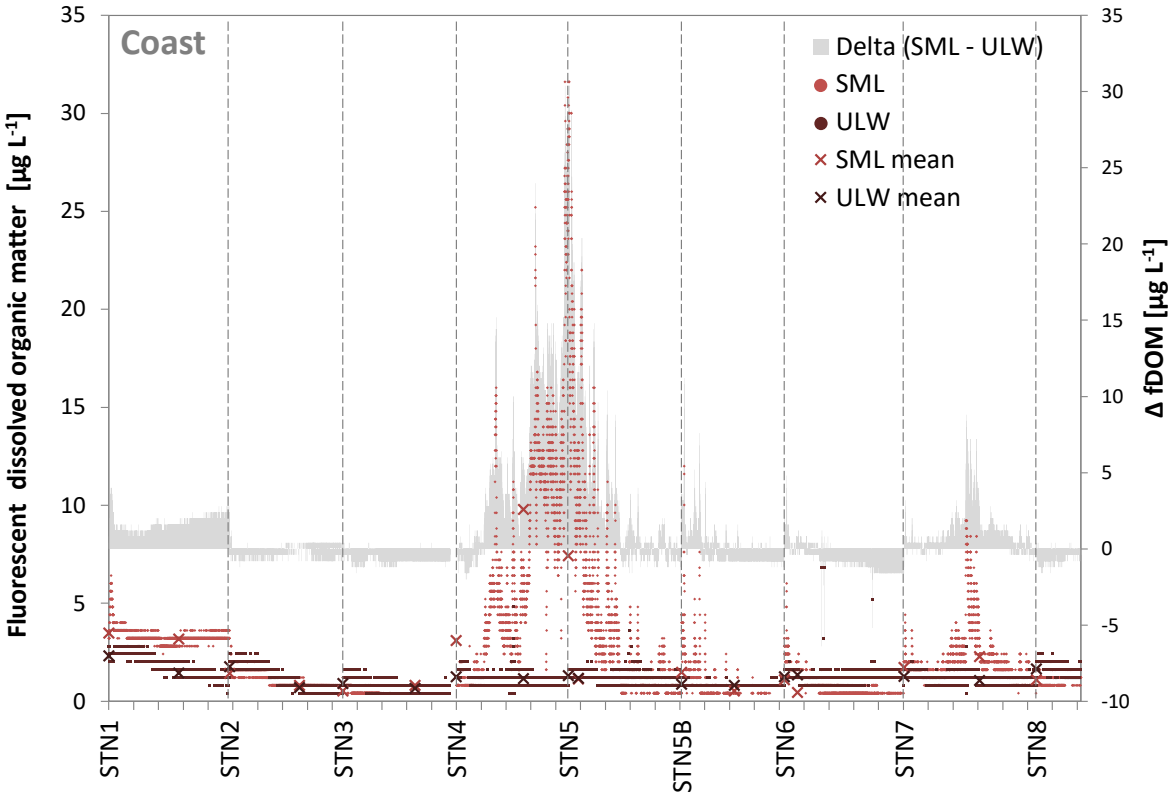

Figure 6.6. Fluorescent dissolved organic matter (fDOM) [µg L^{-1}] measured in the sea surface microlayer (SML) and underlying water (ULW) at coastal stations. Points represent an individual data point, bars represent the difference between the SML and the ULW, and crosses represent the mean for each station at AM and PM sampling times. Data is not continuous between stations, intervals between each station are indicated by dashed gridlines.

Fluorescent chlorophyll-a in the ULW (1 m) was higher at coastal stations (figure 6.7ai) (mean 1.35 µg L^{-1}; range 0.03-24.85 µg L^{-1}) than oceanic stations (mean 0.16 µg L^{-1}; range 0.03 to 3.77 µg L^{-1}) (figure 6.7aii). Discrete chlorophyll-a concentrations also showed a similar trend, and were generally higher in the SML than the ULW at coastal stations (figure 6.7bi) with a mean difference of 7.57 µg L^{-1} that was largely driven by a large peak at station 4. Chlorophyll-a was generally not enriched in the SML at oceanic stations (figure 6.7bii).

Surface active substances (SAS) at coastal stations were on average 2.3 times higher in the SML (mean 972.78 µg Teq L^{-1}; range 63 - 22,200 µg Teq L^{-1}) than the ULW (mean 269.53 µg Teq L^{-1}; range 53 to 4,099 µg Teq L^{-1}) with the exception of station 4, which showed a large peak in the SML that was on average ~6.8 times higher than the ULW. SAS at oceanic stations was only slightly higher (1.1 times) in the SML (mean 102 µg Teq L^{-1}; range 49 - 609 µg Teq L^{-1}) than the (ULW mean 83 µg Teq L^{-1}; range 50 - 613 µg Teq L^{-1}) except at station 11 where the SML was on average 3.6 times higher than the ULW.

The partial pressure of carbon dioxide (pCO_2) at coastal stations (figure 6.9a) was consistently higher in the seawater (mean 470 µatm; range of 432 – 491 µatm) than the air (mean 404 µatm; 401 – 408 µatm), resulting in a mean flux of CO_2 from the sea to the air of 67 µ atm at a rate of 5.07 cm h^{-1}. In contrast, the pCO_2 at oceanic stations (figure 6.9b) was consistently lower in the seawater (mean 358 µatm; range 344-366 µatm) than the air, (mean 370.69 µatm; range 367-399 µatm), resulting in a mean flux of 12 µatm at 59 cm h^{-1} from the air to the sea.

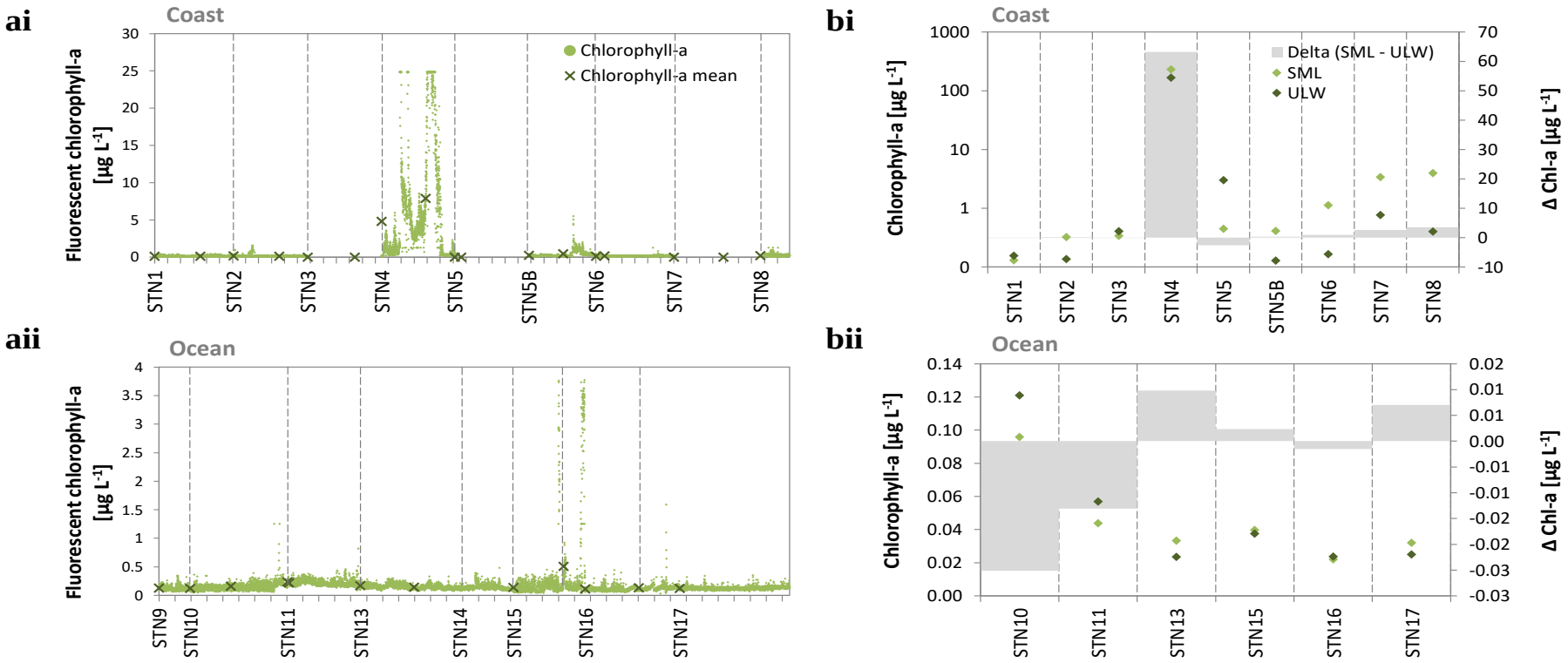

Figure 6.7. Chlorophyll-a measurements a) from fluorescence in the underlying water (ULW) b) from discrete bottle samples of the sea surface microlayer (SML) and ULW at i) coastal stations, ii) oceanic stations. Points represent an individual data point, bars represent the difference between the SML and the ULW, and crosses represent the mean for each station at AM and PM sampling times. Data is not continuous between stations, intervals between each station are indicated by dashed gridlines.

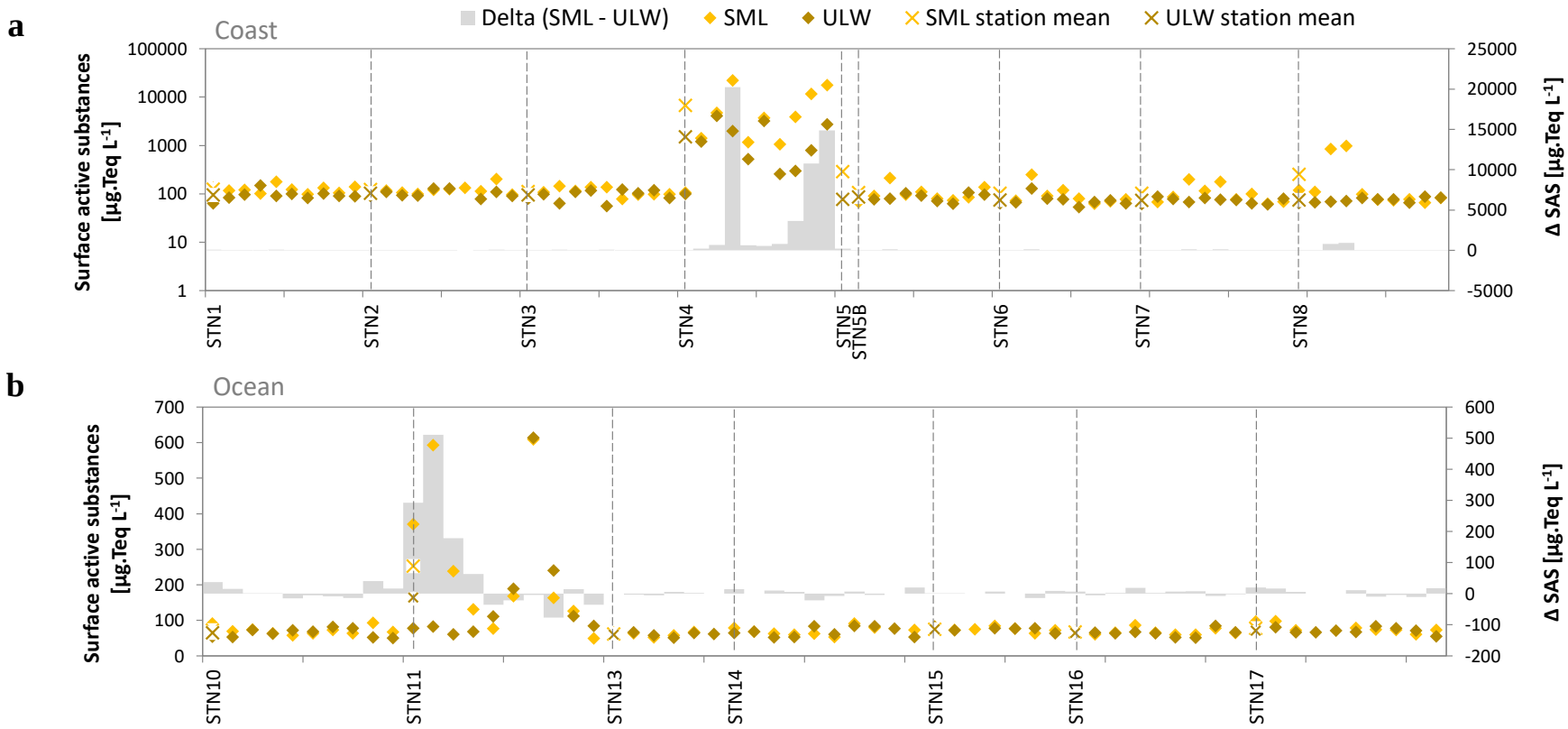

Figure 6.8. Surface active substances (SAS) in the sea surface microlayer (SML) and underlying water (ULW) at a) coastal stations and b) at oceanic stations. Points represent an individual data point, bars represent the difference between the SML and the ULW, and crosses represent the mean for each station at AM and PM sampling times. Data is not continuous between stations, intervals between each station are indicated by dashed gridlines.

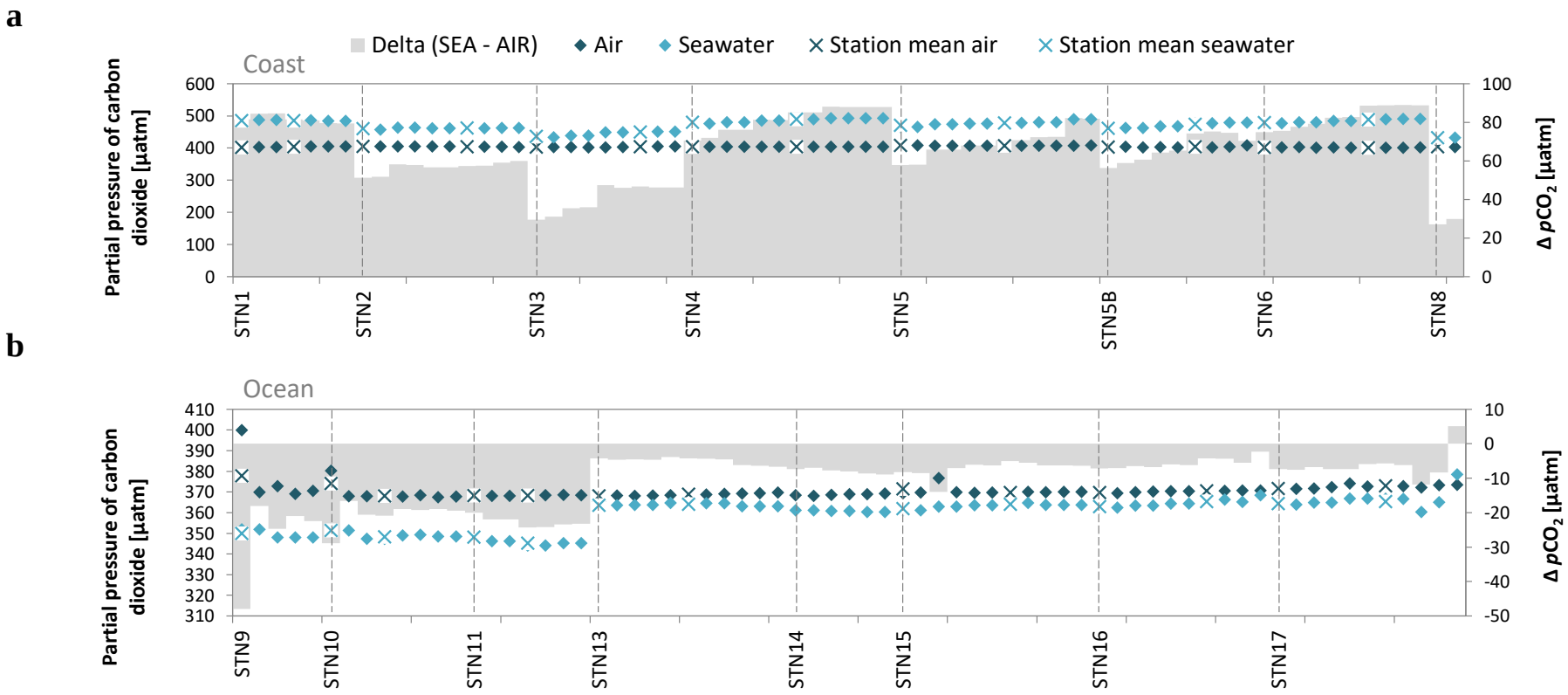

Figure 6.9. Partial pressure of carbon dioxide (pCO_2) [µatm] in seawater and air at a) coastal stations and b) oceanic stations. Points represent an individual data point, bars represent the difference between the sea and the air, and crosses represent the mean for each station at AM and PM sampling times. Data is not continuous between stations, intervals between each station are indicated by dashed gridlines.

The air temperature measured by the Sea Surface Scanner (SSS) and from the ship agreed well and ranged 23.1 to 31.4 °C for the duration of the cruise (figure 6.10a). The mean air temperature during sampling periods at coastal and oceanic stations was 29.4 °C and 27.7 °C respectively. The SSS determined solar radiation ranged from 25-1123 W m^2, and was generally lowest during the morning with the exception of stations 10 and 11, which were low throughout the day. Relative humidity measured from the SSS and from the ship agreed and ranged 34.9 to 100 % over the duration of the cruise. Dew point measured from the SSS and calculated from ship based relative humidity and air temperature also agreed and ranged 16.88 to 25.76 °C (figure 6.4b).

Wind speed measured from the SSS (1 m above sea level) and from the ship (U10N = wind speed 10 m above sea level) agreed well and ranged from 0.0 to 15.4 m s^{-1} (figure 6.11a). Mean wind speed during sampling at the coastal stations was 3.4 m s^{-1}. Wind speeds during sampling at oceanic stations were slightly higher (mean 6.01 m s^{-1}). Wind stress ranged from 0.00-0.47 N/ m^2 for the duration of the cruise (figure 6.11b), with a mean wind stress at 0.02 N/ m^2 at coastal stations and 0.06 N/ m^2 at oceanic stations. Atmospheric boundary layer stability represented by Monin-Obukhov length ranged from -0.42 to -524.29 m for the duration of the cruise (figure 6.11c), with mean values of -11.9 m for coastal stations (with exception of station 2 AM which had a mean of 315.6 m) and -31.45 m for oceanic stations. The low negative values indicate that the atmospheric turbulence at the air-sea boundary was influenced more strongly by buoyant forces than shear forces.

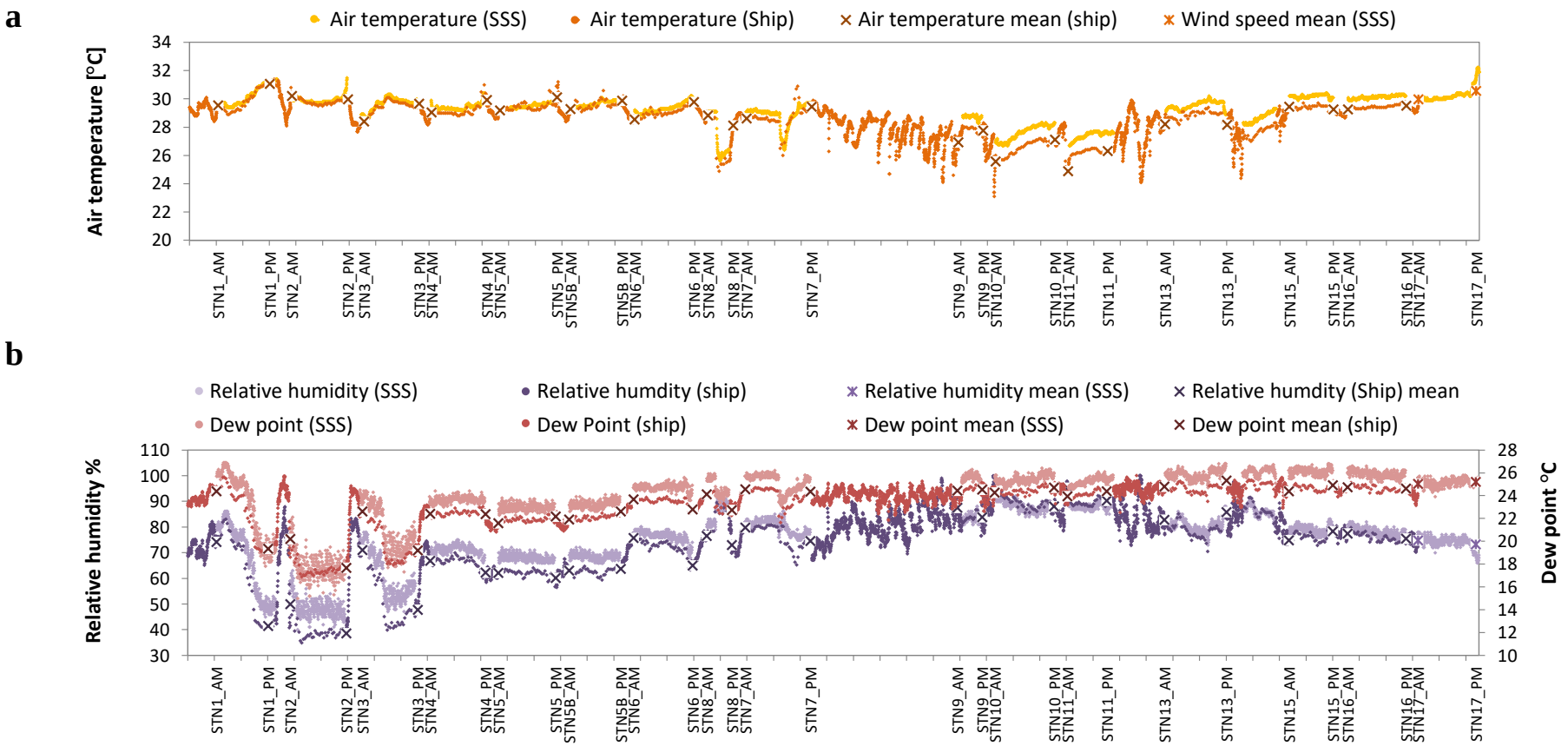

Figure 6.10. Meteorological parameters measured from the sea surface scanner (SSS) and ship. a) air temperature, b) relative humidity and dew point. Points represent an individual data point and crosses represent the mean for each station at AM and PM sampling times.

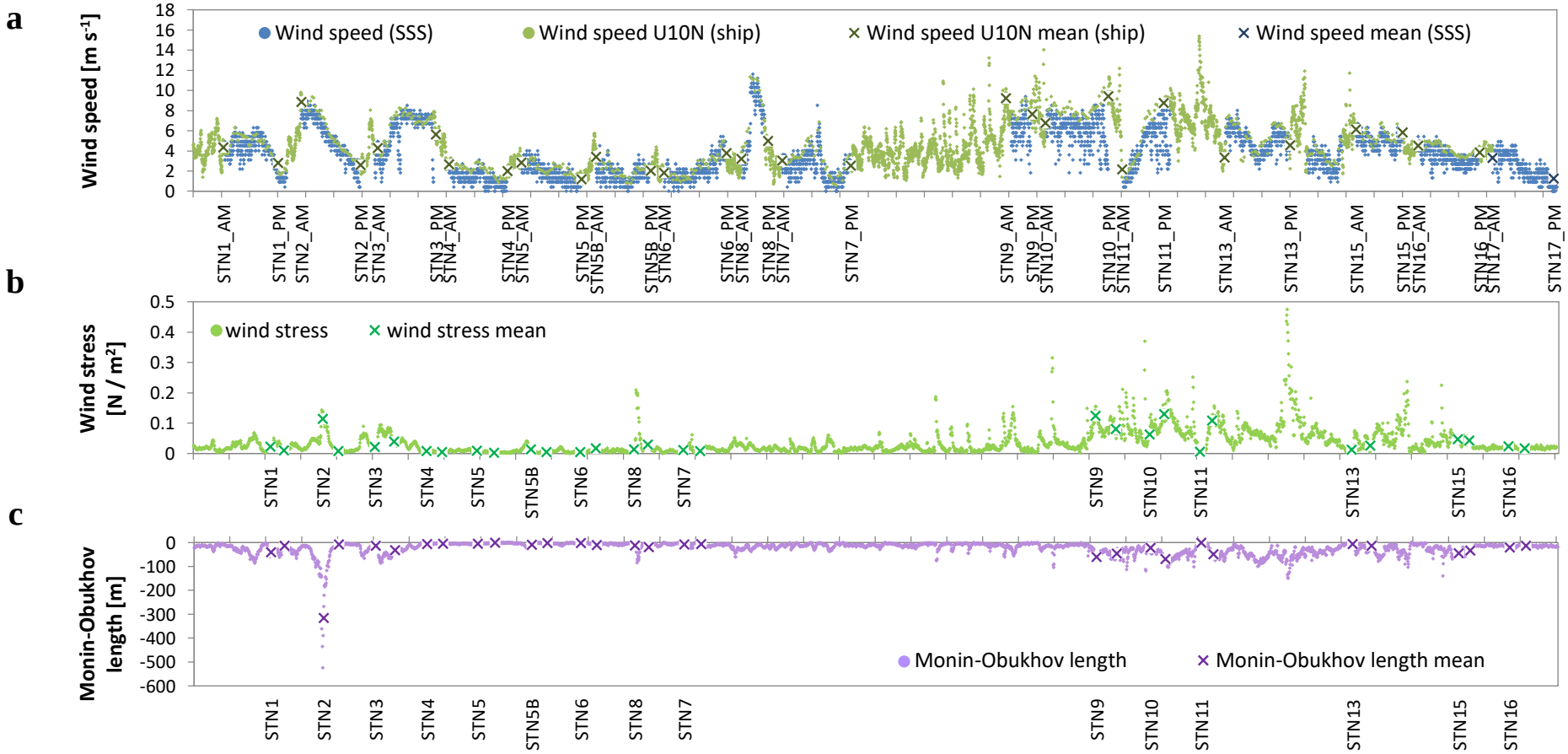

Figure 6.11. Meteorological parameters measured from the sea surface scanner and ship. a) wind speed, b) wind stress, c) Monin-Obukhov length. Points represent an individual data point and crosses represent the mean for each station at AM and PM sampling times.

Dust deposition was 36 times greater at coastal stations (figure 6.12a) than oceanic stations (figure 6.12b), using dust concentration values from aerosol measurements [ng m^{3-3}] as a proxy for flux (Duce et al., 1991), the mean flux of dust from the atmosphere into the sea was calculated as 1444 µg.m^2.d^{-1} and 40 µg.m^2.d^{-1} respectively. At the coastal stations, particulate aluminium (P-Al) was enriched in the SML by a mean factor of 3.8 (figure 6.13ai), particulate iron (P-Fe) by a mean factor of 4.0 (figure 6.13bi) and particulate phosphorous (P-P) by a factor of 3.3 (figure 6.13ci). Even though trace metal concentrations at oceanic stations were very low compared to the coastal stations, P-Al, P-Fe and P-P were still enriched in the SML by a mean factor of 3.4 (figure 6.13aii), 4.6 (figure 6.13bii) and 2.0 (figure 6.13cii) respectively.

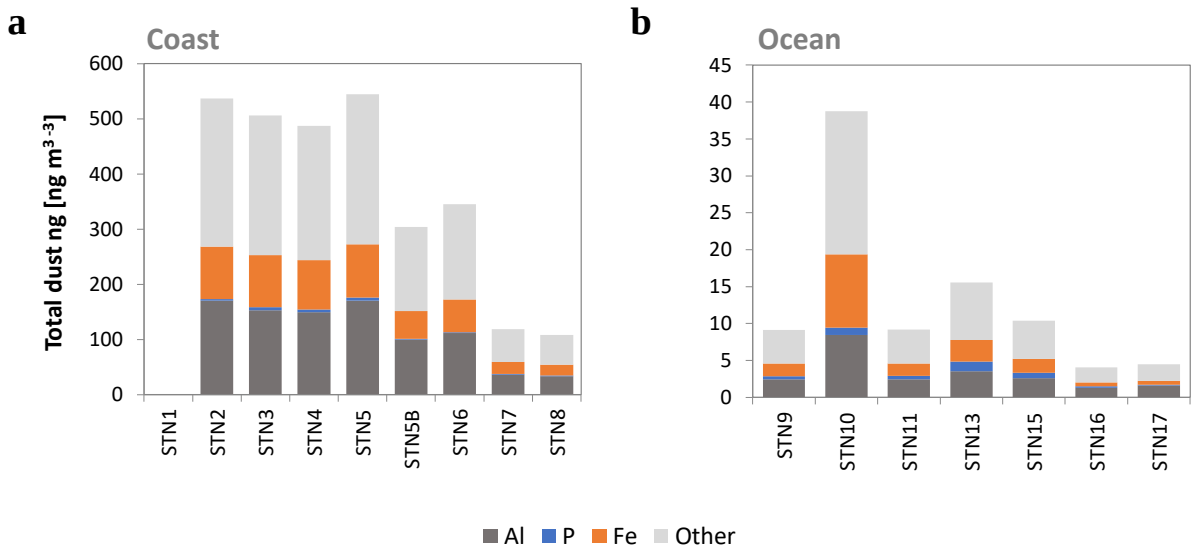

Figure 6.12. Composition of atmospheric dust [ng m^{3-3}] at a) coastal stations and b) oceanic stations.

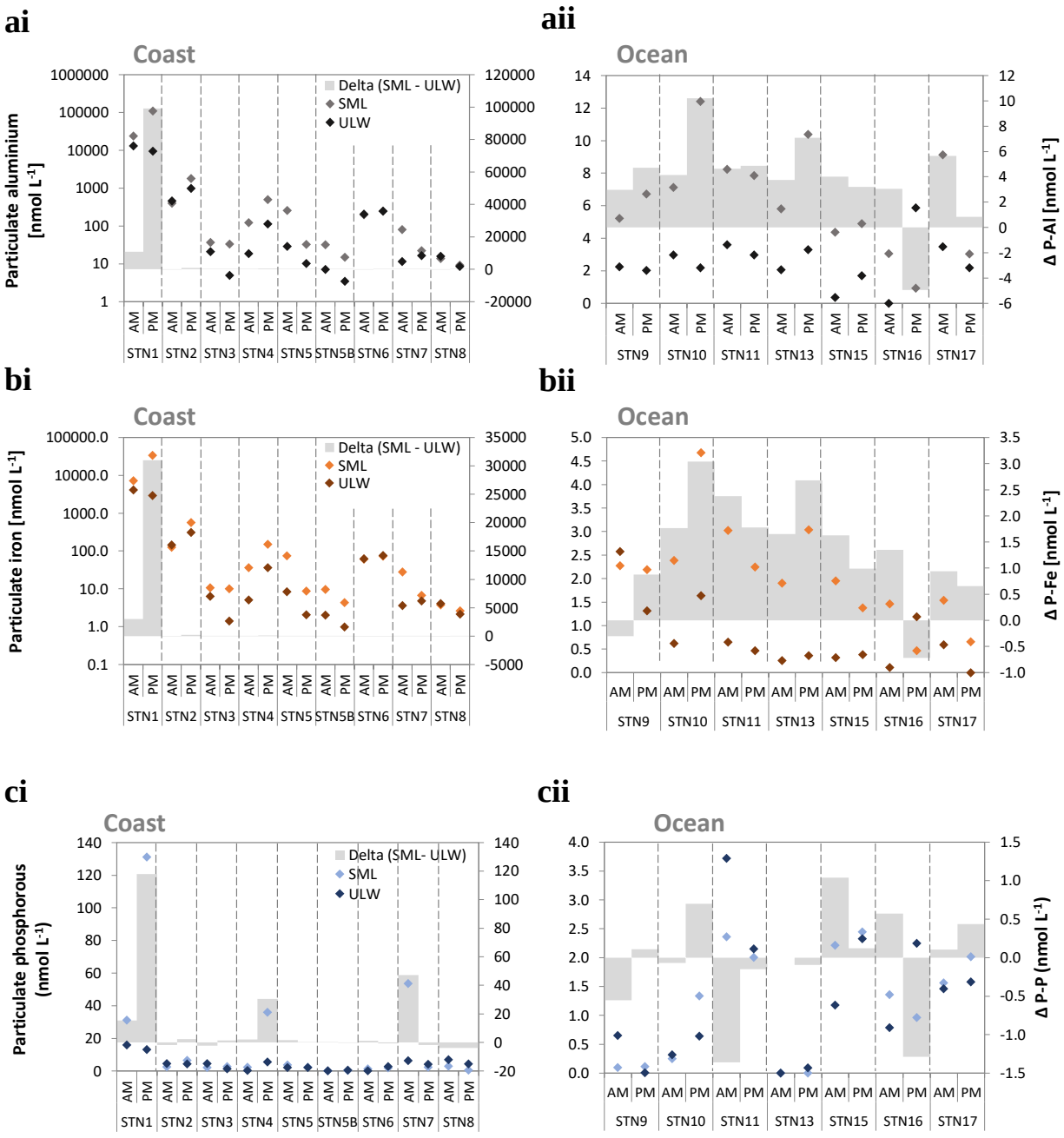

Figure 6.13. Particulate trace metals [nmol L^{-1}] from the sea surface microlayer (SML) and underlying water (ULW). a) particulate aluminium (P-Al), b) particulate iron (P-Fe), c) particulate phosphorous (P-P), d) composition of atmospheric dust at i) coastal stations and ii) oceanic stations.

6.3.2 General bacterial diversity

The bacterioneuston and bacterioplankton communities at the coastal and oceanic stations were assessed by 16S rRNA gene amplicon high-throughput sequencing. Reads were filtered to exclude singletons, eukaryotic, archaeal, and organelle (e.g. chloroplast) sequences and rarefied to a depth of 10,787 per sample resulting in a total of 1,445,458 high quality reads representing 1,251 operational taxonomic units (OTUs) based on 97% similarity. 29 abundant (>0.1 % relative abundance) orders at coastal sites and 32 abundant (>0.1 % relative abundance) orders at oceanic sites were determined. Both coastal and oceanic sites were dominated by the same 5 orders, which accounted for 76 % of the total normalised abundance across all stations (figure 6.14a and b). The SAR11 clade, *Rhodobacterales* and *Flavobacteriales* abundance was consistent between coastal and oceanic sites, comprising approximately 39 %, 7 % and 6% of the community respectively. *Synechococcales* (subsection I) made up 18 % of the community at both coastal and oceanic sites, however the ratio between the genera *Synechococcus* and *Prochlorococcus* varied greatly between sites, from 1:1 at the coastal stations to 1:17 at oceanic stations. The order also varied between sites, accounting for 10 % of relative abundance at the oceanic site and just 1 % of relative abundance at the coastal site.

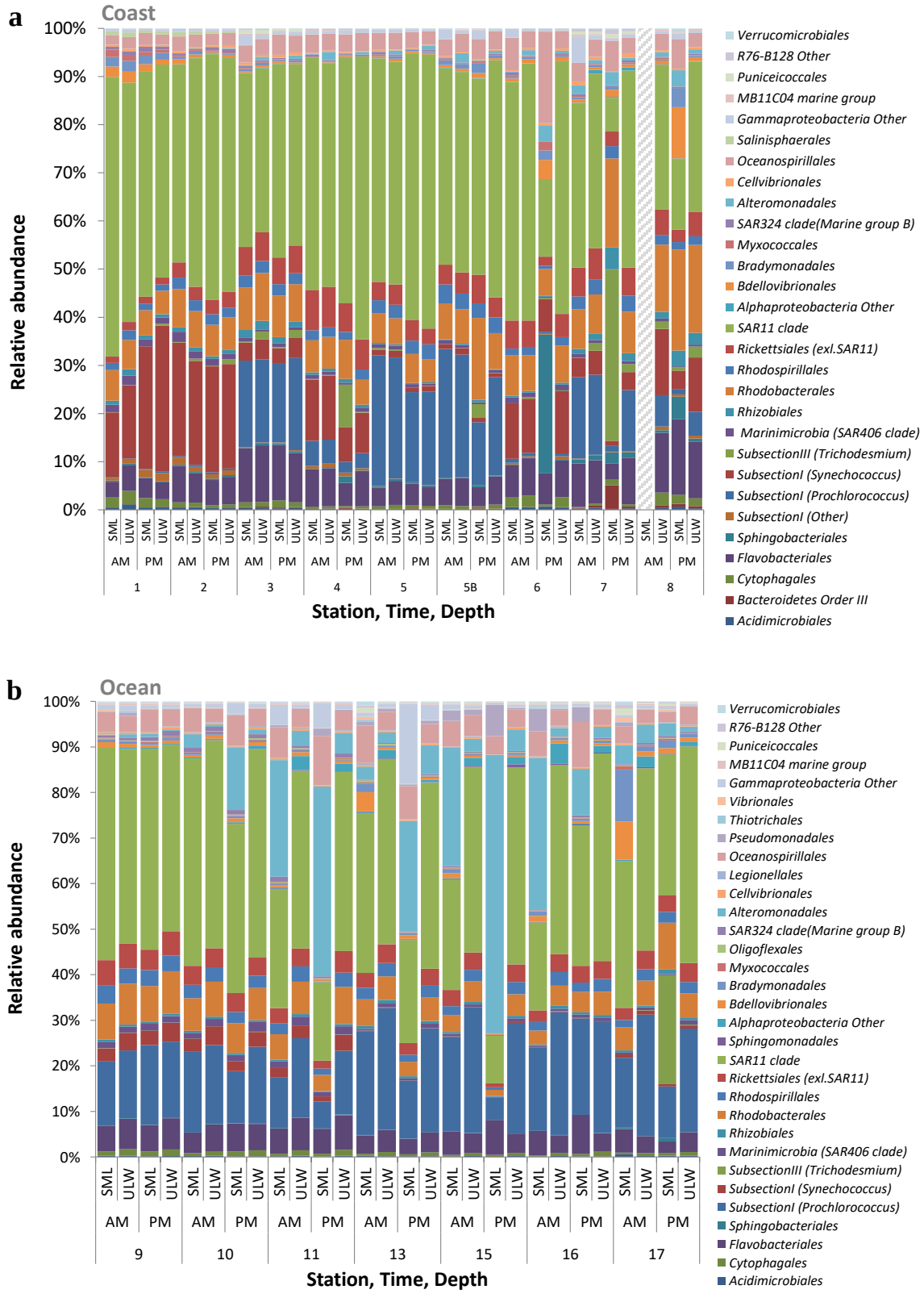

Figure 6.14. Relative abundance showing the distribution of bacterial orders (>0.1% relative abundance) at a) coastal stations and b) oceanic stations. Shaded areas represent missing data points.

6.3.3 Variance in bacterial communities by beta diversity analyses

Based on their geographical location, stations 1 to 8 were defined as coastal and stations 9 to 17 were defined as oceanic in this study. Principle coordinates analysis (PCoA) of all samples showed a separation along the leading diagonal, which loosely grouped the samples into coastal and oceanic sites, with some overlap between the coastal stations 3, 5 and 5B and the oceanic stations (figure 6.15a). The ULW samples were tightly grouped while the SML samples showed more variation. Redundancy analysis (RDA), constraining the PCoA by category's site (i.e. coastal/oceanic) and depth (i.e. SML/ULW) showed the centroids of coastal and oceanic sites were separated along axis dbRDA1 (figure 6.15b), while the centroids of SML and ULW samples were separated along axis dbRDA2. Permutational multivariate analysis of variance (PERMANOVA) of all samples showed that samples grouped by either, station, sample depth or site, were significantly different to each other, however there was no significant difference between the AM or PM samples (table 6.1).

Table 6.1. Permutational multivariate analysis of variance, bold text indicates significant ($p < 0.05$) categories.

Category	All Samples		Coastal Samples		Oceanic Samples	
	Pseudo-F	p Value	Pseudo-F	p Value	Pseudo-F	p Value
Station	**4.70**	**0.00**	**5.77**	**0.00**	1.74	0.06
Depth (SML vs. ULW)	**4.04**	**0.01**	0.92	0.46	**8.86**	**0.00**
Time (AM vs. PM)	0.97	0.41	0.86	0.48	0.83	0.41
Site (coastal vs. ocean)	**13.22**	**0.00**	NA	NA	NA	NA

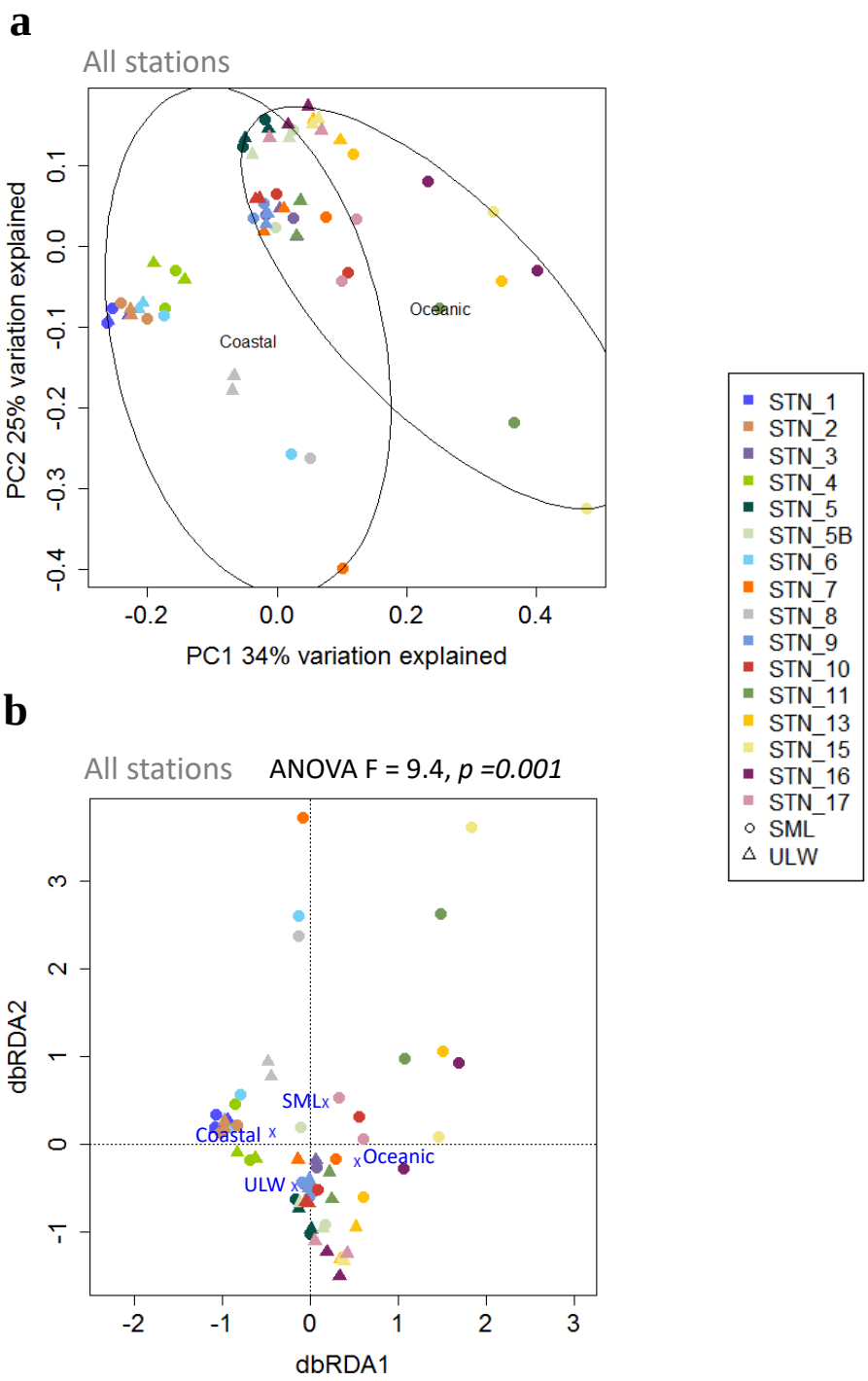

Figure 6.15. a) Principle coordinates analysis of weighted UniFrac distance metrics on all samples. b) Redundancy analysis of weighted UniFrac distance metrics on all samples. Points represent an individual sample and are coloured by station, symbols identify the depth of the sample (circles SML and triangles ULW). The centroids of categorical variables are illustrated by (x).

PCoA of coastal samples showed two station groupings; group A (stations 1, 2, 4 and 6) and group B (stations 3, 5, 5B and 7), with station 8 as an outlier. There was no distinct separation of coastal SML and ULW samples, although stations 6, 7 and 8 had outlying SML samples (figure 6.16a). PERMANOVA of coastal samples showed a significant difference when grouped by station (table 6.1).

PCoA of oceanic samples showed two station groupings separated along axis PC2 (13% variation explained); group C (9 to 11) and group D (13 to 17), with the exception of station 17 SML samples which group with stations 9 to 11 (figure 6.16b). SML and ULW samples are separated along axis PC1 (64 % variation explained), ULW samples clustered tightly within station groups, whereas SML samples showed higher variation between samples and were not distinctly separated into station groups. PERMANOVA of oceanic samples showed a significant difference between SML and ULW samples (table 6.1). RDA and Spearman's rho correlations with the associated physicochemical metadata showed that coastal station group A (supplemental figure 6.1a) was best described by higher pH, trace metals and chlorophyll-a, and coastal group B by higher buoyant stress and humidity. Oceanic station group C (supplemental figure 6.1b) was best described by higher physical stress (e.g. wind speed), and oceanic station group D was described by higher solar radiation.

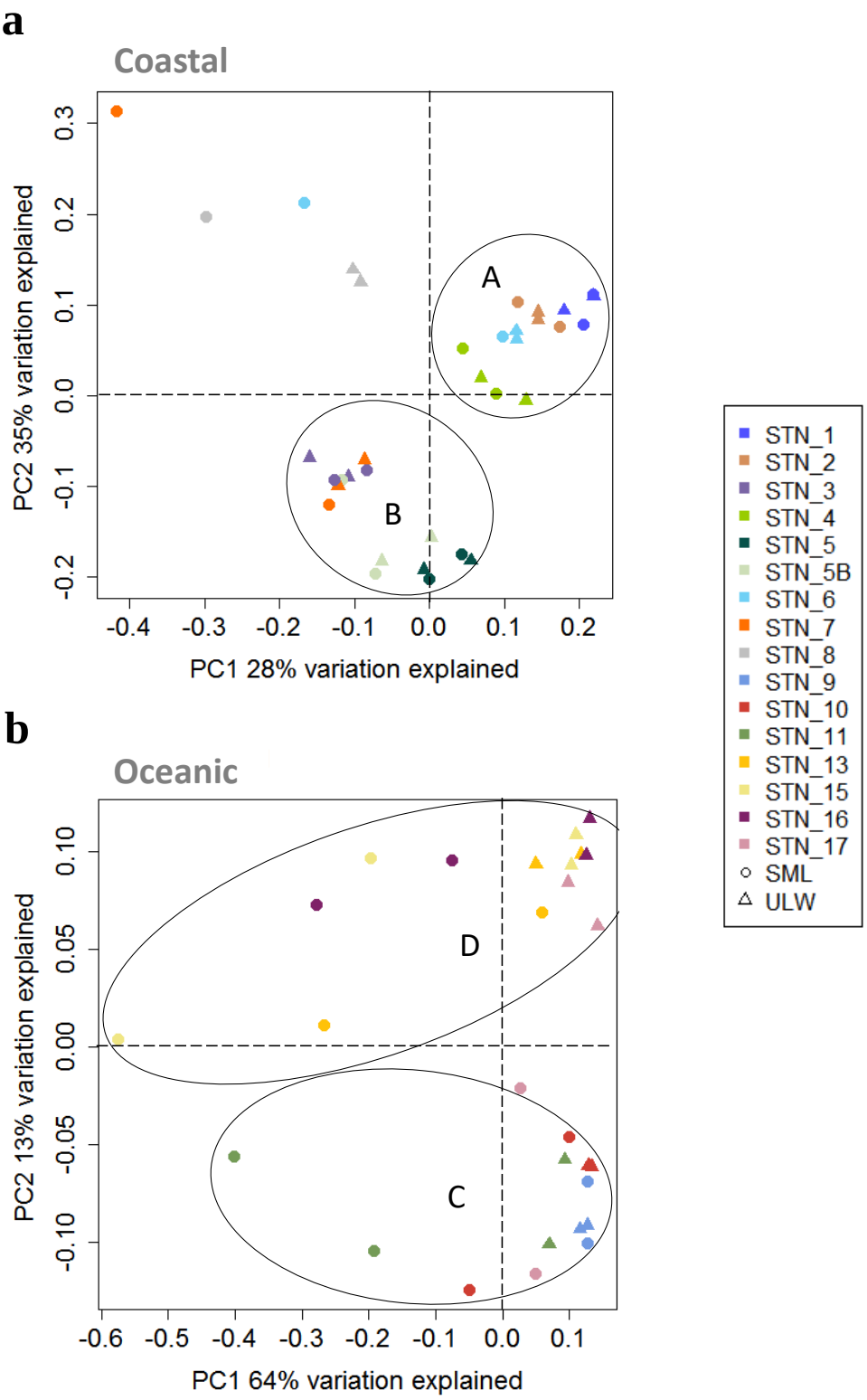

Figure 6.16. Principle coordinates analysis of weighted UniFrac distance metrics on a) coastal and b) oceanic samples. Points represent an individual sample and are coloured by station, symbols identify the depth of the sample.

6.3.4 Enrichment of bacterioneuston

All orders (with the exception of Sphingomonadales) showed a higher abundance in the SML than the ULW in at least one sample (figure 6.17a), however, log-likelihood ratio tests showed that only eight bacterial orders, six at the coastal site (figure 6.14bi), and seven at the oceanic site (figure 6.14bii) were significantly (Bonferroni corrected p values < 0.5) enriched in the SML. The five orders enriched in the SML at both coastal and oceanic sites were 1) The *Bdellovibrionales* which was dominated by the family *Bdellovibrionaceae* (OM27 clade). 2) The *Cyanobacteria* Subsection III, which was identified as *Trichodesmium sp.*, and was dominated by a single OTU (OTU_3). 3) The other *Gammaproteobacteria* was made up of 19 OTUs at the coastal site and 16 OTUs at the oceanic site, and was dominated at both sites by a single OTU (OTU_12) identified as belonging to the family *Pseudoalteromonadaceae*. 4) The *Oceanospirillales* was dominated by the family *Oceanospirillaceae* at the coastal site and by family *Halomonadaceae* at the oceanic site. 5) The *Bradymonadales* was made up of 43 OTUs at the coastal site and 40 OTUs at the oceanic site, and was not dominated by any particular OTU. The remaining three orders were only found to be enriched at either coastal or oceanic stations; The *Sphingobacteriales* was only significantly enriched at the coastal site and was dominated by the family *Chitinophagaceae*. The *Alteromonadales* and *Pseudomonadales* were only significantly enriched at the oceanic site and were dominated by the families *Alteromonadaceae* and *Pseudomonadaceae* respectively. RDA of coastal samples (supplemental figure 6.2) showed the significantly enriched bacterioneuston described (ANOVA F =5.5, p =0.001) the outlying coastal SML samples at station 6, 7 and 8. RDA of the oceanic samples (supplemental figure 6.3) also showed the SML samples are described (ANOVA F =15.97, p =0.001) by a higher abundance of the significantly enriched bacterioneuston, especially the order *Alteromonadales* (ANOVA F =82.69, p =0.001).

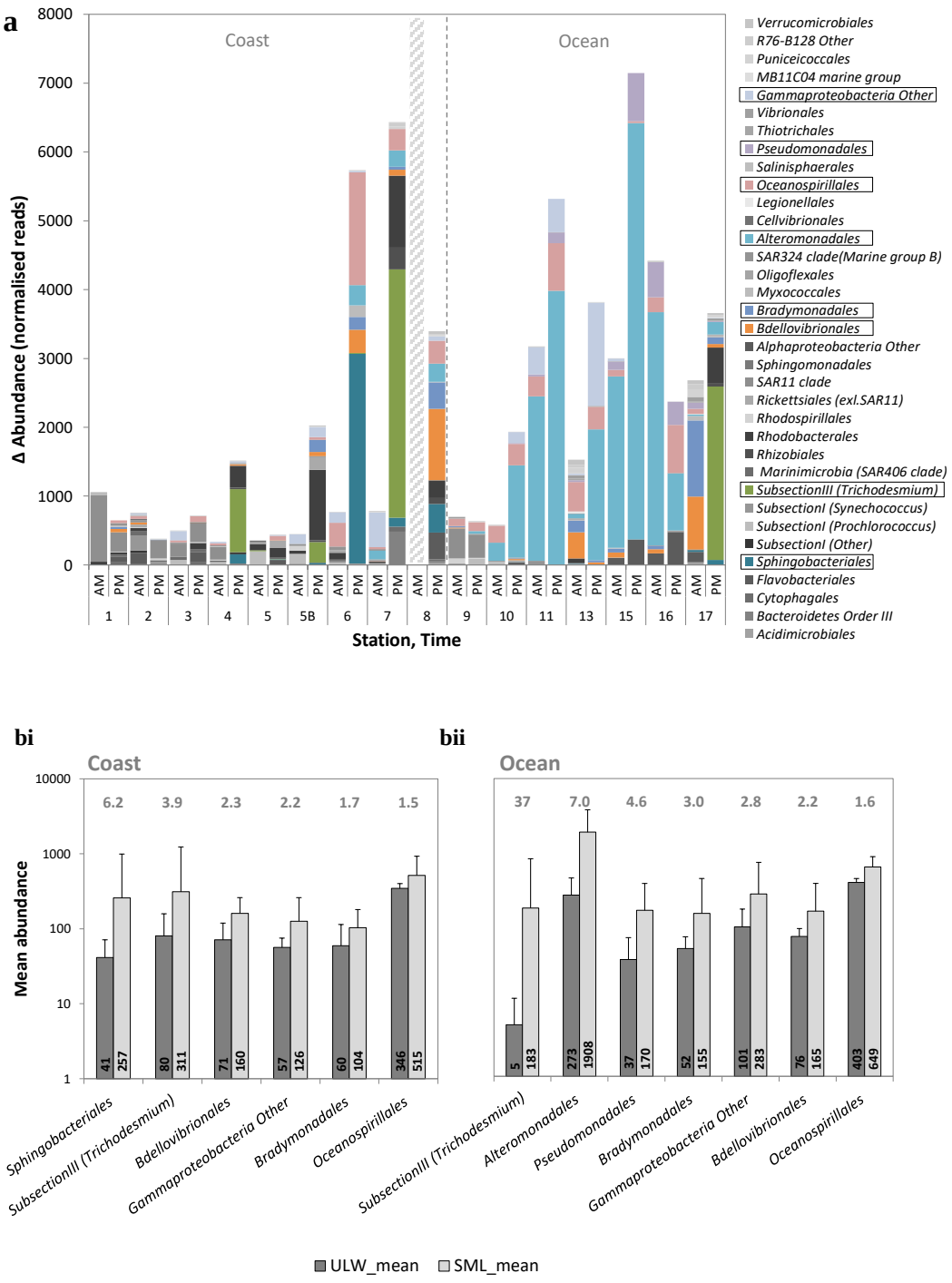

Figure 6.17. Bacterial taxa (>0.1 % relative abundance) with a) a higher abundance in the sea surface microlayer (SML) compared to the underlying water (ULW). b) significantly (Bonferroni p <0.05) higher mean (all stations) abundance in the SML compared to the ULW from bi) coastal and bii) oceanic sampling sites. Values above the bars report the enrichment factor in the SML. Values inside the bars report mean abundance as normalised reads. Error bars show standard deviation.

6.3.5 Relationship of significantly enriched bacterioneuston with physicochemical properties and with other bacterial orders

Spearman's rho correlations were performed between the significantly SML enriched taxa at each site and the associated physicochemical metadata. At coastal sites, the order Bdellovibrionales correlated positively with pH, wind speed and wind stress and negatively with solar radiation, chlorophyll-a and Monin-Obukhov length. Bradymonadales correlated positively with wind speed, wind stress, dew point and negatively with surface active substances, chlorophyll-a and Monin-Obukhov length. Oceanospirillales correlated positively with chlorophyll-a, relative humidity and Monin-Obukhov length and negatively with air temperature, pH, P-Al, P-P and P-Fe. The other *Gammaproteobacteria* correlated positively with relative humidity and negatively with air temperature. *Cyanobacteria* Subsection III (i.e. *Trichodesmium*) correlated positively with dew point. The order Sphingobacteriales did not correlate significantly with any of the physicochemical variables.

At oceanic sites, Bdellovibrionales correlated negatively with chlorophyll-a. The order Bradymonadales correlated negatively with relative humidity and chlorophyll-a and positively with pCO_2 air and air temperature. *Alteromonadales* correlated positively with surface active substances, chlorophyll-a, P-Al and P-P, and negatively with mean pCO_2 air. Oceanospirillales correlated positively with P-Al, P-Fe and negatively with pH and mean *p*CO2 air. The other *Gammaproteobacteria* correlated negatively with air temperature, sea temperature, solar radiation, mean pCO_2 air and water, and positively with relative humidity, salinity, wind speed, P-Al and P-Fe. Pseudomonadales correlated positively with solar radiation. Subsection III (*Trichodesmium*) did not correlate with any physicochemical parameters.

6.4 Discussion

6.4.1 Summary of the characteristics of the coastal and oceanic stations

The coastal site was characterised by a higher seawater pCO_2 and chlorophyll-a concentrations, particulate trace metals and SAS, indicative of an increased status of productivity compared to the open ocean site. Generally, the coastal site was also warmer and more saline, and the oceanic site experienced greater levels of turbulent physical stress. Based on the geographical locations and differences in the physicochemical characteristics of the sites, the stations in the coastal and oceanic sites were separated for further analysis.

Bacterial communities at the coastal site showed variations between stations, and formed two groups. Group A stations were generally warmer and calmer than the stations in group B. Group A stations also had higher particulate trace metal concentrations and seawater pCO_2, suggesting higher respiration and heterotrophic productivity, whereas group B stations, which overlapped with the oceanic station group C, were more oligotrophic. Overall, the SML and ULW communities were not distinct from each other at the coastal stations with the exception of three outlying samples from station 6PM, station 7 PM and station 8PM. These outliers could be attributed to high enrichments of Sphingobacteriales and Oceanospirillales (STN6), *Trichodesmium* sp. (STN7) and Bdellovibrionales and Bradymonadales (STN8).

Although bacterial communities at the oceanic site were more homogeneous between stations, two groups were observed. Group D experienced warmer and calmer conditions than group C, which experienced higher turbulent stress from the prevailing meteorological conditions. There was also a distinction between the chemical characteristics of the two groups, as group D had a higher seawater pCO_2 while group C had higher concentrations of chlorophyll-a and the particulate trace metals aluminium and iron. This suggests that group

D was more oligotrophic than group C, and this was further supported by the overlap of group C bacterial communities with coastal group B.

6.4.2 Enrichment of bacterioneuston in response to particulate material in the sea surface microlayer and underlying water

The bacterioneuston communities were distinct from the bacterioplankton communities principally at the oceanic sites. Generally the SML was no more diverse than the ULW, and the communities were composed of the same OTUs, which indicates that the bacterioneuston is populated from the bacterioplankton as has been previously observed (Agogue et al., 2005a, Joux et al., 2006, Stolle et al., 2011). Variations between bacterioneuston and bacterioplankton communities were positively correlated with P-Al which also correlated with total dust deposition suggesting an atmospheric origin. A recent review by Mahowald et al. (2018) provides a comprehensive summary of studies that show aerosol trace metal deposition into the ocean can enhance both bacterial and phytoplankton production especially in oligotrophic environments.

A positive correlation was also seen with P-P, which in contrast to P-Al was not correlated with atmospheric dust measurements and was generally less enriched in the SML, suggesting that the source of P-P was primarily from the underlying water column. The environmental organic matter pool is difficult to characterise as it comprised of such a diverse range of molecules (Benner, 2002). However, as P-P includes particle-adsorbed phosphorous and live and dead plankton (Paytan and McLaughlin, 2007), it could be used as a proxy for plankton derived organic matter (OM) (Duhamel et al., 2007). The origin of P-P from the ULW is further supported by a positive correlation between P-P and SAS in the microlayer as transport by surface active particles is a primary mechanism of particulate enrichment in the SML (Hunter, 1980). The important coupling between bacterial secondary production and phytoplankton derived OM has been discussed previously (Chapters 4 and

5). The significant relationship between the distinct oceanic bacterioneuston communities and the particulate components of the SML in this study suggests that bacterioneuston become enriched in response to the accumulation of valuable particulate organic matter and trace metals arriving in the SML from both the atmosphere and from the underlying water below.

6.4.3 The effect of physical stress on bacterioneuston

The SML is more stable at winds up to 5 m s^{-1}, after which surface mixing is increased and the SML can be disturbed (Wurl et al., 2011b, Stolle et al., 2011, Rahlff et al., 2017). Our results concur with these previous findings as we saw greater enrichment of taxa in the SML at the calmer group D stations when wind speeds were generally below 5 m s^{-1} than the more turbulent group C stations when wind speeds were between 5 - 10 m s^{-1}. Despite the higher wind speeds associated with the group C stations, distinct bacterioneuston communities were still observed with wind speeds close to 10 m s^{-1}. Stolle et al. (2011) found that only wind speed history (~6h prior to sampling) was related to differences between bacterioneuston and bacterioplankton communities. This study used wind speed expressed as a mean over the hour prior to sampling plus the sampling time, but when taken over 6 hr mean wind speeds were reduced. This result suggests that the enrichment of taxa in the SML is dependant not only on wind speed, but also on the duration of stress acting on the surface (Stolle et al., 2011).

Interestingly, the station 10PM sample that had the highest 6 hr wind speed (8.2 m s^{-1}) showed distinction between bacterioneuston and bacterioplankton communities. At the oceanic site, chlorophyll-a was highest at station 10 suggesting phytoplankton, the primary gel particle producers (Hoagland et al., 1993, Myklestad, 1995), were more abundant. Also, the most abundant enriched taxa, *Alteromonadales* are known to be particle associated (Ivars-Martinez et al., 2008). Gel particles can be positively buoyant (Azetsu-Scott and

Passow, 2004) and have been suggested to aid the enrichment of particle-associated bacteria in remaining in the SML under higher stress conditions (Stolle et al., 2011). Recent studies have shown that transparent exopolymer particles (TEP) are more enriched in the SML in oligotrophic environments (Jennings et al., 2017, Zäncker et al., 2017) and that oceanic TEP export by sinking is inhibited by reduced aggregation (Jennings et al., 2017). Also Wurl et al. (2011a) suggested that TEP production is likely to be enhanced by higher wind speeds. Our findings suggest that buoyant particles in surface waters may aid in the enrichment of particle-associated bacteria making the SML bacterioneuston enrichment more resistant to turbulent stress.

A recent study that utilised a wind-wave tunnel to investigate the effect of wind speed on the enrichment of bacterioneuston concluded no significant enrichment was seen at wind speeds >5.6 m s^{-1}. The lack of enrichment at higher wind speeds under a controlled environment supports the suggestion made previously that the SML in the environment behaves differently to the SML under artificial experimental conditions (Cunliffe et al., 2013). The threshold at which the SML is considered stable cannot be defined by one variable but is dependent on complex interactive effects of the physicochemical characteristics of the SML.

6.4.4 Gammaproteobacteria in the oceanic sea surface microlayer

The dominance of the *Gammaproteobacteria* in the SML in this and other studies (Agogue et al., 2005a, Franklin et al., 2005) suggests that these bacteria are adapted to the SML. The significantly enriched *Gammaproteobacteria* orders (i.e. *Alteromonadales*, *Oceanospirillales*, *Pseudomonadales* and other *Gammaproteobacteria*) identified in this study are motile and able to utilise a diverse range of organic substrates chemoorganotrophically (Palleroni, 1981, de la Haba et al., 2014, Ivanova et al., 2014, López-Pérez and Rodriguez-Valera, 2014). Although there are some features shared by these

taxa, some evidence of niche partitioning was seen in this study, which is unsurprising given the phylogenetic and metabolic diversity of the class (Williams et al., 2010). The holistic approach of this study gives some insight into the different ecological strategies employed.

Pseudomonadales showed greater enrichment in the SML at the warmer and calmer stations, and were positively correlated with high UV. Members of the *Pseudomonadales* have previously been shown to be tolerant to UV and solar radiation (Agogue et al., 2005b, Marizcurrena et al., 2017). *Pseudomonadales* was dominated by the family *Pseudomonadaceae*, which are the only predominantly 'free living' bacteria (Palleroni, 1981) amongst the significantly enriched *Gammaproteobacteria* in this study. Their low SML enrichment at the more turbulent stations suggests they may be more susceptible to turbulent stress than the other particle-associated *Gammaproteobacteria*. The distribution of the *Pseudomonadales* in this study suggests this order is competitive at exploiting calm, high light oligotrophic SML environments.

In contrast the unassigned other *Gammaproteobacteria* showed greater enrichment at the cooler and more turbulent stations, showing a negative relationship with solar radiation, which suggests that this group may be susceptible to solar stress. The dominant OTU of the other *Gammaproteobacteria* was identified as belonging to the family *Pseudoalteromonadaceae*, which is often associated with eukaryotic organisms (Holmstrom and Kjelleberg, 1999) and is known to produce extracellular polysaccharides (Holmstrom and Kjelleberg, 1999, Ivanova et al., 2014) that may aid with buoyancy and potentially allowing the taxa to exploit a more turbulent SML.

The *Oceanospirillales* (mainly the family *Halomonadaceae*) showed no specific relationships with any of the physicochemical parameters and were enriched at nearly all stations, suggesting that this order contains generalists well adapted to a variety of habitats.

The *Alteromonadales* were enriched at nearly all ocean stations, and were the most abundant significantly enriched member of the bacterioneuston. The order is well known to

be particle-associated (Ivars-Martinez et al., 2008) and contains taxa that are tolerant to solar stress (Agogue et al., 2005b, Marizcurrena et al., 2017). As discussed previously, possessing these ecological traits could make *Alteromonadales* better adapted to cope with the physical stresses (solar and turbulent) present in the SML.

Alteromonadales was dominated by a single OTU (OTU_4) which belonged to the family *Alteromonadacea* and was further identified as being most similar (ID 100%; cover 100%) to *Alteromonas macleodii*. *Alteromonadacea*, including *A. macleodii*, are typical r strategists that can rapidly respond to and utilise a diverse range of complex organic compounds and increase in abundance to high densities (López-Pérez and Rodriguez-Valera, 2014). The enrichment of *Alteromonadales* in the bacterioneuston showed a positive relationship with P-P (possible plankton derived OM), and their total abundance also showed a positive relationship with SAS. *Alteromonadales* have previously been shown using bottle incubations and mesocosm studies to utilise a range of phytoplankton derived organic matter, including dissolved organic carbon (DOC) (Sarmento and Gasol, 2012, Nelson and Carlson, 2012), polysaccharide microgels (Taylor and Cunliffe, 2017) and other organic substrates particularly amino acids and protein (Bryson et al., 2017). Pedler et al. (2014) demonstrated that a single strain of *Alteromonas* sp. was capable of consuming the entire labile DOC pool. Organic matter is often enriched in the SML (Reinthaler et al., 2008, Wurl and Holmes, 2008, Engel and Galgani, 2016) and *Alteromonadales* have been identified in SML samples from mesocosm experiments (Rahlff et al., 2017, Taylor and Cunliffe, 2017) and in the environment (Cunliffe et al., 2008). *Alteromonadales* are clearly an ecologically important member of the bacterioneuston and potentially play a key role in the marine carbon cycle transferring carbon through the microbial loop and through the marine food web (Pedler et al., 2014).

6.4.5 Other bacteria in the oceanic sea surface microlayer

Bdellovibrionales and *Bradymonadales* (*Deltaproteobacteria*) and the cyanobacterium *Trichodesmium* were also significantly enriched in the SML compared to the ULW. *Bradymonadales* and *Bdellovibrionales* were enriched in low numbers at most stations but were most abundant at station 17 AM. Little is known about the novel order *Bradymonadales* within the class *Deltaproteobacteria* (Wang et al., 2015). *Bdellovibrionales* were dominated by the family *Bdellovibrionaceae*, which are known to predate other gram negative bacteria (Rotem et al., 2014). There is no obvious driver for the enrichment of these two orders from the physicochemical data, however, they were very strongly correlated with each other. It is possible that *Bdellovibrionales* were predating *Bradymonadales* and are enriched in response to the increase in prey abundance.

Trichodesmium, other than a large enrichment at station 17PM, was present at a very low abundance and was not enriched in the SML at other stations. *Trichodesmium* are diazotrophs and are known to form large visible surface blooms in nutrient limited tropical open ocean environments (Capone et al., 1997) such as those seen at station 17. These huge surface blooms require large amounts of dissolved iron and are able to readily dissolve P-Fe (Rubin et al., 2011, Polyviou et al., 2017). P-Fe was not as high at station 17 as other oceanic stations, however dissolved iron was measured at station 17 and was very high (2.76 nmol L^{-1}) and was enriched in the SML by a factor of 7 (supplemental figure 6.4). It is possible that *Trichodesmium* bloomed at station 17AM during favourable warm and calm conditions in response to an increase of iron in the SML from atmospheric deposition (Langlois et al., 2012).

Strong negative correlations with the enriched *Gammaproteobacteria* and positive correlations with several other taxa in the SML, including the *Rhodobacterales*, suggests that *Trichodesmium* bloom events may alter the bacterioneuston community presumably through the increase in organic matter produced by the bloom. The sampling of co-occurring

data missed the bloom at station 17, highlighting the potential spatial and temporal localisation of bloom events. A large bloom of *Trichodesmium* seen in the SML at coastal station 4 coincided with peaks in fDOM concentrations (Wurl et al., 2018). *Trichodesmium* are known to affect nutrient flow by increasing the concentration of dissolved organic nitrogen (DON) and dissolved amino acids (LaRoche and Breitbarth, 2005) and have the potential to significantly alter co-occurring bacterial communities (West et al., 2008) as well as the physicochemical properties of the SML such as temperature (Kahru et al., 1993, Wurl et al., 2018), salinity (Wurl et al., 2018) and wave dampening (Wurl et al., 2016) by slick formation (Sieburth and Conover, 1965). These findings suggest *Trichodesmium* sp. are potentially important to nutrient supply in the oligotrophic tropical open ocean.

6.4.6 Conclusions

This study has been the first to use co-occurring *in situ* biological, chemical and physical data to investigate the SML, and has shown that physicochemical interactions are more complex and important in determining bacterioneuston community composition than previously considered (figure 6.18).

The SML is often conceptualised as a homogeneous habitat within the upper 1 mm of the surface ocean. Here, we show that distinct differences between coastal and oceanic SML environments occur over a relatively conserved area and propose some consideration be given to the different biogeochemical regions when comparing and defining the characteristics of the SML.

The buoyant properties of particulate matter potentially aid in sustaining the enrichment of particle-associated bacterioneuston during prolonged periods of physical stress. Current studies potentially underestimate the resilience of the SML ecosystem to turbulent processes.

This study has also shown that the bacterioneuston (primarily *Gammaproteobacteria*) are responding rapidly to resources arriving in the SML from the ULW and/or from the atmosphere, which provides novel evidence that the SML plays an important role in determining the fate of valuable organic nutrients and trace metals in the open ocean.

We have demonstrated that key taxa can be assigned to single populations and can significantly contribute to the bacterioneuston, such as *Trichodesmium sp.* and *Alteromonas sp.* This study provides new evidence to link *in situ Alteromonadales* blooms in the SML with plankton derived organic matter from the ULW. We also show acute events such as *Trichodesmium* blooms can dramatically alter bacterioneuston communities. Future studies should focus on high resolution phylogenetic identification and include functional classification to identify the metabolic pathways that determine the fate of valuable nutrients in the oligotrophic open ocean.

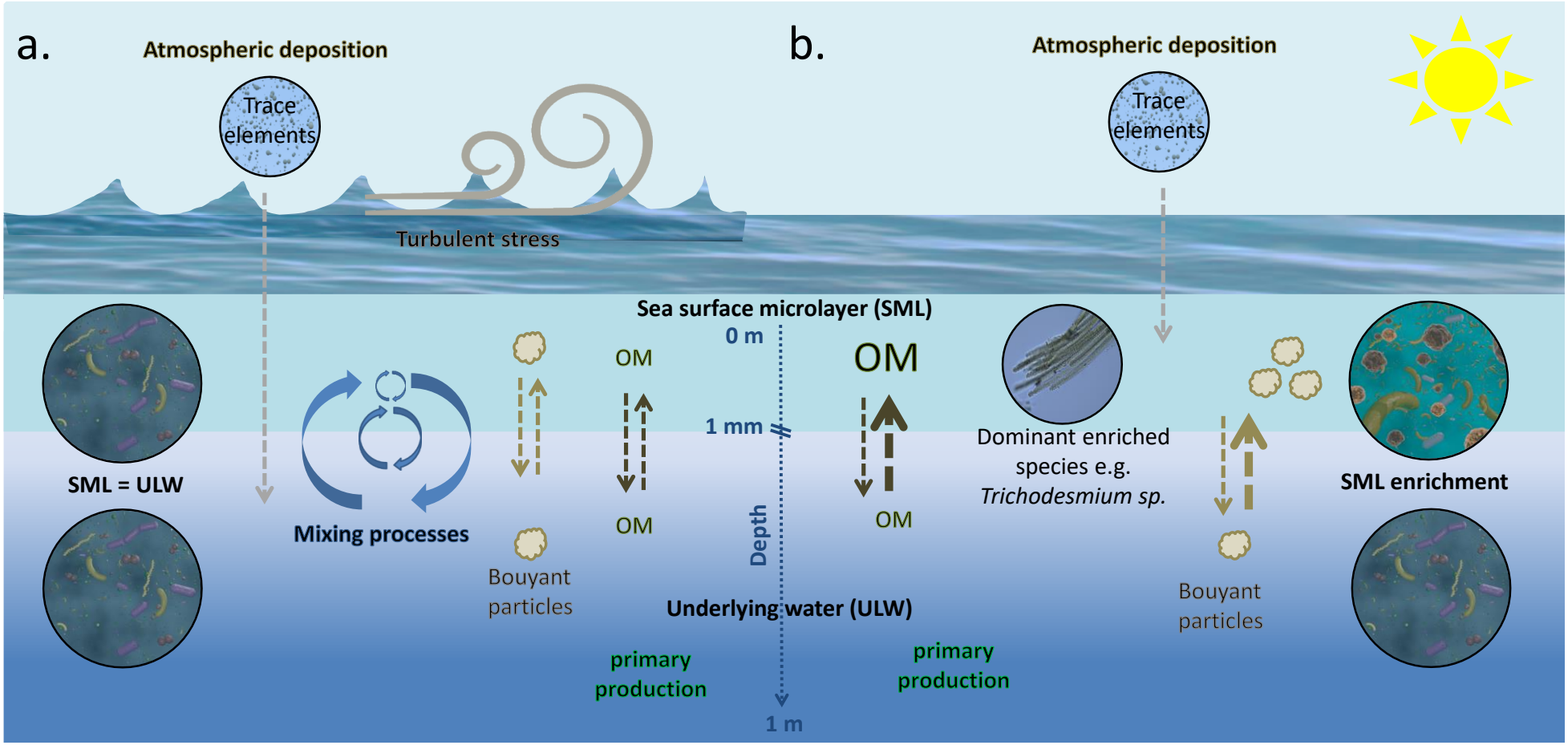

Figure 6.18. Conceptual diagram of the of sea surface microlayer environmental under a) high and b) low stress conditions, illustrating the drivers of bacterial enrichment which lead to distinct sea surface microlayer and underlying water bacterial community composition.

6.5 Supplementary material

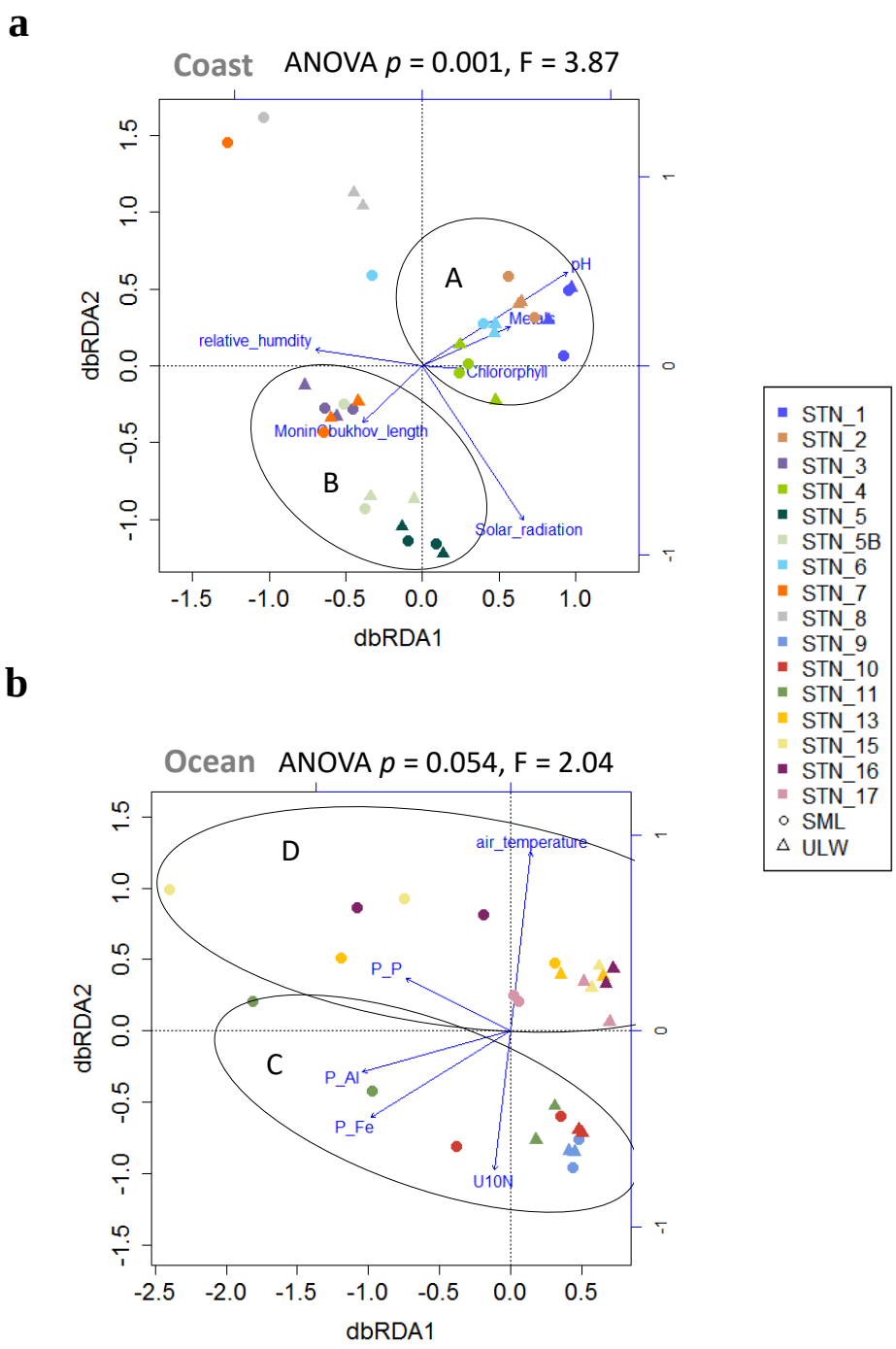

Supplemental figure 6.1. Redundancy analysis of weighted UniFrac distance metrics on a) coastal samples and b) oceanic samples. Ordination is constrained by selected significantly correlated physicochemical metadata. Points represent an individual sample and are coloured by station, symbols identify the depth of the sample. Arrows represent continuous explanatory variables fitted to the ordination; direction indicates the maximum change whereas the length indicates the magnitude of change for a variable.

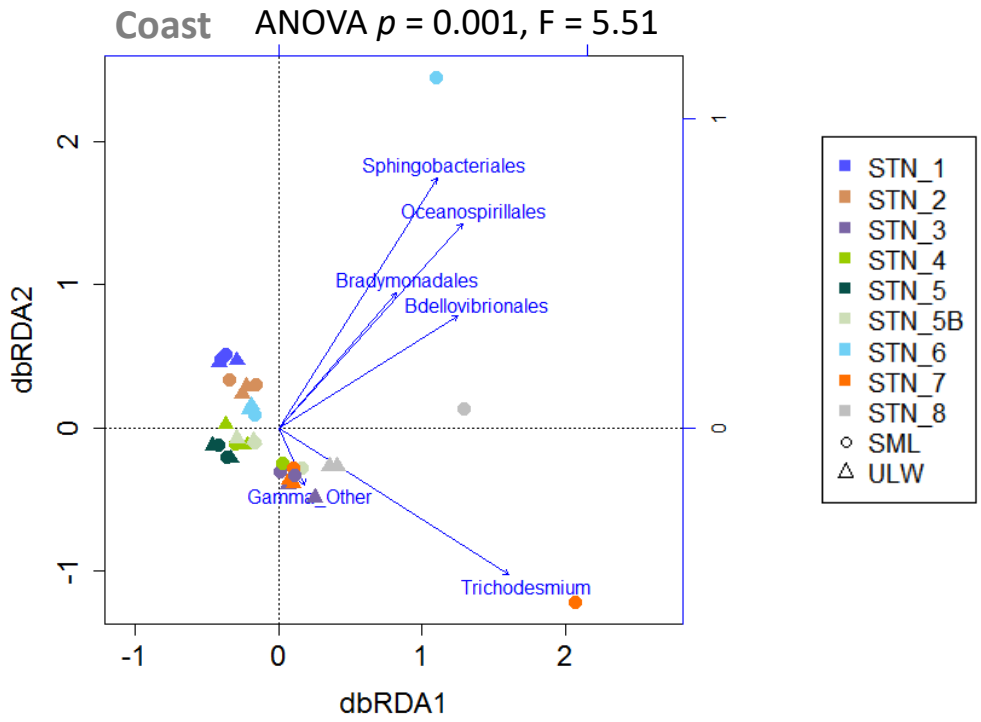

Taxa	Pseudo-F	*p* value
Trichodesmium	11.91	0.001
Bdellovibrionales	4.42	0.011
Bradymonadales	5.58	0.001
Gamma. other	3.97	0.043
Oceanospirillales	5.86	0.020
Sphingobacteriales	1.30	0.268

Supplemental figure 6.2. Redundancy analysis (RDA) of weighted UniFrac distance metrics on coastal samples. Ordination is constrained by significantly enriched bacterioneuston taxa. Points represent an individual sample and are coloured by station, symbols identify the depth of the sample. Arrows represent continuous explanatory variables fitted to the ordination; direction indicates the maximum change whereas the length indicates the magnitude of change for a variable. The table shows the results of analysis of variance (ANOVA) for each individual taxa used in the RDA.

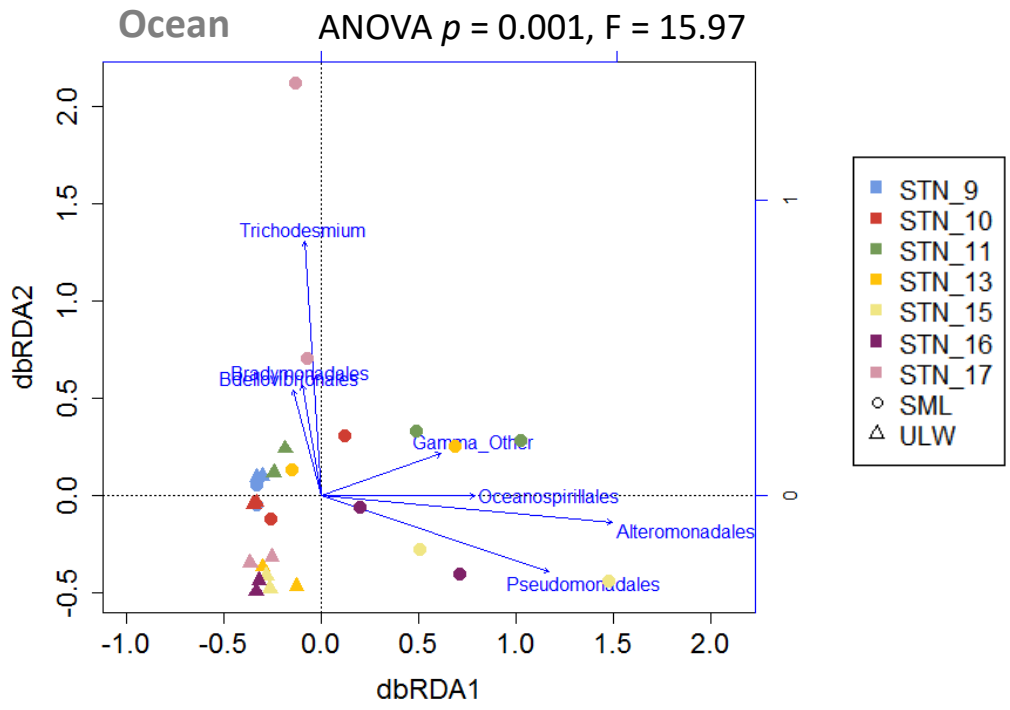

Taxa	Pseudo-F	*p* value
Trichodesmium	8.37	0.026
Bdellovibrionales	5.88	0.032
Bradymonadales	1.57	0.193
Gamma other	3.63	0.043
Oceanospirillales	4.68	0.024
Alteromonadales	82.69	0.001
Pseudomonadales	5.00	0.016

Supplemental figure 6.3. Redundancy analysis (RDA) of weighted UniFrac distance metrics on oceanic samples. Ordination is constrained by significantly enriched bacterioneuston taxa. Points represent an individual sample and are coloured by station, symbols identify the depth of the sample. Arrows represent continuous explanatory variables fitted to the ordination; direction indicates the maximum change whereas the length indicates the magnitude of change for a variable. The table shows the results of analysis of variance (ANOVA) for each individual taxa used in the RDA.

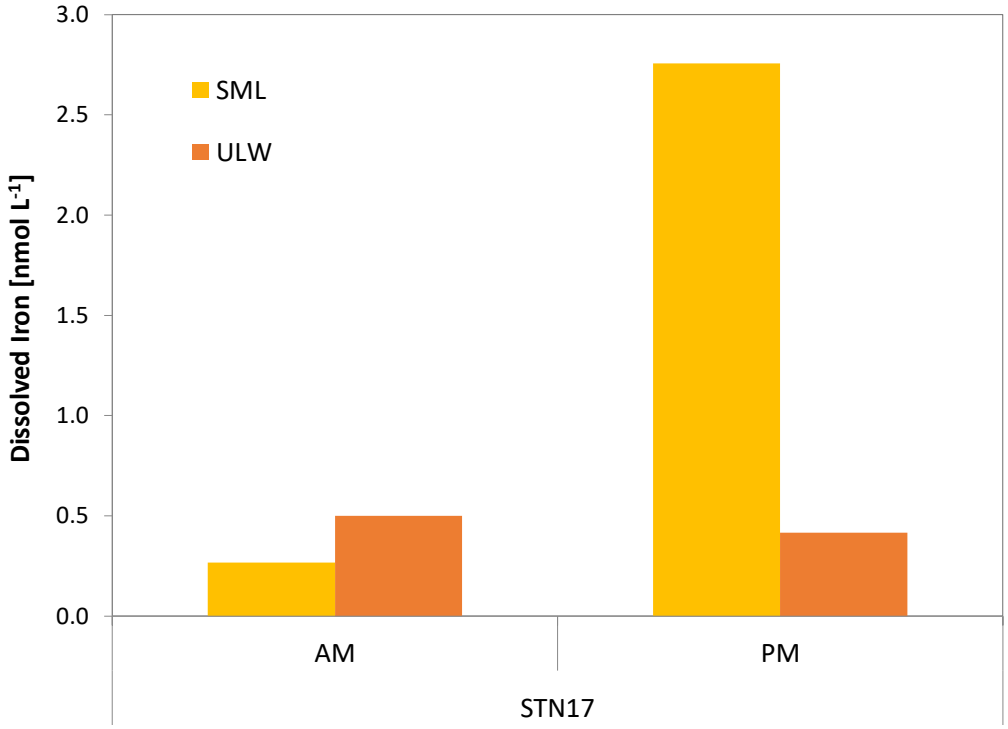

Supplemental figure 6.4. Dissolved Iron [nmol L^{-1}] from the sea surface microlayer and underlying water at oceanic station 17.

Chapter 7

General Discussion

7.1 Summary of the key findings from each chapter

The results presented in this thesis have shown that the overarching drivers selecting for bacterial communities are nutrient regime, substrate origin, physical processes, light & temperature. These environmental drivers lead to a predictable community at a broad level over spatial and temporal scales; temperate regions are characterised by higher relative abundance and activity of heterotrophs and copiotrophs whereas tropical regions are characterised by a higher relative abundance and activity of phototrophs and oligotrophs. Subtropical regions appear to be transitional between temperate and tropical regions sharing similarities with both temperate and tropical communities. Coastal environments are generally characterised by high eukaryotic derived organic matter sources with high physicochemical variation selecting for a dynamic community dominated by copiotrophic heterotrophs. In contrast the open ocean is a high light, low nutrient environment characterised by prokaryotic derived organic matter sources and low physicochemical variability which selects for a stable community dominated by autotrophs and oligotrophic heterotrophs. The individual chapters in this thesis also investigated if the importance of environmental drivers differ on a more local scale by focusing on specific habitats such as the sea surface microlayer and key taxonomic groups such as the CO-oxidisers.

Chapter 3. Carboxydovory in the ecologically-relevant model marine bacterioplankton Ruegeria pomeroyi DSS-3.

I set out to confirm the function of the *coxL* gene in the ecologically relevant and important model marine bacterium Ruegeria pomeroyi DSS-3.

- I have successfully linked CO-oxidation specifically with the *coxL* Form I gene function and shown chemolithoheterotrophy in the model MRC CO-oxidiser *R. pomeroyi* DSS-3.

Chapter 4. Seasonal diversity of bacterioplankton coxL genes: a time series study at the coastal Station L4 and open shelf Station E1 in the Western English Channel.

In this chapter, I aimed to analyse and compare weekly-scale dynamics of two temperate coastal bacterioplankton communities over a spring phytoplankton bloom transition, in relation to prevailing physicochemical drivers.

- I have made the first characterisation of bacterioplankton community dynamics at both Station L4 and E1 and shown that the bacterioplankton present at both stations are typical of previous studies and exhibit strong seasonal patterns in response to physicochemical and biological influences.
- I also show that the bacterioplankton community at the coastal Station L4 and open-shelf Station E1 show slight differences in the timing of seasonal changes and the dominant taxa within community due to differences in the meteorological and hydrographic conditions.
- This study was also the first to characterise bacterioplankton throughout the entire water column which has revealed vertical changes in the bacterioplankton community composition in relation to thermal stratification that were previously unknown.
- Building on from Chapter 3, I have developed functional gene probes to investigate the diversity and distribution of marine carboxydovores, and have successfully demonstrated the use of a trait-based approach to characterise potential CO-oxidising bacterioplankton amongst the Rhodobacteraceae and identified seasonal changes in the CO-oxidising community in relation to the spring phytoplankton bloom.

Chapter 5. Diversity and distribution of total and active bacterioplankton communities in relation to light along a transect of the Atlantic Ocean.

In this chapter, I investigated the bacterioplankton communities in the euphotic zone of the Atlantic Ocean, to gain a better understanding of their biogeographical distribution. I also investigated the activity of the bacterioplankton in these communities to gain insight into the relative contributions these taxa make to bacterial productivity. In addition, I investigated whether light affected the composition and distribution of bacterioplankton communities vertically through the water column.

- I have shown that the bacterioplankton community composition was typical of the environments investigated (e.g. open ocean and coastal), and exhibited strong biogeographical variation in response to prevailing seawater characteristics.
- By comparing total and active bacterioplankton communities, I have shown that bacterioplankton activity is decoupled from abundance throughout the Atlantic, although the two community types show similar patterns in beta diversity.
- I found that light and time of day did not significantly affect the overall structure of the active community. However, ecologically important members of the community did show distinct differences in activity in response to light and time of day.

Chapter 6. A multidisciplinary approach to studying the sea surface microlayer reveals the complexity of physicochemical influences on bacterioneuston diversity.

In this chapter, I investigated bacterial diversity at the air-sea interface using a collaborative multidisciplinary approach in order to better understand the interactive effects of the physicochemical characteristics of the sea surface microlayer on the bacterioneuston.

- I have for the first time used co-occurring *in situ* biological, chemical and physical data to investigate the SML, and shown that physicochemical interactions are both complex and important in determining bacterioneuston community composition.

- I have shown that distinct differences between coastal and oceanic SML environments occur over a relatively conserved area.
- The buoyant properties of particulate matter potentially aid in sustaining the enrichment of particle-associated bacterioneuston during prolonged periods of physical stress.
- I have also shown that the bacterioneuston (primarily *Gammaproteobacteria*) are responding rapidly to resources arriving in the SML from the ULW and/or from the atmosphere.
- I have demonstrated that key taxa can be assigned to single populations and can significantly contribute to the bacterioneuston.
- I have provided new evidence to link *in situ Alteromonadales* blooms in the SML with plankton derived organic matter from the ULW, and also shown that acute events such as *Trichodesmium* blooms can dramatically alter bacterioneuston communities.

7.2 Geographical distribution of bacteria diversity

This thesis has characterised the diversity of marine bacteria in the euphotic zone from the top 1 mm of the surface to down to 250 m deep, covering eleven Longhurst provinces in the northern and southern hemispheres, from coastal waters and shelf seas to the open ocean (figure 7.1). Of the abundant orders (>0.1 % relative abundance), 31 % were shared between all studies. In agreement with previous studies (Rappe et al., 2000, Zinger et al., 2011, Sunagawa et al., 2015), bacterial communities at all study sites were largely (~80 %) composed of bacteria belonging to the orders Synechococcales (i.e. *Cyanobacteria*), SAR11 clade, *Rhodobacterales*, and *Flavobacteriales*, however, the relative contribution of these orders to the community varied geographically, with differences seen on local (i.e. within provinces) and broader (i.e. between provinces and ocean basins) scales. The diversity of the abundant fraction of the community (>0.1 % relative abundance) at the taxonomic level of order was greater at open ocean sites than coastal sites following trends previously reported (Pommier et al., 2007, Fuhrman et al., 2008). The beta diversity of the bacterial communities from each study was also compared and found to vary geographically, with the greatest variation seen between studies. Samples grouped by geographical features, such as province and domain, also varied significantly.

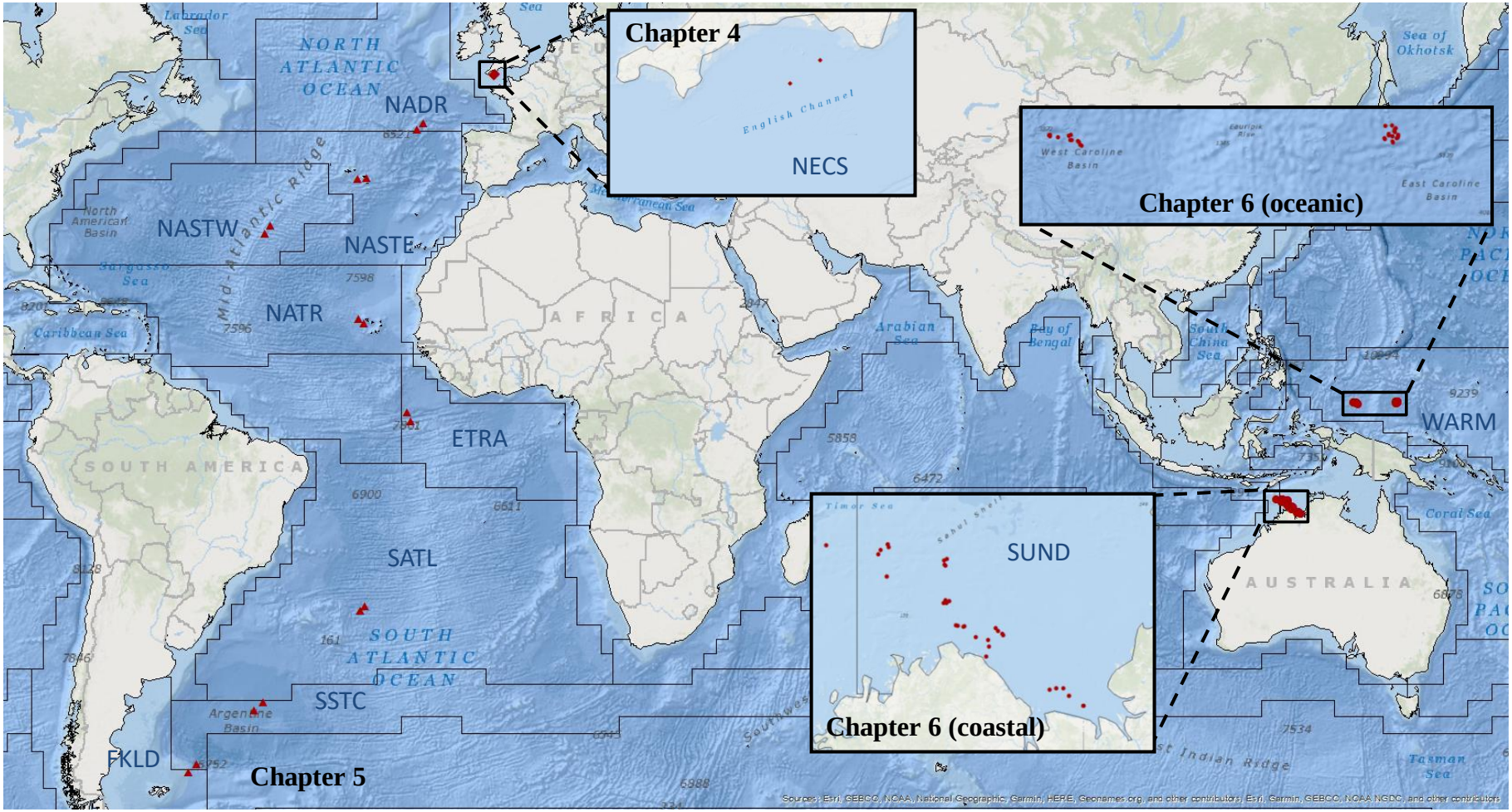

Figure 7.1. Map of all environmental sampling sites in this thesis. Diamonds = Chapter 4, triangles = Chapter 5 and circles = Chapter 6.

7.2.1 Variation of bacterioplankton communities between Oceans

The surface bacterioplankton communities of the Pacific and Atlantic were distinct from each other. The tropical Pacific was dominated by the SAR11 clade, whereas the tropical Atlantic was dominated by *Prochlorococcus*. Interestingly, despite sharing 47 % of the abundant orders, the combined data set showed these communities are distinct at the OTU level (97 % similarity), with only two OTUs (<0.01 % relative abundance) shared by the Pacific and Atlantic studies. This suggests that the communities originate from a local pool of taxa, and supports previous suggestions that the majority of taxa are not shared between ocean basins (Sunagawa et al., 2015).

7.2.2 Coastal versus Open Ocean

It has previously been suggested that coastal communities are phylogenetically similar to open ocean communities (Rappe et al., 2000, Zinger et al., 2011), but are distinguished by a higher abundance of copiotrophs and lower abundance of oligotrophs (Zinger et al., 2011). Although this was broadly true of the coastal and ocean locations investigated in this thesis, oligotrophs were found to dominate the 'coastal' communities in the Pacific (Chapter 6). Also the similarity of bacterioplankton community composition in the coastal and ocean sites were higher within oceans than between oceans. This shows that while there are some universal characteristics of coastal bacterial communities, their composition cannot necessarily be predicted by their proximity to the coast alone and that other factors such as climate should also be considered. For example, the Atlantic coastal domains were in temperate regions, whereas the Pacific coastal domain was in a tropical region. Overall this suggests that environmental characteristics of a particular coastal location have a stronger influence on the bacterial community composition than the location itself as has been shown for temporal studies (Fuhrman et al., 2015).

7.2.3 Seasonal variation in bacterioplankton

Seasonal variation was more apparent in coastal communities than open ocean communities (Chapter 4 and 5), suggesting that coastal domains are more strongly influenced by seasonal changes in environmental conditions, presumably as result of proximity to the terrestrial environment. Northern and southern temperate spring communities from the North Atlantic Shelf (NECS), the South West Atlantic Shelf (FKLD) and South Subtropical Convergence Zone (SSTC) showed a high degree of relatedness to each other (figure 7.2). Interestingly pre-spring bloom communities at the temperate Station E1 (NECS) were more closely related to tropical spring communities of Sunda-Afura shelf (SUND) than to autumn communities at the same Station E1 (figure 7.2). Spring and summer communities in province NECS shared 24 % of OTUs with Pacific communities but only 0.2 % with Atlantic communities, which included autumn samples from the same and neighbouring provinces. This observation of higher similarity across hemispheres and across ocean basins suggests that seasonal environmental characteristics strongly influence the composition of bacterial communities and, conversely to the open ocean environments, suggests bacteria may be 'selected' from a more global pool of taxa.

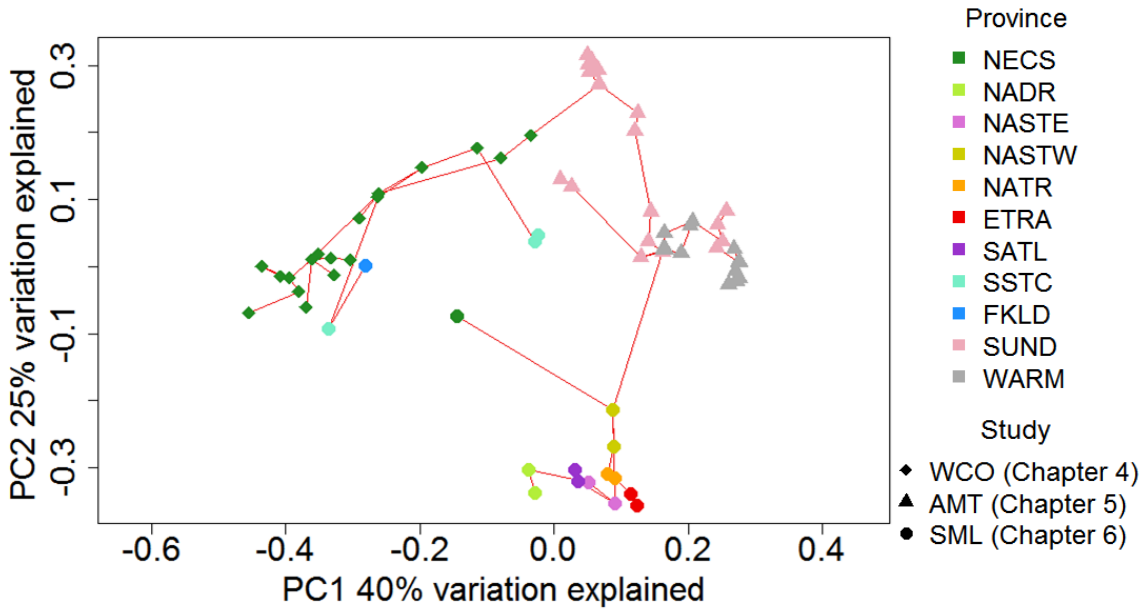

Figure 7.2. Principle coordinates analysis of weighted UniFrac distance metrics of surface (<5 m) samples from Chapters 4, 5 and 6, with minimum spanning tree analysis (red line).

7.2.4 Vertical distribution of bacterioplankton diversity

Bacterial communities in the euphotic zone did not vary as strongly by depth as they did geographically or seasonally. In fact, bacterioplankton communities throughout the upper 250 m of the Atlantic were relatively homogeneous, as were spring bacterioplankton communities throughout the water column in the Western English Channel. Some significant depth related patterns were apparent between surface and deep communities during summer stratification in the Western English Channel, and at the very surface of the ocean between the sea surface microlayer and the surface waters 1 m below.

7.3 Drivers of diversity in marine bacterial communities

The variation in beta diversity seen in this thesis is not directly influenced by depth, geographical location or season but rather is a response of the bacterial community to the prevailing meteorological, physicochemical and biological characteristics of a particular environment at a particular time, i.e. 'the environment selects' (Baas-Becking, 1934, Fuhrman et al., 2006, Caporaso et al., 2012). Key factors selecting for bacterial communities identified in this thesis were trophic regime, substrate origin, physical processes, light and temperature (figure 7.3).

7.3.1 Temperature and light

Temperature was a major influence on the beta diversity of bacterial communities in all studies. In agreement with previous studies, seawater temperature driven by prevailing climatic conditions strongly influenced the geographical and seasonal distribution on bacteria (Pommier et al., 2007, Sunagawa et al., 2015, Bunse and Pinhassi, 2017). Light, however, was not a major driver of bacterial community composition, which is surprising as light stress can be inhibitory to bacterial metabolism and activity (Bailey et al., 1983, Herndl et al., 1993, Müller-Niklas et al., 1995, Sommaruga et al., 1997), and some bacteria have metabolic requirements linked to light and light-dependent processes such as phototrophy (e.g. the SAR11 clade and the *Cyanobacteria*) (Moran and Miller, 2007, Six et al., 2007) or carboxydovory (e.g. the MRC) (Moran and Miller, 2007). It is possible that bacterial taxa have ecotypes that occupy different light niches that cannot be resolved by an OTU similarity of 97 %, as seen for *Prochlorococcus* (Zinser et al., 2007). Therefore, light is likely more important in determining the distribution and activity of individual populations of bacteria within the major bacterial orders that make up the total community.

7.3.2 Physical processes and dispersal

Thermal stratification and physical mixing processes affected the vertical distribution of bacteria. There was also some evidence of mixing processes influencing dispersal between neighbouring provinces. The variability in the similarity between open shelf Station E1 and neighbouring Atlantic provinces shows the dispersal potential of bacterioplankton between the Atlantic and the open shelf of the Western English Channel changes throughout the year. In addition, the bacterioplankton communities in the tropical Atlantic were relatively homogeneous, and coastal (SUND) and open ocean (WARM) communities from the tropical Pacific were closely related, suggesting that there is some degree of dispersal of taxa between neighbouring provinces. As noted previously (Martiny et al., 2006, Pommier et al., 2007, Fuhrman, 2009, Sul et al., 2013, Sunagawa et al., 2015), however, it is hard to tease out dispersal effects from environmental drivers, as these patterns could also be explained by homogeneity or heterogeneity in other environmental characteristics.

7.3.3 Trophic regime and primary producers

Trophic regime (productivity) also seemed to strongly influence the geographical distribution of bacterioplankton, and in the spring appeared to be a more influential driver of seasonal changes in community composition than temperature. In this thesis, coastal bacterial communities, which had a higher abundance of typically particle-associated copiotrophic bacteria were linked with higher concentrations of oxygen, chlorophyll-a and eukaryote phytoplankton abundance. In addition, copiotrophs became enriched in the sea surface microlayer in response to phytoplankton derived organic matter.

The coupling between phytoplankton productivity and bacterioplankton communities is well known (Buchan et al., 2014), however, this thesis shows that this relationship may be more complex. Lower levels of heterotrophic activity seen in *Prochlorococcus* dominated environments and a higher heterotrophic activity seen in

Synechococcus and eukaryotic phytoplankton dominated environments, suggest that there are relationships between the dominant primary producer and the composition and activity of the heterotrophic community, as suggested by Sarmento and Gasol (2012), who showed that interactions between phytoplankton derived DOM and different heterotrophs varies according to the DOM source organism. As such, the composition of DOM varies according to phytoplankton community structure and between ecosystems (Becker et al., 2014). Niche partitioning according to preferential substrate degradation (Christie-Oleza et al., 2015, Sarmento et al., 2016, Bryson et al., 2017) may explain this relationship and agrees with previous suggestions that bacterial communities are influenced by the composition of organic matter (Sapp et al., 2007, Pete et al., 2010). Another possibility is that small *Prochlorococcus* cells may leak less and or produce less extracellular substrates than generally larger eukaryotes, affecting the quantity of organic matter available to heterotrophs, which has also been shown to affect niche partitioning in substrate utilisation (Sarmento et al., 2016). Given that marine bacteria play a major role in shaping the marine DOM pool (Lechtenfeld et al., 2015), these communities may also be influenced by cross feeding through positive feedback mechanisms driven by the primary OM degraders.

7.3.4 Atmospheric inputs

There was also evidence that atmospheric deposition can influence bacterial communities in the oligotrophic open ocean. This was primarily observed in the sea surface microlayer study (Chapter 6), but increases in the abundance of *Trichodesmium,* which are known to readily respond to iron inputs from dust deposition (Langlois et al., 2012, Polyviou et al., 2017) were also seen in provinces of the Atlantic (Chapter 5) that are seasonally influenced by Saharan dust (Baker et al., 2006). Dust deposition events have been shown to promote bloom formation of certain taxa such as *Vibrio* spp. (Westrich et al., 2016) and *Trichodesmium* spp. (Langlois et al., 2012, Polyviou et al., 2017) and can even supply airborne microbes into the

surface ocean. Dust deposition represents an important source of nutrients into the marine environment, and has potential to influence biogeochemical cycles by altering the metabolism of autochthonous taxa, affecting the overall trophic status of an environment (Hill et al., 2010, Lekunberri et al., 2010). Furthermore the enrichment of trace metal utilising bacteria in the sea surface microlayer could influence the availability of these nutrients in the water column below. But currently, relatively little is known about the transformation of atmospheric nutrients by bacterial communities in the surface ocean (Wurl et al., 2017).

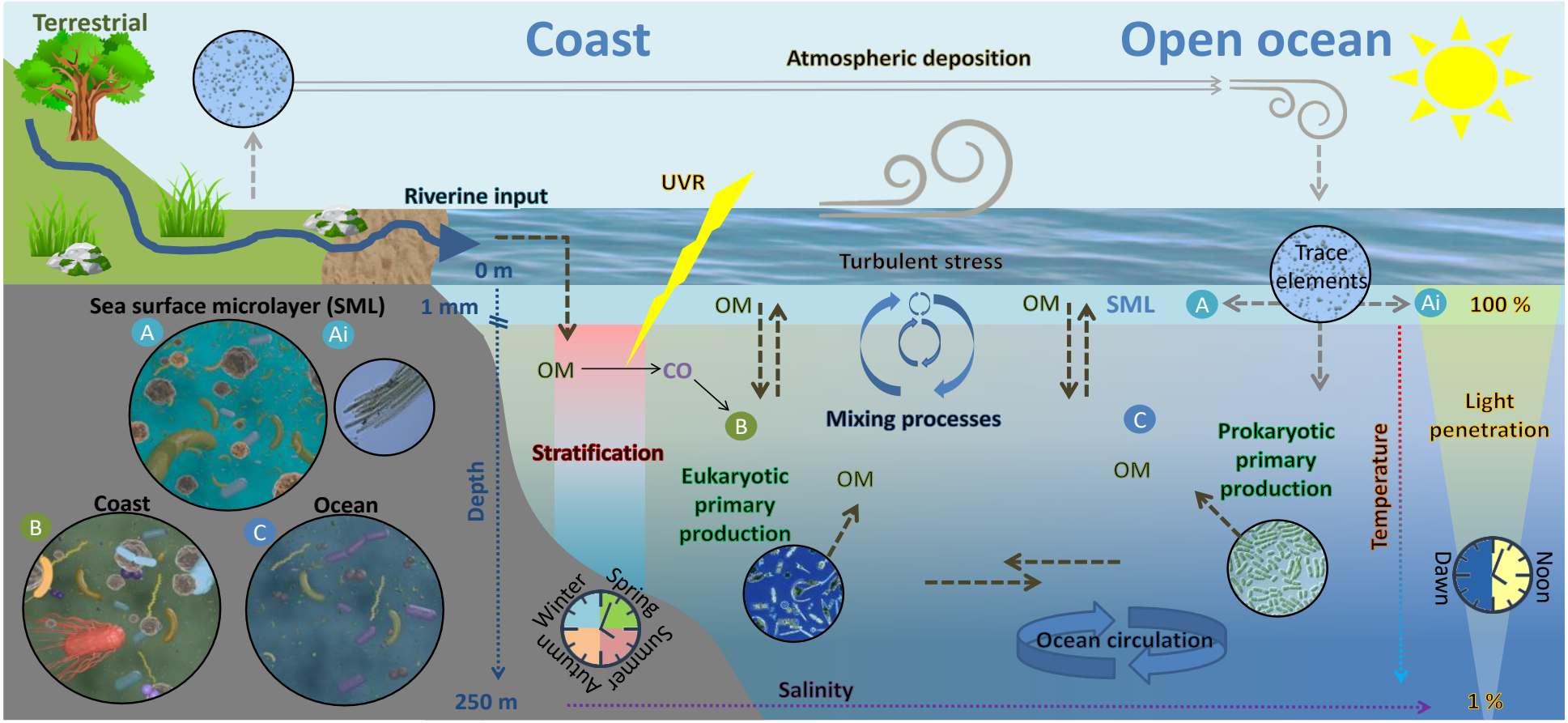

Figure 7.3.Conceptual diagram of environmental drivers of bacterial diversity in the marine environment. A = cartoon of sea surface microlayer bacterioneuston community and Ai = *Trichodesmium*, B = cartoon of coastal bacterial community and C = cartoon of open ocean bacterial community.

7.4 Ecology of bacteria

The distribution of oligotrophs (bacteria adapted to growth at low nutrient levels) and copiotrophs (bacteria that are adapted for growth at high nutrient levels) (Koch, 2001), reflected the nutrient regimes of the environments studied in this thesis. However, the patterns in bacterial diversity, ecological, and metabolic strategies were in reality more complex than this simple classification implies. Acute inputs of atmospheric and water column organic/inorganic matter and physical stress selected for dynamic enrichments of copiotrophic, particle-associated heterotrophs and opportunistic diazotrophs in the sea surface microlayer (figure 7.3 A). In coastal environments high eukaryotic derived OM and high physicochemical variation selected for a dynamic community dominated by phytoplankton-associated copiotrophic heterotrophs (figure 7.3 B). Conversely, high light, low nutrient level, prokaryotic derived OM and low physicochemical variability selects for a stable community dominated by oligotrophic autotrophs and heterotrophs in the open ocean (figure 7.3 C).

7.4.1 Rhodobacterales and Flavobacteriales

The *Rhodobacterales* and *Flavobacteriales* were an abundant part of all communities characterised in this thesis. RNA:DNA ratios suggest that their activity as well as their abundance is associated with productive coastal and shelf sea environments most likely in relation to organic matter composition and concentration as discussed earlier. Both are metabolically diverse, making them well adapted to respond to the pulses of phytoplankton derived OM occurring in coastal environments (Buchan et al., 2014). Occupying slightly different substrate niches (high-molecular weight vs low molecular weight) these bacteria function synergistically in the ecosystem to degrade the larger fractions of phytoplankton derived OM (Buchan et al., 2014, Taylor et al., 2014). Interestingly, in Chapter 5, RNA:DNA

ratios revealed that this synergistic approach may also be diurnally synchronised to optimise metabolism of high-molecular weight and low-molecular weight substrates.

7.4.2 The SAR11 clade

The SAR11 clade were also an abundant part of all communities characterised in this thesis. The activity levels identified in Chapter 5 and previous studies (Lami et al., 2009, Campbell et al., 2011, Hunt et al., 2013) suggest that SAR11 are not as active in the community as their potential, as evidenced by enrichment studies, suggests (Malmstrom et al., 2004, Mary et al., 2006b, Laghdass et al., 2012). As discussed by Giovannoni (2017), these mismatches could be explained by the correlation of growth rates with RNA:DNA ratios, but comparability to other taxa aside, Chapter 5 still showed variation in SAR11 RNA:DNA ratios in different provinces of the Atlantic. One reason for this may be due to substrate type or availability. SAR11 are specialised in the uptake of small labile substrates such as dissolved amino acids and simple sugars (Giovannoni, 2017), but the oligotrophic lifestyle of SAR11 means it cannot compete with fast growing copiotrophs that occupy the same trophic niche (Klappenbach et al., 2000, Giovannoni, 2017) (e.g. in the Arctic Ocean (Alonso-Saez et al., 2008) and Delaware estuary (Elifantz et al., 2005)). Thus, it is thought SAR11 cannot respond to increases in substrate due to their low growth rates (Giovannoni, 2017). Previous studies have shown that SAR11 activity varies with time of year (Alonso-Sáez et al., 2007) and between ecosystems. For example, SAR11 are dominant in the uptake of glucose and amino acids in the Sargasso Sea (Malmstrom et al., 2005) and the North Sea (Alonso and Pernthaler, 2006). Alonso and Pernthaler (2006) also showed that SAR11 growth was maximal at 1 nM glucose and was reduced to 0.1 nM. Later it was shown that glycolysis is a trait more common to coastal ecotypes of SAR11 (Rappé et al., 2002, Stingl et al., 2007, Schwalbach et al., 2010). SAR11 activity in this study was higher in the more productive sub-tropical and temperate provinces of the Atlantic. Concentrations of amino

acids in the marine environment are higher in abundance with proximity to the coast (Lee & Bada, 1977) and where total OM degradation is higher (Rich et al., 1997, Jørgensen et al., 2014). This suggests that SAR11 can respond to increases in substrate availability in stable oligotrophic environments where the balance between competition and substrate levels is optimal.

The distinct OTU composition of SAR11, and higher abundance seen in the Pacific compared to the Atlantic shown here could also be explained by the existence of ecotypes with different trophic requirements. The concentration of amino acids have also been shown to be higher in the Pacific than the Atlantic (Lee and Bada, 1977), and Coleman and Chisholm (2010) suggested that P limitation in the Atlantic is a primary mechanism for divergence between Atlantic and Pacific populations of SAR11.

7.4.3 The Gammaproteobacteria

Gammaproteobacteria such as the *Alteromonadales*, are less abundant but invest in high growth and/or activity when conditions are optimal. Peaks in *Gammaproteobacteria* abundance were seen in all chapters, possibly in response to inputs of both allochthonous and autochthonous substrates. *Alteromonadales* were increased in Atlantic provinces influenced by atmospheric deposition, to my knowledge this is a novel observation. The family *Alteromonadaceae* are associated with iron metabolism as are other *Gammaproteobacteria*, such as family *Vibrionaceae* (Haggerty and Dinsdale, 2017), which have been associated with dust deposition processes previously (Westrich et al., 2016). *Alteromonadales* also showed a peak in abundance in week 21 at the Western Channel Observatory, which was higher at the bottom of the water column than at the surface suggesting a benthic source of substrate.

In contrast to the communities at 1 m depth and other communities in the euphotic water column, *Gammaproteobacteria* (especially *Alteromonadales*) dominated SML

communities in the Pacific Ocean, again in response to atmospheric deposition and also to the accumulation of particulate phosphorous in the SML from the water column below. The patterns and drivers of *Gammaproteobacteria* abundance identified in this thesis suggest they play a crucial role in 'rapid input' biogeochemical processes especially in the oligotrophic ocean.

7.4.4 Chemolithoheterotrophy

The range and supply of organic matter in the marine environment is complex (Koch et al., 2005), therefore bacteria with a range of different metabolic traits are at an advantage in this dynamic environment (Moran, 2015). In Chapter 3, I identified that CO-oxidation supports higher heterotrophic growth in *R. Pomeroyi* during carbon starvation, and in agreement with previous studies, in Chapter 4 I identified a large potential for carboxydovory among the MRC in productive coastal seas (Tolli et al., 2006, Cunliffe, 2011). The MRC (e.g. *R. pomeroyi*) are metabolically diverse (Buchan et al., 2005, Moran et al., 2007, Newton et al., 2010), as are many other globally dominant heterotrophs. The ability to take advantage of different energy sources may aid ecologically important heterotrophic bacteria such as the MRC to persist abundantly in the marine environment even during suboptimal circumstances such as low nutrient conditions (Moran, 2015). Understanding specific metabolic processes such as CO-oxidation and being able to measure these processes in the environment has potential to advance our understanding of the fate of organic matter in the marine ecosystem (Lechtenfeld et al., 2015).

7.5 Future direction and perspectives

The results of these chapters have shown that despite the general predictability of bacterioplankton communities at a broad taxonomic and geographical scale there is still a lot to be investigated at the fine scale to fully understand how the chemical, physical and

biological environment influences bacterioplankton community structure and the individual taxa that compose it, these details could help to improve biogeochemical models and allow us to better understand how the marine ecosystem may respond to climate change. Some key areas for consideration in future studies are:

- Using higher sampling frequencies to look into temporal dynamics of bacterial communities.
- Including depth resolved sampling approaches, especially where physicochemical features such as stratification are present.
- Conducting culture based experimentation with environmentally important taxa in order to relate metabolic processes to genes or RNA concentration in the environment.
- Using new genomic technologies / methods to better resolve bacterial community composition in order to understand niche separation within closely related taxa and improve taxonomic representation within genomic databases.
- Investigate in more detail the origins of organic matter and the resulting effect on bacterial community structure and activity.
- Investigate the role of bacterioplankton in the transformation of atmospheric inputs.

16S rRNA diversity and activity alone cannot determine whether the function of bacterial communities is also distinct between oceans, especially as a recent study by Parks et al., (2018) has shown that bacterial taxonomy based on protein phylogeny may be more accurate than historic taxonomy based on evolutionary relationships determined by 16S rRNA. Metagenomics and metatranscriptomics have potential to advance our knowledge of phylogenetic and functional bacterial diversity, however, as the majority of these studies identify genes that are not yet characterised, we cannot exploit these new technologies to

their full potential. Therefore, there is an increasing need for culture and enrichment based studies to identify functional traits and link them with ecological processes.

While the communities identified from different environments in this thesis appeared distinct at the order level, sharing 31 % of bacterial orders, their distinction at the OTU level was far greater, with no shared OTUs at a 97 % similarity cut off. Although evidence suggests that function is less affected by variation at the OTU level than phylogenetic composition (Gilbert et al., 2010a, Gilbert et al., 2010b, Sunagawa et al., 2015), given the diversity and distribution of different metabolic and environmental niches of the bacteria comprising these communities, it is likely that taxonomic resolution could affect how we assign ecosystem function to different communities. Amplicon sequence variants (ASVs) are a recent development in the analysis of gene sequencing that allows variation in the sequenced gene region to be resolved down to the level of a single-nucleotide difference (Callahan et al., 2017). ASVs would allow differentiation of ecotypes amongst closely related taxa, such as substrate niches in SAR11 and light niches in *Prochlorococcus*, improving the ecological relevance of phylogenetic diversity studies.

Bacterial communities are generally predictable by their environment, but the interactions with underlying chemical, physical and biological niches at a high and low taxonomic resolution are complex. We are only just beginning to be able to characterise the individual components within the dynamic marine environment and now must work toward linking together the details of these complex interactions. In order to achieve this, multidisciplinary/holistic approaches such as those demonstrated in this thesis are required to not only characterise the diversity of bacteria and their metabolism, but to also characterise the diversity and distribution of their drivers, such as substrate composition at a higher resolution.

Abbreviations

°C	Degrees Celsius
°N	Degrees north
°S	Degrees south
%	Percent
®	Registered
µ	Growth rate
µatm	Micro atmospheres
µg	Microgram
µm	Micrometre
µm	Microliter
µM	Micromoles
16S rRNA	16S ribosomal RNA
AM	Ante meridiem
AMT	Atlantic Meridional Transect
ANOVA	Analysis of variance
ASV	Amplicon sequence variants
AU	Australia
BIOM	Biological Observation Matrix
BLAST	Basic local alignment search tool
bp	Base pair
C	Carbon

CARD-FISH	Catalysed reporter deposition Fluorescence *In Situ* Hybridization
cDNA	Complementary DNA
CDOM	Chromophoric Dissolved Organic Matter
CGEB	Centre for Comparative Genomics and Evolutionary Bioinformatics
CHIN	China Sea province
cm	Centimetre
CO	Carbon monoxide
CO_2	Carbon dioxide
CODH	Carbon monoxide dehydrogenase
coxL	Carbon monoxide dehydrogenase large sub unit gene
CTD	Conductivity, temperature, depth
DCM	Deep chlorophyll maximum
DGGE	Denaturing gradient gel electrophoresis
DIVA	Data-Interpolating Variational Analysis
DNA	Deoxyribonucleic acid
DOC	Dissolved organic carbon
DOM	Dissolved organic matter
DON	Dissolved organic nitrogen
DSMZ	Deutsche Sammlung von Mikroorganismen und Zellkulturen
EDTA	Ethylenediaminetetraacetic acid
ETRA	Eastern tropical Atlantic province
excl.	Excluding
Fe	Iron

fDOM	Fluorescent Dissolved Organic Matter
FKLD	Southwest Atlantic shelves province
G	Total growth
g	Gram
G (as unit)	G-force
GMT	Greenwich mean time
Gt	Giga ton
h	Hour
HCl	Hydrochloric Acid
HTS	High-throughput sequencing
ID	Identity
IMR	Integrated Microbiome Resource
IMS	Industrial methylated spirits
incl.	Including
INSDC	International Nucleotide Sequence Database Collaboration
kaiBC	Cyanobacterial clock gene cluster
L	Litre
LMO	Linnaeus Microbial Observatory
ln	Natural logarithm
log	Base 10 logarithm
LTD	Limited
m	Meter
M	Molar

MAMS	Marine ammonium mineral salts
MBA	Marine Biological Association UK
MEDI	Mediterranean Sea province
MEGA	Molecular Evolutionary Genetics Analysis
mg	Milligram
min	Minute
mL	Millilitre
mm	Millimetre
MRC	Marine Roseobacter Clade
MST	Minimum spanning tree
MUSCLE	Multiple Sequence Comparison by Log-Expectation
N	Nitrogen
n	Number
N (as a unit)	Newtons
NADR	North Atlantic Drift province
Na-EDTA	Sodium Ethylenediaminetetraacetic acid
NASTE	Northeast Atlantic subtropical gyral
NASTW	Northwest Atlantic subtropical gyral
NATR	North Atlantic tropical gyral province
NCBI	National Centre for Biotechnology Information
NERC	Natural Environment Research Council
NECS	Northeast Atlantic shelves
NEODAAS	NERC Earth Observation Data Acquisition and Analysis Service

NIOZ	Royal Netherlands Institute for Sea Research
nm	Nanometre
NWCS	Northwest Atlantic shelves province
Ø	Diameter
OD600	Optical density at 600 nm
ODV	Ocean Data View
OM	Organic matter
OMG	Oligotrophic marine *Gammaproteobacteria*
OTU	Operational taxonomic unit
P	Phosphorous
P-Al	Particulate aluminium
PAR	Photosynthetically Active Radiation
PBS	Phosphate buffered saline
***p*CO$_2$**	Partial pressure of carbon dioxide
PCoA	Principal Coordinates Analysis
PCR	Polymerase chain reaction
PERMANOVA	Permutational multivariate analysis of variance
P-Fe	Particulate iron
PM	Post meridiem
POC	Particulate organic carbon
P-P	Particulate phosphorous
ppm	Parts per million
PSU	Practical salinity unit

Pty	Proprietary company
prx	Circadian marker peroxiredoxin
pyrG	CTP synthase gene
QIIME	Quantitative Insights Into Microbial Ecology
qPCR	Quantitative real-time PCR
RA	Relative abundance
RDA	Redundancy analysis
RFLP	Restriction Fragment Length Polymorphism
RFU	Relative fluorescence unit
RNA	Ribonucleic acid
rpoB	β subunit of bacterial RNA polymerase gene
RT	Reverse transcription
s	Second
SAS	Surface active substance
SATL	South Atlantic gyral province
SML	Sea surface microlayer
sp.	Species pluralis
spp.	Species
SSS	Sea surface scanner
SSTC	South subtropical convergence province
SUND	Sunda-Arafura shelves province
TAE	Tris base, acetic acid and ethylenediaminetetraacetic acid
TEP	Transparent exopolymer particles

Teq	Triton X-100
Tg	Teragram
™	Trade mark
U10N	Wind speed at 10 m above sea level
UK	United Kingdom
ULW	Underlying water
US	United States
UTC	Coordinated universal time
UV	Ultraviolet
UVR	Ultraviolet radiation
v/v	Volume/volume
vs.	Versus
W	Watt
w/v	Weight/volume
WARM	Western Pacific warm pool province
WCO	Western Channel Observatory
YTSS	Yeast, tryptone and sea salts
Δ	Delta

List of References

AGOGUE, H., CASAMAYOR, E. O., BOURRAIN, M., OBERNOSTERER, I., JOUX, F., HERNDL, G. J. & LEBARON, P. 2005a. A survey on bacteria inhabiting the sea surface microlayer of coastal ecosystems. *FEMS Microbiology Ecology,* 54**,** 269-280.

AGOGUE, H., JOUX, F., OBERNOSTERER, I. & LEBARON, P. 2005b. Resistance of marine bacterioneuston to solar radiation. *Applied and Environmental Microbiology,* 71**,** 5282-5289.

AIKEN, J., REES, N., HOOKER, S., HOLLIGAN, P., BALE, A., ROBINS, D., MOORE, G., HARRIS, R. & PILGRIM, D. 2000. The Atlantic Meridional Transect: overview and synthesis of data. *Progress in Oceanography,* 45**,** 257-312.

ALDERKAMP, A.-C., SINTES, E. & HERNDL, G., J. 2006. Abundance and activity of major groups of prokaryotic plankton in the coastal North Sea during spring and summer. *Aquatic Microbial Ecology,* 45**,** 237-246.

ALONSO-SÁEZ, L., BALAGUÉ, V., SÀ, E. L., SÁNCHEZ, O., GONZÁLEZ, J. M., PINHASSI, J., MASSANA, R., PERNTHALER, J., PEDRÓS-ALIÓ, C. & GASOL, J. M. 2007. Seasonality in bacterial diversity in north-west Mediterranean coastal waters: assessment through clone libraries, fingerprinting and FISH. *FEMS Microbiology Ecology,* 60**,** 98-112.

ALONSO-SAEZ, L., DIAZ-PEREZ, L. & MORAN, X. A. 2015. The hidden seasonality of the rare biosphere in coastal marine bacterioplankton. *Environmental Microbiology,* 17**,** 3766-3780.

ALONSO-SÁEZ, L. & GASOL, J. M. 2007. Seasonal Variations in the contributions of different bacterial groups to the uptake of low-molecular-weight compounds in Northwestern Mediterranean coastal waters. *Applied and Environmental Microbiology,* 73**,** 3528-3535.

ALONSO-SAEZ, L., GASOL, J. M., LEFORT, T., HOFER, J. & SOMMARUGA, R. 2006. Effect of natural sunlight on bacterial activity and differential sensitivity of natural bacterioplankton groups in northwestern Mediterranean coastal waters. *Applied and Environmental Microbiology,* 72**,** 5806-5813.

ALONSO-SAEZ, L., SANCHEZ, O., GASOL, J. M., BALAGUE, V. & PEDROS-ALIO, C. 2008. Winter-to-summer changes in the composition and single-cell activity of near-surface Arctic prokaryotes. *Environmental Microbiology,* 10**,** 2444-2454.

ALONSO, C. & PERNTHALER, J. 2006. Roseobacter and SAR11 dominate microbial glucose uptake in coastal North Sea waters. *Environmental Microbiology,* 8**,** 2022-2030.

ALTSCHUL, S. F., GISH, W., MILLER, W., MYERS, E. W. & LIPMAN, D. J. 1990. Basic local alignment search tool. *Journal of Molecular Biology,* 215**,** 403-410.

ANDERSSON, A. F., RIEMANN, L. & BERTILSSON, S. 2010. Pyrosequencing reveals contrasting seasonal dynamics of taxa within Baltic Sea bacterioplankton communities. *The ISME Journal,* 4**,** 171-181.

ARAR, E. J. & COLLINS, G. B. 1997. *Method 445.0: In vitro determination of chlorophyll a and pheophytin a in marine and freshwater algae by fluorescence,* United States Environmental Protection Agency, Office of Research and Development, National Exposure Research Laboratory Cincinnati.

ARNOSTI, C. & STEEN, A. D. 2013. Patterns of extracellular enzyme activities and microbial metabolism in an Arctic fjord of Svalbard and in the northern Gulf of Mexico: contrasts in carbon processing by pelagic microbial communities. *Frontiers in Microbiology,* 4**,** fmicb.2013.00318.

ARNOSTI, C., STEEN, A. D., ZIERVOGEL, K., GHOBRIAL, S. & JEFFREY, W. H. 2011. Latitudinal gradients in degradation of marine dissolved organic carbon. *PLOS ONE,* 6**,** e28900.

ARRIETA, J. M., WEINBAUER, M. G. & HERNDL, G. J. 2000. Interspecific variability in sensitivity to UV radiation and subsequent recovery in selected isolates of marine bacteria. *Applied and Environmental Microbiology,* 66**,** 1468-1473.

AZAM, F. 1998. Microbial Control of Oceanic Carbon Flux: The Plot Thickens. *Science,* 280**,** 694-696.

AZAM, F., FENCHEL, T., FIELD, J. G., GRAY, J., MEYER-REIL, L. & THINGSTAD, F. 1983. The ecological role of water-column microbes in the sea. *Marine ecology progress series,*10**,** 257-263.

AZAM, F. & MALFATTI, F. 2007. Microbial structuring of marine ecosystems. *Nature Reviews Microbiology,* 5**,** 782-791.

AZETSU-SCOTT, K. & PASSOW, U. 2004. Ascending marine particles: Significance of transparent exopolymer particles (TEP) in the upper ocean. *Limnology and Oceanography,* 49**,** 741-748.

BAAS-BECKING, L. G. M. 1934. *Geobiologie; of inleiding tot de milieukunde,* WP Van Stockum & Zoon NV.

BAILEY, C. A., NEIHOF, R. A. & TABOR, P. S. 1983. Inhibitory effect of solar radiation on amino acid uptake in Chesapeake Bay bacteria. *Applied and environmental microbiology,* 46**,** 44-49.

BAKER, A. R., JICKELLS, T. D., BISWAS, K. F., WESTON, K. & FRENCH, M. 2006. Nutrients in atmospheric aerosol particles along the Atlantic Meridional Transect. *Deep Sea Research Part II: Topical Studies in Oceanography,* 53**,** 1706-1719.

BAR-ON, Y. M., PHILLIPS, R. & MILO, R. 2018. The biomass distribution on Earth. *Proceedings of the National Academy of Sciences,* 115**,** 6506-6511.

BECKER, J., BERUBE, P., FOLLETT, C., WATERBURY, J., CHISHOLM, S., DELONG, E. & REPETA, D. 2014. Closely related phytoplankton species produce similar suites of dissolved organic matter. *Frontiers in Microbiology,* 5. fmicb.2014.00111

BEHRENFELD, M. J., O'MALLEY, R. T., SIEGEL, D. A., MCCLAIN, C. R., SARMIENTO, J. L., FELDMAN, G. C., MILLIGAN, A. J., FALKOWSKI, P. G., LETELIER, R. M. & BOSS, E. S. 2006. Climate-driven trends in contemporary ocean productivity. *Nature,* 444**,** 752-755.

BENNER, R. 2002. Chemical composition and reactivity. *Biogeochemistry of marine dissolved organic matter,* 3**,** 56-90.

BIANCHI, T. S. 2011. The role of terrestrially derived organic carbon in the coastal ocean: A changing paradigm and the priming effect. *Proceedings of the National Academy of Sciences,* 108**,** 19473-19481.

BLAZEWICZ, S. J., BARNARD, R. L., DALY, R. A. & FIRESTONE, M. K. 2013. Evaluating rRNA as an indicator of microbial activity in environmental communities: limitations and uses. *The ISME Journal,* 7**,** 2061-2068.

BODC. 2015. *cruise JR15001 (AMT, JR864)* [Online]. British Oceanographic Data Centre. Available: https://www.bodc.ac.uk/data/bodc_database/nodb/search/ [Accessed 2016].

BOUMAN, H. A., ULLOA, O., SCANLAN, D. J., ZWIRGLMAIER, K., LI, W. K., PLATT, T., STUART, V., BARLOW, R., LETH, O. & CLEMENTSON, L. 2006.

Oceanographic basis of the global surface distribution of *Prochlorococcus* ecotypes. *Science,* 312**,** 918-921.

BOYD, P. W. & ELLWOOD, M. J. 2010. The biogeochemical cycle of iron in the ocean. *Nature Geoscience,* 3**,** 675-682.

BOYD, P. W., ELLWOOD, M. J., TAGLIABUE, A. & TWINING, B. S. 2017. Biotic and abiotic retention, recycling and remineralization of metals in the ocean. *Nature Geoscience,* 10**,** 167-173.

BREWER, P. G. & RILEY, J. P. 1965. The automatic determination of nitrate in sea water. *Deep Sea Research and Oceanographic Abstracts,* 12**,** 765-772.

BROWN, M. V., LAURO, F. M., DEMAERE, M. Z., MUIR, L., WILKINS, D., THOMAS, T., RIDDLE, M. J., FUHRMAN, J. A., ANDREWS-PFANNKOCH, C., HOFFMAN, J. M., MCQUAID, J. B., ALLEN, A., RINTOUL, S. R. & CAVICCHIOLI, R. 2012. Global biogeography of SAR11 marine bacteria. *Molecular Systems Biology,* 8**,** 595-595.

BRYSON, S., LI, Z., CHAVEZ, F., WEBER, P. K., PETT-RIDGE, J., HETTICH, R. L., PAN, C., MAYALI, X. & MUELLER, R. S. 2017. Phylogenetically conserved resource partitioning in the coastal microbial loop *The ISME Journal,* 11**,** 2781-2792.

BUCHAN, A., GONZALEZ, J. M. & MORAN, M. A. 2005. Overview of the marine roseobacter lineage. *Applied and Environmental Microbiology,* 71**,** 5665-5677.

BUCHAN, A., LECLEIR, G. R., GULVIK, C. A. & GONZÁLEZ, J. M. 2014. Master recyclers: features and functions of bacteria associated with phytoplankton blooms. *Nature Reviews Microbiology,* 12**,** 686-698.

BUNSE, C. & PINHASSI, J. 2017. Marine Bacterioplankton Seasonal Succession Dynamics. *Trends in Microbiology,* 25**,** 494-505.

CAI, X., HUTCHINS, D. A., FU, F. & GAO, K. 2017. Effects of ultraviolet radiation on photosynthetic performance and N 2 fixation in *Trichodesmium erythraeum* IMS 101. *Biogeosciences,* 14**,** 4455-4466.

CALLAHAN, B. J., MCMURDIE, P. J. & HOLMES, S. P. 2017. Exact sequence variants should replace operational taxonomic units in marker-gene data analysis. *The ISME Journal,* 11**,** 2639-2643.

CAMPBELL, B. J., YU, L., HEIDELBERG, J. F. & KIRCHMAN, D. L. 2011. Activity of abundant and rare bacteria in a coastal ocean. *Proceedings of the National Academy of Sciences of the United States of America,* 108**,** 12776-12781.

CAMPBELL, B. J., YU, L., STRAZA, T. R. A. & KIRCHMAN, D. L. 2009. Temporal changes in bacterial rRNA and rRNA genes in Delaware (USA) coastal waters. *Aquatic Microbial Ecology*, 57**,** 123-135.

CAPONE, D. G., ZEHR, J. P., PAERL, H. W., BERGMAN, B. & CARPENTER, E. J. 1997. *Trichodesmium*, a Globally Significant Marine Cyanobacterium. *Science,* 276**,** 1221-1229.

CAPORASO, J. G., KUCZYNSKI, J., STOMBAUGH, J., BITTINGER, K., BUSHMAN, F. D., COSTELLO, E. K., FIERER, N., PENA, A. G., GOODRICH, J. K., GORDON, J. I., HUTTLEY, G. A., KELLEY, S. T., KNIGHTS, D., KOENIG, J. E., LEY, R. E., LOZUPONE, C. A., MCDONALD, D., MUEGGE, B. D., PIRRUNG, M., REEDER, J., SEVINSKY, J. R., TURNBAUGH, P. J., WALTERS, W. A., WIDMANN, J., YATSUNENKO, T., ZANEVELD, J. & KNIGHT, R. 2010. QIIME allows analysis of high-throughput community sequencing data. *Nature Methods,* 7**,** 335-336.

CAPORASO, J. G., PASZKIEWICZ, K., FIELD, D., KNIGHT, R. & GILBERT, J. A. 2012. The Western English Channel contains a persistent microbial seed bank. *The ISME Journal,* 6**,** 1089-1093.

CASOTTI, R., BRUNET, C., ARONNE, B. & D'ALCALA, M. R. 2000. Mesoscale features of phytoplankton and planktonic bacteria in a coastal area as induced by external water masses. *Marine Ecology Progress Series,* 195**,** 15-27.

CHEN, Y., TOVAR-SANCHEZ, A., SIEFERT, R. L., SAÑUDO-WILHELMY, S. A. & ZHUANG, G. 2011. Luxury uptake of aerosol iron by *Trichodesmium* in the western tropical North Atlantic. *Geophysical Research Letters,* 38, L18602.

CHO, J.-C. & GIOVANNONI, S. J. 2004. Cultivation and growth characteristics of a diverse group of oligotrophic marine *Gammaproteobacteria*. *Applied and Environmental Microbiology,* 70**,** 432-440.

CHRISTIE-OLEZA, J. A., PIÑA-VILLALONGA, J. M., BOSCH, R., NOGALES, B. & ARMENGAUD, J. 2012. Comparative proteogenomics of twelve Roseobacter exoproteomes reveals different adaptive strategies among these marine bacteria. *Molecular & Cellular Proteomics,* 11, M111.013110.

CHRISTIE-OLEZA, J. A., SOUSONI, D., LLOYD, M., ARMENGAUD, J. & SCANLAN, D. J. 2017. Nutrient recycling facilitates long-term stability of marine microbial phototroph–heterotroph interactions. *Nature Microbiology,* 2**,** 17100.

CHRISTIE-OLEZA, J. A., SCANLAN, D. J. & ARMENGAUD, J. 2015. "You produce while I clean up", a strategy revealed by exoproteomics during *Synechococcus*–Roseobacter interactions. *Proteomics,* 15**,** 3454-3462.

COLEMAN, M. L. & CHISHOLM, S. W. 2010. Ecosystem-specific selection pressures revealed through comparative population genomics. *Proceedings of the National Academy of Sciences,* 107**,** 18634-18639.

COMEAU, A. M., DOUGLAS, G. M. & LANGILLE, M. G. 2017. Microbiome Helper: a custom and streamlined workflow for microbiome research. *mSystems,* 2, e00127-16.

CONRAD, R. & SEILER, W. 1980. Photooxidative production and microbial consumption of carbon monoxide in seawater. *FEMS Microbiology Letters,* 9**,** 61-64.

ĆOSOVIĆ, B. & VOJVODIĆ, V. 1998. Voltammetric analysis of surface active substances in natural seawater. *Electroanalysis,* 10**,** 429-434.

COX, J. & MANN, M. 2008. MaxQuant enables high peptide identification rates, individualized p.p.b.-range mass accuracies and proteome-wide protein quantification. *Nature Biotechnology,* 26**,** 1367-1372.

CRAM, J. A., CHOW, C.-E. T., SACHDEVA, R., NEEDHAM, D. M., PARADA, A. E., STEELE, J. A. & FUHRMAN, J. A. 2014. Seasonal and interannual variability of the marine bacterioplankton community throughout the water column over ten years. *The ISME Journal,* 9**,** 563-580.

CUNLIFFE, M. 2011. Correlating carbon monoxide oxidation with *cox* genes in the abundant Marine Roseobacter Clade. *The ISME Journal,* 5**,** 685-691.

CUNLIFFE, M. 2013. Physiological and metabolic effects of carbon monoxide oxidation in the model marine bacterioplankton *Ruegeria pomeroyi* DSS-3. *Applied and Environmental Microbiology,* 79**,** 738-740.

CUNLIFFE, M. 2016. Purine catabolic pathway revealed by transcriptomics in the model marine bacterium *Ruegeria pomeroyi* DSS-3. *FEMS Microbiology Ecology,* 92, fiv150.

CUNLIFFE, M., ENGEL, A., FRKA, S., GAŠPAROVIĆ, B., GUITART, C., MURRELL, J. C., SALTER, M., STOLLE, C., UPSTILL-GODDARD, R. & WURL, O. 2013. Sea surface microlayers: A unified physicochemical and biological perspective of the air–ocean interface. *Progress in Oceanography,* 109**,** 104-116.

CUNLIFFE, M. & MURRELL, J. C. 2009. The sea-surface microlayer is a gelatinous biofilm. *The ISME Journal,* 3**,** 1001-1003.

CUNLIFFE, M., SALTER, M., MANN, P. J., WHITELEY, A. S., UPSTILL-GODDARD, R. C. & MURRELL, J. C. 2009. Dissolved organic carbon and bacterial populations in the gelatinous surface microlayer of a Norwegian fjord mesocosm. *FEMS Microbiology Letters,* 299**,** 248-254.

CUNLIFFE, M., SCHAFER, H., HARRISON, E., CLEAVE, S., UPSTILL-GODDARD, R. & MURRELL, J. C. 2008. Phylogenetic and functional gene analysis of the bacterial and archaeal communities associated with the surface microlayer of an estuary. *The ISME Journal,* 2**,** 776-789.

CUNLIFFE, M., UPSTILL-GODDARD, R. C. & MURRELL, J. C. 2011. Microbiology of aquatic surface microlayers. *FEMS Microbiol Rev,* 35**,** 233-246.

CUNLIFFE, M. & WURL, O. 2014. Guide to best practices to study the ocean's surface. Plymouth, UK: Occasional Publications of the Marine Biological Association of the United Kingdom, Plymouth, UK. 118 pp.

DE LA HABA, R. R., ARAHAL, D. R., SÁNCHEZ-PORRO, C. & VENTOSA, A. 2014. The family *Halomonadaceae*. *In:* ROSENBERG, E., DELONG, E. F., LORY, S., STACKEBRANDT, E. & THOMPSON, F. (eds.) *The prokaryotes: Gammaproteobacteria*. Berlin, Heidelberg: Springer Berlin Heidelberg.

DEL GIORGIO, P. A. & SCARBOROUGH, G. 1995. Increase in the proportion of metabolically active bacteria along gradients of enrichment in freshwater and marine plankton: implications for estimates of bacterial growth and production rates. *Journal of Plankton Research,* 17**,** 1905-1924.

DELONG, E. F. & PACE, N. R. 2001. Environmental diversity of bacteria and archaea. *Systems Biology,* 50**,** 470-478.

DELONG, E. F., PRESTON, C. M., MINCER, T., RICH, V., HALLAM, S. J., FRIGAARD, N. U., MARTINEZ, A., SULLIVAN, M. B., EDWARDS, R., BRITO, B. R., CHISHOLM, S. W. & KARL, D. M. 2006. Community genomics among stratified microbial assemblages in the ocean's interior. *Science,* 311**,** 496-503.

DENMAN, K.L., G. BRASSEUR, A. CHIDTHAISONG, P. CIAIS, P.M. COX, R.E. DICKINSON, D. HAUGLUSTAINE, C. HEINZE, E. HOLLAND, D. JACOB, U. LOHMANN, S RAMACHANDRAN, P.L. DA SILVA DIAS, S.C. WOFSY AND X. ZHANG. 2007: *Couplings between Changes in the Climate System and Biogeochemistry. In:* SOLOMON, S., D. QIN, M. MANNING, Z. CHEN, M. MARQUIS, K.B. AVERYT, M.TIGNOR AND H.L. MILLER (eds.). *Climate Change 2007: The physical science basis. contribution of working group I to the*

fourth assessment report of the Intergovernmental Panel on Climate Change. Cambridge University Press, Cambridge, United Kingdom and New York, NY, USA.

DIXON, J. L., SARGEANT, S., NIGHTINGALE, P. D. & COLIN MURRELL, J. 2013. Gradients in microbial methanol uptake: productive coastal upwelling waters to oligotrophic gyres in the Atlantic Ocean. *The ISME Journal,* 7**,** 568-580.

DONEY, S. C., ABBOTT, M. R., CULLEN, J. J., KARL, D. M. & ROTHSTEIN, L. 2004. From genes to ecosystems: the ocean's new frontier. *Frontiers in Ecology and the Environment,* 2**,** 457-468.

DUCE, R. A., LISS, P. S., MERRILL, J. T., ATLAS, E. L., BUAT-MENARD, P., HICKS, B. B., MILLER, J. M., PROSPERO, J. M., ARIMOTO, R., CHURCH, T. M., ELLIS, W., GALLOWAY, J. N., HANSEN, L., JICKELLS, T. D., KNAP, A. H., REINHARDT, K. H., SCHNEIDER, B., SOUDINE, A., TOKOS, J. J., TSUNOGAI, S., WOLLAST, R. & ZHOU, M. 1991. The atmospheric input of trace species to the world ocean. *Global Biogeochemical Cycles,* 5**,** 193-259.

DUCKLOW, H. 2000. Bacterial production and biomass in the oceans. *Microbial ecology of the oceans,* Wiley-Liss inc, New Jersey, 85-120.

DUHAMEL, S., MOUTIN, T., VAN WAMBEKE, F., VAN MOOY, B., RIMMELIN, P., RAIMBAULT, P. & CLAUSTRE, H. 2007. Growth and specific P-uptake rates of bacterial and phytoplanktonic communities in the Southeast Pacific (BIOSOPE cruise). *Biogeosciences,* European Geosciences Union, 2007, 4**,** 941-956.

EBLING, A. M. & LANDING, W. M. 2015. Sampling and analysis of the sea surface microlayer for dissolved and particulate trace elements. *Marine Chemistry,* 177**,** 134-142.

EBLING, A. M. & LANDING, W. M. 2017. Trace elements in the sea surface microlayer: rapid responses to changes in aerosol deposition. *Elementa: Science of the Anthropocene,* 5, 10.1525/elementa.237.

EDGAR, R. C. 2004. MUSCLE: multiple sequence alignment with high accuracy and high throughput. *Nucleic Acids Research,* 32**,** 1792-1797.

EDGAR, R. C. 2010. Search and clustering orders of magnitude faster than BLAST. *Bioinformatics,* 26**,** 2460-2461.

EDSON, J. B., JAMPANA, V., WELLER, R. A., BIGORRE, S. P., PLUEDDEMANN, A. J., FAIRALL, C. W., MILLER, S. D., MAHRT, L., VICKERS, D. & HERSBACH,

H. 2013. On the exchange of momentum over the open ocean. *Journal of Physical Oceanography,* 43**,** 1589-1610.

EILER, A. 2006. Evidence for the ubiquity of mixotrophic bacteria in the upper ocean: implications and consequences. *Applied and Environmental Microbiology,* 72**,** 7431-7437.

ELIFANTZ, H., MALMSTROM, R. R., COTTRELL, M. T. & KIRCHMAN, D. L. 2005. Assimilation of polysaccharides and glucose by major bacterial groups in the Delaware Estuary. *Applied and Environmental Microbiology,* 71**,** 7799-7805.

ELOIRE, D., SOMERFIELD, P. J., CONWAY, D. V., HALSBAND-LENK, C., HARRIS, R. & BONNET, D. 2010. Temporal variability and community composition of zooplankton at station L4 in the Western Channel: 20 years of sampling. *Journal of Plankton Research,* 32**,** 657-679.

ENGEL, A., BANGE, H. W., CUNLIFFE, M., BURROWS, S. M., FRIEDRICHS, G., GALGANI, L., HERRMANN, H., HERTKORN, N., JOHNSON, M., LISS, P. S., QUINN, P. K., SCHARTAU, M., SOLOVIEV, A., STOLLE, C., UPSTILL-GODDARD, R. C., VAN PINXTEREN, M. & ZÄNCKER, B. 2017. The ocean's vital skin: toward an integrated understanding of the sea surface microlayer. *Frontiers in Marine Science,* 4, fmars.2017.00165.

ENGEL, A. & GALGANI, L. 2016. The organic sea-surface microlayer in the upwelling region off the coast of Peru and potential implications for air–sea exchange processes. *Biogeosciences,* 13**,** 989-1007.

FALKOWSKI, P. G., BARBER, R. T. & SMETACEK, V. 1998. Biogeochemical controls and feedbacks on ocean primary production. *Science,* 281**,** 200-206.

FASHAM, M. J., BOYD, P. W. & SAVIDGE, G. 1999. Modeling the relative contributions of autotrophs and heterotrophs to carbon flow at a Lagrangian JGOFS station in the Northeast Atlantic: the importance of DOC. *Limnology and Oceanography,* 44**,** 80-94.

FENCHEL, T. & FINLAY, B. J. 2004. The ubiquity of small species: patterns of local and global diversity. *BioScience,* 54**,** 777-784.

FENG, B.-W., LI, X.-R., WANG, J.-H., HU, Z.-Y., MENG, H., XIANG, L.-Y. & QUAN, Z.-X. 2009. Bacterial diversity of water and sediment in the Changjiang estuary and coastal area of the East China Sea. *FEMS Microbiology Ecology,* 70**,** 236-248.

FIELD, C. B., BEHRENFELD, M. J., RANDERSON, J. T. & FALKOWSKI, P. 1998. Primary production of the biosphere: integrating terrestrial and oceanic components. *Science,* 281**,** 237-240.

FIELD, K. G., GORDON, D., WRIGHT, T., RAPPE, M., URBACK, E., VERGIN, K. & GIOVANNONI, S. J. 1997. Diversity and depth-specific distribution of SAR11 cluster rRNA genes from marine planktonic bacteria. *Applied and Environmental Microbiology,* 63**,** 63-70.

FLOMBAUM, P., GALLEGOS, J. L., GORDILLO, R. A., RINCON, J., ZABALA, L. L., JIAO, N., KARL, D. M., LI, W. K., LOMAS, M. W., VENEZIANO, D., VERA, C. S., VRUGT, J. A. & MARTINY, A. C. 2013. Present and future global distributions of the marine *Cyanobacteria Prochlorococcus* and *Synechococcus*. *Proceedings of the National Academy of Sciences of the United States of America,* 110**,** 9824-9829.

FRANKIGNOULLE, M. & BORGES, A. V. 2001. European continental shelf as a significant sink for atmospheric carbon dioxide. *Global Biogeochemical Cycles,* 15**,** 569-576.

FRANKLIN, M. P., MCDONALD, I. R., BOURNE, D. G., OWENS, N. J., UPSTILL-GODDARD, R. C. & MURRELL, J. C. 2005. Bacterial diversity in the bacterioneuston (sea surface microlayer): the bacterioneuston through the looking glass. *Environmental Microbiology,* 7**,** 723-736.

FRIAS-LOPEZ, J., SHI, Y., TYSON, G. W., COLEMAN, M. L., SCHUSTER, S. C., CHISHOLM, S. W. & DELONG, E. F. 2008. Microbial community gene expression in ocean surface waters. *Proceedings of the National Academy of Sciences of the United States of America,* 105**,** 3805-3810.

FUHRMAN, J. A. 2009. Microbial community structure and its functional implications. *Nature,* 459**,** 193-199.

FUHRMAN, J. A. & AZAM, F. 1982. Thymidine incorporation as a measure of heterotrophic bacterioplankton production in marine surface waters: Evaluation and field results. *Marine Biology,* 66**,** 109-120.

FUHRMAN, J. A., CRAM, J. A. & NEEDHAM, D. M. 2015. Marine microbial community dynamics and their ecological interpretation. *Nature Reviews Microbiology,* 13**,** 133-146.

FUHRMAN, J. A., HEWSON, I., SCHWALBACH, M. S., STEELE, J. A., BROWN, M. V. & NAEEM, S. 2006. Annually reoccurring bacterial communities are predictable

from ocean conditions. *Proceedings of the National Academy of Sciences of the United States of America,* 103**,** 13104-13109.

FUHRMAN, J. A., STEELE, J. A., HEWSON, I., SCHWALBACH, M. S., BROWN, M. V., GREEN, J. L. & BROWN, J. H. 2008. A latitudinal diversity gradient in planktonic marine bacteria. *Proceedings of the National Academy of Sciences,* 105**,** 7774-7778.

GASOL, J. M., DOVAL, M. D., PINHASSI, J., CALDER, XF, N-PAZ, J. I., GUIXA-BOIXAREU, N., XFA, RIA, VAQU, XE, DOLORS, PEDR, XF, S, A., XF & CARLOS 1998. Diel variations in bacterial heterotrophic activity and growth in the northwestern Mediterranean Sea. *Marine Ecology Progress Series,* 164**,** 107-124.

GHIGLIONE, J. F. & MURRAY, A. E. 2012. Pronounced summer to winter differences and higher wintertime richness in coastal Antarctic marine bacterioplankton. *Environmental Microbiology,* 14**,** 617-629.

GIBBONS, S. M., CAPORASO, J. G., PIRRUNG, M., FIELD, D., KNIGHT, R. & GILBERT, J. A. 2013. Evidence for a persistent microbial seed bank throughout the global ocean. *Proceedings of the National Academy of Sciences of the United States of America,* 110**,** 4651-4655.

GILBERT, J. A., FIELD, D., SWIFT, P., NEWBOLD, L., OLIVER, A., SMYTH, T., SOMERFIELD, P. J., HUSE, S. & JOINT, I. 2009. The seasonal structure of microbial communities in the Western English Channel. *Environmental Microbiology,* 11**,** 3132-3139.

GILBERT, J. A., FIELD, D., SWIFT, P., THOMAS, S., CUMMINGS, D., TEMPERTON, B., WEYNBERG, K., HUSE, S., HUGHES, M., JOINT, I., SOMERFIELD, P. J. & MUHLING, M. 2010a. The taxonomic and functional diversity of microbes at a temperate coastal site: a 'multi-omic' study of seasonal and diel temporal variation. *PLoS One,* 5**,** e15545.

GILBERT, J. A., MEYER, F., SCHRIML, L., JOINT, I. R., MÜHLING, M. & FIELD, D. 2010b. Metagenomes and metatranscriptomes from the L4 long-term coastal monitoring station in the Western English Channel. *Standards in Genomic Sciences,* 3**,** 183-193.

GILBERT, J. A., STEELE, J. A., CAPORASO, J. G., STEINBRUCK, L., REEDER, J., TEMPERTON, B., HUSE, S., MCHARDY, A. C., KNIGHT, R., JOINT, I., SOMERFIELD, P., FUHRMAN, J. A. & FIELD, D. 2012. Defining seasonal marine microbial community dynamics. *The ISME Journal,* 6**,** 298-308.

GIOVANNONI, S. J. 2017. SAR11 Bacteria: The Most Abundant Plankton in the Oceans. *Annual Review of Marine Science,* 9**,** 231-255.

GIOVANNONI, S. J., RAPPÉ, M. S., VERGIN, K. L. & ADAIR, N. L. 1996. 16S rRNA genes reveal stratified open ocean bacterioplankton populations related to the Green Non-Sulfur bacteria. *Proceedings of the National Academy of Sciences of the United States of America,* 93**,** 7979-7984.

GIOVANNONI, S. J. & STINGL, U. 2005. Molecular diversity and ecology of microbial plankton. *Nature,* 437**,** 343-348.

GIOVANNONI, S. J., TRIPP, H. J., GIVAN, S., PODAR, M., VERGIN, K. L., BAPTISTA, D., BIBBS, L., EADS, J., RICHARDSON, T. H., NOORDEWIER, M., RAPPE, M. S., SHORT, J. M., CARRINGTON, J. C. & MATHUR, E. J. 2005. Genome streamlining in a cosmopolitan oceanic bacterium. *Science,* 309**,** 1242-1245.

GIOVANNONI, S. J. & VERGIN, K. L. 2012. Seasonality in ocean microbial communities. *Science,* 335**,** 671-676.

GOHL, D. M., VANGAY, P., GARBE, J., MACLEAN, A., HAUGE, A., BECKER, A., GOULD, T. J., CLAYTON, J. B., JOHNSON, T. J., HUNTER, R., KNIGHTS, D. & BECKMAN, K. B. 2016. Systematic improvement of amplicon marker gene methods for increased accuracy in microbiome studies. *Nature Biotechnology,* 34**,** 942-949.

GREEN, J. & BOHANNAN, B. J. M. 2006. Spatial scaling of microbial biodiversity. *Trends in Ecology & Evolution,* 21**,** 501-507.

HAGGERTY, J. M. & DINSDALE, E. A. 2017. Distinct biogeographical patterns of marine bacterial taxonomy and functional genes. *Global Ecology and Biogeography,* 26**,** 177-190.

HAGSTRÖM, A., AZAM, F., ANDERSSON, A., WIKNER, J. & RASSOULZADEGAN, F. 1988. Microbial loop in an oligotrophic pelagic marine ecosystem: possible roles of *cyanobacteria* and nanoflagellates in the organic fluxes. *Marine ecology progress series,* 49**,** 171-178.

HAGSTRÖM, Å., PINHASSI, J. & ZWEIFEL, U. L. 2000. Biogeographical diversity among marine bacterioplankton. *Aquatic Microbial Ecology,* 21**,** 231-244.

HARRELL JR, F. E. 2016. with contributions from Charles Dupont and many others: Hmisc: Harrell Miscellaneous. R package version 3.13-0.

HARVEY, G. W. 1966. Microlayer collection from the sea surface: a new method and initial results. *Limnology and Oceanography,* 11**,** 608-613.

HERNDL, G. J., MÜLLER-NIKLAS, G. & FRICK, J. 1993. Major role of ultraviolet-B in controlling bacterioplankton growth in the surface layer of the ocean. *Nature,* 361**,** 717-719.

HIGHFIELD, J. M., ELOIRE, D., CONWAY, D. V. P., LINDEQUE, P. K., ATTRILL, M. J. & SOMERFIELD, P. J. 2010. Seasonal dynamics of meroplankton assemblages at station L4. *Journal of Plankton Research,* 32**,** 681-691.

HILL, P. G., ZUBKOV, M. V. & PURDIE, D. A. 2010. Differential responses of Prochlorococcus and SAR11-dominated bacterioplankton groups to atmospheric dust inputs in the tropical Northeast Atlantic Ocean. *FEMS Microbiology Letters,* 306**,** 82-89.

HOAGLAND, K. D., ROSOWSKI, J. R., GRETZ, M. R. & ROEMER, S. C. 1993. Diatom extracellular polymeric substances: function, fine structure, chemistry and physiology. *Journal of Phycology,* 29**,** 537-566.

HOLMSTROM, C. & KJELLEBERG, S. 1999. Marine *Pseudoalteromonas* species are associated with higher organisms and produce biologically active extracellular agents. *FEMS Microbiology Ecology,* 30**,** 285-293.

HORNER-DEVINE, C. M., LEIBOLD, M. A., SMITH, V. H. & BOHANNAN, B. J. M. 2003. Bacterial diversity patterns along a gradient of primary productivity. *Ecology Letters,* 6**,** 613-622.

HÖRNLEIN, C., CONFURIUS-GUNS, V., STAL, L. J. & BOLHUIS, H. 2018. Daily rhythmicity in coastal microbial mats. *npj Biofilms and Microbiomes,* 4**,** 10.1038/s41522-018-0054-5.

HUNT, D. E., LIN, Y., CHURCH, M. J., KARL, D. M., TRINGE, S. G., IZZO, L. K. & JOHNSON, Z. I. 2013. Relationship between abundance and specific activity of bacterioplankton in open ocean surface waters. *Applied and Environmental Microbiology,* 79**,** 177-184.

HUNTER, K. A. 1980. Processes affecting particulate trace metals in the sea surface microlayer. *Marine Chemistry,* 9**,** 49-70.

HUSON, D. H. & SCORNAVACCA, C. 2012. Dendroscope 3: an interactive tool for rooted phylogenetic trees and networks. *Systems Biology,* 61**,** 1061-1067.

IRIGOIEN, X., FLYNN, K. J. & HARRIS, R. P. 2005. Phytoplankton blooms: a 'loophole' in microzooplankton grazing impact? *Journal of Plankton Research,* 27**,** 313-321.

IRIGOIEN, X., HARRIS, R. P., HEAD, R. N. & HARBOUR, D. 2000. North Atlantic Oscillation and spring bloom phytoplankton composition in the English Channel. *Journal of Plankton Research,* 22**,** 2367-2371.

IVANOVA, E. P., NG, H. J. & WEBB, H. K. 2014. The family *Pseudoalteromonadaceae*. *In:* ROSENBERG, E., DELONG, E. F., LORY, S., STACKEBRANDT, E. & THOMPSON, F. (eds.) *The prokaryotes: Gammaproteobacteria.* Berlin, Heidelberg: Springer Berlin Heidelberg.

IVARS-MARTINEZ, E., MARTIN-CUADRADO, A. B., D'AURIA, G., MIRA, A., FERRIERA, S., JOHNSON, J., FRIEDMAN, R. & RODRIGUEZ-VALERA, F. 2008. Comparative genomics of two ecotypes of the marine planktonic copiotroph Alteromonas macleodii suggests alternative lifestyles associated with different kinds of particulate organic matter. *The ISME Journal* , 2**,** 1194-212.

JENNINGS, M. K., PASSOW, U., WOZNIAK, A. S. & HANSELL, D. A. 2017. Distribution of transparent exopolymer particles (TEP) across an organic carbon gradient in the western North Atlantic Ocean. *Marine Chemistry,* 190**,** 1-12.

JIAO, N., HERNDL, G. J., HANSELL, D. A., BENNER, R., KATTNER, G., WILHELM, S. W., KIRCHMAN, D. L., WEINBAUER, M. G., LUO, T., CHEN, F. & AZAM, F. 2010. Microbial production of recalcitrant dissolved organic matter: long-term carbon storage in the global ocean. *Nature Reviews Microbiology,* 8**,** 593-599.

JOHNSON, C. H., ZHAO, C., XU, Y. & MORI, T. 2017. Timing the day: what makes bacterial clocks tick? *Nature Reviews Microbiology,* 15**,** 232-242.

JOHNSON, Z. I., ZINSER, E. R., COE, A., MCNULTY, N. P., WOODWARD, E. M. S. & CHISHOLM, S. W. 2006. Niche partitioning among *Prochlorococcus* ecotypes along ocean-scale environmental gradients. *Science,* 311**,** 1737-1740.

JOINT, I., MÜHLING, M. & QUERELLOU, J. 2010. Culturing marine bacteria – an essential prerequisite for biodiscovery. *Microbial biotechnology,* 3**,** 564-575.

JONES, R. D. 1991. Carbon monoxide and methane distribution and consumption in the photic zone of the Sargasso Sea. *Deep Sea Research Part A. Oceanographic Research Papers,* 38**,** 625-635.

JONES, R. D. & AMADOR, J. A. 1993. Methane and carbon monoxide production, oxidation, and turnover times in the Caribbean Sea as influenced by the Orinoco River. *Journal of Geophysical Research: Oceans,* 98**,** 2353-2359.

JOUX, F., AGOGUÉ, H., OBERNOSTERER, I., CHRISTINE, D., REINTHALER, T., HERNDL, G., J & LEBARON, P. 2006. Microbial community structure in the sea

surface microlayer at two contrasting coastal sites in the northwestern Mediterranean Sea. *Aquatic Microbial Ecology,* 42**,** 91-104.

KAHRU, M., LEPPANEN, J. M. & RUD, O. 1993. Cyanobacterial Blooms Cause Heating of the Sea-Surface. *Marine Ecology-Progress Series,* 101**,** 1-7.

KANG, B. S. & KIM, Y. M. 1999. Cloning and molecular characterization of the genes for carbon monoxide dehydrogenase and localization of molybdopterin, flavin adenine dinucleotide, and iron-sulfur centers in the enzyme of *Hydrogenophaga pseudoflava*. *J Bacteriol,* 181**,** 5581-5590.

KARL, D. M. 2002. Hidden in a sea of microbes. *Nature,* 415**,** 590-591.

KARL, D. M. 2007. Microbial oceanography: paradigms, processes and promise. *Nature Reviews Microbiology,* 5**,** 759-769.

KARL, D. M. & CHURCH, M. J. 2014. Microbial oceanography and the Hawaii Ocean Time-series programme. *Nature Reviews Microbiology,* 12**,** 699-713.

KATTNER, G. G. & BROCKMANN, U. H. 1978. Fatty-acid composition of dissolved and particulate matter in surface films. *Marine Chemistry,* 6**,** 233-241.

KIESSLING, M. & MEYER, O. 1982. Profitable oxidation of carbon monoxide or hydrogen during heterotrophic growth of Pseudomonas carboxydoflava. *FEMS Microbiology Letters,* 13**,** 333-338.

KIM, Y. J. & KIM, Y. M. 1989. Induction of carbon monoxide dehydrogenase during heterotrophic growth of *Acinetobacter sp*. strain JC1 DSM 3803 in the presence of carbon monoxide. *FEMS Microbiology Letters,* 59**,** 207-210.

KING, G. M. 2003. Molecular and culture-based analyses of aerobic carbon monoxide oxidizer diversity. *Applied and Environmental Microbiology,* 69**,** 7257-7265.

KING, G. M. & WEBER, C. F. 2007. Distribution, diversity and ecology of aerobic CO-oxidizing bacteria. *Nature Reviews Microbiology,* 5**,** 107-118.

KIRKWOOD, D. S. 1989. Simultaneous determination of selected nutrients in seawater. International Council for the Exploration of the Sea (ICES)**,** CM1989/C:29.

KLAPPENBACH, J. A., DUNBAR, J. M. & SCHMIDT, T. M. 2000. rRNA operon copy number reflects ecological strategies of bacteria. *Applied and Environmental Microbiology,* 66**,** 1328-1333.

KLINDWORTH, A., MANN, A. J., HUANG, S., WICHELS, A., QUAST, C., WALDMANN, J., TEELING, H. & GLÖCKNER, F. O. 2014. Diversity and activity of marine bacterioplankton during a diatom bloom in the North Sea assessed by total RNA and pyrotag sequencing. *Marine Genomics,* 18, Part B**,** 185-192.

KOCH, A. L. 2001. Oligotrophs versus copiotrophs. *Bioessays,* 23**,** 657-661.

KOCH, B. P., WITT, M., ENGBRODT, R., DITTMAR, T. & KATTNER, G. 2005. Molecular formulae of marine and terrigenous dissolved organic matter detected by electrospray ionization Fourier transform ion cyclotron resonance mass spectrometry. *Geochimica et Cosmochimica Acta,* 69**,** 3299-3308.

KRAUSE, S., LE ROUX, X., NIKLAUS, P. A., VAN BODEGOM, P. M., LENNON, J. T., BERTILSSON, S., GROSSART, H.-P., PHILIPPOT, L. & BODELIER, P. L. E. 2014. Trait-based approaches for understanding microbial biodiversity and ecosystem functioning. *Frontiers in Microbiology,* 5**,** fmicb.2014.00251.

KRÜGER, B. & MEYER, O. 1984. Thermophilic *Bacilli* growing with carbon monoxide. *Archives of Microbiology,* 139**,** 402-408.

LAANE, R. W. P. M., SOUTHWARD, A. J., SLINN, D. J., ALLEN, J., GROENEVELD, G. & DE VRIES, A. 1996. Changes and causes of variability in salinity and dissolved inorganic phosphate in the Irish Sea, English Channel, and Dutch coastal zone. *ICES Journal of Marine Science,* 53**,** 933-944.

LAGHDASS, M., CATALA, P., CAPARROS, J., ORIOL, L., LEBARON, P. & OBERNOSTERER, I. 2012. High contribution of SAR11 to microbial activity in the north west Mediterranean Sea. *Microbial ecology,* 63**,** 324-333.

LAMI, R., GHIGLIONE, J. F., DESDEVISES, Y., WEST, N. J. & LEBARON, P. 2009. Annual patterns of presence and activity of marine bacteria monitored by 16S rDNA–16S rRNA fingerprints in the coastal NW Mediterranean Sea. *Aquatic Microbial Ecology,* 54**,** 199-210.

LANE, D. 1991. *16S/23S rRNA sequencing,* New York, NY, John Wiley and Sons.

LANGLOIS, R. J., MILLS, M. M., RIDAME, C., CROOT, P. & LAROCHE, J. 2012. Diazotrophic bacteria respond to Saharan dust additions. *Marine Ecology Progress Series,* 470**,** 1-14.

LAROCHE, J. & BREITBARTH, E. 2005. Importance of the diazotrophs as a source of new nitrogen in the ocean. *Journal of Sea Research,* 53**,** 67-91.

LECHTENFELD, O. J., HERTKORN, N., SHEN, Y., WITT, M. & BENNER, R. 2015. Marine sequestration of carbon in bacterial metabolites. *Nature Communications,* 6**,** ncomms7711.

LEE, C. & BADA, J. L. 1977. Dissolved amino acids in the equatorial Pacific, the Sargasso Sea, and Biscayne Bay1. *Limnology and Oceanography,* 22**,** 502-510.

LEKUNBERRI, I., LEFORT, T., ROMERO, E., VÁZQUEZ-DOMÍNGUEZ, E., ROMERA-CASTILLO, C., MARRASÉ, C., PETERS, F., WEINBAUER, M. & GASOL, J. M. 2010. Effects of a dust deposition event on coastal marine microbial abundance and activity, bacterial community structure and ecosystem function. *Journal of Plankton Research,* 32**,** 381-396.

LILLEY, M. D., DE ANGELIS, M. A. & GORDON, L. I. 1982. CH_4, H_2, CO and N_2O in submarine hydrothermal vent waters. *Nature,* 300**,** 48-50.

LINDH, M. V., SJOSTEDT, J., ANDERSSON, A. F., BALTAR, F., HUGERTH, L. W., LUNDIN, D., MUTHUSAMY, S., LEGRAND, C. & PINHASSI, J. 2015. Disentangling seasonal bacterioplankton population dynamics by high-frequency sampling. *Environmental Microbiology,* 17**,** 2459-2476.

LIVAK, K. J. & SCHMITTGEN, T. D. 2001. Analysis of relative gene expression data using real-time quantitative PCR and the $2^{-\Delta\Delta CT}$ method. *Methods,* 25**,** 402-408.

LLABRÉS, M. & AGUSTÍ, S. 2006. Picophytoplankton cell death induced by UV radiation: evidence for oceanic Atlantic communities. *Limnology and Oceanography,* 51**,** 21-29.

LOCHTE, K. & TURLEY, C. M. 1988. Bacteria and *cyanobacteria* associated with phytodetritus in the deep sea. *Nature,* 333**,** 67-69.

LONG, R. A. & AZAM, F. 2001. Antagonistic interactions among marine pelagic bacteria. *Applied and Environmental Microbiology,* 67**,** 4975-4983.

LONGHURST, A., SATHYENDRANATH, S., PLATT, T. & CAVERHILL, C. 1995. An estimate of global primary production in the ocean from satellite radiometer data. *Journal of Plankton Research,* 17**,** 1245-1271.

LÓPEZ-PÉREZ, M. & RODRIGUEZ-VALERA, F. 2014. The family *Alteromonadaceae*. *In:* ROSENBERG, E., DELONG, E. F., LORY, S., STACKEBRANDT, E. & THOMPSON, F. (eds.) *The prokaryotes: Gammaproteobacteria.* Berlin, Heidelberg: Springer Berlin Heidelberg.

LOZA-CORREA, M., GOMEZ-VALERO, L. & BUCHRIESER, C. 2010. Circadian clock proteins in prokaryotes: hidden rhythms? *Frontiers in Microbiology,* 1**,** fmicb.2010.00130.

LOZUPONE, C. & KNIGHT, R. 2005. UniFrac: a new phylogenetic method for comparing microbial communities. *Applied and Environmental Microbiology,* 71**,** 8228-8235.

MAHOWALD, N. M., HAMILTON, D. S., MACKEY, K. R. M., MOORE, J. K., BAKER, A. R., SCANZA, R. A. & ZHANG, Y. 2018. Aerosol trace metal leaching and

impacts on marine microorganisms. *Nature Communications,* 9**,** s41467-018-04970-7.

MALMSTROM, R. R., COTTRELL, M. T., ELIFANTZ, H. & KIRCHMAN, D. L. 2005. Biomass production and assimilation of dissolved organic matter by SAR11 bacteria in the Northwest Atlantic Ocean. *Applied and Environmental Microbiology,* 71**,** 2979-2986.

MALMSTROM, R. R., KIENE, R. P., COTTRELL, M. T. & KIRCHMAN, D. L. 2004. Contribution of SAR11 bacteria to dissolved dimethylsulfoniopropionate and amino acid uptake in the North Atlantic Ocean. *Applied and Environmental Microbiology,* 70**,** 4129-4135.

MARIZCURRENA, J. J., MOREL, M. A., BRANA, V., MORALES, D., MARTINEZ-LOPEZ, W. & CASTRO-SOWINSKI, S. 2017. Searching for novel photolyases in UVC-resistant Antarctic bacteria. *Extremophiles,* 21**,** 409-418.

MARTIN-PLATERO, A. M., CLEARY, B., KAUFFMAN, K., PREHEIM, S. P., MCGILLICUDDY, D. J., ALM, E. J. & POLZ, M. F. 2018. High resolution time series reveals cohesive but short-lived communities in coastal plankton. *Nature Communications,* 9**,** s41467-017-02571-4.

MARTINY, J. B. H., BOHANNAN, B. J. M., BROWN, J. H., COLWELL, R. K., FUHRMAN, J. A., GREEN, J. L., HORNER-DEVINE, M. C., KANE, M., KRUMINS, J. A., KUSKE, C. R., MORIN, P. J., NAEEM, S., ØVREÅS, L., REYSENBACH, A.-L., SMITH, V. H. & STALEY, J. T. 2006. Microbial biogeography: putting microorganisms on the map. *Nature Reviews Microbiology,* 4**,** 102-112.

MARY, I., CUMMINGS, D., BIEGALA, I., BURKILL, P., ARCHER, S. & ZUBKOV, M. 2006a. Seasonal dynamics of bacterioplankton community structure at a coastal station in the western English Channel. *Aquatic Microbial Ecology,* 42**,** 119-126.

MARY, I., HEYWOOD, J., FUCHS, B., AMANN, R., TARRAN, G., BURKILL, P. & ZUBKOV, M. 2006b. SAR11 dominance among metabolically active low nucleic acid bacterioplankton in surface waters along an Atlantic meridional transect. *Aquatic Microbial Ecology,* 45**,** 107-113.

MCDONALD, D., CLEMENTE, J. C., KUCZYNSKI, J., RIDEOUT, J. R., STOMBAUGH, J., WENDEL, D., WILKE, A., HUSE, S., HUFNAGLE, J. & MEYER, F. 2012. The Biological Observation Matrix (BIOM) format or: how I learned to stop worrying and love the ome-ome. *GigaScience,* 1**,** 2047-217X-1-7.

MELLA-FLORES, D., SIX, C., RATIN, M., PARTENSKY, F., BOUTTE, C., LE CORGUILLE, G., MARIE, D., BLOT, N., GOURVIL, P., KOLOWRAT, C. & GARCZAREK, L. 2012. *Prochlorococcus* and *Synechococcus* have evolved different adaptive mechanisms to cope with light and UV stress. *Frontiers in Microbiology,* 3**,** fmicb.2012.00285.

MEYER, O. 1989. Aerobic carbon monoxide-oxidizing Bacteria. *In:* SCHLEGEL, H., G & BOWIEN, B. (eds.) *Autotrophic Bacteria* Madison, WI: Springer Verlag.

MEYER, O., FRUNKE, K. & MORSDORF, G. 1993. Biochemistry of the aerobic utilization of carbon monoxide. *In:* MURRELL, J. C. & KELLY, D. P. (eds.) *Microbial growth on C_1 compounds.* Andover: Intercept.

MEYER, O. & SCHLEGEL, H. G. 1978. Reisolation of the carbon monoxide utilizing hydrogen bacterium *Pseudomonas carboxydovorans* (Kistner) comb. nov. *Archives of Microbiology,* 118**,** 35-43.

MEYER, O. & SCHLEGEL, H. G. 1983. Biology of aerobic carbon monoxide-oxidizing bacteria. *Annual Review of Microbiology,* 37**,** 277-310.

MILICI, M., TOMASCH, J., WOS-OXLEY, M. L., DECELLE, J., JÁUREGUI, R., WANG, H., DENG, Z.-L., PLUMEIER, I., GIEBEL, H.-A., BADEWIEN, T. H., WURST, M., PIEPER, D. H., SIMON, M. & WAGNER-DÖBLER, I. 2016. Bacterioplankton biogeography of the Atlantic Ocean: a case study of the distance-decay relationship. *Frontiers in Microbiology,* 7**,** fmicb.2016.00590.

MILLER, W. L. & ZEPP, R. G. 1995. Photochemical production of dissolved inorganic carbon from terrestrial organic matter: significance to the oceanic organic carbon cycle. *Geophysical Research Letters,* 22**,** 417-420.

MILNE, A., LANDING, W., BIZIMIS, M. & MORTON, P. 2010. Determination of Mn, Fe, Co, Ni, Cu, Zn, Cd and Pb in seawater using high resolution magnetic sector inductively coupled mass spectrometry (HR-ICP-MS). *Analytica chimica acta,* 665**,** 200-207.

MONOD, J. 1978. The growth of bacterial cultures. *Selected Papers in Molecular Biology by Jacques Monod.* Academic Press.

MOPPER, K. & LINDROTH, P. 1982. Diel and depth variations in dissolved free amino acids and ammonium in the Baltic Sea determined by shipboard HPLC analysis1. *Limnology and Oceanography,* 27**,** 336-347.

MORAN, M. A. 2015. The global ocean microbiome. *Science,* 350**,** aac8455.

MORAN, M. A., BELAS, R., SCHELL, M. A., GONZALEZ, J. M., SUN, F., SUN, S., BINDER, B. J., EDMONDS, J., YE, W., ORCUTT, B., HOWARD, E. C., MEILE, C., PALEFSKY, W., GOESMANN, A., REN, Q., PAULSEN, I., ULRICH, L. E., THOMPSON, L. S., SAUNDERS, E. & BUCHAN, A. 2007. Ecological genomics of marine Roseobacters. *Applied and Environmental Microbiology,* 73**,** 4559-4569.

MORAN, M. A., BUCHAN, A., GONZALEZ, J. M., HEIDELBERG, J. F., WHITMAN, W. B., KIENE, R. P., HENRIKSEN, J. R., KING, G. M., BELAS, R., FUQUA, C., BRINKAC, L., LEWIS, M., JOHRI, S., WEAVER, B., PAI, G., EISEN, J. A., RAHE, E., SHELDON, W. M., YE, W., MILLER, T. R., CARLTON, J., RASKO, D. A., PAULSEN, I. T., REN, Q., DAUGHERTY, S. C., DEBOY, R. T., DODSON, R. J., DURKIN, A. S., MADUPU, R., NELSON, W. C., SULLIVAN, S. A., ROSOVITZ, M. J., HAFT, D. H., SELENGUT, J. & WARD, N. 2004. Genome sequence of Silicibacter pomeroyi reveals adaptations to the marine environment. *Nature,* 432**,** 910-913.

MORAN, M. A. & MILLER, W. L. 2007. Resourceful heterotrophs make the most of light in the coastal ocean. *Nature Reviews Microbiology,* 5**,** 792-800.

MORAN, M. A. & ZEPP, R. G. 1997. Role of photoreactions in the formation of biologically labile compounds from dissolved organic matter. *Limnology and Oceanography,* 42**,** 1307-1316.

MOREL, A. & BERTHON, J.-F. 1989. Surface pigments, algal biomass profiles, and potential production of the euphotic layer: relationships reinvestigated in view of remote-sensing applications. *Limnology and Oceanography,* 34**,** 1545-1562.

MORTON, P. L., LANDING, W. M., HSU, S.-C., MILNE, A., AGUILAR-ISLAS, A. M., BAKER, A. R., BOWIE, A. R., BUCK, C. S., GAO, Y., GICHUKI, S., HASTINGS, M. G., HATTA, M., JOHANSEN, A. M., LOSNO, R., MEAD, C., PATEY, M. D., SWARR, G., VANDERMARK, A. & ZAMORA, L. M. 2013. Methods for the sampling and analysis of marine aerosols: results from the 2008 GEOTRACES aerosol intercalibration experiment. *Limnology and Oceanography: Methods,* 11**,** 62-78.

MOU, X., SUN, S., EDWARDS, R. A., HODSON, R. E. & MORAN, M. A. 2008. Bacterial carbon processing by generalist species in the coastal ocean. *Nature,* 451**,** 708-711.

MÜLLER-NIKLAS, G., HEISSENBERGER, A., PUSKARIC, S. & HERNDL, G. J. 1995. Ultraviolet-B radiation and bacterial metabolism in coastal waters. *Aquatic Microbial Ecology,* 9**,** 111-116.

MYKLESTAD, S. M. 1995. Release of extracellular products by phytoplankton with special emphasis on polysaccharides. *Science of The Total Environment,* 165**,** 155-164.

NAUMANN, E. 1917. Beitrage zur Kenntnis des Teichnannoplanktons. II. *Uber das Neuston das Susswassers*.

NELSON, C. E. & CARLSON, C. A. 2012. Tracking differential incorporation of dissolved organic carbon types among diverse lineages of Sargasso Sea bacterioplankton. *Environmental Microbiology,* 14**,** 1500-1516.

NEWTON, R. J., GRIFFIN, L. E., BOWLES, K. M., MEILE, C., GIFFORD, S., GIVENS, C. E., HOWARD, E. C., KING, E., OAKLEY, C. A., REISCH, C. R., RINTA-KANTO, J. M., SHARMA, S., SUN, S., VARALJAY, V., VILA-COSTA, M., WESTRICH, J. R. & MORAN, M. A. 2010. Genome characteristics of a generalist marine bacterial lineage. *The ISME Journal,* 4**,** 784-798.

OBERNOSTERER, I., CATALA, P., REINTHALER, T., HERNDL, G. J. & LEBARON, P. 2005. Enhanced heterotrophic activity in the surface microlayer of the Mediterranean Sea. *Aquatic Microbial Ecology,* 39**,** 293-302.

OBERNOSTERER, I., PIET, R. & J., H. G. 2001. Spatial and diurnal dynamics of dissolved organic matter (DOM) fluorescence and H_2O_2 and the photochemical oxygen demand of surface water DOM across the subtropical Atlantic Ocean. *Limnology and Oceanography,* 46**,** 632-643.

OKSANEN, J., BLANCHET, F. G., KINDT, R., LEGENDRE, P., MINCHIN, P. R., O'HARA, R., SIMPSON, G. L., SOLYMOS, P., STEVENS, M. H. H. & WAGNER, H. 2013. Package 'vegan'. *Community ecology package, version,* 2.

ORTEGA-RETUERTA, E., RECHE, I., PULIDO-VILLENA, E., AGUSTÍ, S. & DUARTE, C. M. 2008. Exploring the relationship between active bacterioplankton and phytoplankton in the Southern Ocean. *Aquatic Microbial Ecology,* 52**,** 99-106.

OTTESEN, E. A., YOUNG, C. R., GIFFORD, S. M., EPPLEY, J. M., MARIN, R., SCHUSTER, S. C., SCHOLIN, C. A. & DELONG, E. F. 2014. Multispecies diel transcriptional oscillations in open ocean heterotrophic bacterial assemblages. *Science,* 345**,** 207-212.

PALLERONI, N. J. 1981. Introduction to the family *Pseudomonadaceae*. *In:* STARR, M. P., STOLP, H., TRÜPER, H. G., BALOWS, A. & SCHLEGEL, H. G. (eds.) *The prokaryotes: A handbook on habitats, isolation, and identification of bacteria.* Berlin, Heidelberg: Springer Berlin Heidelberg.

PARKS, D. H., CHUVOCHINA, M., WAITE, D. W., RINKE, C., SKARSHEWSKI, A., CHAUMEIL, P.-A. & HUGENHOLTZ, P. 2018. A standardized bacterial taxonomy based on genome phylogeny substantially revises the tree of life. *Nature Biotechnology, 36***,** 996-1004.

PARTENSKY, F., HESS, W. R. & VAULOT, D. 1999. *Prochlorococcus*, a marine photosynthetic prokaryote of global significance. *Microbiol Mol Biol Rev,* 63**,** 106-127.

PAYTAN, A. & MCLAUGHLIN, K. 2007. The oceanic phosphorus cycle. *Chemical Reviews,* 107**,** 563-576.

PEDLER, B. E., ALUWIHARE, L. I. & AZAM, F. 2014. Single bacterial strain capable of significant contribution to carbon cycling in the surface ocean. *Proceedings of the National Academy of Sciences of the United States of America,* 111**,** 7202-7207.

PEDROS-ALIO, C. 2006. Marine microbial diversity: can it be determined? *Trends Microbiol,* 14**,** 257-263.

PEDROS-ALIO, C. 2012. The rare bacterial biosphere. *Annual Review of Marine Science,* 4**,** 449-66.

PETE, R., DAVIDSON, K., HART, M. C., GUTIERREZ, T. & MILLER, A. E. J. 2010. Diatom derived dissolved organic matter as a driver of bacterial productivity: The role of nutrient limitation. *Journal of Experimental Marine Biology and Ecology*, 391**,** 20-26.

PFAFFL, M. W., HORGAN, G. W. & DEMPFLE, L. 2002. Relative expression software tool (REST©) for group-wise comparison and statistical analysis of relative expression results in real-time PCR. *Nucleic Acids Research,* 30**,** e36.

PINGREE, R. D. 1980. Chapter 13 Physical oceanography of the Celtic Sea and English Channel. *In:* BANNER, F. T., COLLINS, M. B. & MASSIE, K. S. (eds.) *Elsevier Oceanography Series.* Elsevier.

PINHASSI, J. & HAGSTRÖM, Å. 2000. Seasonal succession in marine bacterioplankton. *Aquatic Microbial Ecology,* 21**,** 245-256.

PITTERA, J., HUMILY, F., THOREL, M., GRULOIS, D., GARCZAREK, L. & SIX, C. 2014. Connecting thermal physiology and latitudinal niche partitioning in marine Synechococcus. *The ISME Journal,* 8**,** 1221-1236.

POLYVIOU, D., BAYLAY, A. J., HITCHCOCK, A., ROBIDART, J., MOORE, C. M. & BIBBY, T. S. 2017. Desert dust as a source of iron to the globally important diazotroph *Trichodesmium*. *Frontiers in Microbiology,* 8**,** fmicb.2017.02683.

POMMIER, T., CANBACK, B., RIEMANN, L., BOSTROM, K. H., SIMU, K., LUNDBERG, P., TUNLID, A. & HAGSTROM, A. 2007. Global patterns of diversity and community structure in marine bacterioplankton. *Molecular Ecology,* 16**,** 867-880.

PUJALTE, M. J., LUCENA, T., RUVIRA, M. A., ARAHAL, D. R. & MACIÁN, M. C. 2014. The family *Rhodobacteraceae*. *In:* ROSENBERG, E., DELONG, E. F., LORY, S., STACKEBRANDT, E. & THOMPSON, F. (eds.) *The prokaryotes: Alphaproteobacteria and Betaproteobacteria.* Berlin, Heidelberg: Springer Berlin Heidelberg.

QUAST, C., PRUESSE, E., YILMAZ, P., GERKEN, J., SCHWEER, T., YARZA, P., PEPLIES, J. & GLÖCKNER, F. O. 2013. The SILVA ribosomal RNA gene database project: improved data processing and web-based tools. *Nucleic Acids Research,* 41**,** D590-D596.

R-CORE-TEAM 2015. R: A language and environment for statistical computing. R foundation for statistical computing. Vienna, Austria: URL https://www.R-project.org/.

RAHLFF, J., STOLLE, C., GIEBEL, H. A., BRINKHOFF, T., RIBAS-RIBAS, M., HODAPP, D. & WURL, O. 2017. High wind speeds prevent formation of a distinct bacterioneuston community in the sea-surface microlayer. *FEMS Microbiology Ecology,* 96**,** fix041.

RAPPÉ, M. S., CONNON, S. A., VERGIN, K. L. & GIOVANNONI, S. J. 2002. Cultivation of the ubiquitous SAR11 marine bacterioplankton clade. *Nature,* 418**,** 630-633.

RAPPE, M. S., VERGIN, K. & GIOVANNONI, S. J. 2000. Phylogenetic comparisons of a coastal bacterioplankton community with its counterparts in open ocean and freshwater systems. *FEMS Microbiology Ecology,* 33**,** 219-232.

REES, A., ROBINSON, C., SMYTH, T., AIKEN, J., NIGHTINGALE, P. & ZUBKOV, M. 2015. 20 years of the Atlantic Meridional Transect—AMT. *Limnology and Oceanography Bulletin,* 24**,** 101-107.

REES, A. P., HOPE, S. B., WIDDICOMBE, C. E., DIXON, J. L., WOODWARD, E. M. S. & FITZSIMONS, M. F. 2009. Alkaline phosphatase activity in the western English Channel: elevations induced by high summertime rainfall. *Estuarine, Coastal and Shelf Science,* 81**,** 569-574.

REINTHALER, T., SINTES, E. & HERNDL, G. J. 2008. Dissolved organic matter and bacterial production and respiration in the sea-surface microlayer of the open Atlantic and the western Mediterranean Sea. *Limnology and Oceanography,* 53**,** 122-136.

REINTJES, G. 2017. *Taxonomic and Functional Analyses of Marine Microbial Polysaccharide Utilisation.* Dr.rer.nat, Universität Bremen: Biologie/Chemie.

REYGONDEAU, G., LONGHURST, A., MARTINEZ, E., BEAUGRAND, G., ANTOINE, D. & MAURY, O. 2013. Dynamic biogeochemical provinces in the global ocean. *Global Biogeochemical Cycles,* 27**,** 1046-1058.

RIBAS-RIBAS, M., KILCHER, L. F. & WURL, O. 2018. Sniffle: a step forward to measure in situ CO2 fluxes with the floating chamber technique. *Elementa,* 6**,** NREL/JA-5000-71252.

RIBAS-RIBAS, M., MUSTAFFA, N. I. H., RAHLFF, J., STOLLE, C. & WURL, O. 2017. Sea Surface Scanner (S3): A catamaran for high-resolution measurements of biogeochemical properties of the sea surface microlayer. *Journal of Atmospheric and Oceanic Technology,* 34**,** 1433-1448.

RICHARDSON, T. L. & JACKSON, G. A. 2007. Small phytoplankton and carbon export from the surface ocean. *Science,* 315**,** 838-840.

RILEY, J. P. (1977). GRASSHOFF, K. [ED.] 1976. *Methods of seawater analysis*. Verlag Chemie, Weinheim and New York, *Limnology and Oceanography*, 6**,** lo.1977.22.6.1103.

ROBINSON, C., POULTON, A. J., HOLLIGAN, P. M., BAKER, A. R., FORSTER, G., GIST, N., JICKELLS, T. D., MALIN, G., UPSTILL-GODDARD, R., WILLIAMS, R. G., WOODWARD, E. M. S. & ZUBKOV, M. V. 2006. The Atlantic Meridional Transect (AMT) Programme: A contextual view 1995–2005. *Deep Sea Research Part II: Topical Studies in Oceanography,* 53**,** 1485-1515.

ROCCA, J. D., HALL, E. K., LENNON, J. T., EVANS, S. E., WALDROP, M. P., COTNER, J. B., NEMERGUT, D. R., GRAHAM, E. B. & WALLENSTEIN, M. D. 2015. Relationships between protein-encoding gene abundance and corresponding process are commonly assumed yet rarely observed. *The ISME Journal,* 9**,** 1693-1699.

ROCHA, D. J., SANTOS, C. S. & PACHECO, L. G. 2015. Bacterial reference genes for gene expression studies by RT-qPCR: survey and analysis. *Antonie Van Leeuwenhoek,* 108**,** 685-693.

RODRÍGUEZ, F., FERNÁNDEZ, E., HEAD, R. N., HARBOUR, D. S., BRATBAK, G., HELDAL, M. & HARRIS, R. P. 2000. Temporal variability of viruses, bacteria, phytoplankton and zooplankton in the western English Channel off Plymouth. *Journal of the Marine Biological Association of the United Kingdom,* 80**,** 575-586.

ROGNES, T., FLOURI, T., NICHOLS, B., QUINCE, C. & MAHE, F. 2016. VSEARCH: a versatile open source tool for metagenomics. *PeerJ,* 4**,** e2584.

ROONEY-VARGA, J. N., GIEWAT, M. W., SAVIN, M. C., SOOD, S., LEGRESLEY, M. & MARTIN, J. L. 2005. Links between phytoplankton and bacterial community dynamics in a coastal marine environment. *Microbial Ecology,* 49**,** 163-175.

ROTEM, O., PASTERNAK, Z. & JURKEVITCH, E. 2014. Bdellovibrio and like organisms. *In:* ROSENBERG, E., DELONG, E. F., LORY, S., STACKEBRANDT, E. & THOMPSON, F. (eds.) *The Prokaryotes: Deltaproteobacteria and Epsilonproteobacteria.* Berlin, Heidelberg: Springer Berlin Heidelberg.

RUBIN, M., BERMAN-FRANK, I. & SHAKED, Y. 2011. Dust-and mineral-iron utilization by the marine dinitrogen-fixer *Trichodesmium*. *Nature Geoscience,* 4**,** 529-534.

RUSCH, D. B., HALPERN, A. L., SUTTON, G., HEIDELBERG, K. B., WILLIAMSON, S., YOOSEPH, S., WU, D., EISEN, J. A., HOFFMAN, J. M., REMINGTON, K., BEESON, K., TRAN, B., SMITH, H., BADEN-TILLSON, H., STEWART, C., THORPE, J., FREEMAN, J., ANDREWS-PFANNKOCH, C., VENTER, J. E., LI, K., KRAVITZ, S., HEIDELBERG, J. F., UTTERBACK, T., ROGERS, Y. H., FALCON, L. I., SOUZA, V., BONILLA-ROSSO, G., EGUIARTE, L. E., KARL, D. M., SATHYENDRANATH, S., PLATT, T., BERMINGHAM, E., GALLARDO, V., TAMAYO-CASTILLO, G., FERRARI, M. R., STRAUSBERG, R. L., NEALSON, K., FRIEDMAN, R., FRAZIER, M. & VENTER, J. C. 2007. The Sorcerer II global ocean sampling expedition: northwest Atlantic through eastern tropical Pacific. *PLoS Biol,* 5**,** e77.

SALTER, I., GALAND, P. E., FAGERVOLD, S. K., LEBARON, P., OBERNOSTERER, I., OLIVER, M. J., SUZUKI, M. T. & TRICOIRE, C. 2014. Seasonal dynamics of active SAR11 ecotypes in the oligotrophic Northwest Mediterranean Sea. *The ISME Journal,* 9**,** 347-360.

SALTER, M. E., UPSTILL-GODDARD, R. C., NIGHTINGALE, P. D., ARCHER, S. D., BLOMQUIST, B., HO, D. T., HUEBERT, B., SCHLOSSER, P. & YANG, M. 2011. Impact of an artificial surfactant release on air-sea gas fluxes during Deep Ocean Gas Exchange Experiment II. *Journal of Geophysical Research: Oceans,* 116**,** C11016.

SALTER, S. J., COX, M. J., TUREK, E. M., CALUS, S. T., COOKSON, W. O., MOFFATT, M. F., TURNER, P., PARKHILL, J., LOMAN, N. J. & WALKER, A. W. 2014. Reagent and laboratory contamination can critically impact sequence-based microbiome analyses. *BMC Biology,* 12**,** s12915-014-0087-z.

SANTOS, A. L., BAPTISTA, I., LOPES, S., HENRIQUES, I., GOMES, N. C., ALMEIDA, A., CORREIA, A. & CUNHA, Â. 2012. The UV responses of bacterioneuston and bacterioplankton isolates depend on the physiological condition and involve a metabolic shift. *FEMS Microbiology Ecology,* 80**,** 646-658.

SAPP, M., SCHWADERER, A. S., WILTSHIRE, K. H., HOPPE, H. G., GERDTS, G. & WICHELS, A. 2007. Species-specific bacterial communities in the phycosphere of microalgae? *Microbiology Ecology,* 53**,** 683-99.

SAPP, M., WICHELS, A., WILTSHIRE, K. H. & GERDTS, G. 2006. Bacterial community dynamics during the winter–spring transition in the North Sea. *FEMS Microbiology Ecology,* 59**,** 622-637.

SARMENTO, H. & GASOL, J. M. 2012. Use of phytoplankton-derived dissolved organic carbon by different types of bacterioplankton. *Environmental Microbiology,* 14**,** 2348-2360.

SARMENTO, H., MORANA, C. & GASOL, J. M. 2016. Bacterioplankton niche partitioning in the use of phytoplankton-derived dissolved organic carbon: quantity is more important than quality. *The ISME Journal,* 10**,** 2582-2592.

SCHAFER, H., ABBAS, B., WITTE, H. & MUYZER, G. 2002. Genetic diversity of 'satellite' bacteria present in cultures of marine diatoms. *FEMS Microbiology Ecology,* 42**,** 25-35.

SCHAUER, M., BALAGUÉ, V., PEDRÓS-ALIÓ, C. & MASSANA, R. 2003. Seasonal changes in the taxonomic composition of bacterioplankton in a coastal oligotrophic system. *Aquatic Microbial Ecology,* 31**,** 163-174.

SCHLITZER, R. 2015. Ocean Data View. http://odv.awi.de/

SCHWALBACH, M., S. , BROWN, M. & FUHRMAN, J., A. 2005. Impact of light on marine bacterioplankton community structure. *Aquatic Microbial Ecology,* 39**,** 235-245.

SCHWALBACH, M. S., TRIPP, H. J., STEINDLER, L., SMITH, D. P. & GIOVANNONI, S. J. 2010. The presence of the glycolysis operon in SAR11 genomes is positively correlated with ocean productivity. *Environmental Microbiology,* 12**,** 490-500.

SELJE, N., SIMON, M. & BRINKHOFF, T. 2004. A newly discovered Roseobacter cluster in temperate and polar oceans. *Nature,* 427**,** 445-448.

SIEBURTH, J. M. 1983. Microbiological and organic-chemical processes in the surface and mixed layers. *In:* LISS, P. S. & SLINN, W. G. N. (eds.) *Air-sea exchange of gases and particles.* Dordrecht: Springer Netherlands.

SIEBURTH, J. M. & CONOVER, J. T. 1965. Slicks associated with *Trichodesmium* Blooms in the Sargasso Sea. *Nature,* 205**,** 830-831.

SIX, C., FINKEL, Z. V., IRWIN, A. J. & CAMPBELL, D. A. 2007. Light variability illuminates niche-partitioning among marine picocyanobacteria. *PLoS One,* 2**,** e1341.

SMYTH, T. J., FISHWICK, J. R., AL-MOOSAWI, L., CUMMINGS, D. G., HARRIS, C., KITIDIS, V., REES, A., MARTINEZ-VICENTE, V. & WOODWARD, E. M. S. 2010. A broad spatio-temporal view of the Western English Channel observatory. *Journal of Plankton Research,* 32**,** 585-601.

SOMMARUGA, R., OBERNOSTERER, I., HERNDL, G. J. & PSENNER, R. 1997. Inhibitory effect of solar radiation on thymidine and leucine incorporation by freshwater and marine bacterioplankton. *Applied and Environmental Microbiology,* 63**,** 4178-4184.

SOUTHWARD, A. J., LANGMEAD, O., HARDMAN-MOUNTFORD, N. J., AIKEN, J., BOALCH, G. T., DANDO, P. R., GENNER, J., JOINT, I., KENDALL, M. A., HALLIDAY, N. C., HARRIS, R. P., LEAPER, R., MIESZKOWSKA, N., PINGREE, R. D., RICHARDSON, A. J., SIMS, D. W., SMITH, T., WALNE, A. W. & HAWKINS, S. J. 2005. A review of long-term research in the western English Channel. *In:* SOUTHWARD, A. J., TYLER, P. A., YOUNG, C. M. & FUIMAN, L. A. (eds.) *Advances in Marine Biology, Vol. 47.* Elsevier Academic Press.

SPRING, S., SCHEUNER, C., GÖKER, M. & KLENK, H.-P. 2015. A taxonomic framework for emerging groups of ecologically important marine *gammaproteobacteria* based on the reconstruction of evolutionary relationships using genome-scale data. *Frontiers in Microbiology,* 6**,** fmicb.2015.00281.

STINGL, U., TRIPP, H. J. & GIOVANNONI, S. J. 2007. Improvements of high-throughput culturing yielded novel SAR11 strains and other abundant marine bacteria from the Oregon coast and the Bermuda Atlantic Time Series study site. *The ISME Journal,* 1**,** 361-371.

STOLLE, C., LABRENZ, M., MEESKE, C. & JÜRGENS, K. 2011. Bacterioneuston community structure in the southern baltic sea and its dependence on meteorological conditions. *Applied and environmental microbiology,* 77**,** 3726-3733.

STOLLE, C., NAGEL, K., LABRENZ, M. & JÜRGENS, K. 2010. Succession of the sea-surface microlayer in the coastal Baltic Sea under natural and experimentally induced low-wind conditions. *Biogeosciences,* 7**,** 2975-2988.

STUBBINS, A., UHER, G., KITIDIS, V., LAW, C. S., UPSTILL-GODDARD, R. C. & WOODWARD, E. M. S. 2006. The open-ocean source of atmospheric carbon monoxide. *Deep Sea Research Part II: Topical Studies in Oceanography,* 53**,** 1685-1694.

SUL, W. J., OLIVER, T. A., DUCKLOW, H. W., AMARAL-ZETTLER, L. A. & SOGIN, M. L. 2013. Marine bacteria exhibit a bipolar distribution. *Proceedings of the National Academy of Sciences,* 110**,** 2342-2347.

SUNAGAWA, S., COELHO, L. P., CHAFFRON, S., KULTIMA, J. R., LABADIE, K., SALAZAR, G., DJAHANSCHIRI, B., ZELLER, G., MENDE, D. R., ALBERTI, A., CORNEJO-CASTILLO, F. M., COSTEA, P. I., CRUAUD, C., OVIDIO, F., ENGELEN, S., FERRERA, I., GASOL, J. M., GUIDI, L., HILDEBRAND, F., KOKOSZKA, F., LEPOIVRE, C., LIMA-MENDEZ, G., POULAIN, J., POULOS, B. T., ROYO-LLONCH, M., SARMENTO, H., VIEIRA-SILVA, S., DIMIER, C., PICHERAL, M., SEARSON, S., KANDELS-LEWIS, S., BOWLER, C., DE VARGAS, C., GORSKY, G., GRIMSLEY, N., HINGAMP, P., IUDICONE, D., JAILLON, O., NOT, F., OGATA, H., PESANT, S., SPEICH, S., STEMMANN, L., SULLIVAN, M. B., WEISSENBACH, J., WINCKER, P., KARSENTI, E., RAES, J., ACINAS, S. G. & BORK, P. 2015. Structure and function of the global ocean microbiome. *Science,* 348**,** science.1261359.

SUZUKI, M. T., TAYLOR, L. T. & DELONG, E. F. 2000. Quantitative analysis of small-subunit rRNA genes in mixed microbial populations via 5′-Nuclease assays. *Applied and Environmental Microbiology,* 66**,** 4605-4614.

SZYMCZYCHA, B., WINOGRADOW, A., KULIŃSKI, K., KOZIOROWSKA, K. & PEMPKOWIAK, J. 2017. Diurnal and seasonal DOC and POC variability in the land-locked sea. *Oceanologia,* 59**,** 379-388.

TAMURA, K., STECHER, G., PETERSON, D., FILIPSKI, A. & KUMAR, S. 2013. MEGA6: Molecular evolutionary genetics analysis version 6.0. *Molecular Biology and Evolution,* 30**,** 2725-2729.

TAYLOR, J. D., BIRD, K. E., WIDDICOME, C. E. & CUNLIFFE, M. 2018. Active bacterioplankton community response to dissolved 'free' deoxyribonucleic acid (dDNA) in surface coastal marine waters. *FEMS Microbiology Ecology,* 94**,** fiy132.

TAYLOR, J. D., COTTINGHAM, S. D., BILLINGE, J. & CUNLIFFE, M. 2014. Seasonal microbial community dynamics correlate with phytoplankton-derived polysaccharides in surface coastal waters *The ISME Journal,* 8**,** 245-248.

TAYLOR, J. D. & CUNLIFFE, M. 2017. Coastal bacterioplankton community response to diatom-derived polysaccharide microgels. *Environmental Microbiology Reports,* 9**,** 151-157.

TEELING, H., FUCHS, B. M., BECHER, D., KLOCKOW, C., GARDEBRECHT, A., BENNKE, C. M., KASSABGY, M., HUANG, S., MANN, A. J. & WALDMANN, J. 2012. Substrate-controlled succession of marine bacterioplankton populations induced by a phytoplankton bloom. *Science,* 336**,** 608-611.

TEELING, H., FUCHS, B. M., BENNKE, C. M., KRUGER, K., CHAFEE, M., KAPPELMANN, L., REINTJES, G., WALDMANN, J., QUAST, C., GLOCKNER, F. O., LUCAS, J., WICHELS, A., GERDTS, G., WILTSHIRE, K. H. & AMANN, R. I. 2016. Recurring patterns in bacterioplankton dynamics during coastal spring algae blooms. *Elife,* 5**,** e11888.

TODD, J. D., KIRKWOOD, M., NEWTON-PAYNE, S. & JOHNSTON, A. W. B. 2011. DddW, a third DMSP lyase in a model Roseobacter marine bacterium, *Ruegeria pomeroyi* DSS-3. *The ISME Journal,* 6**,** 223-226.

TOLLI, J. D., SIEVERT, S. M. & TAYLOR, C. D. 2006. Unexpected diversity of bacteria capable of carbon monoxide oxidation in a coastal marine environment, and contribution of the Roseobacter-associated clade to total CO oxidation. *Applied and Environmental Microbiology,* 72**,** 1966-1973.

TOLLI, J. D. & TAYLOR, C. D. 2005. Biological CO oxidation in the Sargasso sea and in vineyard sound, Massachusetts. *Limnology and oceanography,* 50**,** 1205-1212.

TRAVING, S. J., ROWE, O., JAKOBSEN, N. M., SØRENSEN, H., DINASQUET, J., STEDMON, C. A., ANDERSSON, A. & RIEMANN, L. 2017. The effect of increased loads of dissolved organic matter on estuarine microbial community composition and function. *Frontiers in Microbiology,* 8**,** fmicb.2017.00351.

TREUSCH, A. H., VERGIN, K. L., FINLAY, L. A., DONATZ, M. G., BURTON, R. M., CARLSON, C. A. & GIOVANNONI, S. J. 2009. Seasonality and vertical structure of microbial communities in an ocean gyre. *The ISME Journal,* 3**,** 1148-1163.

UITZ, J., CLAUSTRE, H., GENTILI, B. & STRAMSKI, D. 2010. Phytoplankton class-specific primary production in the world's oceans: Seasonal and interannual variability from satellite observations. *Global Biogeochemical Cycles,* 24**,** 2009GB003680.

VAN LEUSSEN, W., RADACH, G., VAN RAAPHORST, W., COLIJN, F. & LAANE, R. 1996. The North-West European Shelf Programme (NOWESP): integrated analysis of shelf processes based on existing data sets and models. *ICES Journal of Marine Science,* 53**,** 926-932.

VERGIN, K. L., DONE, B., CARLSON, C. A. & GIOVANNONI, S. J. 2013. Spatiotemporal distributions of rare bacterioplankton populations indicate adaptive strategies in the oligotrophic ocean. *Aquatic Microbial Ecology,* 71**,** 1-13.

WALSH, E. A., KIRKPATRICK, J. B., RUTHERFORD, S. D., SMITH, D. C., SOGIN, M. & D'HONDT, S. 2016. Bacterial diversity and community composition from seasurface to subseafloor. *The ISME Journal,* 10**,** 979-989.

WALTERS, W., HYDE, E. R., BERG-LYONS, D., ACKERMANN, G., HUMPHREY, G., PARADA, A., GILBERT, J. A., JANSSON, J. K., CAPORASO, J. G., FUHRMAN, J. A., APPRILL, A. & KNIGHT, R. 2016. Improved bacterial 16S rRNA gene (V4 and V4-5) and fungal internal transcribed spacer marker gene primers for microbial community surveys. *mSystems,* 1**,** e00009-15

WANG, Q., GARRITY, G. M., TIEDJE, J. M. & COLE, J. R. 2007. Naive Bayesian classifier for rapid assignment of rRNA sequences into the new bacterial taxonomy. *Applied and Environmental Microbiology,* 73**,** 5261-5267.

WANG, Z. J., LIU, Q. Q., ZHAO, L. H., DU, Z. J. & CHEN, G. J. 2015. *Bradymonas sediminis* gen. nov., sp. nov., isolated from coastal sediment, and description of *Bradymonadaceae* fam. nov. and *Bradymonadales* ord. nov. *International Journal of Systematic and Evolutionary Microbiology,* 65**,** 1542-1549.

WEST, N. J., OBERNOSTERER, I., ZEMB, O. & LEBARON, P. 2008. Major differences of bacterial diversity and activity inside and outside of a natural iron-fertilized phytoplankton bloom in the Southern Ocean. *Environmental Microbiology,* 10**,** 738-756.

WEST, N. J. & SCANLAN, D. J. 1999. Niche-partitioning of *Prochlorococcus* populations in a stratified water column in the Eastern North Atlantic Ocean. *Applied and Environmental Microbiology,* 65**,** 2585-2591.

WESTRICH, J. R., EBLING, A. M., LANDING, W. M., JOYNER, J. L., KEMP, K. M., GRIFFIN, D. W. & LIPP, E. K. 2016. Saharan dust nutrients promote *Vibrio* bloom formation in marine surface waters. *Proceedings of the National Academy of Sciences,* 113**,** 5964-5969.

WIDDEL, F. 2007. Theory and measurement of bacterial growth. *Di dalam Grundpraktikum Mikrobiologie,* 4**,** 1-11.

WIDDICOMBE, C., ELOIRE, D., HARBOUR, D., HARRIS, R. & SOMERFIELD, P. 2010. Long-term phytoplankton community dynamics in the Western English Channel. *Journal of Plankton Research,* 32**,** 643-655.

WILLIAMS, K. P., GILLESPIE, J. J., SOBRAL, B. W., NORDBERG, E. K., SNYDER, E. E., SHALLOM, J. M. & DICKERMAN, A. W. 2010. Phylogeny of *gammaproteobacteria*. *Journal of Bacteriology,* 192**,** 2305-2314.

WINTER, C., MOESENEDER, M. M. & HERNDL, G. J. 2001. Impact of UV radiation on bacterioplankton community composition. *Applied and Environmental Microbiology,* 67**,** 665-672.

WRIGHT, R. T. & COFFIN, R. B. 1983. Planktonic bacteria in estuaries and coastal waters of Northern Massachusetts - spatial and temporal distribution. *Marine Ecology Progress Series,* 11**,** 205-216.

WURL, O., BIRD, K., CUNLIFFE, M., LANDING, W. M., MILLER, U., MUSTAFFA, N. I. H., RIBAS-RIBAS, M., WITTE, C. & ZAPPA, C. J. 2018. Warming and inhibition of salinization at the ocean's surface by *Cyanobacteria*. *Geophysical Research Letters,* 45**,** 4230-4237.

WURL, O., EKAU, W., LANDING, W. M. & ZAPPA, C. J. 2017. Sea surface microlayer in a changing ocean–A perspective. *Elementa: Science of the Anthropocene,* 5**,** elementa.228.

WURL, O. & HOLMES, M. 2008. The gelatinous nature of the sea-surface microlayer. *Marine Chemistry,* 110**,** 89-97.

WURL, O., MILLER, L., RÖTTGERS, R. & VAGLE, S. 2009. The distribution and fate of surface-active substances in the sea-surface microlayer and water column. *Marine Chemistry,* 115**,** 1-9.

WURL, O., MILLER, L. & VAGLE, S. 2011a. Production and fate of transparent exopolymer particles in the ocean. *Journal of Geophysical Research: Oceans,* 116**,** 2011JC007342.

WURL, O., STOLLE, C., VAN THUOC, C., THE THU, P. & MARI, X. 2016. Biofilm-like properties of the sea surface and predicted effects on air–sea CO2 exchange. *Progress in Oceanography,* 144**,** 15-24.

WURL, O., WURL, E., MILLER, L., JOHNSON, K. & VAGLE, S. 2011b. Formation and global distribution of sea-surface microlayers. *Biogeosciences,* 8**,** 121-135.

WWW.BEARSBYTHESEA.CO.UK. 2018. Available: www.bearsbythesea.co.uk [Accessed 2015].

WWW.WESTERNCHANNELOBSERVATORY.ORG.UK. 2011. Available: www.westernchannelobservatory.org.uk [Accessed 2015].

XIE, H., ZAFIRIOU, O. C., UMILE, T. P. & KIEBER, D. J. 2005. Biological consumption of carbon monoxide in Delaware Bay, NW Atlantic and Beaufort Sea. *Marine Ecology Progress Series,* 290**,** 1-14.

YE, J., COULOURIS, G., ZARETSKAYA, I., CUTCUTACHE, I., ROZEN, S. & MADDEN, T. L. 2012. Primer-BLAST: a tool to design target-specific primers for polymerase chain reaction. *BMC Bioinformatics,* 13**,** 1471-2105-13-134.

YEH, Y.-C., NEEDHAM, D. M., SIERADZKI, E. T. & FUHRMAN, J. A. 2018. Taxon disappearance from microbiome analysis reinforces the value of mock communities as a standard in every sequencing run. *mSystems***,** 3, e00023-18.

ZAFIRIOU, O. C., ANDREWS, S. S. & WANG, W. 2003. Concordant estimates of oceanic carbon monoxide source and sink processes in the Pacific yield a balanced global "blue-water" CO budget. *Global Biogeochemical Cycles,* 17**,** 2001GB001638.

ZÄNCKER, B., BRACHER, A., RÖTTGERS, R. & ENGEL, A. 2017. Variations of the organic matter composition in the sea surface microlayer: a comparison between open ocean, coastal, and upwelling sites off the Peruvian coast. *Frontiers in Microbiology,* 8**,** fmicb.2017.02369.

ZAVARZIN, G. A. & NOZHEVNIKOVA, A. N. 1977. Aerobic carboxydobacteria. *Microbial ecology,* 3**,** 305-236.

ZHANG, Z., LIU, L., LIU, C. & CAI, W. 2003. Studies on the sea surface microlayer: II. The layer of sudden change of physical and chemical properties. *Journal of Colloid and Interface Science,* 264**,** 148-159.

ZINGER, L., AMARAL-ZETTLER, L. A., FUHRMAN, J. A., HORNER-DEVINE, M. C., HUSE, S. M., WELCH, D. B. M., MARTINY, J. B. H., SOGIN, M., BOETIUS, A. & RAMETTE, A. 2011. Global patterns of bacterial beta-diversity in seafloor and seawater ecosystems. *PLoS ONE,* 6**,** e24570.

ZINSER, E. R., JOHNSON, Z. I., COE, A., KARACA, E., VENEZIANO, D. & CHISHOLM, S. W. 2007. Influence of light and temperature on *Prochlorococcus* ecotype distributions in the Atlantic Ocean. *Limnology and Oceanography,* 52**,** 2205-2220.

ZUBKOV, M. V., SLEIGH, M. A. & BURKILL, P. H. 2000. Assaying picoplankton distribution by flow cytometry of underway samples collected along a meridional transect across the Atlantic Ocean. *Aquatic Microbial Ecology,* 21**,** 13-20.

ZWIRGLMAIER, K., HEYWOOD, J. L., CHAMBERLAIN, K., WOODWARD, E. M., ZUBKOV, M. V. & SCANLAN, D. J. 2007. Basin-scale distribution patterns of picocyanobacterial lineages in the Atlantic Ocean. *Environmental Microbiology,* 9**,** 1278-1290.

Appendicies

Appendix 1

Details of Sea Surface Scanner on-board sensors including manufacturers and specifications taken from Ribas-Ribas et al., (2017).

Parameter	Manufacturer	Model	Range, unit, and resolution	Sensitivity	Accuracy	Sample[a]
pH	VWR	MU 6100 H	−2.000 to 19.999		±0.005	SML and UW
Salinity[b]	VWR	MU 6100 H	0.0–70.0		±0.2%	SML and UW
Oxygen, concentration	VWR	MU 6100 H	0–20.00 or 20.0–90.0 mg L^{-1}		±0.5%	SML and UW
Oxygen, saturation	VWR	MU 6100 H	0%–200.0% or 0%–600%		±0.5%	SML and UW
Temperature or [c]	VWR	MU 6100 H	−5.0° to 105.0°C		±0.1°C	SML and UW
pH	EuTech Instruments	PCD650	−2.000 to 20.000		±0.002	SML and UW
Salinity[b]	EuTech Instruments	PCD650	0.0–80.0		±1%	SML and UW
Oxygen, concentration	EuTech Instruments	PCD650	0–90.00 mg L^{-1}		±0.2 mg L^{-1}	SML and UW
Oxygen, saturation	EuTech Instruments	PCD650	0%–600%		±0.2%	SML and UW
Temperature	EuTech Instruments	PCD650	−10.0°C to 110.0°C		±0.5°C	SML and UW
FDOM	TriOS	MicroFlu	0.0–20.0 or 0.0–200.0 μg L^{-1}	0.2 μg L^{-1}		SML and UW
HPT	Dostmann Electronic GmbH	P795	−200.000° to 200.000°C		±0.015°C	2 and 15 cm
Chlorophyll-*a*	Turner Designs	Phytoflash	0–150.00 μg L^{-1}	0.15 μg L^{-1}		SML or UW
Photosynthetic yield as ratio Fv/Fm	Turner Designs	Phytoflash	0.000–1.000			SML or UW
Air temperature	Davis Instruments	Vantage Pro2	−40.0°C to 65.0°C		±0.3°C	Atmosphere
Humidity	Davis Instruments	Vantage Pro2	0%–100%		±2%	Atmosphere
Wind speed 1	Davis Instruments	Vantage Pro2	0.5–89 m s^{-1}		±1 m s^{-1} or ± 5%[c]	Atmosphere
Wind speed 2	PCE Instruments	PCE-KWG2	0.8–40 m s^{-1}		±0.5 m s^{-1} or ± 5%[d]	Atmosphere
Wind direction	Davis Instruments	Vantage Pro2	0°–360°		±3°	Atmosphere
Rain rate	Davis Instruments	Vantage Pro2	0–100 mm h^{-1}		±4%	Atmosphere
UV radiation dose (280–360 nm)	Davis Instruments	Vantage Pro2	0.1–19.9 MEDs or 20–199 MEDs		±5%	Atmosphere
UV radiation index (280–360 nm)	Davis Instruments	Vantage Pro2	0.0–16.0 index		±5%	Atmosphere
Solar radiation (400–1100 nm)	Davis Instruments	Vantage Pro2	0–1800 W m^{-2}		±5%	Atmosphere
PAR	Apogee Instruments	MQ-220	0–3000 μmol m^{-2} s^{-1}		±5%	Atmosphere
GPS	Canmore	GT-730FL-S	Latitude and longitude (°)		3 m	

[a] SML refers to a operationally defined thickness ranging from 60 to 100 μm. UW refers to a depth of 1 m.
[b] Derived from the measurement of conductivity.
[c] Depending on operational needs (see text).
[d] Whichever is greater.

Appendix 2

The list of detected peptides and polypeptides is provided in a table electronically in appendix 2.1.

Appendix 3

Sources of metadata used in this thesis. Any metadata from closed sources (i.e. Chapter 6) is provided in a table electronically in appendix 3.1.

Chapter	Metadata Type	Status	Source
Chapter 4	Physicochemical (Temperature, Fluorescence, Depth, Density, Salinity, Transmission, PAR, Oxygen)	Open access	https://www.westernchannelobservatory.org.uk
	Nutrients (Nitrite, Nitrate+Nitrite, Ammonia, silicate, Phosphate)	Open access	
	Phytoplankton and microzooplankton counts	Open access	
	Meteorological	Open access	http://www.bearsbythesea.co.uk
Chapter 5	Physicochemical	Open access, on request	https://www.bodc.ac.uk
	Nutrients	Open access, on request	
	Phytoplankton	Open access, on request	
Chapter 6	Meteorological from sea surface scanner	Data provided for this thesis is available electronically in Appendix 2.2 for the purposes of examination only, for any other use please contact Dr Wurl	Intellectual property of Dr Oliver Wurl Carl von Ossietzky Universität Oldenburg The Institute for Chemistry and Biology of the Marine Environment (ICBM) EG 003 Schleusenstraße 1 D-26382 Wilhelmshaven Germany Phone: 04421 / 944-228 oliver.wurl@uni-oldenburg.de
	Partial pressure of carbon dioxide		
	Chlorophyll-a (discrete)		
	Surface active substances (discrete)		
	Physicochemical (Temperature, Salinity, fDOM, Fluorescence, pH)		

Chapter	Metadata Type	Status	Source
Chapter 6	Trace metals (Al, P, Fe, Total dust)	Data provided for this thesis is available electronically in Appendix 2.2 for the purposes of examination only, for any other use please contact Dr landing	Intellectual property of Dr William Landing Earth, Ocean, and Atmospheric Science College of Arts and Sciences Florida State University Tallahassee, Florida 32306-4320 Phone: (850) 644-6037 Fax: (850) 644-2581 E-mail: wlanding@fsu.edu
	Ocean physics and ship board meteorological	Data provided for this thesis is available electronically in Appendix 2.2 for the purposes of examination only, for any other use please contact Dr Zappa	Intellectual property of Dr Christopher Zappa Lamont-Doherty Earth Observatory (LDEO) 206B Oceanography P.O. Box 1000 61 Route 9W Palisades NY 10964 Phone:845-365-8547 Fax:845-365-8157 E-Mail:zappa@ldeo.columbia.edu

Appendix 4

Western Channel Observatory nutrient protocol

This document includes:

Chemistry/Nutrients/Nitrate concentration parameters in the water column
Chemistry/Nutrients/Nitrite concentration parameters in the water column
Chemistry/Nutrients/Silicate concentration parameters in the water column
Chemistry/Nutrients/Phosphate concentration parameters in the water column
Chemistry/Nutrients/Ammonium concentration parameters in the water column

at both L4 and E1.

Sample collection

1) Take a water sample from the surface, this should be from a clean pumped supply, or from the sampling CTD Rosette bottle;
2) Put on gloves (ensure these are Duratouch);
3) Take some surface water sample direct from the rosette bottle or the pump supply straight into one of the sample bottles (labelled), and fill with about 20-30 mls of seawater, swill the bottle and discard, do this three times to clean the bottle. Then fill the sample bottle and screw the lid on. Label as to where it was sampled, depth etc. Ensure this is kept clean at all times. Put the sample bottle into the cool box;
4) If another sample is taken from 10 metres or elsewhere then carry out the same protocol for taking the first sample;
5) Return the water samples back to land in the cool box provided;
6) Return all the equipment and samples to PML as soon as possible.

Calculations and analysis

1. Phosphate

The analytical method is based upon the production of the phospho-molybdinum-blue complex by reaction with molybdate and ascorbic acid, and the catalyst of potassium antimony tartrate. The pH needs to be kept <1 in order to avoid a competitive reaction from silicate.

Reference: J-Z Zhang and J. Chi (2002), Automated analysis of nanomolar concentrations of phosphate in natural waters with liquid waveguides, Env. Sci. and Tech., 36(5).

2. Silicate

The analytical method here involves the reaction of inorganic silicate with the ammonium molybdate to form mainly silicomolybdic acid. This is reduced by the ascorbic acid to form a silico-molybdenum blue complex. The oxalic acid ensures that there is no competitive reaction from phosphates.

Reference: D.S. KIRKWOOD, ICES CM 1989/ C: 29 Simultaneous determination of selected nutrients in sea water.

3. Nitrate

The analysis is for the total of nitrate and nitrite ions. The reaction is for the reduction of nitrate to nitrite, using a copper/cadmium column, in an ammonium chloride solution (pH = 8.5). The nitrite ions react with an acidic sulphanilamide solution to form a diazo compound. This is then reacted with the N-1-naphthylethylenediamine dihydrochloride(NEDD), to form a reddish purple azo dye. The concentration of nitrate is obtained by subtracting the nitrite concentration from the combined concentration obtained here for the total of nitrate plus nitrite.
Reference: BREWER and RILEY, 1965, Deep Sea Research, 12: 765 - 772. The automatic determination of nitrate in sea water. (modified to increase sensitivity, by decreasing the ammonium chloride concentration in the reaction.)

4. Nitrite
The chemistry is the same as the nitrate channel for nitrite analysis.
Reference: A modified GRASSHOFF, K, (1976). Methods of seawater analysis, Verlag chemie, Weiheim: pp. 317.

5. Ammonia
The analysis technique is based upon the production of the indophenol-blue complex. This method is very dependent upon the reaction pH, which is optimum at 10.6. Temperature optimisation for sensitivity is at 55 degrees C. The reaction must then be cooled prior to detection.
Reference: MANTOURA, R.F.C, and WOODWARD, E.M.S., (1983). Estuarine, Coastal and Shelf Science, (1983), 17, 219-224. Optimization of the indophenol blue method for the automated determination of ammonia in estuarine waters.

Data stored
In WCO database – new data delivered every three months.

Appendix 5

Maximum Likelihood analysis (1000 bootstrap replications) of an alignment of the forward 250 bp of the *coxL* Form I amplicon from OMPF and NGSR primers using the same reference sequences from which new primer NGSR was designed see figure 2.8.

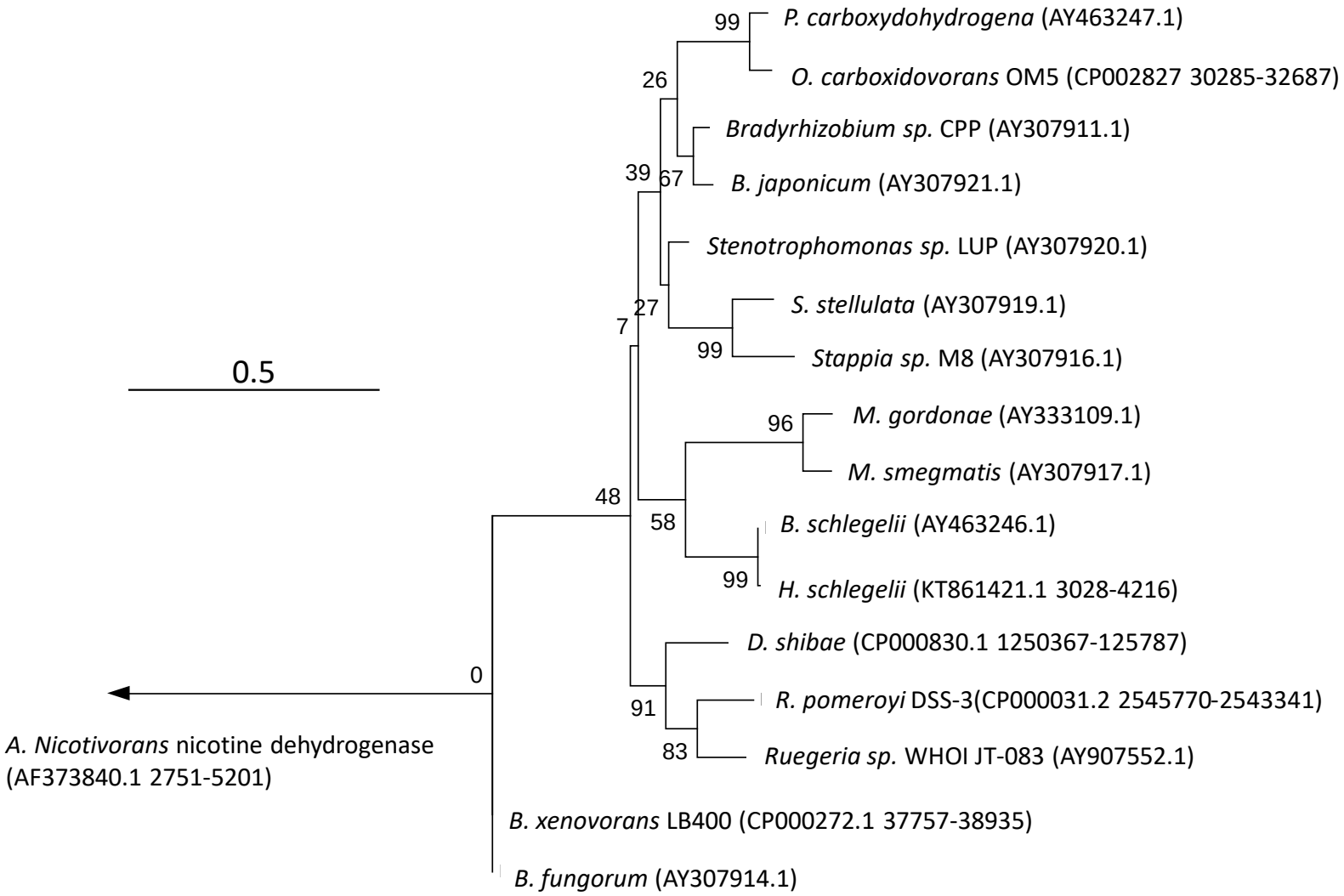
99
P. carboxydohydrogena (AY463247.1)
26
O. carboxidovorans OM5 (CP002827 30285-32687)
Bradyrhizobium sp. CPP (AY307911.1)
39
67
B. japonicum (AY307921.1)
Stenotrophomonas sp. LUP (AY307920.1)
27
S. stellulata (AY307919.1)
7
99
Stappia sp. M8 (AY307916.1)
0.5
96
M. gordonae (AY333109.1)
M. smegmatis (AY307917.1)
48
58
B. schlegelii (AY463246.1)
99
H. schlegelii (KT861421.1 3028-4216)
D. shibae (CP000830.1 1250367-125787)
0
R. pomeroyi DSS-3(CP000031.2 2545770-2543341)
91
83
Ruegeria sp. WHOI JT-083 (AY907552.1)
A. Nicotivorans nicotine dehydrogenase
(AF373840.1 2751-5201)
B. xenovorans LB400 (CP000272.1 37757-38935)
B. fungorum (AY307914.1)

Appendix 6

WURL, O., BIRD, K., CUNLIFFE, M., LANDING, W. M., MILLER, U., MUSTAFFA, N. I. H., RIBAS-RIBAS, M., WITTE, C. & ZAPPA, C. J. 2018. Warming and Inhibition of Salinization at the Ocean's Surface by *Cyanobacteria*. *Geophysical Research Letters*, 45**,** 4230-4237.

Geophysical Research Letters

RESEARCH LETTER
10.1029/2018GL077946

Warming and Inhibition of Salinization at the Ocean's Surface by Cyanobacteria

O. Wurl[1], K. Bird[2], M. Cunliffe[2,3], W. M. Landing[4], U. Miller[5], N. I. H. Mustaffa[1], M. Ribas-Ribas[1], C. Witte[5], and C. J. Zappa[5]

[1]Institute for Chemistry and Biology of the Marine Environment, Carl von Ossietzky University Oldenburg, Wilhelmshaven, Germany, [2]Marine Biological Association of the United Kingdom, Plymouth, UK, [3]Marine Biology and Ecology Research Centre, School of Biological and Marine Sciences, Plymouth University, Drake Circus, Plymouth, UK, [4]Department of Earth, Ocean, and Atmospheric Science, Florida State University, Tallahassee, FL, USA, [5]Lamont-Doherty Earth Observatory, Columbia University, Palisades, NY, USA

Abstract This paper describes high-resolution in situ observations of temperature and, for the first time, of salinity in the uppermost skin layer of the ocean, including the influence of large surface blooms of cyanobacteria on those skin properties. In the presence of the blooms, large anomalies of skin temperature and salinity of 0.95°C and −0.49 practical salinity unit were found, but a substantially cooler (−0.22°C) and saltier skin layer (0.19 practical salinity unit) was found in the absence of surface blooms. The results suggest that biologically controlled warming and inhibition of salinization of the ocean's surface occur. Less saline skin layers form during precipitation, but our observations also show that surface blooms of *Trichodesmium* sp. inhibit evaporation decreasing the salinity at the ocean's surface. This study has important implications in the assessment of precipitation over the ocean using remotely sensed salinity, but also for a better understanding of heat exchange and the hydrologic cycle on a regional scale.

Plain Language Summary We provide high-resolution in situ observations of large cyanobacterial blooms floating in a biofilm-like microlayer on the ocean's surface. Our observations show biologically controlled warming and freshening of the surface by the surface blooms that are essential in understanding global heat exchange and the hydrologic cycle. Our study describes a new phenomenon to force "apparent" freshening of the sea surface—in the literature assumed to occur only by precipitation. It further challenges the development of algorithms and validation of remotely sensed temperature and salinity from space. Our finding of active microbial communities in the sea surface microlayer highlights the sea surface as another environment for extreme habitats and microbial adaptation. Our discovery of their influence on satellite observations of sea surface temperature and salinity is fundamental for future research in remote sensing, marine microbiology, air-sea interaction, and climate regulation.

Key Points:
- Warming and inhibition of salinization of the sea surface are controlled by cyanobacterial surface blooms
- In the absence of surface blooms, skin layer is generally cooler and saltier
- A new phenomenon of "apparent" freshening of the sea surface is described, which has been assumed to occur only by precipitation

Supporting Information:
- Supporting Information S1

Correspondence to:
O. Wurl
oliver.wurl@uni-oldenburg.de

Citation:
Wurl, O., Bird, K., Cunliffe, M., Landing, W. M., Miller, U., Mustaffa, N. I. H., et al. (2018). Warming and inhibition of salinization at the ocean's surface by cyanobacteria. *Geophysical Research Letters, 45*, 4230–4237. https://doi.org/10.1029/2018GL077946

Received 27 NOV 2017
Accepted 26 APR 2018
Accepted article online 2 MAY 2018
Published online 12 MAY 2018

1. Introduction

Satellite observations of climate variables in the ocean are crucial to understand the magnitude of the global water cycle, ocean circulation, primary productivity, and climate change (Martin, 2014). Cyanobacteria are photosynthetic microorganisms that can significantly increase in abundance (bloom) at the ocean's surface and become visible from space (Capone et al., 1997), and also change the physical features of the sea surface (Frka et al., 2012). Floating cyanobacteria colonies are embedded in a gelatinous matrix sharing properties with biofilms, and subsequently form visibly smooth patches, also known as slicks, caused by capillary wave damping (Wurl et al., 2016). Cyanobacteria slicks exhibit significant effects on the sea surface temperature (SST) and heat exchange between the ocean and atmosphere (Kahru et al., 1993).

The effects of slicks on SST include different emissivity of slicks and nonslick surfaces based on investigations of artificial oil films (Zhou et al., 2017), decrease of evaporation rates (La Mer & Healy, 1965), and additional layer thickness due to reduced turbulence in the absence of capillary waves (Saunders, 1967). An increase of SST by 1.5°C has been observed in the presence of large cyanobacterial surface blooms in the Baltic Sea (Kahru et al., 1993) due to enhanced solar absorption by cyanobacteria. The prediction of SST in the presence of slicks, however, remains uncertain as slicks not induced by cyanobacteria have a cooling signature compared to the SST of ambient water surfaces (Marmorino & Smith, 2006). Such knowledge is essential for the evaluation of satellite observations because of the frequent appearance (Romano, 1996) and large size

(up to 1,300 km^2) of slicks (Capone et al., 1998; Kahru et al., 1993). Slicks induced by the large filamentous cyanobacterium *Trichodesmium* sp. have been reported during calm sea states in tropical regions (Capone et al., 1998; Sieburth & Conover, 1965; Wurl et al., 2011). So far, no observations have been published for the magnitude and direction of associated salinity anomalies. Salinity of the skin layer is forced by evaporation and precipitation (Soloviev & Lukas, 2006), and model approaches have shown salinity anomalies of 0.15 to 0.25 practical salinity unit (PSU; Song et al., 2015; Yu, 2010; Zhang & Zhang, 2012).

Here we show, using high-resolution in situ measurements, that slicks formed by cyanobacteria both warm the upper <1 mm of the ocean's surface compared to the near-surface mixed layer and inhibit salinization of the ocean's surface. Considering that the ocean absorbs 90% of the "anthropogenic" heat trapped by greenhouse gases (Levitus et al., 2012), these observations of biologically controlled warming and inhibition of salinization of the surface are essential in understanding heat exchange, the development of algorithms to reliably interpret SST and sea surface salinity (SSS) from satellites, and ultimately in the prediction of regional warming.

2. Methods

Observations were made in the Indo-West Pacific during cruise FK161010 (11 October to 10 November 2016; *R/V* Falkor). Similar to earlier observations from the Sargasso Sea (Sieburth & Conover, 1965), we observed patchy and banded slicks of cyanobacterial surface blooms (Figure S1) in the Joseph Bonaparte Gulf (Timor Sea; centered at 12.45°S, 126.62°E) over several hours on the 14 and 15 October 2016 (UTC).

The thermal boundary layer has been reported to vary between 500 and 1,000 μm in thickness (Donlon et al., 2002). The thickness of the salinity boundary layer is 200 μm thick due to different diffusivity scaling relationships (Katsaros, 1980). SST, SSS (derived from conductivity), and fluorescent dissolved organic matter (FDOM) were measured in a layer of ~80 μm thickness with a rotating glass disk sampler mounted on the remote-controlled catamaran Sea Surface Scanner (S^3; Ribas-Ribas et al., 2017). The 80-μm layer adheres to the disks through surface tension, is removed from the ascending side of the disk assembly by wipers, and pumped through onboard sensors. We estimate a time delay of approximately 7 s for water adhering to the discs to enter the pump tubing, protected from direct exposure of solar radiation, considering the following: (i) rotational speed of the disks of approximately 8 s per rotation, (ii) the fact that the disks are immersed to a depth equivalent to about one third of their diameter (8 s * 0.66 = 5.3 s), and (iii) run-off time from the wipers of 2 s resulting in the time delay of 7 s. The disks are shaded by a low-transmitting dark-colored shield, and their positions between the hulls minimize the warming of the disks and adhering water as well evaporative cooling. In addition, continuous immersion prevents warming of the disks.

Simultaneously, temperature, salinity, and FDOM were measured at 1 m depth, from which $\Delta S = S_{S3} - S_{1m}$ and $\Delta T = T_{S3} - T_{1m}$ were determined. S_{S3} and T_{S3} are the average salinity and temperature measured in the top 80 μm of the sea surface skin layer, respectively. The accuracy of the temperature and conductivity sensors was ±0.1°C and ±0.2%, respectively (Ribas-Ribas et al., 2017). The enrichment factor (EF) of FDOM was calculated as the ratio between the concentrations in the skin to that of the corresponding water sample from 1 m depth. Data were logged with a frequency of 0.1 Hz, and averaged over each minute of operation. The meteorological and radiation sensors, including wind speed, air temperature, and humidity, were mounted on the catamaran mast at a height of 3 m above the sea surface.

The temperature difference across the skin layer, ΔT_{skin}, is the skin SST minus the subskin SST (Jessup et al., 2009). The skin SST is defined as the radiometric temperature measured across a very small depth of approximately 20 μm. The subskin SST represents the temperature at the base of the thermal skin layer. Skin SST was determined by an infrared (IR) camera installed on the upper deck of the research vessel Falkor along with downward and upward looking IR radiometers. The Stirling-cycle cooled IR camera imagery measured thermal radiation from 7.7 to 9.3 μm emitted by the ocean surface (and reflected by the sky), and brightness temperature was obtained with a resolution of 0.02°C (noise-equivalent temperature difference). Calibration with a blackbody was better than ±0.05°C (Zappa et al., 2012). Brightness temperature was measured by IR imagery at a sampling rate of 100 Hz in 20-min bursts and was measured by IR radiometry at a sampling rate of 1 Hz continuously. The radiometer is calibrated with the same blackbody to ±0.1°C. Both the IR camera and radiometer were corrected for sky reflection (Donlon et al., 2014; Katsaros, 1980) by an upward

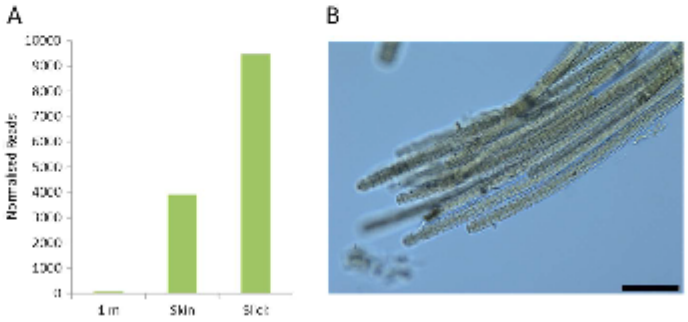

Figure 1. (a) *Trichodesmium* sp. abundance as the number of normalized bacterial 16S rRNA genes (Normalized Reads) in manual samples taken at 04:15 UTC (15 October 2016) from 1 m below the surface, the surface skin, and surface slick. Note that the skin sample was collected between the surrounding banded slicks and cannot be considered as a "clean" skin layer. (b) Micrograph of sampled colonies of *Trichodesmium* sp. Scale bar represents 50 μm.

looking radiometer to estimate the skin SST using known emissivity values for the ocean surface (Downing and Williams, 1975). The difference between the skin and subskin SST, ΔT_{skin}, was calculated directly using the distribution of temperature measured by the IR imager (Jessup et al., 2009), under the assumption that turbulent renewal of the skin layer leads to sampling a range of skin and subskin thermal values. This technique precludes the need for knowledge of the sky reflection. Polarimetric imaging (Zappa et al, 2008; Zappa et al., 2012) from the upper deck of the *R/V* Falkor provided a visible reference of the ocean surface.

In summary, temperature and salinity in the upper 80 μm were measured from the catamaran S^3 (T_{S3} and S_{S3}, respectively), and temperature and salinity anomalies calculated from the reference bulk temperature and salinity at 1 m depth, i.e., $\Delta T = T_{S3} - T_{1m}$ and $\Delta S = S_{S3} - S_{1m}$, respectively. Temperature in the upper 20 μm was measured by an IR camera (skin SST), and its anomaly across the thermal skin layer (approximately the upper 1000 μm) refers to ΔT_{skin}.

Trichodesmium sp. abundance was determined by bacterial 16S rRNA gene high-throughput sequencing. In brief, 0.5 L seawater was sampled from the skin layer using a glass plate (Harvey & Burzell, 1972) and from 1 m below the surface. Samples were filtered onto 0.2 μm membrane filters and stored in RNAlater® (Sigma, UK) at −80°C. DNA was later extracted using a commercially available DNeasy kit (Qiagen, UK). 16S rRNA gene library preparation and sequencing were performed at the Integrated Microbiome Resource at the Centre for Comparative Genomics and Evolutionary Bioinformatics, Dalhousie University (Comeau et al., 2017). Sequences were analyzed in QIIME as previously described (Taylor et al., 2014). Slicks were dominated by a single operational taxonomic unit (OTUB), which was identified as *Trichodesmium* sp. using the National Center for Biotechnology Information BLAST database.

The statistical analysis was performed with GraphPad PRISM version 5.0. Correlation tests were based on Spearman's correlation coefficient and 95% confidence intervals (CIs). All other values were reported as average ± standard deviation based on repeated measurements.

3. Results and Discussion

We identified the cyanobacterium *Trichodesmium* sp. in extremely high abundance in skin samples from slick areas compared to nonslick and underlying water samples (Figure 1).

The EF of FDOM is used as proxy for the presence of slicks (Frew et al., 2004), and Figure 2 shows that slicks appeared after 01:16 UTC (local time is nine and a half hours ahead).

Positive ΔT (i.e., warmer sea surface) and negative ΔS (i.e., fresher sea surface) were coincident with slicks (Figure 2). This measured positive ΔT is due to the presence of the surface slick. To demonstrate the role of

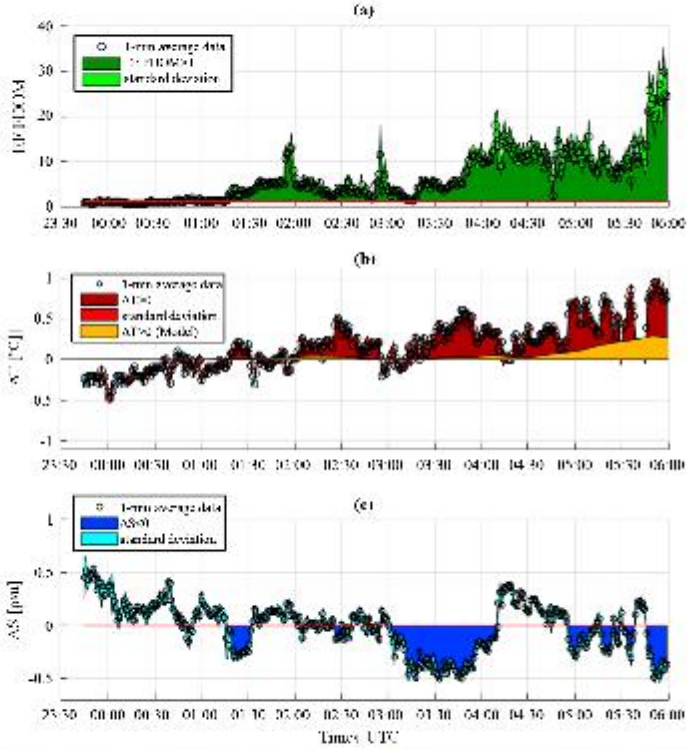

Figure 2. Time series from 23:45 UTC (14 October 2016) to 05:59 UTC (15 October 2016). (a) Enrichment factor (EF) of fluorescent dissolved organic matter (FDOM; the dark green areas indicate the presence of slicks), (b) temperature anomaly (ΔT; the dark red areas indicate the in situ warm surface layer; the orange areas indicate the model surface layer warming according to Price et al., 1986, and noted as Price Weller Pinkel [PWP] for short throughout), and (c) salinity anomaly (ΔS; the dark blue areas indicate the fresher surface layer). Standard deviations are from 1-min averaged data, and the averaged data are represented by black circles.

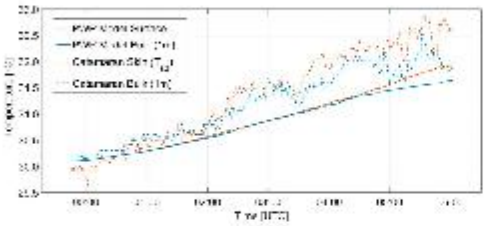

Figure 3. Time series of the in situ temperature measurements from the catamaran (skin T_{S3} and 1 m bulk) and the PWP modeled temperatures (surface and 1 m).

the slick, we ran a one-dimensional diurnal mixed-layer model (Price et al., 1986; Price Weller Pinkel model or in short PWP) that accounts for solar absorption without the impact of surface slicks. In contrast to the observations (Figure 2b), only modest warming occurred in the model, and this was delayed relative to the observations by more than 2 hr. The largest anomalies of ΔT (in situ: 0.95°C at 05:52 UTC; model: 0.30°C at 05:50 UTC; Figure 2b) and ΔS (−0.50 PSU at 03:47 UTC, and −0.49 PSU at 05:51 UTC; Figure 2c) occurred with the largest FDOM enrichments at the surface (EF = 4.90 at 03:47 UTC and EF = 20.44 at 05:52 UTC; Figure 2a). Furthermore, Figure 3 demonstrates that while both the in situ temperatures (T_{S3} and 1 m bulk) and the modeled temperatures (surface and 1 m) both increase, the in situ temperatures in the upper 80-μm layer (T_{S3}) and 1 m bulk water warm more quickly.

While FDOM enrichment in slicks collected by S^3 generally yielded a less saline skin layer, high FDOM enrichments between 04:00 UTC

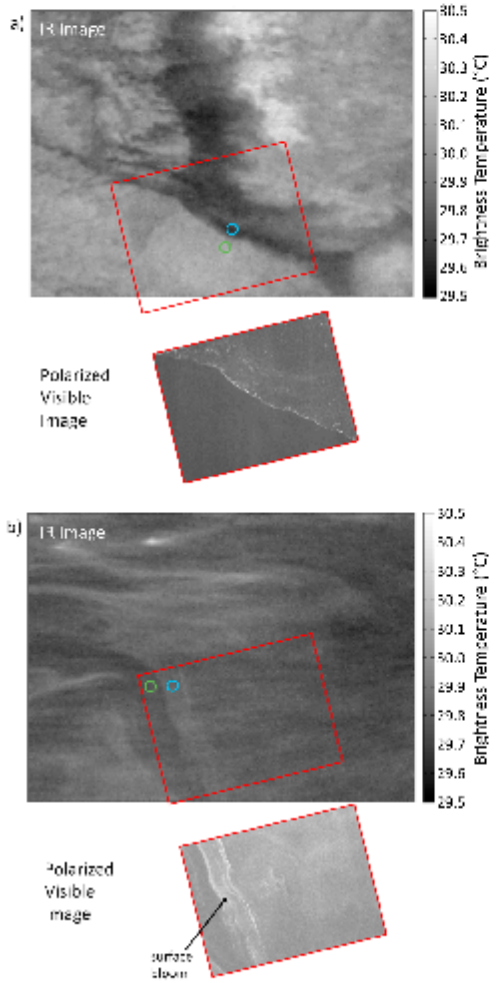

Figure 4. Infrared images (3.50 m × 2.75 m) showing sea surface brightness temperature with bright areas warmer and dark areas cooler, and polarized visible images (1.0 m × 0.8 m). (a) Slick without cyanobacterial bloom showing cooler skin layer, for example, negative in situ ΔT from S[3] (02:56 UTC, 15 October 2016; see Figure 2). For the noncyanobacterial slick, the brightness temperature in the slick is 29.68 °C ± 0.02°C (blue circle) and outside is 30.10°C ± 0.02°C (green circle). (b) Slicks associated with cyanobacterial blooms show a warmer skin layer, for example, positive in situ ΔT (02:24 UTC, 15 October 2016). For the cyanobacteria slick, the brightness temperature in the slick is 29.84°C ± 0.02°C (blue circle) and outside is 29.77°C ± 0.02°C (green circle).

and 04:30 UTC corresponded to a more saline skin layer. Other processes such as dynamic evaporation and associated cooling, thinning of the skin layer by wind-driven dispersion, and photo degradation of FDOM in the skin layer are likely to have contributed to this observation. Both the skin temperature and, to a lesser extent, the subsurface temperature increased and led to the positive ΔT (Figure 3), which deviated less from the FDOM trend than ΔS. Our observation on the greatest degree of warming of the sea surface by 0.95°C is consistent with observations by satellite-based radiometers of regions (>1,000 km^2) warmer by 1.5°C, supposedly caused by cyanobacterial surface blooms and supported by opportunistic ship measurements (Kahru et al., 1993). Without the presence of slicks, we observed a cooler surface (averaged −0.22 ± 0.09°C; Figure 2b) consistent with numerous reports on the "cool skin layer" (Soloviev & Lukas, 2006).

Interestingly, natural slicks that are not associated with cyanobacterial blooms often have a cooler skin, typically 0.1 to 0.4°C compared to ambient nonslick surfaces as observed using aircraft-based IR radiometers (Marmorino & Smith, 2006). Laboratory measurements have shown cool skin layers for varying surfactants, depending on their ability to modulate evaporation, lower surface tension, or change viscosity and therefore alter convective mixing with underlying bulk water (Jarvis, 1962). The IR and polarimetric imagery shows cooling of the skin layer in the presence of slicks without cyanobacteria (Figure 4a). The measurements of skin SST by both IR radiometry and IR imagery is compared in Figure 5 with the in situ skin layer temperature from the catamaran. The two distributions of skin SST are comparable, but the in situ skin layer temperature shows a tendency to warmer temperatures. The skin SST is measured in the top 20 μm of the surface in contrast to the in situ skin layer temperature that is measured in the top 80 μm. Furthermore, our measurements from nonslick areas demonstrate the skin SST to be always lower than the subskin SST (see Figure 2b; 23:45 UTC to 01:15 UTC). The cooling effect is in line with the increased thickness of the thermal conduction layer induced by the wave-damping phenomena reducing near-surface turbulence (McLeish & Putland, 1975). In contrast, slicks may also inhibit evaporation due to a close packed monomolecular film (La Mer & Healy, 1965) and/or, a gel-like matrix (Wurl et al., 2016), which could also include monomolecular surface films. The inhibition of evaporation reduces the heat loss from the sea surface and therefore partly offsets the cooling effect. The combination of multiple effects of slicks on evaporation and near-surface turbulence, for example, thickening thermal boundary layer, existence of closely packed monolayers, and type of surfactants, is a poorly understood process. However, due to the existence of cool slicks of noncyanobacterial origin (Marmorino & Smith, 2006), inhibition of evaporation will only influence the cool skin effect.

For the IR imagery in Figure 4 of the noncyanobacterial slick, the brightness temperature signature of a cooler slick is comparable with previous observations of cooler surface slicks. For the slicks associated with cyanobacterial blooms, the observations of warming are real rather than apparent since any changes in emissivity should have minimal impact, or cooling effect, on the brightness temperature. Hühnerfuss et al. (1986) state that monomolecular surface films do not change the emissivity of the sea surface significantly in contrast to crude-oil films (Grossman et al., 1969; Jarvis &

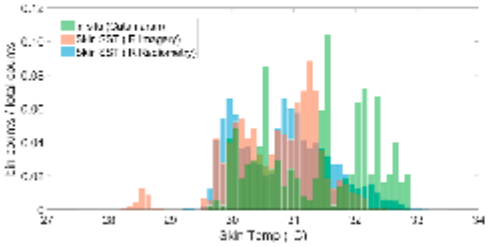

Figure 5. Distribution of skin SST (upper 20 μm) by both IR radiometry and IR imagery in comparison with the in situ 80-μm-layer temperature T_{53} from the catamaran S[3].

Kagarise, 1962). We conclude that the observed warming is directly linked to the cyanobacterial-dominated slicks as shown by the IR and polarimetric imagery (Figure 4b).

Mycosporine-like amino acids are common cyanobacteria pigments (Sinha et al., 1998) that are present in higher concentrations at the ocean's surface (Tilstone et al., 2010), and are known to dissipate 97% of the adsorbed energy to the surroundings as heat (Conde et al., 2004). Cyanobacteria are also known to excrete the extracellular pigments Scytonemin and Gloeocapsin (Sinha et al., 1998) into the ambient gel-matrix. Our slick samples showed more pronounced rose coloration (Figure S2), which indicates synthesis and excretion of the pigment Gloeocapsin (Sinha et al., 1998) by the slick communities. High solar radiation causes strong stratification and traps cyanobacteria close to the surface by losing their buoyancy regulation, a phenomenon called inverted sedimentation (Kahru et al., 1994). As a positive feedback loop, warming of the microlayer is intensified by the synthesis and excretion of pigments on the ocean's surface resulting from the massive surface accumulation of cyanobacteria (Kahru et al., 1994).

Previous studies have assumed that freshening of the ocean's surface occurs only by precipitation (Soloviev & Lukas, 2006); however, we report that slicks also inhibit salinization and produce an apparent freshening. As mentioned above, closely packed monomolecular films retard evaporation from water surfaces, and more disorganized films with complex mixtures of substances retain the capability to reduce evaporation rates (La Mer & Healy, 1965) causing a fresh salinity anomaly ($\Delta S < 0$). We obtained a significant and strong correlation between ΔT and EF FDOM ($r = 0.708$, 95% CI [0.663, 0.748], $n = 374$), but EF FDOM correlated only weakly with ΔS ($r = -0.270$, 95% CI [−0.347, −0.189], $n = 374$; Figure S3). Considering only data in the presence of cyanobacterial slicks, the correlation even weakened in both cases for ΔT ($r = 0.420$, 95% CI [0.336, 0.498], $n = 284$) and ΔS ($r = 0.177$, 95% CI [0.080, 0.270], $n = 284$), probably due to heterogeneity within the slicks or perhaps due to other complex processes in the slick areas. The weaker correlation to ΔS is evident from Figure 2c as a more saline surface was detected between 02:00 UTC and 03:00 UTC as well between 04:10 UTC and 04:55 UTC despite EF FDOM above 4 and 10, respectively. Evaporation rates computed from meteorological bulk formulas increased after 02:00 UTC (Figure S4). The salty lens detected between 04:10 UTC and 04:55 UTC cannot be explained by our observations, for example, no increase in evaporation rates. Evaporation from water surfaces is a complex process, however, and evaporation rates from slicks may be controlled not only by the concentrations and types of film material but also because wave damping reduces the effective area (Garrett, 1971) or the wind profiles (Wu, 1971) over which evaporation can occur.

4. Conclusion

This study shows that concurrent high-resolution in situ measurements of SST and SSS are essential for better understanding SST and SSS dynamics. Our observations demonstrate that large cyanobacteria slicks complicate the evaluation of satellite-based SST and SSS, and therefore the prediction of regional warming and freshwater fluxes over the ocean. As remote sensing of salinity has become an international mission (i.e., SPURS, Salinity Processes in the Upper-ocean Regional Study; Lindstrom et al., 2015) to assess precipitation over the ocean, the wide coverage of the sea surface with biological slicks (Capone et al., 1998; Sieburth & Conover, 1965; Wurl et al., 2016) can bias satellite data with misinterpretation as having had recent precipitation. Aquarius and SMOS satellites retrieve microwave brightness temperature to obtain SSS from the upper 1 cm, equivalent to the penetration depth of the radiation, but its exponential decay at the sea surface leaves satellite measurements sensitive to changes in the skin layer (Yu, 2010). Synthetic aperture radar from satellites has the capability to detect slicks remotely (Espedal et al., 1998) and potentially useful to reduce the biases on SST and SSS reported here. The observed tendency of warmer SST across the upper 80 μm compared to the upper 20 μm indicates the need of real ground-truth in situ data, that is, from depth equivalent to penetration depth of satellite's IR or microwave radiation, to further advance retrieval algorithm for satellite-derived SST and SSS. Such improved assessment of climate variables from satellites is crucial to improve modeled forecasts on future ocean and climate change.

Competing financial interests

The authors declare no competing financial interests.

Acknowledgments
O. W. acknowledges funding by the European Research Council (ERC) project (grant GA336408). M. C. acknowledges funding through an MBA Research Fellowship, and K. B. was awarded a Natural Environment Research Council (NERC) EnvEast Doctoral Training Partnership PhD studentship. W. M. L. acknowledges funding from the Schmidt Ocean Institute and the Scientific Committee on Ocean Research (SCOR). C. J. Z. acknowledges funding by the Schmidt Ocean Institute (award SOI CU16-228S). All authors thank the Schmidt Ocean Institute for providing their research vessel *R/V* Falkor for the expedition AIR‖SEA (cruise no. FK161010) and funding for open access fees. The captain, officers, and crew of the *R/V* Falkor are acknowledged for their invaluable support during the expedition. Cruise track and catamaran data of FK161010 are archived at the PANGAEA data publisher (Wurl et al., 2017) and available upon request (O. W.). C. J. Z. archives IR and polarimetric data products on Columbia Academic Commons (https://academiccommons.columbia.edu/), and raw imagery are available upon request. This is Lamont-Doherty Earth Observatory contribution number 8213.

References

Capone, D. G., Subramaniam, A., Montoya, J. P., Voss, M., Humborg, C., Johansen, A. M., et al. (1998). An extensive bloom of the N_2-fixing cyanobacterium *Trichodesmium erythraeum* in the central Arabian Sea. *Marine Ecology Progress Series, 172*, 281–292. https://doi.org/10.3354/meps172281

Capone, D. G., Zehr, J. P., Paerl, H. W., Bergman, B., & Carpenter, E. J. (1997). Trichodesmium, a globally significant marine cyanobacterium. *Science, 276*(5316), 1221–1229. https://doi.org/10.1126/science.276.5316.1221

Comeau, A. M., Douglas, G. M., & Langille, M. G. (2017). Microbiome helper: A custom and streamlined workflow for microbiome research. *mSystems, 2*(1), e00127-16. https://doi.org/10.1128/mSystems.00127-16

Conde, F. R., Churio, M. S., & Previtali, C. M. (2004). The deactivation pathways of the excited-states of the mycosporine-like amino acids shinorine and porphyra-334 in aqueous solution. *Photochemical & Photobiological Sciences, 3*(10), 960–967. https://doi.org/10.1039/b405782a

Donlon, C. J., Minnett, P. J., Gentemann, C., Nightingale, T. J., Barton, I. J., Ward, B., & Murray, M. J. (2002). Toward improved validation of satellite sea surface skin temperature measurements for climate research. *Journal of Climate, 15*(4), 353–369.

Donlon, C. J., Minnett, P. J., Jessup, A. T., Barton, I., Emery, W., Hook, S., et al. (2014). Ship-borne thermal infrared radiometer systems. *Experimental Methods in the Physical Sciences: Optical Radiometry for Ocean Climate Measurements, 47*(1), 305–404. https://doi.org/10.1016/B978-0-12-417011-7.00011-8

Downing, H. D., & Williams, D. (1975). Optical constants of water in the infrared. *Journal of Geophysical Research, 80*(12), 1656–1661.

Espedal, H. A., Johannessen, O. M., Johannessen, J. A., Dano, E., Lysenga, D. R., & Knulst, J. C. (1998). COASTWATCH'95: ERS 1/2 SAR detection of natural film on the ocean surface. *Journal of Geophysical Research, 103*, 24,969–24,982. https://doi.org/10.1029/98JC01660

Frew, N. M., Bock, E. J., Schimpf, U., Hara, T., Haußecker, H., Edson, J. B., et al. (2004). Air-sea gas transfer: Its dependence on wind stress, small-scale roughness, and surface films. *Journal of Geophysical Research, 109*, C08S17. https://doi.org/10.1029/2003JC002131

Frka, S., Pogorzelski, S., Kozarac, Z., & Ćosović, B. (2012). Physicochemical signatures of natural sea films from middle Adriatic stations. *The Journal of Physical Chemistry. A, 25*, 6552–6559. https://doi.org/10.1021/jp212430a%20|%201021/jp212430a

Garrett, W. D. (1971). A novel approach to evaporation control with monomolecular films. *Journal of Geophysical Research, 76*, 5122–5123. https://doi.org/10.1029/JC076i021p05122

Grossman, R. L., Bean, B. R., & Marlatt, W. E. (1969). Airborne infrared radiometer investigation of water surface temperature with and without an evaporation-retarding monomolecular layer. *Journal of Geophysical Research, 74*, 2471–2476. https://doi.org/10.1029/JB074i010p02471

Harvey, G. W., & Burzell, L. A. (1972). A simple microlayer method for small samples. *Limnology and Oceanography, 17*(1), 156–157. https://doi.org/10.4319/lo.1972.17.1.0156

Hühnerfuss, H., Alpers, W., & Richter, K. (1986). Discrimination between crude-oil spills and monomolecular sea slicks by airborne radar and infrared radiometer- possibilities and limitations. *International Journal of Remote Sensing, 7*(8), 1001–1013. https://doi.org/10.1080/01431168608948905

Jarvis, N. L. (1962). The effect of monomolecular films on surface temperature and convective motion at the water/air interface. *Journal of Colloid Science, 17*(6), 512–522. https://doi.org/10.1016/0095-8522(62)90019-3

Jarvis, N. L., & Kagarise, R. E. (1962). Determination of the surface temperature of water during evaporation studies. A comparison of thermistor with infrared radiometer measurements. *Journal of Colloid Science, 17*(6), 501–511. https://doi.org/10.1016/0095-8522(62)90018-1

Jessup, A. T., Asher, W. E., Atmane, M., Phadnis, K., Zappa, C. J., & Loewen, M. R. (2009). Evidence for complete and partial surface renewal at an air-water interface. *Geophysical Research Letters, 36*, L16601. https://doi.org/10.1029/2009GL038986

Kahru, M., Horstmann, U., & Rud, O. (1994). Satellite detection of increased cyanobacteria blooms in the Baltic Sea: Natural fluctuation or ecosystem change? *Ambio, 23*, 469–472.

Kahru, M., Leppanen, J. M., & Rud, O. (1993). Cyanobacterial blooms cause heating of the sea surface. *Marine Ecology Progress Series, 101*, 1/2), 1–1/2), 7.

Katsaros, K. (1980). Radiative sensing of sea surface temperature. In F. Dobson, L. Hasse, & R. Davis (Eds.), *Air Sea Interaction: Instruments and Methods* (pp. 293–317). New York: Plenum Press. https://doi.org/10.1007/978-1-4615-9182-5_17

La Mer, V. K., & Healy, T. W. (1965). Evaporation of water: Its retardation by monolayers. *Science, 148*(3666), 36–42. https://doi.org/10.1126/science.148.3666.36

Levitus, S., Antonov, J. I., Boyer, T. P., Baranova, O. K., Garcia, H. E., & Zweng, R. A. L., et al. (2012). World ocean heat content and thermosteric sea level change (0–2000 m), 1955–2010. *Geophysical Research Letters, 39*, L10603. https://doi.org/10.1029/2012GL051106

Lindstrom, E., Bryan, F., & Schmitt, R. (2015). SPURS: Salinity Processes in the Upper-Ocean Regional Study: The North Atlantic Experiment. *Oceanography, 28*(1), 14–19. https://doi.org/10.5670/oceanog.2015.01

Marmorino, G. O., & Smith, G. B. (2006). Reduction of surface temperature in ocean slicks. *Geophysical Research Letters, 33*, L14603. https://doi.org/10.1029/2006GL026502

Martin, S. (2014). *An introduction to ocean remote sensing* (2nd ed.). New York: Cambridge University Press.

Mcleish, W., & Putland, G. E. (1975). Measurements of wind-driven flow profiles in the top millimeter of water. *Journal of Physical Oceanography, 5*(3), 516–518.

Price, J. F., Weller, R. A., & Pinkel, R. (1986). Diurnal cycling: Observations and models of the upper ocean response to diurnal heating, cooling, and wind mixing. *Journal of Geophysical Research, 91*, 8411–8427. https://doi.org/10.1029/JC091iC07p08411

Ribas-Ribas, M., Mustaffa, N. I. H., Rahlff, J., Stolle, C., & Wurl, O. (2017). Sea Surface Scanner (S^3): A catamaran for high-resolution measurements of biogeochemical properties of the sea surface microlayer. *Journal of Atmospheric and Oceanic Technology, 34*(7), 1433–1448. https://doi.org/10.1175/JTECH-D-17-0017.1

Romano, J. C. (1996). Sea-surface slick occurrence in the open sea (Mediterranean, Red Sea, Indian Ocean) in relation to wind speed. *Deep Sea Research, Part I, 43*(4), 411–423. https://doi.org/10.1016/0967-0637(96)00024-6

Saunders, P. M. (1967). The temperature at the ocean-air interface. *Journal of the Atmospheric Sciences, 24*(3), 269–273. https://doi.org/10.1175/1520-0469(1967)024%3C0269:TTATOA%3E2.0.CO;2

Sieburth, J. M. N., & Conover, J. T. (1965). Slicks associated with Trichodesmium blooms in the Sargasso Sea. *Nature, 205*(4973), 830–831. https://doi.org/10.1038/205830b0

Sinha, R. P., Klisch, M., Gröniger, A., & Häder, D.-P. (1998). Ultraviolet-absorbing/screening substances in cyanobacteria, phytoplankton and macroalgae. *Journal of Photochemistry and Photobiology B: Biology, 47*(2-3), 83–94. https://doi.org/10.1016/S1011-1344(98)00198-5

Soloviev, A., & Lukas, R. (2006). *The near-surface layer of the ocean*. Dordrecht: Kluwer Academic.

Song, Y. T., Lee, T., Moon, J.-H., Qu, T., & Yueh, S. (2015). Modeling skin-layer salinity with an extended surface-salinity layer. *Journal of Geophysical Research: Oceans, 120*, 1079–1095. https://doi.org/10.1002/2014JC010346

Taylor, J. D., Cottingham, S. D., Billinge, J., & Cunliffe, M. (2014). Seasonal microbial community dynamics correlate with phytoplankton-derived polysaccharides in surface coastal waters. *The ISME Journal, 8*(1), 245–248. https://doi.org/10.1038/ismej.2013.178

Tilstone, G. H., Ailts, R. L., Vicente, V. M., Widdicombe, C., & Llewellyn, C. (2010). High concentrations of mycosporine-like amino acids and colored dissolved organic matter in the sea surface microlayer off the Iberian Peninsula. *Limnology and Oceanography, 55*(5), 1835–1850. https://doi.org/10.4319/lo.2010.55.5.1835

Wu, J. (1971). Evaporation retardation by monolayers: Another mechanism. *Science, 174*(4006), 283–285. https://doi.org/10.1126/science.174.4006.283

Wurl, O., Miller, L., & Vagle, S. (2011). Formation and distribution of transparent exopolymer particles in the ocean. *Journal of Geophysical Research, 116*, C00H13. https://doi.org/10.1029/2011JC007342

Wurl, O., Mustaffa, N. I. H., & Ribas-Ribas, M. (2017). Multiparameter measurement of biochemical properties of the sea surface microlayer in the Pacific Ocean during *R/V Falkor* cruise FK161010. *PANGAEA*. https://doi.org/10.1594/PANGAEA.882430

Wurl, O., Stolle, C., Van Thuoc, C., Thu, P. T., & Mari, X. (2016). Biofilm-like properties of the sea surface and predicted effects on air–sea CO_2 exchange. *Progress in Oceanography, 144*, 15–24. https://doi.org/10.1016/j.pocean.2016.03.002

Yu, L. (2010). On sea surface salinity skin effect induced by evaporation and implications for remote sensing of ocean salinity. *Journal of Physical Oceanography, 40*(1), 85–102. https://doi.org/10.1175/2009JPO4168.1

Zappa, C. J., Banner, M. L., Schultz, H., Corrada-Emmanuel, A., Wolff, L. B., & Yalcin, J. (2008). Retrieval of short ocean wave slope using polarimetric imaging. *Measurement Science and Technology, 19*(5), 055503. https://doi.org/10.1088/0957-0233/19/5/055503

Zappa, C. J., Banner, M. L., Schultz, H., Gemmrich, J. R., Morison, R. P., LeBel, D. A., & Dickey, T. (2012). An overview of sea state conditions and air-sea fluxes during RaDyO. *Journal of Geophysical Research, 117*, C00H19. https://doi.org/10.1029/2011JC007336

Zhang, Y., & Zhang, X. (2012). Ocean haline skin layer and turbulent surface convections. *Journal of Geophysical Research, 117*, C04017. https://doi.org/10.1029/2011JC007464

Zhou, Y., Jiang, L., Lu, Y., Zhan, W., Mao, Z., Qian, W., & Liu, Y. (2017). Thermal infrared contrast between different types of oil slicks on top of water bodies. *IEEE Geoscience and Remote Sensing Letters, 14*(7), 1042–1045. https://doi.org/10.1109/LGRS.2017.2694609

Appendix 7

RAHLFF, J., RIBAS-RIBAS, M., BROWN, S. M., MUSTAFFA, N. I. H., RENZ, J., PECK, M. A., BIRD, K., CUNLIFFE, M., MELKONIAN, K. & ZAPPA, C. J. 2018. Blue pigmentation of neustonic copepods benefits exploitation of a prey-rich niche at the air-sea boundary. *Scientific Reports,* 8**,** 11510.

SCIENTIFIC REPORTS

OPEN

Blue pigmentation of neustonic copepods benefits exploitation of a prey-rich niche at the air-sea boundary

Received: 26 February 2018
Accepted: 19 July 2018
Published online: 31 July 2018

Janina Rahlff[1,6], Mariana Ribas-Ribas[1], Scott M. Brown[2], Nur Ili Hamizah Mustaffa[1], Jasmin Renz[3], Myron A. Peck[4], Kimberley Bird[5], Michael Cunliffe[5], Katharina Melkonian[1] & Christopher J. Zappa[2]

The sea-surface microlayer (SML) at the air-sea interface is a distinct, under-studied habitat compared to the subsurface and copepods, important components of ocean food webs, have developed key adaptations to exploit this niche. By using automated SML sampling, high-throughput sequencing and unmanned aerial vehicles, we report on the distribution and abundance of pontellid copepods in relation to the unique biophysicochemical signature of the SML. We found copepods in the SML even during high exposure to sun-derived ultraviolet radiation and their abundance was significantly correlated to increased algal biomass. We additionally investigated the significance of the pontellids' blue pigmentation and found that the reflectance peak of the blue pigment matched the water-leaving spectral radiance of the ocean surface. This feature could reduce high visibility at the air-sea boundary and potentially provide camouflage of copepods from their predators.

The ocean-spanning sea-surface microlayer (SML) forms the boundary between atmosphere and hydrosphere. Despite having a thickness of < 1 mm, the SML has profoundly different physicochemical and biological characteristics from the underlying water (ULW)[1]. The SML provides a biogenic gelatinous framework[2] and is typically enriched with organic matter[3], heterotrophic microorganisms[4] as well as higher trophic level organisms[5].

Among zooplankton taxa living within the SML, neustonic copepods (phylum Arthropoda, class Crustacea) of the family Pontellidae have been frequently recorded in tropical regions of all oceans[6–8]. The SML is regarded as a challenging or even extreme habitat because organisms are exposed to variable temperatures and high intensities of solar and ultraviolet (UV) radiation[9]. Copepods are the most abundant metazoans on Earth[10] and show impressive short-term adaptation to environmental stressors, e.g. downregulation of the cellular heat stress response[11]. Given their major role in marine food webs and ecosystem functioning[12], knowledge of the tolerance limits of copepods to abiotic factors is essential if we hope to make robust projections of the effects of global change on the world's oceans. The effects of climate-driven warming (and acidification) on the SML ecosystem and neuston-dwelling copepods, although scarcely examined to date, may be particularly dramatic.

A feature of many pontellid copepods is their blue colouring, that also occurs in other surface-dwelling mesozooplankton[13]. The colouring results from a complex of the pigment astaxanthin and a carotenoprotein[14]. Astaxanthin can be produced from dietary sources and was found to be the principal carotenoid in four different blue-pigmented copepod genera as well as in *Oikopleura dioica* of the class Appendicularia indicating convergent evolution of the feature in different neuston inhabitants[15]. Various theories have been developed to explain the significance of the blue colouring in copepods, including protection from strong solar and/or UV radiation[16,17],

[1]Institute for Chemistry and Biology of the Marine Environment (ICBM), Carl von Ossietzky University Oldenburg, Schleusenstraße 1, 26382, Wilhelmshaven, Germany. [2]Lamont-Doherty Earth Observatory, Columbia University, Palisades, NewYork, 10964, USA. [3]German Centre for Marine Biodiversity Research, Senckenberg am Meer, Martin-Luther-King Platz 3, 20146, Hamburg, Germany. [4]Center for Earth System Research and Sustainability (CEN), University of Hamburg, Olbersweg 24, 22767, Hamburg, Germany. [5]Marine Biological Association of the United Kingdom, Plymouth, PL1 2PB, UK. [6]Present address: Group for Aquatic Microbial Ecology (GAME), University of Duisburg-Essen, Campus Essen-Biofilm Centre, Essen, Germany. Correspondence and requests for materials should be addressed to J.R. (email: Janina.rahlff@uni-due.de) or M.R.-R. (email: Mariana.ribas.ribas@uni-oldenburg.de)

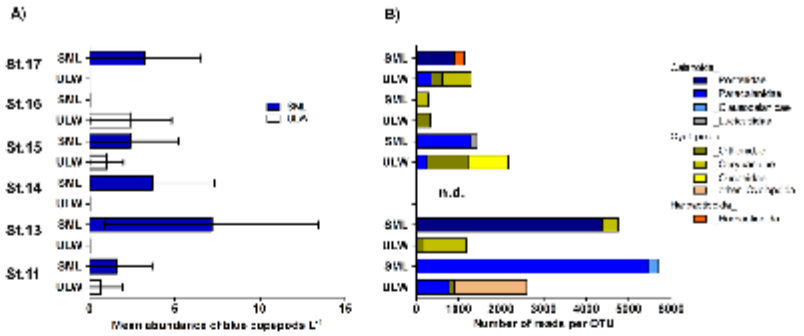

Figure 1. Copepod distribution at the air-sea boundary. **(A)** Mean (±standard deviation) of whole pontellid copepods L^{-1} in SML and ULW. **(B)** Number of reads per OTU assigned for different copepod orders and families from SML and ULW (1 m depth). Stations as in **(A)**. N.d. = not determined, SML = sea-surface microlayer, ULW = underlying water, OTU = operational taxonomic unit, St = Station.

camouflage against visual predators that forage in the uppermost water layers[13] as well as recognition of conspecifics when occurring together with copepods that possess a green fluorescent protein (GFP)-based coloration[18].

In situ sampling was performed on the *R/V* Falkor in the tropical Pacific Ocean, northwest of the Bismarck Sea in October and November 2016 (Supplementary Fig. S1). During daylight hours over six days, the remotely-operated Sea Surface Scanner (S^3)[19] was used to collect paired samples from the SML (uppermost 1 mm) and ULW (1 m reference depth). The S^3 employs rotating glass discs[20] to collect organisms associated with the SML. In addition, conductivity (for calculations of salinity) and temperature within the SML as well as UV radiation in air (3 m above sea level) were recorded onboard the S^3. Spectral absorption of the water surface was measured using an unmanned aerial vehicle (UAV) and compared to the reflectance peak derived from the blue pigment of the pontellids to further investigate the camouflage hypothesis.

Results and Discussion

Blue copepods (prosoma length of ~2 mm) collected with the S^3 were counted and identified to the calanoid copepod family Pontellidae in subsamples from stations 11, 13, 14 and 17 (Supplementary Fig. S1). More precisely, *Ivellopsis denticauda* was found at station 11, whereas *Pontella fera* occurred at stations 13, 14, 17 (Supplementary Fig. S1). Besides the blue pontellids no other copepods were observed in both SML and ULW samples. Neustonic copepods were previously found to be enriched (10–100x) in the uppermost 0–5 cm layer of the ocean, compared to the ULW[21]. Using the S^3 we found higher abundance of pontellids in the SML (the uppermost 1 mm) compared to the ULW at one meter (Fig. 1A). High-throughput sequencing of the total eukaryote 18S ribosomal RNA (rRNA) encoding genes on additional manually-collected SML and ULW samples confirmed predominant SML enrichment for the order Calanoida including the families Pontellidae and Paracalanidae, whereas different copepods of the order Cyclopoida were most prevalent in the ULW (Fig. 1B). Using BLAST analysis, we found that operational taxonomic units (OTUs) from SML samples shared high identity with the blue pontellids *Pontella fera* (100%) and *Anomalocera patersoni* (97%) at two stations (Supplementary Table S1). Due to the lack of reference sequences for copepod species in the Genbank and SILVA database, the true copepod community composition could not be reliably determined. While *Anomalocera patersoni* (97%) was the closest hit in the database, morphological analysis indicating presence of *Ivellopsis denticauda* might provide the better estimate for the true identity of the species. Although pontellids were previously noted in the SML via sampling with a Nytex screen[3] or by sampling of the upper 10 cm using a neuston catamaran[8], this is the first study to link their enrichment at the immediate air-sea boundary with physical characteristics, i.e., salinity and temperature of the SML measured during sampling and with the availability of food, i.e. chlorophyll *a* (chl *a*) as an indicator for autotrophic biomass.

When data were pooled across all five days and stations containing pontellids in the SML (Fig. 1A), the peak abundance occurred at 30.7 °C and a salinity of 33.8 (Supplementary Fig. S2). SML and ULW temperature and salinity were significantly different from each other at most stations (Supplementary Fig. S3a,b, Supplementary Table S2). However, neither SML temperature nor salinity being recorded simultaneously to copepod sampling were significantly correlated to copepod abundance in SML samples (Supplementary Fig. S4a,b, Supplementary Table S3). Previous studies on *Pontella fera* in the South Pacific reported increased abundance in waters >28.5 °C and at salinity <34.5[22], and that this species can be abundant in surface waters during daytime[7]. Our data on copepod presence in the SML match the known abiotic preferences (Supplementary Fig. S2). Compared to the ULW, our data indicate that the SML was often more saline (mean ± standard deviation (STD) difference = 0.3 ± 0.5, n = 95) likely due to evaporation and also colder (mean ± STD difference = −0.3 ± 0.2 °C, n = 108), likely due to its heat flux[23] producing a "cool skin effect". Due to the given profiles of temperature and salinity, the SML is denser compared to the ULW, but its stability and buoyancy is retained by the forces of interfacial tension between SML and ULW and by the surface tension of the SML. These physical characteristics of the SML support the establishment of a unique set of organisms[24] and may be especially advantageous to survival in the tropics. For

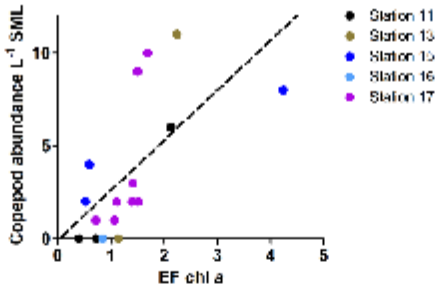

Figure 2. Pontellid abundance in relation to autotrophic biomass. Number of pontellid copepods in SML versus enrichment factor (EF) for chlorophyll *a* (chl *a*), i.e. the ratio of chl *a* concentration in SML over ULW for individual sampling bottles pooled across all stations except for station 14 (no chl *a* readings).

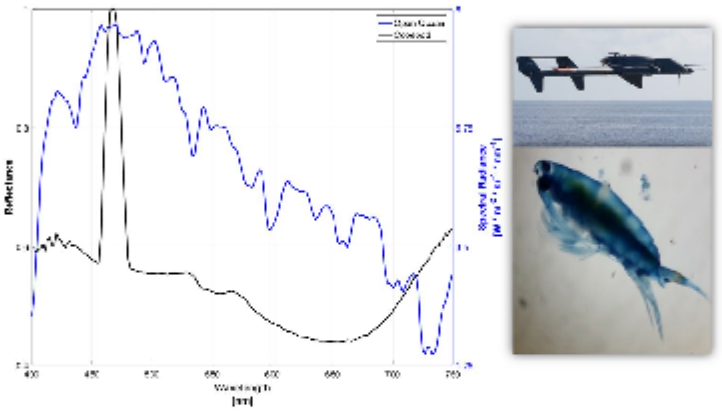

Figure 3. Reflectance spectrum of ocean surface and pontellid copepods. The water-leaving spectral radiance of the ocean surface measured by a hyperspectral visible imaging spectrometer aboard the ship-deployed unmanned aerial vehicle (UAV, upper picture) flying over the S³ during the sampling of the pontellid copepods (lower picture). The same hyperspectral visible imaging spectrometer was used in the *R/V* Falkor's laboratory to measure the reflectance spectrum of copepod pigments.

instance, only at station 16 SML temperature was higher than its ULW counterpart (Supplementary Fig. S3a) and only at this station blue copepods were absent from the SML (Fig. 1A,B).

Additional advantages of living at the immediate air-sea interface include the ability to escape predation by leaping out of the water[25,26] and the ability to reduce energy costs for routine locomotion in this physically stable niche. Surface tension and light availability also favor enrichment of autotrophic biomass (chl *a*) in the SML over ULW. Chl *a* concentration was not significantly different between SML and ULW over all stations (Supplementary Table S4, Supplementary Fig. S5, Mann-Whitney-U-test, U value = 103, $p = 0.16$, $n = 17$), however its enrichment in the SML over ULW was positively and significantly correlated with blue copepod abundance in the SML (Fig. 2, Spearman rank correlation coefficient = 0.70, $p = 0.0017$, $n = 17$). High enrichment of chl *a* -bearing microalgae in the SML over ULW supports suspension feeding by calanoids and, thus, might explain the preference of pontellid copepods to inhabit the SML. It should be noted that enrichment factors (EF) in this dataset (Fig. 2) are even underestimated, because samples for chl *a* originated from the same bottles copepods were counted from, meaning that algal biomass in these samples was already depleted by copepod grazing.

Hyperspectral imaging of the reflectance spectra of the copepod pigment and of the ocean surface water-leaving radiance measured from the UAV are shown in Fig. 3. The spectral peak of the copepod pigment, measured directly after SML sampling, was 466.8 to 468.7 nm with a bandwidth of roughly 455.6 to 479.8 nm. The sharp, narrow spectral peak of the copepod pigment is in striking contrast to the broad absorption spectrum of water-extracted solutions of this blue pigment reported by Herring[16]. The reflectance peak of the copepod pigment measured onboard the *R/V* Falkor lies within the maximum water-leaving radiance spectrum from the

ocean surface. The astaxanthin pigment in these copepods, thus, might provide effective camouflage, potentially reducing risks of visual detection by predators in the SML and/or the ULW[13]. While pigmented copepods generally experience a higher predation risk compared to transparent individuals[27], some blue copepods such as *Pontella mimocerami* can additionally exhibit green fluorescence serving a potential role in counter-shading, a mechanism being analogous to bioluminescence[28]. This might in turn aid the crustaceans to escape predation during the night, e.g. during diel vertical migration. Whether the pontellids we observed at the air-sea interface in the open ocean also expressed GFP-like proteins remains however to be determined.

Moreover, the carotenoid pigment appears to provide protection against UV radiation[29] by holding antioxidant properties and scavenging reactive oxygen species[17]. The abundance of copepods collected with the S^3 seemed unrelated to an index of UV irradiance, i.e. pontellids remained present in the SML at very high UV index values (i.e. $\geq$10, Supplementary Fig. S6) and no enhanced mortality, i.e. increased numbers of carcasses could be observed in our samples being in contrast to other recent findings[30]. Apart from surface avoidance behavior, a typical response of copepods to UV stress[31], and possessing sun screening carotenoids such as astaxanthin, emerging work has shown that UV-protective mycosporine-like amino acids (MAA) have an important role in UV protection of near-surface (top 50 cm) zooplankton communities[32]. Whether pontellid copepods inhabiting the SML rely on MAA in addition to their carotenoid-protein-complex still remains to be determined. At least, the SML and therein accumulating algal biomass might provide a good basis for maintaining both strategies of photo-protection because the synthesis of carotenoids, e.g. astaxanthin from β-carotene, and MAAs is dependent on the availability of algal precursor molecules[15,33]. While recent work has shown that not only UV radiation and fish predation can affect copepod pigmentation, stress responses expressed by colouring can also vary between sex and life-stage of the copepod[34] which we could however not consider in the given study.

Pontellid copepods have a unique life history strategy in the tropical ocean shaped by their ability to tolerate and exploit a prey-rich and slightly cooler SML environment of high physical stability. While being inhospitable to most other meso-zooplankton, pontellids most likely benefit from their pigmentation and adaptive behavior[25,35] to cope with the disadvantages of high visibility and increased solar and UV radiation at the air-sea interface.

Methods

Copepod sampling via the S^3. Copepods were collected by the S^3[19] over a distance of 5–7 km, with an average sampling speed of 2 km h^{-1} at a minimum distance of 100 m from the *R/V* Falkor. Special neuston nets can collect organisms in the 0–5 cm layer[36] but, as only the hydrophobic SML adheres to the glass discs, the S^3 can collect copepods exclusively from the uppermost 1 mm. Sampled volumes are shown in Supplementary Table S5. Copepod subsamples from most stations were later identified by light microscopy (Supplementary Table S6). Water from 1 m was pumped up by the S^3 for reference purposes. Twelve pairs of 1-L bottles were filled with SML and ULW samples during each sampling day, and each bottle filling took approximately 2–3 minutes. Operation of the S^3 was between 11 pm and 7 am UTC time, which corresponds to local daytime. Temperature, conductivity and UV index were measured onboard the S^3 as previously described[19]. Salinity was computed from the conductivity and temperature data using algorithms of the fundamental properties of seawater[37]. Measurements of temperature and salinity were taken from the sensor measurements onboard the S^3 conducted at the same time copepods were sampled. At station 16 salinity from the ULW was not properly recorded due to sensor issues and thus omitted from the data set. The UV index was measured on the mast of the S^3, approximately 3 m above the sea surface, and ranged from 0 to 11 (an index of 10 is equal to an Erythemal Action Spectrum (EAS) weighted irradiance of 0.25 W m^{-2}).

Chlorophyll *a* analysis. Water from random SML and ULW pairs of 1-L bottles was taken for discrete chlorophyll *a* analysis. The fluorometer (JENWAY 6285, Bibby Scientific Ltd., UK) was calibrated before measurements. Readings on standards were taken by using pure chl *a* extracted from spinach (Sigma Aldrich, Germany). Water samples (600–800 mL) were filtered immediately onto glass microfiber filters (GF/F, diameter: 25 mm, Whatman, UK) and were stored at −20 °C for further analysis for up to 4 weeks. The filtered samples were then extracted in 3 mL of 90% ethanol solution for 24 hours and in dark condition, before being measured fluorometrically according to the EPA Method 445.0[38]. The enrichment factor (EF) gives the ratio of the chl *a* concentration in the SML to its ULW counterpart from paired sampling bottles (SML and ULW) derived from stations 11 (n = 3), 13 (n = 2), 15 (n = 3), 16 (n = 1), and 17 (n = 8). An EF >1 indicates an enrichment of chl *a* within the SML, whereas EF < 1 means a depletion.

High-throughput sequencing. In addition, manual glass plate sampling[39] from a small boat and Illumina MiSeq sequencing on the 18S rRNA gene was used to determine the copepod community composition. Sampling was performed shortly before and after S^3 operation and the normalised abundance per operational taxonomic unit (OTU) pooled for each station 11, 13, 15, 16, 17. Seawater samples (500 mL) from the SML and ULW were filtered onto 0.2 µm cellulose nitrate membranes (Whatman, UK), and DNA was extracted using a commercially available DNeasy kit (Qiagen, UK). Primers used for targeting the V4 region of the 18S rRNA gene were 572 F and 1009R[40]. 18S rRNA encoding gene library preparation and sequencing were performed at the Integrated Microbiome Resource (IMR) at the Centre for Comparative Genomics and Evolutionary Bioinformatics (CGEB), Dalhousie University as previously conducted[41]. Sequences were processed in QIIME v1.9.1[42] and USEARCH v9[43] as described elsewhere[44]. OTUs assigned as Copepoda (SILVA 128 database) were filtered from the 18S rRNA data set. Phylogenetic affiliations were determined using the Basic Local Alignment Search Tool (https://blast.ncbi.nlm.nih.gov/Blast.cgi).

UAV operation and spectral analyses. During the cruise, unmanned aerial vehicles (UAVs, Latitude Engineering model HQ-60) were flown. They carried a down-looking Headwall Photonics model Micro-Hyperspec A-Series VNIR hyperspectral visible (400–1000 nm) imaging spectrometer with better than 3 nm spectral resolution for water-leaving spectral radiance measurements to determine ocean color and biogeochemical mapping. The spectrometer measurements from the UAV were performed directly over the ocean surface sampled by the S^3, and the open ocean spectrum in Fig. 3 is an average over 1 km or 1800 spectra. The same hyperspectral imaging spectrometer was used in the *R/V's* laboratory to measure copepod pigments on homogenate of six crushed individuals. The copepod mixture was prepared on a glass slide and illuminated by a diffuse white light source. For the copepod reflectance spectrum, we divided the average of 725 spectra of the copepod mixture by the source spectrum.

Statistical analysis. Non-parametric Spearman rank correlation analysis (two-tailed, 95% confidence level) for EF of chl *a*, temperature and salinity versus copepod abundance in SML was performed. Chl *a*, temperature and salinity differences between SML and ULW were analyzed by means of a two-tailed Mann–Whitney U test. A non-parametric approach was chosen due to the limited number of observations that made it difficult to assess normality and homoscedasticity of the data. All analyses were carried out using GraphPad Prism (v5.00 GraphPad Software, San Diego CA, USA).

Data availability. The datasets generated during and/or analysed during the current study are available from the corresponding author on reasonable request.

References

1. Engel, A. *et al.* The ocean's vital skin: toward an integrated understanding of the sea surface microlayer. *Front. Mar. Sci.* **4**, https://doi.org/10.3389/fmars.2017.00165 (2017).
2. Wurl, O. & Holmes, M. The gelatinous nature of the sea-surface microlayer. *Mar. Chem.* **110**, 89–97, https://doi.org/10.1016/j.marchem.2008.02.009 (2008).
3. Sieburth, J. M. *et al.* Dissolved organic matter and heterotrophic microneuston in the surface microlayers of the North Atlantic. *Science* **194**, 1415–1418, https://doi.org/10.1126/science.194.4272.1415 (1976).
4. Franklin, M. P. *et al.* Bacterial diversity in the bacterioneuston (sea surface microlayer): the bacterioneuston through the looking glass. *Environ. Microbiol.* **7**, 723–736, https://doi.org/10.1111/j.1462-2920.2004.00736.x (2005).
5. Brodeur, R. D. Neustonic feeding by juvenile salmonids in coastal waters of the Northeast Pacific. *Can. J. Zool.* **67**, 1995–2007, https://doi.org/10.1139/z89-284 (1989).
6. Heinrich, A. K. On the near-surface plankton of the eastern South Pacific Ocean. *Mar. Biol.* **10**, 290–294, https://doi.org/10.1007/BF00368087 (1971).
7. Heinrich, A. K. Influence of the monsoon climate on the distribution of neuston copepods in the Northeastern Indian Ocean. *Oceanology* **50**, 549–555, https://doi.org/10.1134/S0001437010040119 (2010).
8. Turner, J. T., Collard, S. B., Wright, J. C., Mitchell, D. V. & Steele, P. Summer distribution of pontellid copepods in the neuston of the Eastern Gulf of Mexico continental-shelf. *B. Mar. Sci.* **29**, 287–297 (1979).
9. Maki, J. S. Neuston microbiology: life at the air-water interface. *Encyclopedia of Environmental Microbiology*. https://doi.org/10.1002/0471263397.env234 (2003).
10. Humes, A. G. How many copepods? In *Ecology and Morphology of Copepods. Developments in Hydrobiology* (eds Ferrari F.D. and Bradley B.P.) Vol. 102 Springer, Dordrecht, 1–7 (1994).
11. Rahlff, J. *et al.* Short-term molecular and physiological responses to heat stress in neritic copepods *Acartia tonsa* and *Eurytemora affinis*. *Comp. Biochem. Physiol. A, Mol. Integr. Physiol.* **203**, 348–358, https://doi.org/10.1016/j.cbpa.2016.11.001 (2017).
12. Mauchline, J. The biology of calanoid copepods. In *Advances in Marine Biology* (eds Blaxter, J.H.S, Southward, A.J. and Tyler, P.A.) Vol. 33 Academic Press, San Diego, 1–702 (1998).
13. Herring, P. J. The pigments of plankton at the sea surface. *Symp. Zool. Soc. Lond* **19**, 215–235 (1967).
14. Zagalsky, P. & Herring, P. J. Studies on a carotenoprotein isolated from the copepod, *Labidocera acutifrons* and its relationship to the decapod carotenoproteins and other polyene-binding proteins. *Comp. Biochem. Physiol. B, Biochem. Mol. Biol.* **41**, 397–415, https://doi.org/10.1016/0305-0491(72)90043-0 (1972).
15. Mojib, N. *et al.* Carotenoid metabolic profiling and transcriptome-genome mining reveal functional equivalence among blue-pigmented copepods and appendicularia. *Mol. Ecol.* **23**, 2740–2756, https://doi.org/10.1111/mec.12781 (2014).
16. Herring, P. J. Blue pigment of a surface-living oceanic copepod. *Nature* **205**, 103–104, https://doi.org/10.1038/205103a0 (1965).
17. Caramujo, M.-J., de Carvalho, C. C., Silva, S. J. & Carman, K. R. Dietary carotenoids regulate astaxanthin content of copepods and modulate their susceptibility to UV light and copper toxicity. *Mar. Drugs* **10**, 998–1018, https://doi.org/10.3390/md10050998 (2012).
18. Shagin, D. A. *et al.* GFP-like proteins as ubiquitous metazoan superfamily: evolution of functional features and structural complexity. *Mol. Biol. Evol.* **21**, 841–850, https://doi.org/10.1093/molbev/msh079 (2004).
19. Ribas-Ribas, M., Mustaffa, N. I. H., Rahlff, J., Stolle, C. & Wurl, O. Sea Surface Scanner (S^3): a catamaran for high-resolution measurements of biogeochemical properties of the sea surface microlayer. *J. Atmospheric Ocean. Technol.* **34**, 1433–1448, https://doi.org/10.1175/jtech-d-17-0017.1 (2017).
20. Shinki, M., Wendeberg, M., Vagle, S., Cullen, J. T. & Hore, D. K. Characterization of adsorbed microlayer thickness on an oceanic glass plate sampler. *Limnol. Oceanogr. Meth.* **10**, 728–735, https://doi.org/10.4319/lom.2012.10.728 (2012).
21. Zaitsev, Y. In *The Sea Surface and Global Change* (eds Liss, P. S. & Duce, R. A.) 371–382 (Cambridge University Press, 2005).
22. Sherman, K. Pontellid copepod occurrence in the central South Pacific. *Limnol. Oceanogr.* **9**, 476–484, https://doi.org/10.4319/lo.1964.9.4.0476 (1964).
23. Saunders, P. M. The temperature at the ocean-air interface. *J. Atmospheric Sci.* **24**, 269–273, https://doi.org/10.1175/1520-0469(1967)024<0269:TTATOA>2.0.CO;2 (1967).
24. Hardy, J. T. The sea surface microlayer: biology, chemistry and anthropogenic enrichment. *Progr. Oceanogr.* **11**, 307–328, https://doi.org/10.1016/0079-6611(82)90001-5 (1982).
25. Gemmell, B. J., Jiang, H., Strickler, J. R. & Buskey, E. J. Plankton reach new heights in effort to avoid predators. *Proc. Biol. Sci.* **279**, 2786–2792, https://doi.org/10.1098/rspb.2012.0163 (2012).
26. Svetlichny, L., Larsen, P. S. & Kiørboe, T. Swim and fly: escape strategy in neustonic and planktonic copepods. *J. Exp. Biol.* **221**, jeb167262, https://doi.org/10.1242/jeb.167262 (2018).
27. Gorokhova, E., Lehtiniemi, M. & Motwani, N. H. Trade-offs between predation risk and growth benefits in the copepod *Eurytemora affinis* with contrasting pigmentation. *Plos One* **8**, e71385, https://doi.org/10.1371/journal.pone.0071385 (2013).
28. Hunt, M. E., Scherrer, M. P., Ferrari, F. D. & Matz, M. V. Very bright green fluorescent proteins from the pontellid copepod *Pontella mimocerami*. *Plos One* **5**, e11517, https://doi.org/10.1371/journal.pone.0011517 (2010).

29. Byron, E. R. The adaptive significance of calanoid copepod pigmentation - a comparative and experimental-analysis. *Ecol.* **63**, 1871–1886, https://doi.org/10.2307/1940127 (1982).
30. Mojib, N., Thimma, M., Kumaran, M., Sougrat, R. & Irigoien, X. Comparative metatranscriptomics reveals decline of a neustonic planktonic population. *Limnol. Oceanogr.* **62**, 299–310, https://doi.org/10.1002/lno.10395 (2017).
31. Alonso, C., Rocco, V., Barriga, J. P., Battini, M. A. & Zagarese, H. Surface avoidance by freshwater zooplankton: field evidence on the role of ultraviolet radiation. *Limnol. Oceanogr.* **49**, 225–232, https://doi.org/10.4319/lo.2004.49.1.0225 (2004).
32. Fileman, E. S. *et al.* Stress of life at the ocean's surface: latitudinal patterns of UV sunscreens in plankton across the Atlantic. *Prog. Oceanogr.* **158**, 171–184, https://doi.org/10.1016/j.pocean.2017.01.001 (2017).
33. Hylander, S. & Jephson, T. UV protective compounds transferred from a marine dinoflagellate to its copepod predator. *J. Exp. Mar. Biol. Ecol.* **389**, 38–44, https://doi.org/10.1016/j.jembe.2010.03.020 (2010).
34. Brüsin, M., Svensson, P. A. & Hylander, S. Individual changes in zooplankton pigmentation in relation to ultraviolet radiation and predator cues. *Limnol. Oceanogr.* **61**, 1337–1344, https://doi.org/10.1002/lno.10303 (2016).
35. Manor, S., Polak, O., Saidel, W. M., Goulet, T. L. & Shashar, N. Light intensity mediated polarotaxis in *Pontella karachiensis* (Pontellidae, Copepoda). *Vision Research* **49**, 2371–2378, https://doi.org/10.1016/j.visres.2009.07.007 (2009).
36. Zaitsev, Y. P. *Marine Neustonology* (translated from Russian). National Marine Fisheries Service, NOAA and National Science Foundation, National Technical Information Service, Springfield, Virginia (1971).
37. Fofonoff, N. & Millard, R. Jr. Algorithms for computation of fundamental properties of seawater. Endorsed by Unesco/SCOR/ICES/IAPSO Joint Panel on Oceanographic Tables and Standards and SCOR Working Group 51. Unesco Technical Papers in Marine Science, No. 44. (1983).
38. Arar, E. J. & Collins, G. B. Method 445.0: *In vitro* determination of chlorophyll a and pheophytin a in marine and freshwater algae by fluorescence. (United States Environmental Protection Agency, Office of Research and Development, National Exposure Research Laboratory Cincinnati, 1997).
39. Harvey, G. W. & Burzell, L. A. A simple microlayer method for small samples. *Limnol. Oceanogr.* **17**, 156–157, https://doi.org/10.4319/lo.1972.17.1.0156 (1972).
40. Comeau, A. M., Li, W. K., Tremblay, J. E., Carmack, E. C. & Lovejoy, C. Arctic Ocean microbial community structure before and after the 2007 record sea ice minimum. *Plos One* **6**, e27492, https://doi.org/10.1371/journal.pone.0027492 (2011).
41. Comeau, A. M., Douglas, G. M. & Langille, M. G. Microbiome helper: a custom and streamlined workflow for microbiome research. *mSystems* **2**, e00127–00116, https://doi.org/10.1128/mSystems.00127-16 (2017).
42. Caporaso, J. G. *et al.* QIIME allows analysis of high-throughput community sequencing data. *Nat. Methods* **7**, 335–336, https://doi.org/10.1038/nmeth.f.303 (2010).
43. Edgar, R. C. Search and clustering orders of magnitude faster than BLAST. *Bioinformatics* **26**, 2460–2461, https://doi.org/10.1093/bioinformatics/btq461 (2010).
44. Taylor, J. D. & Cunliffe, M. High-throughput sequencing reveals neustonic and planktonic microbial eukaryote diversity in coastal waters. *J. Phycol.* **50**, 960–965, https://doi.org/10.1111/jpy.12228 (2014).

Acknowledgements

We thank the cruise chief scientist Oliver Wurl, the captain and crew members of the *R/V* Falkor (cruise FK161010) and Lea Oeljeschläger for assistance with copepod counting. We thank Justin Armer, Scott Bowers, and Joe McDaniel of the Latitude Engineering flight crew for piloting the UAVs aboard the *R/V* Falkor. This work was funded by the European Research Council (ERC) project PASSME (grant number GA336408). C.J.Z. and S.M.B. acknowledge funding by the Schmidt Ocean Institute (Award Number: SOI CU16-2285). This is Lamont-Doherty Earth Observatory contribution number 8233. M.C. acknowledges funding through a MBA Research Fellowship and K.B. was awarded a Natural Environment Research Council (NERC) EnvEast Doctoral Training Partnership PhD studentship. K.M. was funded by the PhD program EcoMol (awarded by Lower Saxony, Germany). We thank the editor and the two anonymous reviewers for the constructive and valuable feedback on our manuscript.

Author Contributions

J.R.1 (the corresponding author) contributed to copepod handling, data analysis and first draft writing; C.J.Z. and S.M.B. were responsible spectral analyses and UAV operation; M.R.R. and N.J.H.M. contributed to S^3 data collection and N.J.H.M. and K.M. additionally to chlorophyll measurements and analyses; J.R.2 contributed to taxonomic analysis; K.B. and M.C. provided copepod sequence data. J.R.1, M.A.P. and C.J.Z. contributed to the idea and concept of the manuscript. All Authors contributed to manuscript discussion and writing.

Additional Information

Supplementary information accompanies this paper at https://doi.org/10.1038/s41598-018-29869-7.

Competing Interests: The authors declare no competing interests.

Publisher's note: Springer Nature remains neutral with regard to jurisdictional claims in published maps and institutional affiliations.